Tommaso Scarabino
Editor

Imaging Gliomas After Treatment

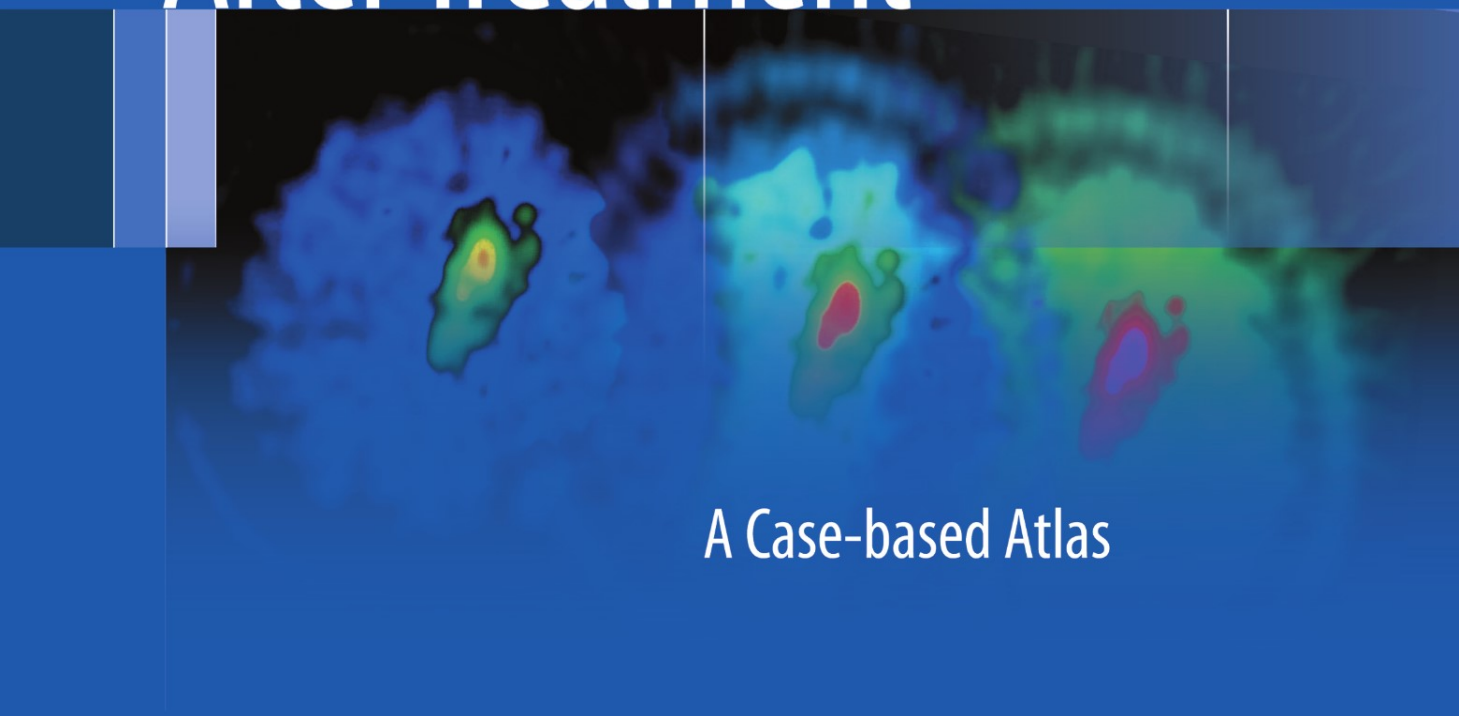

A Case-based Atlas

Springer

Imaging Gliomas After Treatment

Tommaso Scarabino
Editor

Imaging Gliomas After Treatment

A Case-based Atlas

In collaboration with
Ferdinando Caranci, Mario Muto, Teresa Popolizio

and
Saverio Pollice, Armando Tartaro, Gabriele Polonara, Alessandro Stecco, Alessandro Carriero

Springer

Editor

Tommaso Scarabino

Department of Neuroradiology, "L. Bonomo" Hospital, Andria (BT), Italy, and Department of Neuroradiology, Scientific Institute "Casa Sollievo della Sofferenza", San Giovanni Rotondo (FG), Italy

Co-authors

Ferdinando Caranci

Diagnostic Imaging Department, Unit of Neuroradiology, Federico II University, Naples, Italy

Alessandro Carriero

Department of Radiology, "Maggiore della Carità" University Hospital, Novara, Italy, and University of Piemonte Orientale "A. Avogadro", Novara, Italy

Mario Muto

Department of Neuroradiology, "Cardarelli" Hospital, Naples, Italy

Saverio Pollice

Department of Radiology, "L. Bonomo" Hospital, Andria (BT), Italy

Gabriele Polonara

Department of Radiology, University Hospital "Ospedali Riuniti", Ancona, Italy

Teresa Popolizio

Department of Neuroradiology, Scientific Institute "Casa Sollievo della Sofferenza", San Giovanni Rotondo (FG), Italy

Alessandro Stecco

Department of Radiology, "Maggiore della Carità" University Hospital, Novara, Italy

Armando Tartaro

Institute of Advanced Biomedical Technologies, Department of Neurosciences and Imaging, "G. d'Annunzio" University, Chieti-Pescara, Italy

ISBN 978-88-470-2369-7

e-ISBN 978-88-470-2370-3

DOI 10.1007/978-88-470-2370-3

Library of Congress Control Number: 2011934756

Cover design: Ikona S.r.l., Milan, Italy
Typesetting: Ikona S.r.l., Milan, Italy
Printing and binding: Grafiche Porpora S.r.l., Segrate, Milan

Printed in Italy

Springer-Verlag Italia S.r.l. – Via Decembrio 28 – I-20137 Milan
Springer is a part of Springer Science+Business Media

Foreword

Recent years have witnessed important progress in the imaging of brain tumors. In the case of magnetic resonance imaging, increasingly sophisticated contrast agents afford a more comprehensive study of blood-brain barrier abnormalities in clinical practice, and at the same time new techniques have been designed to evaluate the morphology of local and distant metastases. In addition, numerous functional techniques have been introduced, including methods to examine cellularity and cancer spread in the interstitial space (diffusion-weighted MRI), to study tumor vascularization and behavior in the endothelial wall (perfusion-weighted MRI), and to analyze changes in the concentration of normal and pathological metabolites (MR spectroscopy).

Considerable steps forward have also been achieved in the therapeutic approach to brain tumors. With regard to surgery, these have resulted in improved neuronavigation, greater intraoperative control of resection margins, a broadening of surgical indications to include the treatment of aggressive tumors, and earlier resection of slow-growing masses. Further important advances have been highly precise radiation therapy techniques, chemotherapy regimens that attack both tumor cells and the pathological neovasculature, and tumor genotyping studies. Taken together, these developments allow earlier diagnosis and treatment of brain tumors and improve life expectancy. One consequence is the need for more accurate and more frequent follow-up to assess treatment response and consider treatment changes, especially to counter the "evasive resistance" of gliomas to chemotherapy.

Tommaso Scarabino's interest in interdisciplinary cooperation is reflected in the range and volume of his scientific production, especially with regard to the application of MRI to brain tumors. This volume is the result of his collaboration with highly qualified neuroradiologists as well as clinicians. It examines brain tumor imaging after various types of treatment, going beyond the "wait and see" attitude by developing a comprehensive, coordinated approach. I am certain that his latest effort will not only achieve the success it deserves, but also provide a significant contribution to the treatment of brain tumors.

October 2011

Ugo Salvolini
Department of Radiology
University Hospital "Ospedali Riuniti"
Ancona, Italy

Acknowledgements

This book is organized as a text atlas. The first section includes basic information on the different treatment options for brain tumors, while the second presents a series of morphological and functional MR images.

I express my gratitude to all those authors who have contributed to the drafting of several chapters of the book, thereby drawing upon their considerable experience in neuroradiology.

Very important contributions were made by F. Caranci, M. Muto, T. Popolizio and U. Salvolini, who handled the first part of the text, and by A. Tartaro, A. Carriero and A. Stecco, who provided a rich set of clinical cases included in the second part.

Special thanks are due to U. Salvolini, who oversaw the introduction of the book: his important and valuable recommendations have allowed me to achieve important professional goals.

My gratitude is also owed to S. Pollice and M. Lombardi, who helped with the linguistic revision of the text.

Finally, I wish to thank Springer-Verlag Italy and Antonella Cerri for the enthusiasm with which they accepted the scientific initiative that I suggested.

Tommaso Scarabino

Contents

Part D Clinical Cases

Contributors

Raffaele Agati Department of Neurological Sciences, Alma Mater University of Bologna, Bologna, Italy

Lorenzo Alvaro Department of Neurosurgery, University Hospital "Ospedali Riuniti", Ancona, Italy

Anthony Azubuike Obaze Department of Radiology**,** "Maggiore della Carità" University Hospital, Novara, Italy, and University of Piemonte Orientale "A. Avogadro", Novara, Italy

Antonella Bacci Department of Neurological Sciences, Alma Mater University of Bologna, Bologna, Italy

Santa Bambace Department of Radiotherapy, "Di Miccoli" Hospital, Barletta (BT), Italy

Mario Brandi Department of Oncology, "Di Miccoli" Hospital, Barletta (BT), Italy

Chiara Briganti Institute of Advanced Biomedical Technologies, Department of Neurosciences and Imaging, "G. d'Annunzio" University, Chieti-Pescara, Italy

Francesco Briganti Diagnostic Imaging Department, Unit of Neuroradiology, Federico II University, Naples, Italy

Arturo Brunetti Diagnostic Imaging Department, Unit of Neuroradiology, Federico II University, Naples, Italy

Stefania Carbone Department of Radiotherapy, "Di Miccoli" Hospital, Barletta (BT), Italy

Michela Capuano Department of Neuroradiology, "L. Bonomo" Hospital, Andria (BT), Italy

Maria Teresa Cascavilla Department of Neuroradiology, Scientific Institute "Casa Sollievo della Sofferenza", San Giovanni Rotondo (FG), Italy

Antonio Casillo Department of Neuroradiology, Scientific Institute "Casa Sollievo della Sofferenza", San Giovanni Rotondo (FG), Italy

Massimo Caulo Institute of Advanced Biomedical Technologies, Department of Neurosciences and Imaging, "G. d'Annunzio" University, Chieti-Pescara, Italy

Luigi Cirillo Department of Neurological Sciences, Alma Mater University of Bologna, Bologna, Italy

Sossio Cirillo Unit of Neuroradiology, II University of Naples, Naples, Italy

Bianca Cusati Radiology and Diagnostic Imaging Department, S. Maria delle Grazie Hospital, Pozzuoli (NA), Italy

Alessandra D'Amico Diagnostic Imaging Department, Unit of Neuroradiology, Federico II University, Naples, Italy

Vincenzo D'Angelo Department of Neurosurgery, Scientific Institute "Casa Sollievo della Sofferenza", San Giovanni Rotondo (FG), Italy

Alfonso Di Costanzo Department of Neurology, University of Molise, Campobasso, Italy

Gerardo Di Nardo Department of Radiology, "Maggiore della Carità" University Hospital, Novara, Italy, and University of Piemonte Orientale "A. Avogadro", Novara, Italy

Ignazio Divenuto Department of Radiology, "Maggiore della Carità" University Hospital, Novara, Italy

Andrea Elefante Diagnostic Imaging Department, Unit of Neuroradiology, Federico II University, Naples, Italy

Francesco Fabbiano Department of Radiology, "Maggiore della Carità" University Hospital, Novara, Italy, and University of Piemonte Orientale "A. Avogadro", Novara, Italy

Giuseppe Fiscer Department of Radiology, "Maggiore della Carità" University Hospital, Novara, Italy

Lorenzo Fortunelli Department of Radiology, "Maggiore della Carità" University Hospital, Novara, Italy, and University of Piemonte Orientale "A. Avogadro", Novara, Italy

Lucrezia Emanuela Guerra Department of Radiology, "Maggiore della Carità" University Hospital, Novara, Italy, and University of Piemonte Orientale "A. Avogadro", Novara, Italy

Nathalie Herber Department of Radiology, University Hospital "Ospedali Riuniti", Ancona, Italy

Marco Leonardi Department of Neurological Sciences, Alma Mater University of Bologna, Bologna, Italy

Lucia Lombardi Department of Oncology, Scientific Institute "Casa Sollievo della Sofferenza", San Giovanni Rotondo (FG), Italy

Mariangela Lombardi Department of Radiology**,** "Maggiore della Carità" University Hospital, Novara, Italy, and University of Piemonte Orientale "A. Avogadro", Novara, Italy

Angela Lorusso Department of Radiology, "L. Bonomo" Hospital, Andria (BT), Italy

Alberto Maggialetti Department of Radiology, "L. Bonomo" Hospital, Andria (BT), Italy

Evaristo Maiello Department of Oncology, Scientific Institute "Casa Sollievo della Sofferenza", San Giovanni Rotondo (FG), Italy

Emanuele Malatesta Department of Radiology, "Maggiore della Carità" University Hospital, Novara, Italy, and University of Piemonte Orientale "A. Avogadro", Novara, Italy

Raniero Mignini Department of Neurosurgery, "L. Bonomo" Hospital, Andria (BT), Italy

Gilda Morlino Department of Radiology, "Di Venere" Hospital, Bari, Italy

Valentina Panara Institute of Advanced Biomedical Technologies, Department of Neurosciences and Imaging, "G. d'Annunzio" University, Chieti-Pescara, Italy

Alfonso Ragozzino Department of Radiology and Diagnostic Imaging, S. Maria delle Grazie Hospital, Pozzuoli (NA), Italy

Luana Regnicolo Department of Radiology, University Hospital "Ospedali Riuniti", Ancona, Italy

Simone Salice Institute of Advanced Biomedical Technologies, Department of Neurosciences and Imaging, "G. d'Annunzio" University, Chieti-Pescara, Italy

Francesco Sessa Department of Radiology, University Hospital "Ospedali Riuniti", Ancona, Italy

Nicola Sforza Department of Radiology, Scientific Institute "Casa Sollievo della Sofferenza", San Giovanni Rotondo (FG), Italy

Andrea Pietro Sponghini Department of Oncology**,** "Maggiore della Carità" University Hospital, Novara, Italy

Alessandra Stranieri Department of Neuroradiology, Scientific Institute "Casa Sollievo della Sofferenza", San Giovanni Rotondo (FG), Italy

Enrico Tedeschi Diagnostic Imaging Department, Unit of Neuroradiology, Federico II University, Naples, Italy

Domenico Tortora Institute of Advanced Biomedical Technologies, Department of Neurosciences and Imaging, "G. d'Annunzio" University, Chieti-Pescara, Italy

Antonio Volpe Diagnostic Imaging Department, Unit of Neuroradiology, Federico II University, Naples, Italy

Fabio Zeccolini Department of Neuroradiology, "Cardarelli" Hospital, Naples, Italy

Sara Zizzari Department of Radiology, "Maggiore della Carità" University Hospital, Novara, Italy, and University of Piemonte Orientale "A. Avogadro", Novara, Italy

Part A

Introduction

Brain Tumors

1

Saverio Pollice, Gilda Morlino, Michela Capuano
and Tommaso Scarabino

1.1 General Findings

Primary central nervous system (CNS) tumors have an incidence ranging from 5 to 17 cases per 100,000 inhabitants per year, with no significant differences between nations. They cause 2-5% of all cancer deaths [1]. In Italy, the annual incidence of *new* brain tumors ranges from 8.4 to 9.2 per 100,000 per year.

Over the past three decades there has been a progressive increase in the incidence of brain tumors, particularly in subjects about 65 years of age, where the incidence has more than doubled [2]. This increase does not seem attributable only to the increasing availability of new and more sophisticated imaging techniques such as computed tomography (CT) and magnetic resonance (MR) imaging which allow a more accurate diagnosis.

1.2 Classifications

In 2007 the World Health Organization [3] published a revised classification of CNS tumors, which replaced the previous classification of 2000 [4] and to which most neuropathologists today refer (Table 1.1). This classification is based on the identification of different histopathologic groups and includes a scale of malignancy, ranging from grade I benign forms to grade IV forms with rapid growth and poor prognosis.

On the basis of information provided by the WHO classification it is possible to diagnose tumor type and degree of malignancy. In reality, this classification has some limitations because it does not consider the structural heterogeneity of these tumors, in which areas with different degrees of anaplasia-malignancy can coexist. In addition, these tumors over time can undergo malignant transformation which does not appear throughout the lesion at the same time. It follows that histologic diagnosis made on one region of the mass is not necessarily applicable to the whole tumor. Lastly, the location of the tumor, especially when involving eloquent areas, can limit the surgical approach and consequently alter prognosis, even in tumors with the same histopathologic features.

In the new classification, molecular-genetics findings and histologic grade of differentiation have been more precisely assessed [3]. Indeed in neuro-oncology the histologic diagnosis of primary brain tumor is the criterion standard, but only molecular and pathologic tumor tissue assessment may lead to a better characterization of different tumor types (oncotype) and to a better choice of the most appropriate therapeutic strategies [5].

1.3 Glial Tumors

Gliomas are the most common primary intracerebral tumors. Their frequency varies in different statistics between 45 and 62% of the total, with a slight prevalence in males (M/F: 1.3). A common feature of these tumors is the great heterogeneity in neuropathologic appearance, gene expression and prognosis [5].

In the 2007 WHO classification, astrocytic tumor is the prototype referred to the description of the histologic grading. Grade I is assigned to localized tumors with low proliferative level and potentially curable by surgical resection (pilocytic astrocytoma); grade II includes diffusely infiltrative lesions, with cytologic atypia and low prolif-

S. Pollice (✉)
Department of Radiology
"L. Bonomo" Hospital, Andria (BT), Italy

Table 1.1 Classification of central nervous system tumors (WHO 2007)

1. Neuroepithelial tissue tumors
- Astrocytic tumors
  - Astrocytoma (pilocytic, subependymal giant cell) (grade I)
  - Diffuse astrocytomas (pilomyxoid, diffuse, pleomorphic xanthoastrocytoma) (grade II)
  - Anaplastic astrocytoma (grade III)
  - Glioblastoma (giant cell variant, gliosarcoma) (grade IV)
- Oligodendroglial tumors
  - Oligodendroglioma (grade II)
  - Anaplastic oligodendroglioma (grade III)
- Mixed gliomas
  - Oligoastrocytoma (grade II)
  - Anaplastic oligoastrocytoma (grade III)
- Ependymal tumors
  - Ependymoma (grade I)
  - Myxopapillary ependymoma and subependymoma (grade II)
  - Anaplastic ependymoma (grade III)
- Choroid plexus tumors
  - Choroid plexus papilloma (grade I)
  - Atypical choroid plexus papilloma (grade II)
  - Choroid plexus carcinoma (grade III)
- Other neuroepithelial tumors
  - Angiocentric glioma (grade I)
  - Chordoid glioma of III ventricle (grade II)
- Mixed glial and neuronal tumors
  - Gangliocytoma, ganglioglioma (grade I)
  - Anaplastic ganglioglioma (grade III)
  - Desmoplastic infantile astrocytoma and ganglioglioma (grade I)
  - Dysembryoplastic neuroepithelial tumor (grade I)
  - Central neurocytoma (grade II)
  - Extraventricular neurocytoma (grade II)
  - Cerebellar liponeurocytoma (grade II)
  - Spinal paraganglioma (grade I)
  - Papillary glioneuronal tumor (grade I)
  - Glioneuronal tumor forming roses of IV ventricle (grade I)
  - Neuroblastic tumors
  - Olfactory neuroblastoma (esthesioneuroblastoma)
- Pineal tumors
  - Pineocytoma (grade I)
  - Pineal tumor with intermediate differentiation (grade II-III)
  - Papillary tumors of pineal region (grade II-III)
  - Pinealoblastoma (grade IV)
- Embryonal tumor
  - Medulloblastoma (desmoplastic, giant cell, melanocytic, medullomyoblastoma) (grade IV)
  - Primitive neuroectodermal CNS tumors (PNET) (grade IV)
  - Rhabdoid/teratoid atypical tumor (grade IV)

2. Peripheral nerve tumors
- Schwannoma (grade I)
- Neurofibroma (grade I)
- Perineurinoma (grade II-III)
- Peripheral nerve sheath tumors (MPNST) (grade II-IV)

3. Meningeal tumors
- Meningothelial tumors
- Meningioma (grade I)
- Atypical meningioma (grade II)
- Anaplastic or malignant meningioma (grade III)
- Hemangiopericytoma (grade II)
- Anaplastic hemangiopericytoma (grade III)
- Hemangioblastoma (grade I)
- Non meningothelial mesenchymal tumors
- Lipoma, liposarcoma, fibrosarcoma, chondroma, rhabdomyosarcoma, osteosarcoma, hemangiopericytoma etc.
- Melanocytic tumors
  - Diffuse melanocytic, malignant melanoma, diffuse meningeal melanomatosis
- Uncertain origin
  - Hemangioblastoma

4. Hematopoietic tumors
- Lymphoma and plasmacytoma

5. Germ cell tumors
- Germinoma (seminoma), embryonal carcinoma, yolk sac carcinoma, chorion carcinomas, teratomas (mature, immature, with malignant transformation), mixed

6. Sellar region tumors
- Craniopharyngioma (grade I)
- Granular cell tumor of the neurohypophysis (grade I)
- Pituicytoma (grade I)
- Spindle cell oncocytoma of adenohypophysis (grade I)

7. Metastatic tumors

erative activity, which may recur and progress to higher degrees of malignancy (diffuse astrocytoma); grade III consists of tumors with histologic evidence of malignancy, which express nuclear atypia and high mitotic activity (anaplastic astrocytoma); and grade IV includes tumors with malignant cytology, high mitotic activity, tendency to necrosis and microvascular proliferation, with rapid growth, infiltration of surrounding tissues, skull and spinal dissemination and unfavorable outcome (glioblastoma multiforme – GBM). Table 1.2 reports the different degree of glioma distribution in adults.

1.4 Etiology

Tumors are the result of the abnormal and unregulated growth of certain cells. Once the human brain completes its development, most of its cells after birth enter into

Table 1.2 Relative distribution in adults (WHO 2000 Classification)

Low grade
Astrocytoma grade I and II: 4%
Oligodendroglioma: 4%
High grade (malignant gliomas)
Anaplastic astrocytoma grade III: 35%
Glioblastoma multiforme grade IV: 50%
Anaplastic oligoastrocytoma grade III: 4%
Anaplastic oligodendroglioma grade III: 2%

a state of quiescence, devoid of mitotic activity. The only exception to this rule is when a tumor arises. Brain tumor cells resume the *cell cycle* due to changes in some genes that control cell division and growth. Although much is known about the alterations of these genes in brain tumors, the primary reason underlying the changes is currently unknown.

1.5 Hereditary Transmission

Only about 5% of glial tumors have a hereditary component. The role played by genetic predisposition is considered significant in some rare syndromes, in which molecular events are under study (generally inactivation of tumor suppressor genes), commonly known in a family group before a tumor develops in a member. These syndromes include:

- Neurofibromatosis type I (multiple mucosal cutaneous neurofibromas and *cafe au lait* skin rashes) and type II (VIII cranial nerve schwannomas often bilateral)
- Li Fraumeni syndrome (breast cancer, sarcomas, brain tumors, leukemia)
- Turcot syndrome (family polyposis with increased incidence of colon-rectum cancers and astrocytic tumors)
- Von Hippel Lindau syndrome (multiple retinal and intra-axial hemangioblastomas, cysts and renal or pancreatic carcinoma, pheochromocytoma)
- Cowden syndrome (cerebellum dysplastic gangliocytoma, breast cancer, trichilemmomas).

1.6 Risk Factors

Ionizing radiation is considered by some authors the only unequivocal risk factor identified for glial neoplasms. Irradiation of the head, even at low doses, can increase the incidence of glial tumors by a factor of 3 to 7, with a latency period of 10 to more than 20 years after exposure [6]. No other environmental elements or patient behavior has been clearly identified as a risk factor.

Some authors report that proximity to high voltage cables, use of hair dyes, head trauma, diet containing N-nitrosamines, or other nutritional factors may increase the risk of brain tumors [7-9]. The association between type of professional employment and appearance of glioblastomas has been the subject of numerous studies. Workers chronically exposed to vinyl chloride, phenolic compounds and aromatic hydrocarbons have an increased risk [10, 11]. A recent meta-analysis showed an increased risk of gliomas and acoustic neuromas in long-term users (10 years) of cordless or mobile phones [12, 13]. All these data, despite epidemiological importance, however, are considered conflicting and unconvincing [14].

1.7 Pathogenesis

According to the WHO classification there are different genetic alterations leading to glioblastoma [15, 16]. Two particular types of changes can be distinguished:

- Activation of oncogene factors:
  1. EGF/R (epidermal growth factor/receptor)
  2. MDM2 (mouse double minute 2 oncoprotein promotes cell survival and cell cycle progression by inhibiting tumor suppressor TP53)
  3. PDGF/R (platelet-derived growth factor/receptor)
- Deactivation of tumor-suppressor factors:
  1. 10p, 10q, 19q (chromosomes)
  2. DCC (deleted in colorectal cancer tumor suppressor gene)
  3. p16 (tumor suppressor gene/protein)
  4. TP53 (tumor suppressor gene/protein)
  5. PTEN (phosphatase and tensin homolog is a tumor suppressor gene that controls growth, proliferation and cell survival. Its mutation or inhibition can result in the onset of cancer, e.g. prostate, breast, colon and brain)
  6. RB (retinoblastoma tumor suppressor gene, retinoblastoma protein)

Table 1.3 shows mutations that occur in normal cells which can generate glioblastoma [3].

In recent years, molecular studies in neuro-oncology have identified the existence of molecular-biologic changes, such as methylation of MGMT gene promoter

Table 1.3 Astrocytic differentiated cells or precursors or stem cells

TP53 mutation (59%) ↓	*TP53* (59%) mutation ↓	
Diffuse astrocytoma	**Diffuse astrocytoma**	
TP53 Mutation (53%) ↓		
Anaplastic astrocytoma	5.1 years	<3 months (68%) <6 months (84%)
1.9 years		
Loss of heterozygosity on 10q (63%) *EGFR amplification* (8%) *p16*^{INK4a} deletion (19%) *TP53 mutation* (65%) *PTEN mutation* (4%) ↓		Loss of heterozygosity on 10q (70%) *EGFR* amplification (36%) *p16*^{INK4a} detection (31%) *TP53 mutation* (28%) *PTEN mutation* (25%) ↓
Secondary glioblastoma		**Primary glioblastoma**
5% of cases Average age: 45 years M/F ratio: 0.65		95% of cases Average age: 62years M/F ratio: 1.33

and the deletion of chromosomes 1p/19q, able to predict clinical course and response to therapy [17, 18].

The identification of biologic/molecular variables able to characterize the clinical course of disease in the elderly compared to adult patients may allow the identification of targeted treatments which are not only appropriate for the clinical characteristics of elderly patients, but also for biological characteristics of the disease, thus proving more specific, more effective and less toxic.

Genetic analysis of more than 20,000 genes of patients with GBM has detected somatic mutations of the isocitrate dehydrogenase 1 (IDH1) gene in 12% of tumors, more frequently in young patients (mean age 33 years) or with secondary GBM, which has developed from a previous low-grade malignancy type. These mutations are associated with better prognosis [19].

A recent study analyzed the genetic sequence of IDH1 and IDH2 in 445 brain tumors and in 494 other location tumors. Gene mutations have been identified for IDH1 in more than 70% of grade II and III gliomas and secondary glioblastomas. Tumors with mutations in IDH1 and IDH2 have distinct clinical and genetic characteristics and generally have a better prognosis than similar tumors with *wild-type* IDH gene [20].

1.8 Prognostic Factors

Age, performance status and histologic grade are the most important prognostic factors for glial tumors in most randomized trials. Of these, age over 60 years is one of the most important negative prognostic factors in patients with GBM. However, it remains unclear whether this poor prognosis is attributable to the presence of clinical features related to the elderly or to biologic characteristics typical of the disease in the elderly. It has been hypothesized that cancer in elderly patients has different clinical characteristics than in adults given the presence of different molecular genetic profiles. Primary and secondary glioblastomas are probably two distinct diseases, although there is little histologic differentiation. They affect different groups of patients by age and sex and develop through different genetic pathways, with different profiles of mRNA and

Table 1.4 Radiation Therapy Oncology Group prognostic classification

Class	Prognostic factors	Median survival (months)
1	Age <50, anaplastic astrocytoma, surgery, no neurologic deficit	58.6
2	Age ≤50, KPS 70–100, anaplastic astrocytoma, at least three months between onset of symptoms and surgery	37.4
3	Age <50, anaplastic astrocytoma, surgery, neurologic deficit presence Age<50, glioblastoma, KPS 90–100	17.9
4	Age <50, glioblastoma, KPS 90 Age ≤50, KPS 70-100, anaplastic astrocytoma, less than three months from onset of symptoms and surgery Age ≥50, glioblastoma, surgical resection, no neurologic deficit	11.1
5	Age ≤50, KPS 70–100, glioblastoma, surgical resection, Surgery with neurologic deficit or biopsy alone followed by at least 54.4 Gy RT Age ≤ 50, KPS 70, no neurologic deficit	8.9
6	Age ≤50, KPS 70–100, glioblastoma, biopsy alone, less than 54.4 Gy RT Age ≤50, KPS 70, neurologic deficit presence	4.6

KPS, Karnofsky performance status index.

Table 1.5 European Organization for Research and Treatment of Cancer/National Cancer Institute of Canada prognostic classification

Class	Prognostic factors	Median survival (months) (radiotherapy)	Median survival (months) (concomitant and adjuvant temozolomide to radiotherapy)
III	Age <50, glioblastoma, WHO PS 0	15	21
IV	Age <50, glioblastoma, WHO PS 1-2 Age ≥50, glioblastoma, total/partial surgery, MMSE 27	13	16
V	Age ≥50, glioblastoma, MMSE 27, biopsy alone	9	10

PS, performance status; *MMSE*, mini mental state examination.

protein expression. These differences are important, especially because they may influence tumor response to radiation therapy and chemotherapy and may be the target of future therapeutic approaches [21].

The Radiation Therapy Oncology Group (RTOG) has developed a partition of high-grade astrocytic tumors (anaplastic astrocytoma and glioblastoma) in six classes of prognosis according to age, histologic grade, Karnofsky performance status, neurologic function, type of surgery (resection vs. biopsy) and radiation therapy dose delivered (less or more than 54.4 Gy) (Table 1.4) [22].

The European Organization for Research and Treatment of Cancer (EORTC) and the National Cancer Institute of Canada (NCIC) have developed another prognostic classification for patients with GBM treated with radiation therapy alone or adjuvant temozolomide at the same time as radiaton therapy (Table 1.5) [23].

1.9 Symptoms and Complications

The clinical history of glioblastoma is short (less than 3 months in more than 50% of cases), except when cancer develops as the progression of a low-grade astrocytoma (secondary glioblastoma).

The symptoms of a brain tumor depend mainly on its location and its size and consequently on the function of areas involved by the tumor, with a variety of nonspecific symptoms typical of a mass growing inside the skull with increased intracranial pressure. Common symptoms are persistent headache, nausea, vomiting (usually morning), disorders of retina like papilledema caused by the dilatation of cerebral vessels, focal deficit (hemiparesis, hemianesthesia, hemianopsia, diplopia, aphasia) and seizures due to tumor irritation effect (present up to one third of patients); moreover nonspecific neurologic symptoms such as clouding of consciousness and personality changes.

The Karnofsky performance status (KPS) index has been developed to standardize the clinical evaluation of the patient. It gives a score, according to the symptoms, which ranges from the maximum degree of patient autonomy in everyday life (KPS = 100) until death (KPS = 0).

Complications related to the presence of brain tumor can be distinguished from those due to illness (such as

edema, neurologic disorders, visual disturbances, hydrocephalus, leptomeningeal gliomatosis, degradation of cognitive and psychologic state) from those more strictly related to treatment: surgery (infection, neurologic disorders, visual disturbances), radiation therapy (neurologic disorders, visual disturbances, impaired cognitive function), chemotherapy (blood disorders, respiratory disorders, diarrhea, fatigue, neurologic disorders), supportive therapy (anticonvulsants and/or antiinflammatory). Many of these complications are not common and a significant number of them can be effectively controlled with therapy.

1.10 Diagnosis and Staging

Early diagnosis and correct assessment of true tumor extension and relationship with surrounding anatomic structures are important for prognosis and for different treatment approaches and strategies. In many patients, brain tumor diagnosis is delayed by many months after first appearance of symptoms, especially if symptoms are discontinuous and mild. However, there is no significant evidence that earlier diagnosis of most brain tumors favorably influences survival, although it is natural to assume that small tumor lesions can be more easily subjected to radical surgery or respond better to radiation therapy/chemotherapy.

The reference standard examination for the diagnosis of histologic type and grade of brain tumor is the histopathologic study on tissue samples using stereotactic or surgical resection, both of which are invasive methods. Stereotactic biopsy may not always be performed and involves appreciable risk of morbidity and mortality. Sometimes, errors in sampling and mixed malignant and benign histopathologic appearances may limit the diagnostic accuracy of the survey. This underlines the need for a noninvasive technique that could lead to a diagnosis as close as possible to the histologic diagnosis without risk to the patient and with a broader perspective.

MR fits perfectly in this setting and is in fact the investigation of choice for diagnosis and follow-up of patients with brain tumors. This examination should also be recommended to all patients suffering from seizures for which there is no immediate and plausible explanation.

CT is suggested in emergencies (hemorrhage, obstructive hydrocephalus, etc) or in the pursuit of calcification in the context of the lesion (oligodendroglial tumors) or bone erosions of the neurocranium and skull base.

Compared with CT, MR has a greater sensitivity in the detection of lesions. However it is not always easy to access for patients and has some drawbacks: it cannot be done in patients with a pacemaker, a prosthesis incompatible with magnetic field, vascular metal clips, etc.

The MR study should be performed without and with paramagnetic (gadolinium) contrast medium. The use of contrast agent allows the acquisition of information about vascularity and integrity of the blood-brain barrier (BBB), as well as a better definition of tumor lesion and surrounding edema. Once this information has been obtained, the degree of malignancy can be hypothesized.

Contrast enhancement (CE) is not able to distinguish brain tumor from peritumoral edema with certainty. In fact in infiltrating malignant gliomas (such as glioblastoma and anaplastic astrocytoma) anatomopathologic findings may show neoplastic tissue beyond the area of vasogenic edema as shown on MR images.

The presurgical treatment MR study is able to assess the precise location of the lesion and the proximity to (or even the involvement with) vital areas of the brain (eloquent areas). It is also able to evaluate the mechanical effects and consequent changes in the relationship of the tumor with the brain structures such as hydrocephalus and herniation, the effects of which can be fatal.

The morphologic MR study may be supplemented by complementary advanced MR imaging techniques that provide morphofunctional findings very useful for diagnostic and clinical purposes.

The role of positron emission tomography (PET) is very important. This imaging modality is a nuclear technique that uses drugs with positron-emitting isotopes (radiopharmaceuticals). In addition, PET/CT imaging is able to acquire functional metabolic PET images and morphologic CT images using the same system, thus producing a more precise localization of findings. The drug usually used for this study is 18 F-deoxyglucose (FDG) which accumulates in most fast growing lesions and in more aggressive tumors. FDG-PET is indicated in the diagnosis of brain tumors, particularly in the differentiation of metabolically active tumor (persistence/recurrence) from necrotic tissue (radionecrosis) and scarring [24] and in monitoring the response to therapy. False positives are still possible (in cases of non-malignant inflammatory processes) and false negatives (in the presence of small low-grade tumors or high-grade tumors with high anaerobic metabolism) [25].

For the planning of optimal treatment and for post-

treatment monitoring, the medical team should include a neuroradiologist, neurosurgeon, radiation oncologist and oncologist supported by nurses, social workers, psychologists, nutritionists and physical therapists. In this context the neuroradiologist should carefully evaluate post-surgery imaging on the basis of the knowledge of performed treatments.

1.11 Supportive Therapy

Supportive treatment is designed to relieve symptoms and improve the neurologic function of the patient. Supportive primary drugs are anti-epileptics and corticosteroids. Antiepileptic drugs are administered to about 25% of patients who have had seizures at the presentation of the disease. Phenytoin (300-400 mg/d) is the drug most commonly used, but carbamazepine (600-1000 mg/d), phenobarbital (90-150 mg/d) and valproic acid (750-1500 mg/d) are equally effective. Their doses should be adjusted in relation to blood level to provide maximum protection.

New concept anti-epileptics such as levetiracetam, gabapentin, lamotrigine and topiramate are similarly effective. Most of these new drugs have the advantage of causing few cognitive side effects and they do not alter the metabolism of chemotherapy, because they do not induce the hepatic microsomal system. New anticonvulsants are increasingly replacing traditional drugs in first-line anti-epileptic therapy [26]. Prospective clinical trials have yielded negative results to show the effectiveness of the prophylactic use of antiepileptic drugs in brain tumors patients with no previous seizure. Consequently, the medical literature does not recommend its use for this purpose except for the period of surgery, when their use can reduce the incidence of postoperative seizures [26, 27].

Corticosteroids can reduce peritumoral edema, diminishing mass effect of the tumor and reducing intracranial pressure. Their immediate effect is headache relief and improvement in *lateralized* signs.

Corticosteroid dexamethasone is preferable, because of its minimal mineralocorticoid activity. The starting dose is about 16 mg/d. This amount may be increased or decreased to reach the minimum dose needed to control neurologic symptoms.

Prolonged use of corticosteroids is associated with hypertension, diabetes mellitus, hyperosmolar nonketotic hyperglycemic state (a potentially lethal condition), myopathy, weight gain, insomnia and osteoporosis. Therefore, in patients with brain tumor, steroid dose should be reduced gradually *as quickly as possible* once treatment has started. For most patients, the administration of corticosteroids may be discontinued upon completion of radiation therapy.

References

1. Moller-Jensen O, Esteve J, Moller H et al (1990) Cancer in the European Community and its member States. Eur J Cancer 26:1167-1256
2. Werner MH, Phuphanich S, Lyman GH (1995) The increasing incidence of malignant gliomas and primary central nervous system lynphoma in the elderly. Cancer 76:1634-1642
3. Louis DN, Ohgaki H, Wiestler OD, Cavenee WK (eds) (2007) World Health Organization classification of tumours of the central nervous system. IARC, Lyon
4. Kleihues P, Cavenee WK eds (2000) Pathology and genetics of tumours of the nervous system, World Health Organization classification of tumours. IARC, Lyon
5. Brandes AA, Reni M, Carapella C et al (2009) Linee guida in neuro-oncologia a cura dell'AIOM, pp 357-392
6. Walter AW, Hancock ML, Pui CH et al (1998) Secondary brain tumors in children treated for acute lymphoblastic leukemia at St Jude Children's Research Hospital. J Clin Oncol 16:3761-3767
7. Salvatore JR, Weitberg AB, Mehta S (1996) Nonionizing electromagnetic fields and cancer: a review. Oncology 10:563-574
8. Kaplan S, Novikov I, Modan B (1997) Nutritional factors in the etiology of brain tumors: potential role of nitrosamines, fat, and cholesterol. Am J Epidemiol 146:832-841
9. Inskip PD, Mellemkjaer L, Gridley G et al (1998) Incidence of intracranial tumors following hospitalization for head injuries. Cancer Causes Control 9:109-116
10. Rice JM, Wilbourn JD (2000) Tumors of the nervous system in carcinogenic hazard identification. Toxicol Pathol 28:202-214
11. Cordier S, Monfort C, Filippini G et al (2004) Parental exposure to polycyclic aromatic hydrocarbons and the risk of childhood brain tumors: The SEARCH International Childhood Brain Tumor Study. Am J Epidemiol 159:1109-1116
12. Inskip PD, Tarone RE, Hatch EE et al (2001) Cellular-telephone use and brain tumors. N Engl J Med 344:79-86
13. Hardell L, Carlberg M, Soderqvistn F et al (2008) Meta-analysis of long-term mobile phone use and the association with brain tumours. Int J Oncol 32:1097-1103
14. DeAngelis LM (2001) Brain tumors. N Engl J Med 344:114-123
15. Kleihues P et al (2000) Glioblastoma. In: Kleihues P, Cavenee WK (eds) Pathology and genetics of tumours of the nervous system, World Health Organization classification of tumours. IARC, Lyon
16. Kleihues P, Burger PC, Aldape KD et al (2007) Glioblastoma. In: Louis DN, Ohgaki H, Wiestler OD, Cavenee WK (eds) World Health Organization classification of tumours of the central nervous system. IARC, Lyon

17. Van den Bent MJ, Looijenga LH, Langenberg K et al (2003) Chromosomal anomalies in oligodendroglial tumors are correlated with clinical features. Cancer 97:1276-1284
18. Hegi ME, Diserens AC, Gorlia T et al (2005) MGMT gene silencing and benefit from temozolomide in glioblastoma. N Engl J Med 532:997-1003
19. Parsons DW, Sian J, Zhang X et al (2008) An integrating genomic analysis of human glioblastoma multiforme. Science 321:1807-1812
20. Yan H, Parson DW, Jin G et al (2009) IDH1 and IDH2 mutations in gliomas. N Engl J Med 360:765-773
21. Ohgaki H, Kleihues P (2007) Genetic pathways to primary and secondary glioblastoma. Am J Pathol 170:1445-1453
22. Curran WJ, Scott CB, Horton J et al (1993) Recursive partitioning analysis of prognostic factors in three radiation therapy oncology group malignant glioma trials. J Natl Cancer Inst 85:704-710
23. Mirimanoff RO, Gorlia T, Mason W et al (2006) Radiotherapy and temozolomide for newly diagnosed glioblastoma: recursive partitioning analysis of the EORT 26981/122981 – NCIC CE 3 phase III randomized trial. J Clin Oncol 24:2563-2569
24. Doyle WK, Budinger TF, Valk PE et al (1987) Differentiation of cerebral radiation necrosis from tumor recurrence by (18)FDG and 82Rb positron emission tomography. J Comput Assist Tomogr 11:563-570
25. Langleben DD, Segal GM (2000) PET in differentiation of recurrent brain tumor from radiation injury. J Nucl Med 41:1861-1867
26. DeAngelis LM, Loeffler JS, Adam N et al (2007) Primary and metastatic brain tumors. In: Pazdur R, Coia LR, Hoskins WJ, Wagman LD (eds) Cancer management: a multidisciplinary approach, 10th edn. CMPMedica, New York
27. Chang SM, Parney IF, Huang W et al (2005) Glioma Outcomes Project Investigators. Patterns of care for adults with newly diagnosed malignant glioma. JAMA 293:557-564

Part B

Treatment of Gliomas

Surgery

2

Vincenzo D'Angelo, Raniero Mignini and Tommaso Scarabino

2.1 General Findings

The treatment of brain tumors is complex and depends on several factors such as histologic type, location and extension, age and general conditions of the patient. Brain tumors can be treated with surgery, radiation therapy (RT) and chemotherapy, often in combination, in relation to the needs of patient [1].

The first step is to schedule wherever possible a treatment plan that includes the sequence and the individual components of a multidisciplinary approach. Currently, surgery is considered the best available treatment for patients in good health. Surgical resection is chronologically the first therapeutic option and should be as complete as possible according to tumor site and the general conditions of the patient.

For benign tumors, radical excision in most cases is the only and definitive therapy (curative surgery). Where a high risk of morbidity or mortality is associated with radical resection of the mass, it may be preferable to leave a residual tumor and undertake adjuvant therapies for its treatment (mainly RT). For malignant tumors surgery is only a part of a combined RT/chemotherapy treatment. Cytoreductive surgery is more effective the more extensive it is. In this case, the 5-year survival in low grade gliomas increases from 30% to 60%, in glioblastomas from 8 to 13 months, however, it is worse in elderly patients in whom mean survival does not exceed one year.

V. D'Angelo (✉)
Department of Neurosurgery
Scientific Institute "Casa Sollievo della Sofferenza"
San Giovanni Rotondo (FG) Italy

2.2 Surgery

Surgery of brain tumors involves treatment aimed at the removal of the mass. This neurosurgical act follows the removal of a piece of bone (craniotomy or craniectomy) located over the tumor to allow access to the underlying tumor tissue. A craniotomy involves the creation of a bone flap which is then repositioned at the end of the intervention or at a later time. The dura mater underlying the bone is usually sutured along the edges of the bone gap and *suspended* to the same bone while the surgical site is covered with artificial meninges. Craniectomy is instead an opening in the skull with a drill hole and possible widening of the gap with the use of ronguer. The bone removed is replaced with plastic reconstruction or a patch that uses the residual fragments.

Neurosurgical treatment of gliomas is a very complex surgical procedure which requires appropriate neurologic knowledge (anatomic, functional and clinical) and a high level of practical experience. The goals of surgery are to remove as much of the tumor mass as possible and obtain an accurate histopathologic diagnosis, while not affecting brain function or worsening already compromised function, eliminating pathologic vascularization and improving metabolism and blood flow.

Additional benefits of extended surgery are: (1) immediate reduction of intracranial pressure with rapid improvement in symptoms from compression/intracranial hypertension; (2) reduction of cancer mass resulting in better oxygenation of residual tumor in order to promote response to RT; and (3) delay the onset of chemoresistance and thus prevent possible postoperative complications.

Since its origins to today, neurosurgery of brain tumors, particularly gliomas, has undergone significant

change. Over the past 25 years, a range of new operating room instruments has been introduced, new surgical approaches have been designed and anesthetic and resuscitation techniques have been improved. These improvements have allowed a more radical surgery and a significant reduction in mortality and complications, especially for lesions located in *critical* areas in which surgery results in a significant reduction in the quality of life of the patient.

The main advances have focused on: (1) oncologic neurosurgery by neuronavigation, neuro-endoscopy (recommended above in the presence of obstructive hydrocephalus caused by tumor or in biopsy/removal of intraventricular tumors); (2) neuroradiologic diagnosis performed with high field magnetic resonance (MR) imaging, functional MR, ultrasound and/or intraoperative MR / computed tomography (CT); (3) technology supporting surgery with neuroprotection in anesthesia and intensive care; (4) intraoperative neurophysiologic mapping with its monitoring; (5) awake surgery recommended in the removal of lesions adjacent to motor or language areas, during which the patient does tests to assess the onset of motor or sensory aphasia; (6) intraoperative visualization of tumor margins and consequent widening of the removal (by using 5-ALA that renders tumor cells fluorescent); (7) treatment by local chemotherapy (carmustine wafers) and stereotactic radiosurgery.

Even the criteria of operability have changed, allowing an extension of surgical indications so patients that were previously considered inoperable can currently undergo surgery. There are no data in the literature, however, to indicate that these advances are associated with significant improvements in survival. It can be said that certainly an improvement of quality of life post-surgery has been obtained by reducing the appearance of neurologic deficits. Despite the great technologic progress, gliomas remain in most cases an incurable disease that raises still debated and controversial issues: we must first understand where and when to perform surgery in a tumor: there are tumors for which undergoing surgery is not useful and tumors for which surgery is very hard. Neuroradiologic and clinical findings are necessary to take an appropriate decision and moreover an intraoperative evaluation is essential to determine whether removal can be more or less total.

Two factors need to be taken into account to assess whether a glioma is operable: the first is related to the patient, the second to the tumor. Factors related to the patient are primarily age and then general medical conditions, neurologic conditions, clinical history, presence of seizures, any previous therapy and the patient's expectations. Factors related to the tumor are mainly location and extension of disease, relations and effects of the tumor against surrounding brain tissue, number of lesions, rate of growth, characteristics of growth and presumed histopathology classification.

Two requirements moreover must be taken into account: (1) surgery should not cause additional neurologic damage to the patient; (2) the surgeon should try to radically remove the mass to improve survival times, patient clinical condition and response to adjuvant therapies.

The amount of postsurgical residual correlates negatively with prognosis [2, 3], even though it has been noted that tumors in which radical resection is difficult are those that involve vital structures and by their nature have a worse prognosis [4].

A recent systematic review of the literature confirms that the extension of surgery is associated with increased life expectancy in patients with high-grade and low-grade glioma [5]. Immediate surgical treatment is definitely the ideal process for the resolution of the tumor without adverse effects on structures and functions of the central nervous system. Moreover, long-term surgery, alone or in combination with other treatment modalities, should try to contain tumor regrowth both locally and remotely.

The approach to a malignant tumor is different from that for a benign lesion: malignant masses have peculiarities and characteristics for which a neuroradiologic and clinical evaluation before surgery is highly important, considering the concept of the critical areas and critical aspects (e.g. tumor crossed by major vessels).

2.2.1 Low Grade Gliomas

Low grade gliomas (LG) systematically change their biologic nature and evolve into high-grade gliomas (45-86% of cases) with an average time of anaplastic transformation of about 7-8 years, and they become irreversibly fatal after about 10 years.

Their slow but steady growth means that an early surgical approach has become an increasingly approved therapeutic strategy. The amount of surgically removed tumor decisively influences prognosis, even when the differences in the amount removed are small. There are some variables that significantly condition the possibility of performing a complete resection or that even

determine surgical abstention. The most important variable is the involvement of critical areas (25% of supratentorial cancer involve eloquent areas). Delaying treatment may lead to risks such as increased volume of the lesion, anaplastic transformation, onset of non-reversible neurologic deficits or worsening seizures. Delaying surgical treatment may prove logical or rational only in cases of a stable and asymptomatic tumor or with a single symptom such as seizures controlled by medication.

2.2.2 High Grade Gliomas

High grade gliomas (HG) are characterized by short survival and often have a difficult course which is a burden for the patient, their family and society. Surgical resection is chronologically the first therapeutic option and should be as complete as possible according to the tumor site and to the patient's general conditions. The final outcome depends on the age of disease, time between surgery and RT and operator experience.

In theory, the surgical removal of the tumor offers improved quality of life. Gliomatosis cells, however, have high levels of invasiveness toward surrounding healthy tissue; they can in fact be found several inches beyond the macroscopic tumor margins. Consequently, microscopic radical surgery is almost impossible. Unfortunately, recurrence after surgery normally occurs, even in the absence of radiologically evident residual and in over 80% of cases manifests in close proximity to the surgical bed. Although radical excision is not always possible, it should be as wide as possible (as long as it involves no additional risks and deficits of any kind) because this strategy is well correlated with a better outcome. Residual volume, however, influences not only prognosis but also response to chemotherapy and thus survival. However, each case must be evaluated individually. On many occasions, for example, it is considered unnecessary or dangerous to remove the deep component of a tumor that will be subsequently treated with RT.

2.2.3 Recurrence

The operability of a HG glioma, and even more so its reoperability with higher morbidity in relation to previous treatments and greater extension, is an open and debated issue. Recurrence in fact occurs in more than 80% of cases in close proximity to the surgical bed. Various factors affect tumor recurrence, including the infiltrating pattern of the disease, non-radical therapy (surgery and RT), and difficulty of passage of drugs across the blood-brain barrier (BBB). Indications for resurgery predictive of longer survival and better quality of life are age ≤70 years, performance status >70, non-glioblastoma histology, first operation interval greater than 6 months, no disabling neurologic deficit, resolution of clinical symptoms after first surgery, and ability to continue chemotherapy with greater benefit [6]. Often an intensified associated chemotherapy may be useful in further improving prognosis. Repeat surgery logically is useful if we can expect a substantial benefit with improvement in the functional status of the patient. In general, great benefits even with multiple resurgery occur, especially after the first reoperation rather than after subsequent procedures. Even in this case reference should be made to clinical and neuroradiologic criteria.

2.2.4 Critical Areas

In planning tumor treatment, mapping of the brain is very important. This involves assessing the function of *critical* (or eloquent) areas preoperatively and intraoperatively.

Indications for the surgery of tumors in critical areas need to be carefully evaluated. However, surgery must be supported by the use of technologies to prevent serious functional damage (navigation, awake surgery, functional mapping). Brain mapping can help to save critical areas as much as possible that may also improve functionality over time and minimize neurologic deficits. Tumor removal means removing a brain volume with a central part of the tumor and a peripheral part with normally functioning cells and fibers. Brain area functions may be broadly classified into complex functions (such as frontal and parietal functions, which are very hard to evaluate preoperatively and intraoperatively and have a complex anatomic neural substrate) and in simple functions (such as motor functions, which are easier to evaluate especially intraoperatively and are characterized by a more easily accessible neural network).

Motor areas are the most important and studied in the brain. Various techniques exist for this purpose: awake surgery and intraoperative brain mapping with subdural electrodes which monitor motor function make it possible to avoid damaging the patient when operating on those particularly important brain areas. Neuroradi-

ology techniques with cortical activation (fMRI) enable the noninvasive evaluation of preoperative and postoperative resectability.

References

1. Rampling R, James A, Papanastassiou V (2004) The present and future management of malignant brain tumours: surgery, radiotherapy, chemotherapy. J Neurol Neurosurg Psych 75:24-30
2. Wood JR, Green SB, Shapiro et al (1998) The prognostic importance of tumor size in malignant gliomas: a computed tomographic scan study by the Brain Tumor Cooperative Group. J Clin Oncol 6:338-343
3. Lacroix M, Abi-Said D, Fourney DR et al (2001) A multivariate analysis of 416 patients with glioblastoma multiforme: prognosis, extent of resection, and survival. J Neurosurg 95:190-198
4. Hess KR (1999) Extent of resection as a prognostic variable in the treatment of glioma. J Neuro-Oncol 42:227-231
5. Sanai N, Berger MS (2008) Glioma extent if resection and its impact on patient outcome. Neurosurgery 62:753-764
6. Brandes AA, Vastola F, Monfardini S (1999) Reoperation in recurrent high-grade glioma. Literature review of prognostic factors and outcome. Am J Clin Oncol 22:387-390

Radiation Therapy

3

Santa Bambace, Stefania Carbone and Tommaso Scarabino

3.1 General Findings

Radiation therapy (RT) is a nonsurgical treatment that uses radiation to eradicate tumor or to restrict its growth. In the treatment of gliomas, RT may be indicated as an adjuvant therapy to surgery.

The RT target is the surgical bed plus a margin around the mass, as defined in the literature. The aim of treatment is to produce irreversible damage to the DNA of any residual tumor cells that have escaped surgery because they are not microscopically visible (infiltrating more or less distant from the surgical bed).

In RT different types of radiation can be used: X rays, gamma rays and ionizing particles. These forms of radiation have ionizing capabilities which act on the atoms and cause the acquisition or loss of an electron: ions thus obtained interact with normal molecules in the cell (including DNA) producing varying degrees of damage. In dedicated equipment (linear accelerators often shortened to LINAC) electrons are accelerated and, after impact with a target inside the machine, release X-rays.

Gamma rays, instead, are produced from radioactive isotopes which during decay emit radiation or particulate matter, such as secondary products of nuclear reactions.

For some cancer types particularly sensitive to radiation, RT often in combination with chemotherapy may be the only therapeutic approach required. In other cases, RT is used in combination with surgery to remove any residual tumor not removed during surgery. RT can also be used in nonoperable tumors to reduce metastatic spread or relieve symptoms. Radiation can kill cells or block their ability to proliferate. They act, however, both on tumor cells and normal cells. Unlike tumor cells, however, healthy cells have good mechanisms for repairing damage caused by radiation. Generally brain cells are very resistant to irradiation, while other cell types (bone marrow cells, germinal cells, epithelium lining hollow organs) are very sensitive, which is why the approach is to restrict the radiotherapeutic target volume as much as possible. After treatment, it is necessary to wait some time before evaluating the results of RT: during this period, in fact, tumor cells damaged during the course of treatment undergo apoptosis. Often this process produces a degree of edema which can cause symptoms similar to cancer and which in radiologic imaging can simulate tumor growth.

In some cases edema due to tumor cell death may temporarily worsen a pre-existing edema and produce temporary neurologic diseases, thus prompting a temporary interruption to the treatment and a strengthening of anti-edema therapy. At any rate, the dosage of steroid therapy should be limited to the lowest dose able to control the symptoms of intracranial hypertension. Other effects, some of which are permanent and not frequent, may occur long after treatment. These include a decline in intellectual faculties due to the necrosis of healthy tissue and to the degeneration of blood vessels, the possible development of other cancers, hormonal dysfunction and leukoencephalopathy. The main factors that increase the risk of neurologic toxicity due to RT are: (1) age <65 years; (2) increased volume of treatment or whole brain RT; (3) total dose >60 Gy; (4) high linear energy transfer radiation such as neutrons or brachytherapy; (5) brain disorders, concomitant vascular or metabolic disease (diabetes, hypertension, de-

S. Bambace (✉)
Department of Radiotherapy
"Di Miccoli" Hospital, Barletta (BT), Italy

mentia, collagen disease); (6) use of chemotherapy (especially pre-exposure to methotrexate).

3.2 Radiation Therapy Techniques

RT may be given with different treatment modalities

- 3-dimensional conformal RT (3DCRT)
- Intensity-modulated RT (IMRT)
- Brachytherapy
- Stereotactic radiosurgery
- Stereotactic body RT (SBRT)
- RT + chemotherapy
- RT with subatomic particles
- RT + radiosensitizers
- RT + pro drugs switchable with neutrons
- Gliasite

RT plays a key role in the treatment of glioblastoma. With surgery alone, few patients with malignant glioma survive more than 6 months, whereas postoperative RT significantly increases median survival to around 9-10 months for glioblastoma multiforme (GBM) and 36 months for anaplastic astrocytoma [1, 2].

The total radiation dose delivered plays a key role in prognosis. The standard dose for GBM is 60 Gy; the typical fractionation schedule is 2 Gy per day for six weeks of treatment. Below this dose, survival ranges from 8.9 months to 4.6 months. Dose escalation studies have shown that doses above 60 Gy do not produce any advantages in terms of progression free survival and only tend to worsen toxicity. Hypofractionated treatment (40 Gy in 15 fractions) increases the dose per fraction and shortens the total duration of treatment: it does not lead to an increase in survival, but it may be indicated in patients older than 60 years [3].

RT should begin as soon as possible, usually within 4-6 weeks after surgery. A recent retrospective analysis of the Radiation Therapy Oncology Group (RTOG) in 2855 patients with glioblastoma evaluated the impact on survival of a reduction in the time to RT treatment (after surgery) for less than 6 weeks. The study examined periods of 2 weeks, 2-3 weeks, 3-4 weeks and >4 weeks and showed no worsening of survival with increasing time, although RT always began no later than 6 weeks after surgery [4].

Diagnostic imaging with CT and MR is essential for defining the target volume and planning treatment. It is possible to merge images of MR and CT through dedicated software to allow a more precise outline of the target volume.

There are three types of target volume: the gross tumor volume (GTV), the clinical tumor volume (CTV) and the planning target volume (PTV). The GTV is defined as the surgical cavity and any residual disease visualized with contrast enhancement in T1-weighted images of postoperative MR; the CTV is defined as GTV plus an expansion margin of 2 cm where there may be infiltration of tumor cells; the PTV is represented by CTV plus an expansion margin of 1 cm.

When multiple lesions are present in both cerebral hemispheres, whole brain treatment is required with a reduced dose (45-50 Gy).

3D conformal treatment with conventional fractionation (2 Gy per fraction) is the standard, however alternative fractionation schedules have been investigated such as hypofractionation (40 Gy in 15 fractions) or hyperfractionation (72 Gy in 60 fractions in 1.2 Gy twice/day) [5]. These schedules have not always led to an improvement in survival.

Brachytherapy (internal RT) is delivered by placing radiation source(s) inside or next to the area requiring treatment. In brachytherapy, radiation sources are precisely placed directly at the tumor site. This means that the irradiation only affects a highly localized area and exposure to radiation of healthy tissues further away from the sources is reduced. These characteristics provide advantages over external beam RT: the tumor can be treated with very high doses of localized radiation, at the same time reducing the probability of unnecessary damage to surrounding healthy tissues.

This technique can be used as exclusive RT treatment or in addition to conventional external treatment. The feasibility of brachytherapy generally depends on tumor size (less than 5 cm in diameter), on its surgical accessibility and on the absence of metastasis. The most used isotopes are 125I, 192Ir and 203P, which are implanted into the tumor through a surgically placed catheter which is either removed after the procedure or left in place.

Gliasite is a novel treatment approach using intracavitary low-dose rate brachytherapy and has recently received considerable attention for the treatment of primary malignant gliomas. This device consists of an expandable balloon catheter (GliaSite Radiation Therapy System) which is placed in the resection cavity at the time of tumor debulking. Approximately 2 to 4 weeks after surgery, the balloon is filled with an aqueous solution of organically bound 125I for a predetermined amount of time during which a therapeutic dose of radiation is delivered to the edges of the surgical cavity.

Stereotactic radiosurgery (SRS) with LINAC consists in the administration of highly collimated beams of radiation through multiple non-coplanar arcs that intersect at a single point. This method involves the administration of the entire dose in a single session with a rapid fall of the dose to surrounding tissue. In this case an exact target definition is required as well as an appropriate system of patient immobilization.

Stereotactic radiosurgery is feasible for small unifocal tumors (up to 4 cm), metastases, tumors which are unreachable by surgery or recurrence especially in patients already receiving the maximum tolerable radiation dose. Survival is about 7-30 months at the cost of a possible toxicity. This RT technique requires a multidisciplinary team consisting of neuroradiologist, neurosurgeon, radiation oncologist and physicist.

Advanced methods are currently in use in clinical trials such as CyberKnife (real radiating scalpel) and TomoTherapy in order to further reduce the side effects of treatment and administer even higher doses.

The current standard of care for newly diagnosed glioblastoma is the widest surgical resection, followed by adjuvant RT (fractionated focal irradiation in daily fractions of 2 Gy given 5 days per week for 6 weeks, for a total of 60 Gy) plus continuous daily temozolomide (TMZ) (75 mg per m^2 of body-surface area per day, 7 days per week from the first to the last day of RT), followed by six cycles of adjuvant TMZ (150 to 200 mg per m^2 for 5 days during each 28 day cycle). The addition of TMZ to RT in newly diagnosed glioblastoma results in clinically and statistically significant survival benefits with minimal additional toxicity. The addition of TMZ to RT increases median survival from 12.1 months with RT alone to 14.6 months with RT plus TMZ [6, 7].

RT with heavy particles uses protons and heavy ions accelerated in a cyclotron. Currently, this method is still under study, but it seems that its main advantages are increased penetration with a more rapid drop in dose, high linear energy transfer and ability to deposit the entire energy of the beam in a small area.

RT may be associated with radiosensitizing drugs (such as bromodeoxyuridine) that interfere with DNA repair in cells exposed to radiation causing apoptosis.

RT with boron neutron capture (BCNT) is based on tumor cell irradiation with thermal neutron flux. The cells are previously treated with a target molecule (usually a metal with a large section of atomic absorption) to internalize boron. The advantages of this technique seem to be greater safety for healthy tissue, because neutron beams do not cause any damage unless they meet boron. The main disadvantage, however, is the high cost of these instruments, so they are only available in few centers.

The main problem of these tumors is the high incidence of recurrence especially within the field of treatment and the inability to deliver higher doses due to the risk of radionecrosis.

References

1. Walker MD, Alexander E, Hunt WE et al (1978) Evaluation of BCNU and/or radiotherapy in the treatment of anaplastic glioma: a cooperative clinical trial. J Neurosurg 49:333-343
2. Prados MD, Scott C, Curran WJ et al (1999) Procarbazine, lomustine and vincristine (PCV) chemotherapy for anaplastic astrocytoma: a retrospective review of radiation therapy oncology group protocols comparing survical with carmustine or PCV adjuvant chemotherapy. J Clin Oncol 17:2289-3395
3. Roa W, Brasher PM, Bauman G et al (2004) Abbreviated course of radiation therapy in older patients with glioblastoma multiforme: a prospective randomized clinical trial. J Clin Oncol 22:1583-1588
4. Blumenthal DT, Won M, Mehta MP et al (2009) Short delay in initiation of radiotherapy may not affect outcome of patients with glioblastoma: a secondary analysis from the radiation therapy oncology group database. J Clin Oncol 27:733-739
5. Nomiya T, Nemoto K, Kumabe T et al (2008) Prospective single-arm study of 72 Gy hyperfractionated radiation theraphy and combination chemotheraphy for anaplastic astrocytomas. BMC Cancer 16:8-14
6. Stupp R, Mason WR, Van Den Bent MJ et al (2005) Radiotherapy plus concomitant and adjuvant temozolomide for glioblastoma. N Engl J Med 352:987-996
7. Stupp R, Hegi M (2007) Methylguanine methyltransferase testing in glioblastoma: when and how? J Clin Oncol 25:1459-1460

Chemotherapy

4

Evaristo Maiello, Lucia Lombardi, Mario Brandi
and Tommaso Scarabino

4.1 General Findings

Chemotherapy involves the use of drugs in the treatment of brain tumors and can usually be taken in combination with other therapeutic approaches such as RT or surgery. There are currently no indications for chemotherapy prior to surgery.

Generally, drugs used include cytotoxins (substances that can kill cancer cells), hormones, steroids and radiosensitizing substances. Other products that are occasionally grouped in this category are called *biological response modifiers*, which are molecules normally produced by the body capable of regulating the activity of the immune system, and are therefore categorized as immunotherapeutic products.

Anti-cancer drugs may act in two distinct ways, either directly attacking cancer cells or killing them while replicating. However, these products are toxic to some types of normal cells and so cause the onset of some side effects which may be somewhat mitigated by a proper dosage. Due to the presence of different cell types within the tumor mass, a combination of multiple drugs is often used simultaneously.

High chemoresistance of glial tumors and the presence of BBB are the main obstacles that have slowed the application of chemotherapy in gliomas.

Experience in the field of chemotherapy of glioblastoma has not been particularly good over the years. Nitrosoureas, studied since the late 1970s, have long been the main drugs used for the treatment of glial tumors, both as adjuvant at the end of RT or at the recurrence or radiologic progression of disease in previously irradiated patients. Although individual phase II trials have reported significant response rates, several randomized trials have failed to demonstrate a significant impact on overall survival compared with RT alone. Subsequent meta-analysis demonstrated a statistically significant although slight advantage in patient survival with malignant glioma already treated with surgery. The absolute increase varies from 5 to 10% in two years.

4.2 Temozolomide

Only recently has the advent of temozolomide (TMZ) changed clinical practice of postsurgical glioblastomas. TMZ is an orally administered alkylating agent able to cross the BBB which is relatively well tolerated (low blood effects) and operative mainly in grade III tumors.

The standard protocol of treatment used around the world (Stupp scheme) involves postsurgical (within 6 weeks) RT for 6 weeks with or without concomitant treatment with TMZ (75 mg/m^2 per day), then 4 weeks after the interruption of chemotherapy/RT the treatment is resumed with adjuvant TMZ alone (150-200 mg/m^2 x 5 days/28 days x 6 cycles) [1]. In the course of concomitant therapy, prophylaxis with sulfamethoxazole/trimethoprim or pentamidine is recommended. In to the event of response to treatment by the end of 6 cycles, an extension of maintenance chemotherapy with TMZ for up to 12 cycles can be considered [2].

This scheme has proven better than RT performed alone and provides significant advantage in terms of survival. There is in particular an increase in median survival from 12 months to 14.6 months, but also an increase in the proportion of long-term survivors (26%

E. Maiello (✉)
Department of Oncology
Scientific Institute "Casa Sollievo della Sofferenza"
San Giovanni Rotondo (FG), Italy

at 2 years, 16% at 3 years, 10% at 4-5 years). A reduction in mortality by 37% and in disease progression by 46% was also documented.

In this study a tumor protein was also identified (methylguanine-methyltransferase - MGMT) that can approximately predict (and thus is useful in clinical practice) which patients will benefit from the combined protocol.

MGMT is an enzyme that repairs methylation damage caused by TMZ. Recent studies have enabled a group of patients to be selected that best takes advantage of TMZ treatment in the presence of the form of glioblastoma with methylated MGMT. In these patients, in fact, prognosis in terms of survival is greatly improved compared to non-methylated forms. With this test it is therefore possible to improve patient outcome.

Glioblastoma can develop resistance to alkylating drugs that carry out their action by altering the DNA, leading to apoptosis. Recent studies have shown that MGMT is playing a key role in this mechanism of resistance. Patients with methylation of this gene achieved a median survival of 21.7 months when treated with RT and TMZ against 15.3 months if they received only RT, whereas patients without gene methylation obtained with TMZ and RT a median survival of 12.7 months versus 11.8 months (RT alone) [3].

4.3 Other Drugs

Therefore, the Stupp system finds its indication after surgery. At the onset of recurrence/progression of disease after surgery and RT alone, the chemotherapy options are the following:

1. Reuse TMZ (150-200 mg/m^2 for 5 days every 4 weeks);
2. Use other drugs such as nitrosoureas (see fotemustine - FTM) with initial weekly dosing for 3 consecutive weeks and then, after 5 weeks, with thriceweekly administration with possible important bone marrow toxicity that can lead to the suspension of treatment;
3. Use anti-angiogenic drug bevacizumab (BEVA), anti-vascular endothelial growth factor antibody VEGF, suitable in glioblastomas that are known to be particularly vascularized tumors.

   The mechanisms of antitumoral action of BEVA are controversial. In particular, it is unclear whether and when BEVA induces hypoxia in gliomas. Normalization of tumor vasculature with decrease in tumor interstitial pressure improves access of cytoreductive drugs and then RT efficacy due to increased oxygen delivery. However, these drugs may rapidly restore the low permeability characteristics of the BBB and counteract the beneficial effect, so the results may be decreased therapeutic efficacy [4].

   Moreover, some important toxic effects are possible (hypertension, hemorrhage, arterial and venous thromboembolism), especially in combination with other chemotherapy drugs, although the results are better.

   Lastly, new chemotherapy techniques have been developed in malignant gliomas along with local radioimmunotherapy using biodegradable copolymer implants containing chemotherapeutic agents (BCNU, Gliadel Wafers), as well as techniques of convective distribution (chemotherapy, cytotoxic proteins, radiolabeled monoclonal antibodies).

   Treatment with BCNU wafers (Gliadel) in patients with malignant glioma subjected to surgery and postoperative RT results in a statistically significant increase in survival compared to patients treated with surgery and RT alone (13.9 months vs. 11.6 months, p=0.03). It should however be noted that this level of significance was reached by considering a subgroup of patients. When analyzing only patients with glioblastoma (n=101), the difference in survival was not significant [5].

References

1. Stupp R, Mason WR, Van Den Bent MJ et al (2005) Radiotherapy plus concomitant and adjuvant temozolomide for glioblastoma. N Engl J Med 352:987-996
2. Mason WP, Del Maestro R, Eisenstat D et al (2008) Canadian recommendations for the treatment of glioblastoma multiforme. Curr Oncol 14:110-117
3. Hegi ME, Diserens AC, Gorlia T et al (2005) MGMT gene silencing and benefit from temozolomide in glioblastoma. N Engl J Med 532:997-1003
4. Thompson EM, Frenkel EP, Neuwelt EA (2011) The paradoxical effect of bevacizumab in the theraphy of malignant gliomas. Neurology 76:87-93
5. Westphal M, Hilt DC, Bortey E et al (2003) A phase 3 trial of local chemotherapy with biodegradable carmustine (BCNU) wafers (Gliadel wafers) in patients with primary malignant glioma. Neuro-Oncology 5:79-88

Future Developments

5

Saverio Pollice, Gilda Morlino, Michela Capuano
and Tommaso Scarabino

5.1 General Findings

Despite many recent developments that have involved the diagnosis and treatment of these tumors, glioblastoma is the most aggressive glioma and its cure is in practice almost impossible.

Fixed points related to the treatment are:

1. The surgical approach remains the choice in the most radical way possible;
2. Combination chemotherapy-RT according to Stupp is the standard postsurgical treatment;
3. FTM is particularly active and well tolerated in recurrent glioblastoma;
4. BEVA is useful even though many questions remain.

Therefore a rapid response from research is needed to find new ways to treat these incurable diseases (targeted chemotherapy, immunotherapy, stem cell research in tumor tissue). In this context a multidisciplinary approach involving the surgeon, medical oncologist, radiation oncologist, neurologist and research in the field of biology is essential.

The main obstacle to the radical treatment of this disease is currently the inability to transfer molecular and therapeutic agents to each tumor cell. The future hope lies in vaccines, from neural stem cells or viral vectors as a vehicle for molecules, gene therapy, local antiproliferative and antiangiogenic therapies and the molecular approach (nanotechnology) which will hopefully improve the prognosis of these aggressive tumors.

5.2 Neural Stem Cells

Analysis of glioblastoma tissue has uncovered the mechanism of action of cancer stem cells. It has been shown that instead of recruiting healthy blood vessels to feed itself, glioblastoma creates its own network of blood vessels using stem cells that turn into endothelial cells lining vessel walls. Endothelial cells are normally delegated to the formation of blood vessels needed to supply oxygen and nutrients to our body. To confirm this assumption it was found that in most cases endothelial cells have the same genetic profile as the tumor cells, which means that this endothelium has a neoplastic origin. The formation of aberrant vessels (neoangiogenesis) is hosted not only in glioblastoma but also in other aggressive tumors.

This discovery may have important therapeutic implications because the identification of drugs that block this process could be an effective therapy for the treatment of these tumors [1].

Stem cells are important in the process of angiogenesis and cancer having mechanisms that allow themselves to overcome apoptosis and senescence. They are also able to self-renew and generate all cell strains. Cancer stem cells, in the same way as healthy stem cells, are able to generate tumors with the same histopathologic features of the tumor of origin. Hence the need to be extremely careful when transplanting human neural stem cells because they potentially have the ability to turn into cancer. For this reason, these cell lines are studied to understand why they become cancer.

S. Pollice (✉)
Department of Radiology
"L. Bonomo" Hospital, Andria (BT), Italy

5.2 Gene Therapy

Gene therapy involves the transfer of a therapeutic gene in a target cell. In the case of brain tumors, gene therapy appears as a typical example of local treatment, mainly because of locally recurrent behavior of GBM [2, 3].

Moreover, gene therapy may indicate manipulation of the genome of cancer cells. Gene transfer or manipulation of the genome involves the use of vectors to transfer genetic material. These vectors can be derived from plasmids or viruses and in the latter case, the viral genome is modified to prevent it being pathogenic. This can be achieved by preventing absolute vector replication (defective vector) or allowing a selective replication in tumor cells. This manipulation can be made using simple strands of DNA, for example oligonucleotides: in this case, the entry of DNA into the target cell is facilitated in different ways. In clinical practice, liposomes and artificial lipid vesicles are typically used, they may contain DNA and facilitate entry into the cell by merging with its plasma membrane.

5.3 Antiproliferative Therapy

These medications block telomerase enzymes, resulting in the reduction and inhibition of tumor growth. In particular, telomerase (found in glioblastomas) is an enzyme that rebuilds telomeres (the ends of chromosomes) when replicating. When a cell multiplies, telomeres divide until they reach a minimum length at which point they stop multiplying. In the absence of telomerase, the telomere is reduced gradually until the cell goes into senescence and dies. If the cell becomes a cancer cell, it must have telomerase, which rebuilds telomeres that allow itself to replicate, to overcome senescence and then to live. In studies concerning other types of tumors, experimental drugs such as Imetelstat (or GRN-163L) have been developed. These drugs are able to cross the BBB and thus block the action of telomerase in stem cancer cell and in tumor cells, killing them. The maximum effectiveness of these drugs is achieved by combining the administration of the molecule with RT and standard chemoterapy [4].

5.4 Vaccine

This technique is based on the use of dendritic cells, which are very powerful cells of the immune system present in the blood that, when modified in the laboratory and then reintroduced into the body, can attack and destroy cancer cells. One limitation is that they can only be used to treat donor cells.

References

1. Ricci-Vitiani L, Pallini R, Biffoni M et al (2010) Tumour vascularization via endothelial differentiation of glioblastoma stem-like cells. Nature 468:824-828
2. Chiocca EA (2003) Gene therapy: a primer for neurosurgeons. Neurosurgery 53:364-373
3. Rainov NG, Ren H (2003) Gene therapy for human malignant brain tumors. Cancer J 9:180-188
4. Marian CO, Cho SK, McEllin BM et al (2010) The telomerase antagonist, imetelstat, efficiently targets glioblastoma tumor-initiating cells leading to decreased proliferation and tumor growth. Clin Cancer Res 16:154-163

Part C

Post-treatment Neuroradiologic Imaging

Magnetic Resonance Techniques

6

Saverio Pollice, Teresa Popolizio and Tommaso Scarabino

6.1 General Findings

Each form of treatment alters the normal anatomy and structural framework of the region where it is administered. Therefore, the interpretation of images needs to be supported by a sound knowledge of anatomy, pathophysiology, drug compliance, radiotherapy and surgery, because the images represent the *digital translation* of the anatomic reality.

Neuroradiologic imaging after treatment has the role of documenting the anatomic condition modified by the iatrogenic event and the normal postsurgical changes in relation to type of surgical approach (sequelae). It also has the task of detecting the presence of complications and assessing the response to treatment with follow-up, in order to provide the surgeon (and/or radiation oncologist and/or medical oncologist) with detailed information about the surgical bed and adjacent structures involved.

In this setting, computed tomography (CT) and morphologic magnetic resonance (MR) are able in different ways and with different levels of sensitivity to translate the density changes in CT and signal changes in MR into neuropathologic macroscopic changes. However, these imaging modalities fail to detect cellular and subcellular changes. In contrast, functional MR (fMR), with its use of spectroscopy, diffusion, perfusion and cortical activation, is revolutionizing neuroradiology by overcoming the limitations of ultrastructure and in many cases making possible an earlier and more specific diagnosis.

S. Pollice (✉)
Department of Radiology
"L. Bonomo" Hospital, Andria (BT), Italy

6.2 Morphologic Magnetic Resonance Imaging

Under ideal conditions and thanks to its many advantages which include multiplanar and multiparameter features, excellent contrast resolution and noninvasiveness, MR is able to identify the lesion, define its precise location, propose treatment planning and monitor posttreatment. However, some cases can be difficult to interpret both for the neuroradiologist and the neuropathologist. The extreme heterogeneity of brain tumors and moderate specificity of MR may make difficult a clear *histologic diagnosis* which only in typical cases is simple. In MR imaging of glioblastoma, the solid part of the tumor shows hypointense signal in T1-weighted sequences and hyperintense in T2, with higher signal in areas of greater cellularity. Necrotic areas, which always appear hyperintense in T2, may be hypo-, iso- or hyperintense in T1 due to products of protein or hemoglobin degradation. Enhancement after administration of contrast medium is usually intense and irregular at the tumor margins and identifies the cellular *proliferation* component of the tumor. Punctate and serpiginous areas of no signal caused by flow associated with neovascularization are common. These newly formed pathologic vessels are devoid of blood-brain barrier (BBB), which explains both their marked enhancement and perilesional vasogenic edema, due to the passage of fluid in the extracellular space.

Morphologic MR is not always able to distinguish with certainty a tumor (persistence/recurrence) from the effects of surgical treatment, radiation therapy (RT) (radionecrosis) or chemotherapy (fake progression), such that monitoring with imaging is necessary for a clearer characterization.

The neuroradiologic follow-up protocol in treated patients usually includes the following MR examinations:

- within 2-3 days after surgery to evaluate the radicality of surgery;
- 30 days after surgery (often the first follow-up examination!);
- 30 days after completing treatment;
- every 3 months (high-grade gliomas) and every 6 months (low-grade gliomas) to evaluate tumor growth.

The MR study with and without contrast agent administration should include T2 and FLAIR sequences, best performed in 3D, generally in axial or coronal views, and T1-weighted sequences with and without contrast medium in the three planes in space. The preoperative MR study may be completed by MR angiography to clarify intratumoral circulation and thus enable improved planning of surgical treatment. In carrying out these studies, the examination technique should be standardized as much as possible. Ideally the same magnetic field, the same methods of examination and appropriate and readable imaging (often in relation to different centers) should be used. Correct use of contrast medium is especially important (correct dose, same type, optimal time delay in the acquisition).

6.3 Functional Magnetic Resonance Imaging

In many cases the MR morphologic study should be integrated with advanced *functional* MR techniques, which should become an integral part of a routine study. These techniques, which provide metabolic (spectroscopy), structural (diffusion) and hemodynamic (perfusion and cortical activation) information, improve the diagnostic accuracy, sensitivity and specificity of MR and supply a more accurate and comprehensive diagnosis to the surgeon [1-3]. Advanced MR techniques are able to provide a quantitative as well as a qualitative assessment. Generally, the use of quantitative methods (analysis by ROI and/or by histogram) is less subject to methodologic and sampling errors and it is easy to statistically analyze. Moreover, it enables the creation of common databases in various centers to provide greater statistical power to clinical trials and longitudinal studies. These studies are very useful in neuro-oncology; for example, diffuse tumor lesions are very difficult to differentiate from the surrounding healthy tissue, but they may instead be characterized by quantitative data, because the absolute value of alterations measured in the ROI is independent of the surrounding tissue.

6.3.1 Spectroscopy

Proton spectroscopy magnetic resonance (1H-MRS) is a noninvasive technique that provides information about the metabolic status of normal and pathologic tissue. The physical principle used in 1H-MRS is the *chemical shift* that varies according to differences in the precession frequency of atoms belonging to individual molecules (metabolites). By identifying these frequencies, different molecules may be identified to indirectly assess their spatial distribution and their concentration [4, 5].

The metabolic pattern may be acquired with a single voxel technique (with isolated VOI from conventional MR image) or multivoxel (with reconstruction of metabolic maps showing the distribution of metabolites for each individual slice of acquisition) [6].

The metabolites mostly involved in the diagnosis of gliomas include choline (Cho), creatinine (Cr), N-acetylaspartate (NAA), lactate (Lac) and lipids (Lip). Cho is considered a membrane marker, directly related with cellularity and proliferation index. Cr is a cellular energy metabolism marker and is often used as a benchmark in metabolite ratios. NAA is considered a neuronal marker, being present only in neurons, so it is indicative of morphofunctional integrity. Lac indicates the status of anaerobic conditions. Lip are related with necrosis, since their presence is due to the consumption of cell membranes.

In neuro-oncology a Cho/NAA ratio >2:1 is indicative of cell proliferation as observed in tumors. A reduction in the NAA and Cr peaks is common in glial tumors whereas the presence of Lac and Lip is an expression of the most malignant forms.

However, spectroscopy is not always definitive due to the common overlap and coexistence of different disease patterns [7]. Another important limitation of the method concerns lesions in proximity to the skull base which are difficult to study due to the magnetic susceptibility artifacts that these structures produce.

6.3.2 Diffusion

MR diffusion weighted imaging (DWI) is a noninvasive technique that studies the diffusion and random movement of free water molecules in the tissue being examined. Diffusion data are obtained with the use of par-

ticular sequences consisting in the application of additional gradients sensitive to molecular motion during a base sequence.

Diffusion imaging can be done in different forms with increasing complexity and are used in accordance with their requirements:

1. The diffusion-weighted (DWI) study is obtained by measuring the signal loss which is proportional to the diffusion coefficient of the substance and to the T2 relaxation time.
2. The apparent diffusion coefficient (ADC) map shows ADC voxel by voxel, the value of which describes the diffusivity of water molecules in the presence of factors that restrict it.
3. Diffusion tensor imaging (DTI) measures the diffusive motion of water molecules in at least six directions in space. This movement in the white matter is restricted by the orientation of nerve fibers, such that it is greater along the longitudinal axis of the fibers (anisotropy).
4. Tractography is the three-dimensional representation of nerve pathways.

Generally, useful information for tissue characterization may be obtained by considering the extent of diffusion of water molecules [8, 9]. The diffusion of water molecules varies with variations in tissue cellularity, because the higher the cellularity, the greater the number of cell membrane interfaces and therefore the lower the diffusion. DWI can therefore provide information especially about tumor cell increase, which causes a restriction of the extracellular space and thus hinders water diffusion in tissues.

ADC is reduced with inverse proportion to cellularity, which is one of the factors determining histopathologic grading. Accordingly, high cellularity malignant tumors have lower ADC values than those of benign low cellularity tumors.

Coexistence of vasogenic edema and tumor infiltration may affect the interpretation of the diffusion study. Peritumoral edema increases ADC values, masking its reduction determined by infiltration of tumor cells. Therefore, diffusion imaging alone cannot indicate the real extension of the tumor.

6.3.3 Perfusion

MR perfusion-weighted imaging (PWI) is a very useful noninvasive technique with rapid execution which measures microvascular tissue dynamics. Brain perfusion is increasingly used in tumor characterization. The perfusion parameters which can be measured include cerebral blood volume (CBV), mean transit time (MTT), cerebral blood flow (CBF) and the product of surface permeability times blood flow. In clinical practice the method used is usually based on variation in the characteristics of susceptibility in an ROI, obtained at the first step of intravenous bolus (usually at a rate of 5.0 mL/s - dose of 0.2 mL/kg) of a paramagnetic contrast agent (DSCE Dynamic Susceptibility Contrast Enhanced) during acquisitions of echoplanar (EPI) T2-weighted sequences [10].

In normal conditions there is signal intensity reduction at the passage of the bolus, while in pathologic conditions the signal varies in relation to the microvasculature density of the anatomic region examined. The most commonly used hemodynamic parameter is CBV, which varies in relation to the vascularization of the lesion with altered BBB.

In neuro-oncology, an increase in microvessel density and neovascularization (angiogenesis) is an essential histologic criterion for determining the biological malignancy of gliomas. An increase in CBV is one of the strongest predictors of tumor aggressiveness and survival in different histologic types [11-13], although it is not always synonymous with malignancy, e.g. oligodendroglioma and meningioma, which are characterized by high CBV but not by malignant behavior [14, 15].

An inaccurate estimation of CBV may be due to the presence of petecchiae in the setting of tumor recurrence which cause susceptibility artifacts or even in the presence of a disrupted BBB.

Similar information can also be obtained with CT perfusion after contrast injection (usually 50 mL) at a flow rate of 5 mL/s with the subsequent calculation of the permeability surface map (PS).

Information about hypervascularity is more important than information about BBB injury. In this regard it is essential not to confuse the presence of newly formed vessels without BBB that determine lesion enhancement and hypervascularity, responsible for increased CBV in perfusion studies, which provide information about neo-angiogenesis even in the absence of altered BBB. In fact tumor grade better correlates with an increase in blood flow than with BBB changes. In fact high-grade tumors may have high CBV without contrast enhancement (CE). Therefore, an absence of CE does not rule out malignancy.

Moreover, with the recent development of new therapeutic techniques aimed at reducing neo-angiogenesis (targeted chemotherapy and RT), PWI can take on a primary role in the simple and immediate evaluation of treatment efficacy.

6.3.4 Cortical Activation

Cortical activation (fMR) allows the mapping of functional activity of brain areas. With the blood oxygen level dependent (BOLD) technique and with acquisition of a large number of dynamic images, the changes in blood oxygen level can be quantified (endogenous contrast agent). These variations are induced by neuronal stimulation resulting in an increase in blood flow in a specific area and then a relative reduction in the concentration of deoxyhemoglobin (deoxyHb is a strongly paramagnetic substance able to shorten T2*). In BOLD fMR, changes in signal intensity of blood circulation are then determined by paramagnetic properties of deoxyHb.

Information obtained with this technique is useful especially in preoperative planning. The most common clinical application of fMR is in fact the presurgical identification of eloquent cortical areas and their relationship with the lesion in order to optimally guide the surgical decision (resection/biopsy) and to plan the best surgical approach to the lesion. The purpose of neurosurgery is in fact to maximize the resection of the lesion and at the same time preserve normal brain function as much as possible.

6.4 Multimodal Magnetic Resonance Imaging

The use of a single pattern of advanced MR imaging in the diagnosis of gliomas may not be enough to define the histologic grading, for optimal treatment planning and for appropriate post-treatment follow-up [16]. Combined studies are able to increase MR diagnostic accuracy. This is particularly important since recently developed new and more effective anticancer treatments require a complete morphofunctional MRI study to noninvasively obtain an *in vivo neuropathologic* evaluation and thus an interpretation of the biologic heterogeneity typical of these tumors.

These advanced techniques are used for qualitative and quantitative assessment. Quantitative data, especially when combined, provide some real biomarkers which are important for the characterization of tumor tissue. Only by combining data from various different imaging techniques is it possible to obtain essential information able to provide real clinical benefits in patient management.

6.5 High-field Magnetic Resonance Imaging

1.5 Tesla MR has long been considered the criterion standard for the study of all body areas. In fact, major technologic improvements have made 1.5 T MR a very powerful and versatile technique such that it can be used in clinical studies of CNS disease. Until recently, higher field MR was used exclusively for research and not for clinical purposes. 3T MR has since been used not only for research, but also for new and more sophisticated clinical applications, first of all with important benefits for neuroradiology. 3T MR provides adjunctive and more advanced diagnostic methods with excellent image resolution and a significant reduction in acquisition time thanks to the high field intensity and high power of the gradients [3, 8]. The best high field intensity advantage is certainly the improvement of the signal-to-noise ratio (SNR) which increases linearly with the main magnetic field, B0.

A high SNR in a 3T scanner makes it possible to perform a brain examination in the same time as a 1.5 T system while obtaining greater image quality. Similarly, a shorter examination time is needed to achieve the same image quality as a 1.5 T system (thus no change in matrix dimension), thus favoring patient comfort. The high SNR, which reduces the examination time, also makes it possible to use the saved time for performing additional morphologic and functional imaging sequences (diffusion, perfusion, spectroscopy, fMR) [3].

The benefits of a high field in morphologic imaging are improvement of contrast and spatial resolution with consequent better diagnostic performance and significant reduction in acquisition time.

In PWI magnetic susceptibility is increased in a higher magnetic field. In particular, compared to 1.5 T systems, the sensitivity of these studies improves with a lower dose of contras media [18].

In DWI, spatial resolution increases and it is also possible to study phenomena such as anisotropy or diffusion tensor that cannot be studied with 1.5 T systems.

Spectroscopy also benefits from a high field by an

increase in SNR and chemical shift resolution. This implies improved spectral resolution and the possibility of measuring both common metabolites (NAA, CHO, CRE) and lower concentration metabolites usually not measurable with 1.5 T MR systems [5].

High field MR provides its most important advantage in functional imaging, thanks to the increased effects of magnetic susceptibility which emphasize the BOLD effect and to an improvement in voxel spatial resolution. In this way, additional areas and submillimeter structures can be mapped in a short time. Moreover, it is possible to perform real time cortical activation during stimulation (real time fMR).

References

1. Al-Okaili RN, Krejza J, Wang S et al (2006) Advanced MR imaging in the diagnosis of intraaxial brain tumors in adults. Radiographics 26:5173-5189
2. Jenkinson MD, Du Plessis DG, Waljer C et al (2007) Advanced MRI in the management of adult gliomas. Br J Neurosurg 21:550-561
3. Scarabino T, Giannatempo GM, Popolizio T et al (2007) 3.0 T functional brain imaging: a five-year experience. Radiol Med 112:97-112
4. Howe FA, Barton SJ, Cudlip SA et al (2003) Metabolic profiles of human brain tumors using quantitative in vivo ^{1}H magnetic resonance spectroscopy. Magn Reson Med 49:223-232
5. Di Costanzo A, Trojsi F, Tosetti M et al (2007) Proton MR spectroscopy of the brain at 3 T: an update. Eur Radiol 17:1651-1662
6. Nelson SJ (2003) Multivoxel magnetic resonance spectroscopy of brain tumors. Mol Cancer Ther 2:497-507
7. Rock JP, Scarpace L, Hearshen D et al (2004) Associations among magnetic resonance spectroscopy, apparent diffusion coefficients, and image-guided histopathology with special attention to radiation necrosis. Neurosurgery 54:1111-1117
8. Kono K, Inoue Y, Nakayama K et al (2001) The role of diffusion-weighted imaging in patients with brain tumors. AJNR 22:1081-1088
9. Brunberg JA, Chenevert TL, McKeever PE et al (2005) In vivo MR determination of water diffusion coefficients and diffusion anisotropy: correlation with structural alteration in gliomas of the cerebral hemisferes. AJNR 16: 361-371
10. Barbier E, Lamalle L, Decorps M (2001) Methodology of brain perfusion imaging. J Magn Reson Imag 13:496-520
11. Leon SP, Folkerth RD, Black PM (1996) Microvessel density is a prognostic indicator for patients with astroglial brain tumors. Cancer 77:362-372
12. Covarrubias DJ, Rosen BR, Lev MH (2004) Dynamic magnetic resonance perfusion imaging of brain tumors. Oncologist 9:528-537
13. Chaskis C, Stadnik T, Michotte A et al (2006) Prognostic value of perfusion-weighted imaging in brain glioma: a prospective study. Acta Neurochir 148:277-285
14. Lev MH, Ozsunar Y, Henson JW et al (2004) Glial tumor grading and outcome prediction using dynamic spin-echo MR susceptibility mapping compared with conventional contrast-enhanced MR: confounding effect of elevated rCBV of oligondendrogliomas. AJNR 25:214-221
15. Hakyemez B, Erdogan C, Bolca N et al (2006) Evaluation of different cerebral mass lesions by perfusion-weighted MR imaging. J Magn Reson Imag 24:817-824
16. Scarabino T, Popolizio T, Trojsi F, et al (2009) Rule of new advanced MR imaging modalities in the diagnosis of cerebral gliomas. Radiol Med 114:448-60
17. Salvolini U, Scarabino T (2006) High field Brain MRI. Use in clinical practice. Springer, Heidelberg
18. Di Costanzo A, Pollice S, Trojsi F, et al (2008) Role of perfusion-weighted imaging at 3 Tesla in the assessment of malignancy of cerebral gliomas. Radiol Med 113:134-143

Postsurgical Morphologic MR Imaging

7

Ferdinando Caranci, Saverio Pollice and Tommaso Scarabino

7.1 General Findings

The postsurgical neuroradiologic study is designed to assess physiologic (normal sequelae), or pathologic changes (complications). In addition, the study should also evaluate, although this is more difficult, the presence of any residual disease after surgical resection of the mass. Subsequently, periodic monitoring is required to follow the course of the disease and to assess if progression or recurrence occur. Knowledge of the type of surgical approach and procedures performed is necessary to better interpret postsurgical neuroradiologic findings and to clarify their meaning.

7.2 Postsurgical Sequelae

Normal postsurgical sequelae can be divided into early and late changes. Early changes include bone alterations in relation to the type of surgical approach (craniotomy or craniectomy), extracranial soft tissue alterations at the site of surgical access (edema, swelling, air component) and condition of the surgical bed (edema, blood or air component). Normal late sequelae include scar tissue at the surgical bed, *ex vacuo* dilatation of adjacent structures with retraction of ventricular spaces and cavitation bounded by a gliotic wall. Partial or total recalcification of the bone flap may also be present at the craniotomy.

Postsurgical pathologic complication can also be divided into early and late changes. Early complications include malposition of the bone flap, drainage tubes, cerebro-spinal fluid (CSF) shunts, reconstruction patch, surgical scar infection, edema-ischemia of brain tissue surrounding the surgical bed and the presence of extracerebral hematomas from torn tumor vessels.

Late pathologic changes include infectious complications (scar suppuration, osteitis and osteomyelitis), subdural empyema, meningitis, ventriculitis and cerebral abscesses. In these cases the diffusion weighted imaging (DWI) is essential for diagnostic purposes, as it shows a significant reduction in diffusion coefficients.

Other possible complications include CSF rhinorrea secondary to breaks in the skull base, resulting in the passage of CSF in nasal cavities (CSF fistulas), and subgaleal CSF collections due to craniotomy.

Hydrocephalus is another important complication, which is usually caused by a blockage of the CSF pathways, by hemorrhage or tumor spread along the pathways themselves.

7.3 Neuroradiologic Imaging

Normal and pathologic findings can be documented, especially in the early stage after surgery, with CT thanks to its easy access (even in uncooperative patients requiring intensive care), its high sensitivity to recent bleeding, rapid execution and low costs. The CT study performed in the early stage can easily show the presence of bone changes (malposition of bone flap in particular) and soft tissue swelling, as well as it provides information about the surgical bed, such as the presence of air and blood.

Moreover, CT can provide information about early complications that sometimes require a second-look surgery. In particular, bleeding is the most common postoperative complication and it is characterized over

F. Caranci (✉)
Diagnostic Imaging Department, Unit of Neuroradiology, Federico II University, Naples, Italy

time by different imaging signs which are easily demonstrable at CT (especially in the acute phase).

Sometimes, however, CT is not enough, especially when clinical deterioration cannot be explained.

MR is used primarily in cases of disagreement between CT findings and clinical symptoms.

In particular, in the early stage MR shows the presence of ischemic changes surrounding the surgical bed, especially using DWI [1]. Ischemic areas may be caused by pathologic disruption of medullary vessels, by shrinkage of brain tissue or even by compression of small vessels at the resection margins. This occurs mainly in the removal of supratentorial tumors (in 60% of patients treated for glioblastoma it appears within 72 hours) as a result of direct surgical trauma. Clinically, ischemia is associated with new neurologic deficits, which nonetheless improve within a few days. This finding, which should not be confused with residual tumor, shows contrast enhancement (CE) in the subacute phase and then evolves into brain cavitation.

MR is used moreover in late assessment, with the possibility of providing more diagnostic information about tumor progression and prognosis, thanks to its superior contrast resolution and better tissue characterization. In these cases it is useful to associate functional studies with baseline MR imaging.

Association with advanced techniques (diffusion, tractography) contributes to the assessment of complications and of the integrity of white matter tracts [3].

MR imaging is able to accurately assess the evolution in scar tissue or cavitation of the surgical bed and to define the physiologic changes that occur over time: reabsorption of air content and then of hemorrhagic component (in variable times depending on the initial extent of hemorrhage). Subsequently CE of reactive tissue disappears, while meningeal enhancement lasts longer.

A major issue is the identification of residual cancer, which may or may not present pathologic enhancement. In cases of neoplastic lesions without enhancement, the MR diagnosis of residual tumor is based on morphologic criteria, through precise and accurate comparison between pre- and postsurgical imaging and knowledge of the treatment performed.

Usually, serial MR controls allow the course of the disease to be followed and then show the presence of possible progression/recurrence. Rarely, fMR may be necessary to confirm the diagnosis.

In case of neoplastic lesions with pathologic enhancement, CE morphology may be helpful. Typically, enhancement >1 cm or clearly nodular is indicative of residual tumor, while linear enhancement is generally due to transient blood-brain barrier (BBB) changes.

Therefore, CE due to residual tumor must be distinguished from enhancement of the surgical bed margins caused by the iatrogenic effect of surgery on the BBB. This benign and reactive enhancement does not appear immediately, because BBB injury is small or absent within 48-72 hours after surgery. At this stage, a CE MR T1-weighted sequence generally does not demonstrate enhancement, although earlier enhancement has been described after the surgical resection of highly vascularized tumors. Therefore, contrast enhancement in early postoperative MR (within the first 24 hours) is usually neoplastic. This period represents the *diagnostic window* for the relief of any residual tumor. Assessment of postsurgical residual performed at this stage is highly important, since its size is a considerable prognostic factor that influences the subsequent treatment.

On the 4th-5th post-operative day, injury to the BBB appears as linear enhancement along the edges of the surgical cavity, which usually disappears after 1-3/6-8 months, but in some cases it may persist for one year or more [2, 3]. An earlier disappearance of CE along the surgical margins may be due to steroid therapy, while the persistence for years is due to the replacement of granulation with collagen tissue.

The CE pattern makes it possible to distinguish surgery with a radical outcome, characterized by the absence of enhancement in early postoperative studies, from surgery with incomplete tumor removal, which is usually characterized by variable nodular or rim enhancement [4]. Considering these findings, total resection, subtotal resection (with residue less than 10% of the original mass) and partial resection (with residue more than 10%) can be distinguished. The interpretation of MR findings is often hampered by the presence of blood: in these cases it is difficult to differentiate blood from pathologic CE, except in presence of areas of nodular enhancement.

MR assessment in later phases, associated with advanced techniques, is able to study the presence of possible tumor recurrence.

References

1. Ulmer S, Braga TA, Barker FG et al (2006) Clinical and radiographics features of peritumoral infarction following resection of glioblastoma. Neurology 67:1668-1670

2. Ren A, Gao P, Sun Y (2002) Correlation of MR imaging and histopathology after partial resection of normal rabbit brain. Chin Med J 115:247-253
3. Lazar M, Alexander AL, Thottakara PJ et al (2006) White matter reorganization after surgical resection of brain tumors and vascular malformations. Am J Neuroradiol 27:1258-1271
4. Ekinci G, Akpinar IN, Baltagioglu F et al (2003) Early-postoperative magnetic resonance imaging in glial tumors: prediction of tumor regrowth and recurrence. Eur J Radiol 45:99-107

Post Radiation-therapy Morphologic MR Imaging

8

Mario Muto, Saverio Pollice and Tommaso Scarabino

8.1 General Findings

Radiation therapy (RT) is responsible for cellular damage that affects not only cancer cells but also healthy brain and endothelial cells causing toxic effects on enzyme systems. These effects continue in the targeted organ for many months to reach the optimal performance after at least 3-6 months and in some cases, years after the end of treatment, although effects on healthy cells persist over time. In many cases post-RT alterations are associated with concomitant chemotherapy changes which strengthen the harmful effect.

8.2 Neuroradiologic Imaging

In post-RT, the diagnostic options available include CT, which is currently underused in follow-up, and especially morphologic and functional MR, (diffusion, perfusion, spectroscopy, cortical activation). PET has lost much ground with the advent of new advanced MR techniques.

These studies should first be performed within 24-36 h after surgery to obtain early information useful to minimize doubts in subsequent patient evaluation. Regular follow-up examinations are then necessary in relation to the clinical conditions of the patient and histologic findings in order to evaluate the presence of residual tumor or recurrence, and especially the typical changes brought about by RT, which is often associated with chemotherapy.

M. Muto (✉)
Department of Neuroradiology
"Cardarelli" Hospital, Naples, Italy

The CNS effects of RT can be divided into:

1. Acute complications occurring during treatment or shortly after the end of treatment, usually transient and reversible, caused by edema and BBB alterations. The clinical presentation varies according to the extent of edema, and symptoms are usually those of a mild intracranial hypertension which responds to steroid treatment. MR can be negative or may show small hyperintense signal changes in T2 and FLAIR sequences in the white matter of both hemispheres.
2. Sub-acute complications that appear from 3-6 weeks to 3 months, sometimes reversible, but unfortunately often permanent. These are characterized by toxic effects to the endothelium resulting in increased capillary permeability and thus onset of edema, as well as oligodendrocyte damage and subsequent demyelination. Wallerian degeneration is not infrequent and may progress in a retrograde fashion from the site treated to deeper areas and affect axons and their myelin sheaths. The clinical presentation is quite variable: patients may be asymptomatic or present a worsening of neurologic symptoms (intracranial hypertension, dysphagia, dysarthria). Sometimes steroid drugs are administered to control symptoms. MR shows regions of edema in white matter of both hemispheres, in the basal ganglia and cerebral peduncles in the form of areas of T2 and FLAIR signal hyperintensity.
3. Late complications are evident from 3 months up to 10 years (70% in 2 years), are progressive and irreversible, and are characterized by endothelial damage that can lead to a series of pathologic conditions: lacunar infarcts, occlusion of major vessels, vascular malformations (cavernous angioma, telangiectasia), visual pathways necrosis, leukoencephalopathy and focal necrosis. Generally they are quite common

where RT is administered with medium-high doses for each fraction, with large irradiation fields and when radiosensitizers are administered simultaneously. In the presence of combined RT and chemotherapy, determining which is responsible for the damage can be difficult. Symptoms are characterized by difficulty in walking, mnesic deficits, behavior problems, disorientation and coma. MR shows extensive confluent T2 and FLAIR hyperintense areas in the periventricular white matter of both hemispheres and cerebral atrophy.

Although these sequelae in relationship to the time of onset are schematically divided into acute, subacute and late, it is reasonable to assume that they are the result of a dynamic process which, according to the case (patient condition, immune status, integrity vascular tissue, methods of RT used), may terminate leaving only a scar or progress until tissue necrosis.

Pathophysiologic mechanisms in RT-induced CNS lesions depend on the total dose delivered, type of fractionation, the amplitude of the field, the possible combination with chemotherapy, the age of the patient and the duration of survival. In addition, the pathophysiologic mechanisms are thought to include vascular endothelial injury, glial and white matter damage, effects on fibrinolytic enzyme system and immune mechanism.

Whereas in acute vascular lesions there is a transient vasodilatation and vasogenic edema that may regress, in the late phase there is endothelial damage with vasogenic/cytotoxic edema, appearance of ectasia-telangiectasia, hyalinosis of vessel walls that leads to thickening with thrombosis until necrosis. These events can be evaluated by imaging.

In glial and white matter RT injury oligodendrocyte injury with demyelination occurs. Fibrinolytic system injury leads to the emergence of cytotoxic edema with necrosis of tissues. Immune-mediated mechanism results in auto-immunoglobulin response with tissue damage and release of normally segregated substances.

Histopathologic radio-induced changes are divided into:

1. Early, occurring at the molecular level. These are investigated in experimental animals but have no equivalent in diagnostic imaging. These changes may lead to early induction of genes, apoptosis, inhibition of neurogenesis, hypoxia, white matter necrosis and BBB injury.
2. Late, influenced by many variables (dose, fractionation type, individual response, etc). These are studied in vivo with diagnostic imaging. Endothelial injury may lead to a hyalinization, fibrinoid necrosis, thrombosis and thus focal necrosis, diffuse white matter alterations, atrophy, mineralizing microangiopathy, telangiectasia, optic neuritis and large vessel wall damage. Late alterations may also lead to DNA damage, repair mechanism damage, changes in oncogene expression and then induction of delayed cancer [1].

The criteria for validating the relation between radiation delivered and induced tumor include the irradiated area, histologic type different from the primary tumor, time elapsed since treatment, and increased incidence of induced tumor type compared to the general population.

RT-induced damage can be focal (radionecrosis, lesion with pathologic CE) or diffuse (disseminated or necrotizing leukoencephalopathy). There are also several rarer forms: 1) radionecrosis of the cranial nerves characterized by perineural CE and subsequent atrophy [2]; 2) mineralizing microangiopathy typical in pediatric-age patients and characterized by calcium deposits in the putamen and at the border between the basal ganglia and perforating cortical arteries.

Leukoencephalopathy clinically manifests as abnormal deambulation, urinary incontinence and cognitive slowing. Its incidence described in the literature is widely variable. MR shows focal or diffuse (disseminated form) signal alterations of the periventricular white matter, associated with subsequent cerebral atrophy and enlargement of peripheral and ventricular CSF spaces with an *ex vacuo* mechanism. The necrotizing form is more extensive and progressive, due to the combined effects of RT and chemotherapy. In addition to typical scattered and confluent white matter alterations, the lesions may present CE, small hemorrhages or calcification. The differential diagnosis with disease progression is difficult both clinically and radiologically.

Focal necrosis of the CNS is one of the major problems that occurs after RT. Its incidence is variable (5-24%) in relation to various risk factors such as total dose of radiation, radiation field, number and frequency of doses, and age at the time of treatment. It may occur as a result of treatment of intracranial tumors, extracerebral lesions (meningiomas) and extracranial (e.g. nasopharynx, paranasal sinuses, pituitary tumors). It can develop months or years after the completion of RT due to a mechanism of damage which is not yet clear. Several theories have been proposed: direct injury

to irradiated brain tissue, vessel damage, autoimmunization, and free radical cellular damage. The latter two hypotheses usually involve chronic and late damage of irradiated tissue.

Most of the time it is progressive and irreversible and it may require surgery to reduce the mass effect and edema. In this case recurrent radiation necrosis may be observed. At other times it can stabilize or regress.

Radionecrosis tends to occur in white matter, especially in periventricular areas (sparing subcortical arcuate fibers), usually around vessels with a pattern characterized by a necrotic center with no residual tumor, surrounded by a larger area consisting of fibrinoid necrosis of arterioles, telangiectasia, glial proliferation and lymphocytic infiltration. It develops at the site of treated cancer, even after whole brain irradiation due to the sensitizing effect of edema.

Clinically, symptoms are those produced by an expansive lesion. In addition, it may lead to focal neurologic deficits and intracranial hypertension. Treatment involves steroid therapy or surgical resection.

Conventional MR and CT findings are nonspecific. The most common pattern consists of an expansive formation with edema and mass effect, often with bleeding. Usually there is rim enhancement produced by vasogenic edema of moderate intensity with possible subsequent necrosis. CE can also be nodular, linear or curved, single or multiple, with dimensions which may remain stable or progress. An increase in size with associated edema and mass effect is suggestive of progression in radionecrosis.

The differential diagnosis with tumor recurrence is important since the location of the lesion is adjacent to the treated tumor and CE is present (sometimes mimicking secondary lesions), often increasing in size over time, with edema and consequent increase in the mass effect. Multiple lesions may be observed, or lesions in the contralateral hemisphere or subependymal lesions which can therefore mimic metastatic lesions, multifocal glioma or multiple sclerosis.

The literature reports cases of a *Swiss cheese* appearance characterized by extensive enhancement of peripheral white matter, involving subcortical "U" fibers with multiple small internal foci of necrosis. This is caused by diffuse necrosis involving both white matter and cortex.

Current conventional diagnostic methods available for the differentiation between recurrence and radiation necrosis are not always definitive, even though spatial and temporal patterns can help in solving doubts and suggest the hypothesis of radionecrosis in the presence of:

- a nonenhancing lesion prior to surgical treatment that subsequently develops CE internally or peripherally;
- an enhancing lesion that develops after primary glioma;
- an enhancing lesion that develops in the periventricular white matter, involving the corpus callosum;
- an enhancing lesion with the *Swiss cheese* appearance.

Therefore, marked tumoral tissue heterogeneity and changes induced by various therapies often make the differentiation between recurrence and necrosis difficult. In fact it is hoped that specific biomarkers will be discovered in the future. In this context, however, *advanced* MR techniques (in addition to morphologic studies) and follow-up have an important role to play.

References

1. Edelman RR, Hesselink JR, Zlatkin MB et al (2006) Clinical magnetic resonance imaging. Saunders, Philadelphia
2. Kumar AJ, Leeds NE, Fuller GN et al (2000) Malignant gliomas: MR imaging spectrum of radiation therapy – and chemotherapy-induced necrosis of the brain after treatment. Radiology 217:377–384

Post Chemotherapy Morphologic MR Imaging

9

Teresa Popolizio, Saverio Pollice and Tommaso Scarabino

9.1 General Findings

Neurotoxicity of drugs is a pathologic condition which is on the rise due to both the wider use of specific antiblastic therapies and the improved clinical and neuroradiologic performance that allow early and specific diagnosis.

Chemotherapy is often carried out with a combination of drugs and may be neurotoxic, especially when associated with RT, such that RT should only be used after chemotherapy. It has been shown that the damaging effects on the endothelium induced by brain irradiation can promote BBB alterations and allow the passage and retention of molecules which are potentially damaging to brain structures. Polychemotherapy treatment in combination with RT can result in toxicity and it is very difficult and even impossible in many cases to accurately establish the injury being caused by each treatment, as in most cases they are radiologically similar. There are, however, typical radiation-induced and/or chemotherapy-induced effects which must be recognized not only for evaluating the effectiveness of treatment, but also for applying effective and timely treatment.

9.2 Neuroradiologic Imaging

While RT and neurosurgical procedures morphologically modify the target tissue, drug treatments act *at a distance* and can cause organ damage and toxicity even in tissues not directly targeted by the treatment. Therefore, brain MR should be included in the follow-up of patients undergoing chemotherapy. Morphologic MR should be performed before beginning neurotoxic therapy, to provide the neuroradiologist with a reference for follow-up and to define and clarify doubts and problems on the findings observed. Exact knowledge regarding the pre-drug treatment imaging is even more important in the follow-up of neoplastic brain disease treated primarily with surgery. In these cases, MR with gadolinium performed within 2–3 days after surgery is the neuroradiologic reference.

Combined temozolomide (TMZ) and RT treatment in patients with glioblastoma must be carefully evaluated. In these cases, combination therapy may produce the appearance in MR images of lesions with a progressive development and appreciable as CE areoles. These lesions tend to appear immediately after the end of treatment (usually at 30 days after treatment) and may persist for up to three months and sometimes longer. These findings, known as *pseudo-progression*, are almost indistinguishable from real disease progression and are found in approximately 22–31% of cases [1-3]. Therefore caution is recommended in the assessment of neuroradiologic examinations carried within a month after the end of combination therapy.

Pseudo-progression is caused by the destruction of many tumor and endothelial cells, which results in the necrosis of the neoplastic lesion and an increase in BBB damage. These findings occur more frequently and earlier with combination treatment than with RT alone. These lesions decrease in size over time or become stable without additional treatment. Often they remain clinically asymptomatic and sometimes can explain clinical deterioration following completion of chemotherapy. Simple MR follow-up can readily dif-

T. Popolizio (✉)
Department of Neuroradiology
Scientific Institute "Casa Sollievo della Sofferenza"
San Giovanni Rotondo (FG), Italy

ferentiate between pseudo-progression and real progression based on the evaluation of changes over time. Moreover, a hypothesis of pseudo-progression rather than true clinically asymptomatic progression, especially in the first three months after the end of chemotherapy, should recommend the continuation of adjuvant therapy with TMZ.

This phenomenon, which is presumably related to radionecrosis, is correlated with the methylation of the MGMT gene which encodes the 06-methylguanine-DNA methyltransferase enzyme. This enzyme is able to repair the alkylating induced damage and thus protect the tumor cell. Conversely, if MGTM is methylated (inactive), chemotherapy appears to be effective.

On the basis of current scientific knowledge, determining the methylation status of the MGMT gene should be performed in all clinical trials on malignant gliomas involving the use of alkylating drugs. In daily clinical practice outside of clinical trials the methylation status of the MGMT gene is not currently validated as a decision parameter in the choice of the diagnostic and therapeutic pathway [4].

Assessment of the response to chemotherapy should take into consideration the radiologic findings, the clinical conditions of the patient, the type of treatment and the use of steroids [5]. Based on a thorough patient history, clinical examination and neuroradiologic study, four evaluations are possible:

- complete remission: characterized by the disappearance of CE in the tumor on consecutive CT scans or MR images performed at least 4 weeks apart in the absence of steroid therapy and with improved or stable clinical conditions;
- partial remission: characterized by a reduction of at least 50% of CE tumor area measured by the product of the two largest perpendicular diameters, in the presence of stable or reduced steroid therapy and with improved or stable clinical conditions;
- progression of disease: characterized by an increase of 25% of CE tumor area or the appearance of new tumor in the presence of stable or increased steroid therapy and deteriorated clinical conditions;
- stable disease: characterized by stability of the neuroradiologic status compared to the reference examination performed at least two months after starting treatment.

Moreover, not always is there direct correspondence between MR findings and clinical conditions and in some cases it is not possible to discriminate between tumor recurrence and radio-induced injury. Therefore, it is very important to correlate neuroimaging data with the patient's clinical condition, the time between the treatment and characteristics of the therapy.

Morphologic MR and functional studies (spectroscopy, DWI and PWI) are playing a leading role in the evaluation of neuroradiologic findings such as pseudo-progression and in the assessment of response to anti-angiogenic therapy which reduces the amount of CE. In this regard, spectroscopy is considered useful for measuring the true extent of neoplastic tissue, for evaluating the response to chemotherapy, for the early detection of recurrence and in the differential diagnosis between radio-necrosis and progression\recurrence.

The neurotoxic effects caused by drugs used in extracranial neoplastic diseases or in lymphoproliferative, hematologic and not tumoral disorders would require a chapter of their own. In this regard important agents include methotrexate, used in the treatment of leukemia, L-asparagine used in acute lymphocytic leukemia, 5-fluoro-uracil, cyclosporin A, vincristine, capecitabine, cytarabine, cisplatin, steroids and other drugs like morphine and amphetamines.

The combination of several drugs can strengthen the toxic effects of each, as in the combination of methotrexate and cisplatin. The neurotoxic effect is further amplified by superselective intra-arterial or intrathecal administration (e.g. methotrexate in chemical meningitis) of some drugs, used in the treatment of primary brain tumors or lymphoproliferative disorders. Neurotoxic effects are also favored by other predisposing factors such as cerebrovascular disease and advanced age; in these cases neurotoxicity may manifest in ischemic stroke, hemorrhage or acute edema, conditions which often are reversible. Alterations of peripheral blood counts (patients with leukemia or lymphoma) can promote a synergistic negative effect and induce intracranial hemorrhage. The effects of neurotoxic drugs (isolated or associated with RT) according to their onset over time are distinguished in:

1. Acute: occurring during treatment or within a maximum of 50 days from the end of therapy.
2. Subacute or delayed; occurring after treatment and within 3 months after the end of therapy.
3. Late: arising as much as several years after treatment.

Acute and subacute forms may be reversible while late effects leave permanent damage.

Acute effects include:

- stroke-like forms. Methotrexate is the most com-

monly involved drug. The likely cause of brain damage is an increase in blood homocysteine concentration which is thought to induce a direct detrimental action on the cerebrovascular endothelium. Symptoms are stroke related and the prognosis depends on the timeliness of treatment;

- acute thrombosis of the dural sinuses. L-asparaginase is the most commonly involved drug. The etiology is based on a direct action on coagulation. Symptoms include headache, convulsions and coma. The prognosis depends on the timeliness of treatment;
- posterior reversible encephalopathy syndrome (PRES). This syndrome, which was first recognized in association with eclampsia, cyclosporine therapy after transplantation and severe hypertension, is a complex drug-induced neurotoxicity, with well-defined clinical and neuroradiologic findings. It can also promote myocardial ischemia and hemorrhage. The most important feature of the syndrome is bilateral and symmetrical edema which mainly involves the parietal and occipital lobes, followed by the frontal lobes, the temporal-occipital junction and the inferior cerebellum. There are two pathogenetic mechanisms describing this syndrome, and both support the vasogenic hypothesis of edema. The first and more reliable considers hypoperfusion to be the cause of disease, determined by alternation of vasospasm and vasodilatation, as documented by MR angiography in eclampsia. The second theory supports the etiopathogenetic role of hyperperfusion secondary to dysregulation of blood pressure and capillary vasodilatation, which results in a malfunction of the BBB and extravasation of macromolecules and fluid in the interstitium.

Vasogenic edema, related to endothelial dysregulation, was also evidenced as a result of immunosuppressive treatment and drug-induced hypomagnesemia. MR imaging typically shows focal regions of bilateral and symmetrical edema with signal hyperintensity in long TR sequences. These findings have no correspondent in DWI imaging, except in untreated cases in which hyperintense signal areas appear due to progression in cytotoxic edema, which sometimes is irreversible. In this sense, DWI can be considered as a means for prognostic evaluation.

Subacute effects include delayed leukoencephalopathy with stroke-like presentation syndrome. This is a rare pathologic condition caused by methotrexate with intrathecal administration. Its etiology is based on direct endothelial damage. Symptoms mimic a cerebrovascular accident, and they may be fluctuating with alternating involvement of both hemispheres. Prognosis is related to the timeliness of treatment. MR imaging is characterized by T2-weighted focal signal hyperintensity especially in periventricular areas (semi-oval center, corona radiata, internal capsule) that do not show a clear correspondence in DWI imaging, while they are markedly hypointense on ADC maps, with rapid normalization. Increased signal in T2-weighted sequences with no correspondent in DWI could be due to the accumulation of water between myelin sheaths, a condition readily reversible if treated promptly. There is no CE.

Late effects include leukoencephalopathy. This is usually persistent (may be transient in children), and is drug and dose dependent. It is characterized by axonal and myelin loss, pallor, rarefaction, spongiosis and gliosis of white matter probably secondary to chronic ischemia caused by extensive radio-endothelial damage. The preferred site is periventricular white matter and semi-oval centers, even though compromise of all deep and subcortical white matter is not rare. Axonal loss is thought to be responsible for serious and irreversible clinical conditions, characterized by progressive deterioration and worsening of executive functions which may result in dementia.

Initial symptoms are often misunderstood or overlooked, especially because they affect patients already clinically compromised by the underlying disease. Generally, confusion and short-term memory loss can be seen initially, whereas later symptoms may include urinary incontinence, dysphasia, aphasia and visual disturbances. In the most severe forms, there may be dementia caused a dysfunction of the associative pathways.

On T2-weighted FLAIR images, signal hyperintensity appears in the subcortical white matter and especially in deep periventricular and retrotrigonal areas. These findings are not evident on DWI. Generally there is no CE, except in rare cases of punctate enhancement, which is usually reversible.

References

1. Brandes AA, Franceschi E, Tosoni A et al (2008) MGMT promoter methylation status can predict the incidence and outcome of pseudoprogression after concomitant radiochemiotherapy in newly diagnosed glioblastoma patients. J Clin Oncol 26:2192-2197
2. Brandsma D, Stalpers L, Taal et al (2008) Clinical features, mechanisms, and management of pseudoprogression in ma-

lignant gliomas. Lancet Oncol 9:453-461
3. Sanghera P, Perry J, Sahgal A et al (2010) Pseudoprogression following chemoradiotherapy for glioblastoma multiforme. Can J Neurol Sci 37:36-42
4. Stupp R, Hegi M (2007) Methylguanine methyltransferase testing in glioblastoma: when and how? J Clin Oncol 25:1459-1460
5. Macdonald DR, Cascino TL, Schold SC et al (1990) Response criteria for phase II studies of supratentorial malignant glioma. J Clin Oncol 8:1277-1280

Advanced MR Imaging

10

Teresa Popolizio, Saverio Pollice and Tommaso Scarabino

10.1 General Findings

The MR morphologic study, consisting of the acquisition of sequences without and with contrast agent, can be completed with new advanced MR techniques (spectroscopy, diffusion and perfusion), which are particularly useful in cases of diagnostic doubt. These techniques are not usually used in the evaluation of normal and pathologic sequelae after treatment, as these can be well documented with morphologic MR, but they become essential especially in combination when assessing treatment response. Their use is often essential in the differential diagnosis between scar tissue vs. residual tumor, stability vs. progression/recurrence and recurrence vs. radionecrosis.

10.2 Role of Spectroscopy

MR spectroscopy has a higher sensitivity than conventional MR in detecting changes of common metabolites in the absence of radiologically visible morphologic changes [1]. In the literature there is extensive documentation on its usefulness in the diagnosis and post-treatment follow-up in a wide variety of CNS tumors.

10.2.1 Response to Treatment

Surgery and/or RT treatment tumor response usually involves an initial reduction in NAA, which may be evident before Cho and Cr changes. Then Cho, Cr and NAA decrease (NAA may even be absent) with the possible appearance of the Lac/Lip peak, indicating radiation necrosis [2].

10.2.2 Stability vs. Progression/Recurrence

Spectroscopy is able to demonstrate disease progression, showing spectral anomalies at the resection margins or outside the surgical bed, even in the absence of CE and before an increase in it is registered [3]. Changes in the Cho signal and the Cho/Cr and Cho/NAA ratios are predictive of tumor progression. An increase in Cho of more than 45% with respect to the contralateral healthy hemisphere is indicative of disease progression, whereas a value equal to or less than 35% is indicative of stability [4]. With regard to the other ratios, the differentiation between progression and stability has a sensitivity of 93.8% and a specificity of 85.7% [5]. An increase in the Lip signal can be an early marker of malignant transformation [6].

In postsurgical [7] and post-radiosurgery [3] follow-up, areas with high Cho/NAA and Cho/Cr ratios usually undergo contrast-medium enhancement. Tissue volume with an abnormal spectrum correlates inversely with the time of appearance of new enhancement.

In post-chemotherapy, the Cho/Cr and Lac/Cr ratios are the most useful markers for the follow-up of low-grade gliomas. In CE areas, an increase in Lac/Cr during treatment has a significant association with progression and reduced survival. In contrast, a low NAA/Cr in normal appearing brain tissue adjacent to tumor without CE is associated with reduced progression and increased survival. Moreover, an increase in the Cho/Cr and Lac/Cr ratios in normal appearing brain tissue adjacent to tumor may become evident several months before

T. Popolizio (✉)
Department of Neuroradiology
Scientific Institute "Casa Sollievo della Sofferenza"
San Giovanni Rotondo (FG), Italy

disease progression can be visualized in MR morphologic images [8].

10.2.3 Recurrence vs. Radionecrosis

Spectroscopy can detect a characteristic metabolic pattern. In the presence of radionecrosis, a peak in Lac/Lip may appear in the absence of other metabolic signals and persist for several months [2]. This is in contrast to what happens in cases of recurrence, which instead are characterized by an increase in Cho. The distinction between recurrence and radiation injury can be made using the Cho/NAA, Cho/Cr and NAA/Cr ratios: the former two are the main markers for the differential diagnosis. They are in fact significantly higher in recurrence than in radiation injury and even higher than the apparently healthy white matter. The NAA/Cr ratio has instead an opposite trend [9, 10].

However, where necrosis and recurrence coexist (a common occurrence in clinical practice), spectroscopy is not always definitive and it is not always possible to distinguish between radionecrosis and tumor necrosis because of their frequent coexistence and overlapping of events [11]. In this case, serial metabolic changes may be more informative than transversal data collected at a certain time after therapy.

10.3 Role of Diffusion

DWI can be used not only to characterize and define tumor grade on the basis of cellularity, but also to assess how cellularity changes with treatment.

10.3.1 Treatment Response

In the immediate postoperative period, ADC is more useful than CE in defining the persistence or absence of disease thanks to a reduction in ADC caused by acute brain injury [12].

At a later stage, during the initial post-treatment period, cellular changes within the tumor (cell swelling, cell lysis, cell necrosis, apoptosis) may influence DWI and thus the ADC map. In fact, when cells are not responsive there is no change in ADC, whereas in the presence of cell swelling, there is a decrease in ADC. Eventual cell lysis due to hypoxic-ischemic events leads to increased diffusivity which occurs even when apoptosis directly occurs.

In the early stage, DWI can document the presence of ischemic changes surrounding the surgical bed [13]. Tractography moreover can also highlight the preservation of white matter tracts, such as motor fibers, and thus obtain prognostic information about functional recovery of neurologic conditions.

10.3.2 Stability vs. Progression/Recurrence

Functional diffusion mapping (FDM) has been recently proposed as a noninvasive method to assess the quantitative response to therapy of the disease, with the comparison of diffusion maps before and after treatment [14, 15]. FDM done 3 weeks after treatment can already predict whether the tumor is responsive or not in relation to early abnormalities in tumor diffusion values. In such cases it is not necessary to wait the traditional 10 weeks to evaluate treatment response. Comparison between FDM after 3 weeks and changes after 10 weeks is therefore an early quantitative biomarker for predicting response to treatment, its effectiveness, progression time and median survival. The association between FDM and neuroradiologic findings provides a more accurate prediction of survival with respect to the quantitative parameter alone [16]. Clinical implications then become very useful for optimizing patient management to avoid expensive and toxic therapies and other kinds of treatment.

10.3.3 Recurrence vs. Radionecrosis

In the follow-up of treated high-grade glioma, radioinduced injuries may present with a variety of DWI patterns, usually hypointense with high ADC, but sometimes hyperintense with low ADC, for example due to the presence of bleeding, viscous mucinous components or coagulation necrosis [17].

ADC can be used to differentiate RT effects from tumor recurrence, as it is significantly higher in radionecrosis than in recurrence (due to the high cellularity), even though some overlap is possible as a result of various factors such as cellularity, viscosity and permeability [18]. In fact, it is possible to differentiate tumor from necrosis, but ADC is not always able to obtain more information than spectroscopy in discriminating mixed tumor and necrosis from pure tumor or necrosis alone [10, 11].

Diffusion tensor imaging (DTI) provides more accurate data, showing a lower ADC ratio and higher FA in recurrence than in necrosis [19].

In the evaluation of enhancing lesions, cellularity is not the only factor that can influence ADC after therapy. The contribution of other components (necrosis, gliosis, scarring, granulation tissue) may alter ADC values. This suggests the need to study only the average absolute value of ADC in order to minimize the influence of all these components. The use of the ADC ratio certainly improves differentiation between the two entities, reducing the overlapping of data [18].

The quantitative ADC study in theory would then be able to distinguish between radionecrosis and recurrence, but the structural complexity and heterogeneity of a lesion undergoing dynamic changes often involves abnormal values (i.e. an increase in ADC in the presence of increased cellularity and thus recurrence). This state depends on the inclusion or not of vascular structures and necrosis in the peritumoral district. These findings consequently could create confusion as the measure of ADC is often made in enhancing areas, which have low specificity in distinguishing the two entities.

In this regard, imaging based on magnetic susceptibility has recently been used to better visualize the heterogeneous pattern of tumor tissue. Using the same contrast-enhanced sequence, clinically useful information can be gathered such as tumor microvasculature, degree of intratumoral necrosis, and the presence of small alterations of the BBB in the surrounding tissue. The ability of contrast enhanced susceptibility weighted imaging (CE-SWI) to distinguish these pathologic findings thus provides a new mechanism for evaluating ADC within the parenchymal tissue with abnormal BBB, which is often the location of tumor recurrence. Used as a guide in an ADC quantitative diffusion study, especially in CE areas, CE-SWI can therefore distinguish districts anatomically related to vascular, blood and/or necrotic components. Therefore, in recurrence, compared to stable disease, a correlation has been found between increased CE in CE-SWI maps and low ADC in CE areas [20]. Moreover, in the CE lesion, ADC has been shown to be significantly higher in perilesional edema and in radiation injury than in recurrence [21].

10.4 Role of Perfusion

PWI is useful in the post-treatment monitoring of gliomas, especially in lesions with extensive neovascularization and microvessel density. An increase in angiogenesis, which is a typical feature of the more aggressive gliomas, is an essential histologic criterion for determining the biologic behavior of these lesions, which is shown by an increase in cerebral blood volume (CBV), considered one of the strongest predictors of tumor aggressiveness and survival in gliomas [22, 23].

10.4.1 Treatment Response

Initial tumor response to surgery and/or to RT is usually measured by a reduction in CBV. This feature is further supported in relation to the size of the necrotic component [24].

10.4.2 Stability vs. Progression/Recurrence

PWI plays a prominent role especially in the presence of diffuse CE lesions, which may arise as the result of other nonsurgical treatments. In cases of residual or progressive tumor, PWI shows a higher rCBV values than in normal white matter. This finding is also confirmed with morphologic MR studies.

10.4.3 Recurrence vs. Radionecrosis

Since it is correlated with angiogenesis, CBV is significantly higher in recurrence than in radio-necrosis, although there is some overlap of findings in relation to non-high spatial resolution, tissue heterogeneity and the frequent coexistence of vascularized recurrence and radionecrosis with hyperplastic and enlarged vessels [25].

The presence of petecchiae in recurrence can cause susceptibility artifacts and reduce CBV. An inaccurate estimation of CBV may also be due to severe disruption or absence of the BBB [26].

Some authors use other hemodynamic variables in addition to CBV, such as RPH (peak height) and rPSR (percentage of signal intensity recovery).

RPH is a quantifiable measure of tumor vascularity which is highly correlated with CBV and therefore with tumor vascularity and histopathologic grade. For this reason, it has been suggested that it may reflect total vascular volume within the ROI and it is therefore high, like CBV, in CE recurrence, in contrast to what happens in radionecrosis.

rPSR is significantly different in the two states. In particular, it is lower in tumor recurrence in relation to alterations of the BBB which becomes more permeable

to macromolecular contrast agents. This parameter is more useful than the Ktrans value, which is a measure of capillary permeability in relation to T1 relaxation changes (T1 DSC) that occur during the infusion of contrast media or during washout of the CE lesion [27].

Perfusion may be useful for distinguishing pseudo-progression from real progression [28].

In a study using a parametric response map (PRM), an innovative voxel-by-voxel method of image analysis in patients with progressive disease, a significantly reduced CBV was noted after 3 weeks with respect to the patients with pseudo-progression [28].

10.5 Multimodal Magnetic Resonance Imaging

The use of the morphologic or advanced MR examination alone in the diagnosis of gliomas is not enough for defining the histologic grading, optimal treatment planning and correct post-treatment follow-up. Therefore, the use of combined studies is necessary to increase MR diagnostic accuracy, as a function of recent development and of new and more effective anticancer treatments that require a complete morphofunctional MR study. With these techniques an *in vivo* neuropathologic interpretation of the typical biologic heterogeneity of these tumors can be obtained noninvasively.

These advanced techniques should be used for a qualitative and quantitative assessment. The combination of quantitative data can provide real biomarker findings, which are very important for tumor tissue characterization, as well as allow multicenter studies, clinical trials and longitudinal studies. Only by combining data from various imaging techniques, which are often quite different, can essential information with an effective clinical influence be found.

In this setting, we conducted a multimodal study [29] by combining MR imaging with spectroscopy, diffusion and perfusion in order to minimize the low specificity of each of these methods and especially to provide the surgeon oncologist with more accurate and comprehensive information to assist in planning more accurate treatment.

The study involved 31 patients with cerebral gliomas of different degrees. All parameters used, with the exception of ADC, helped to differentiate low-grade gliomas from high-grade tumors. In particular, metabolic information provided by levels of Lac/Lip and CBV were sufficient for a correct classification of 100% of the tumors. In addition, we studied spatial changes in metabolic structural and hemodynamic findings, in gliomas and surrounding tissues. By combining this information, we sought to identify the true tumor margins, the exact definition of which is essential for accurate treatment planning and prognosis.

Zeng et al. [30] found a significant difference in Cho/Cr, Cho/NAA and ADC ratio. Cho/Cr, Cho/NAA and ADC ratio were found to be the key to distinguishing recurrence from radionecrosis. The ADC ratio, in addition to spectroscopy, further improved the differentiation ability of spectroscopy. The accuracy of the differential diagnosis with combined spectroscopy and ADC ratio was higher than spectroscopy alone.

Bobek-Billewicz et al. [31] documented the role of perfusion compared to diffusion and spectroscopy in the differential diagnosis between recurrence and radiation injury. In particular, the mean value of CBV was more discriminating than the maximum value of CBV, while spectroscopy and diffusion did not seem to differentiate the two entities in a significant way, despite lower ADC values in recurrence compared to radiation injury.

Voglein et al. [32] demonstrated the greater efficacy of perfusion imaging compared to spectroscopy in identifying disease progression and predicting response to treatment.

Kim et al. [33] and Prat et al. [34], compared the effectiveness of PET and perfusion in the differential diagnosis between recurrence and radionecrosis, and found MR superior to PET (using both FDG and methionine radiotracers).

References

1. Howe FA, Opstad KS (2003) ^{1}H MR spectroscopy of brain tumours and masses. NMR Biomed 16:123-131
2. Möller-Hartmann W, Herminghaus S, Krings T et al (2002) Clinical application of proton magnetic resonance spectroscopy in the diagnosis of intracranial mass lesions. Neuroradiology 44:371-381
3. Graves EE, Nelson SJ, Vigneron DB et al (2001) Serial proton MR spectroscopic imaging of recurrent malignant gliomas after gamma knife radiosurgery. AJNR 22:613-624
4. Tedeschi G, Lundbom N, Raman R et al (1997) Increased choline signal coinciding with malignant degeneration of cerebral gliomas: a serial proton magnetic resonance spectroscopy imaging study. J Neurosurg 87:516-524
5. Lichy MP, Bachert P, Hamprecht F et al (2006) Application of ^{1}H-MRS spectroscopic imaging in radiation oncology:

choline as a marker for determining the relative probability of tumor progression after radiation of glial brain tumors. Rofo 178:627-339
6. Murphy PS, Rowland IJ, Viviers L et al (2003) Could assessment of glioma methylene lipid resonance by in vivo ^{1}H-MRS be of clinical value? Br J Radiol 76:459-463
7. Pirzkall A, Mcknight TR, Graves EE et al (2001) MR-spectroscopy guided target delineation for high-grade gliomas. Int J Radiat Oncol Biol Phys 50:915-928
8. Balmaceda C, Critchell D, Mao X et al (2006) Multisection 1H magnetic resonance spectroscopic imaging assessment of glioma response to chemiotherapy. J Neurooncol 76:185-191
9. Weybright P, Sundgren PC, Maly P et al (2005) Differentiation between brain tumor recurrence and radiation injury using MR spectroscopy. Am J Roentgenol 185:1471-1476
10. Zeng QS, Li CF, Zhang K et al (2007) Multivoxel 3D proton MR spectroscopy in the distinction of recurrent glioma from radiation injury. J Neurooncol 84:63-69
11. Rock JP, Scarpace L, Hearshen D et al (2004) Associations among magnetic resonance spectroscopy, apparent diffusion coefficients, and image-guided histopathology with special attention to radiation necrosis. Neurosurgery 54:1111-1117
12. Smith JS, Cha S, Mayo MC et al (2005) Serial diffusion-weighted magnetic resonance imaging in cases of glioma: distinguishing tumor recurrence from postresection injury. J Neurosurg 103:428-438
13. Ulmer S, Braga TA, Barker FG et al (2006) Clinical and radiographics features of peritumoral infarction following resection of glioblastoma. Neurology 67:1668-1670
14. Moffat BA, Chenevert TL, Lawrence TS et al (2005) Functional diffusion map: a non invasive MRI biomarker for early stratification of clinical brain tumor response. Proc Natl Acad Sci USA 102:5524-5529
15. Moffat BA, Chenevert TL, Meyer CR et al (2006) The functional diffusion map: an imaging biomarker for the early prediction of cancer treatment outcome. Neoplasia 8:259-267
16. Hamstra DA, Galban CJ, Meyer CR et al (2008) Functional diffusion map as an early imaging biomarker for high-grade glioma: correlation with conventional radiologic response and overall survival. J Clin Oncol 26:3387-3394
17. Asao CH, Korogi Y, Kitajima M et al (2005) Diffusion weighted imaging of radiation-induced brain injury for differentiation from tumor recurrence. AJNR 26:1455-1460
18. Hein PA, Eskey CJ, Dunn JF et al (2004) Diffusion-weighted imaging in the follow-up of treated high-grade gliomas: tumor recurrence versus radiation injury. AJNR 25:201-209
19. Xu J-L, Li YL, Liam JM, et al (2010) Distinction between postoperative recurrent glioma and radiation injury using MR diffusion tensor imaging. Neuroradiology 52:1193-1199
20. Al Sayyari A, Buckley R, McHenery C et al (2011) Distinguishing recurrent primary brain tumor from radiation injury: a preliminary study using a susceptibility-weighted MR imaging-guided apparent diffusion coefficient analysis strategy. AJNR Am J Neuroradiol 31:1049-1054
21. Sudgren PC, Fan X, Weibright P et al (2006) Differentiation of recurrent brain tumor versus radiation injury using diffusion tensor imaging in patients with new contrast-enhancing lesions. Magn Reson Imaging 24:1131-1142
22. Leon SP, Folkerth RD, Black PM (1996) Microvessel density is a prognostic indicator for patients with astroglial brain tumors. Cancer 77:362-372
23. Covarrubias DJ, Rosen BR, Lev MH (2004) Dynamic magnetic resonance perfusion imaging of brain tumors. Oncologist 9:528-537
24. Chaskis C, Stadnik T, Michotte A et al (2006) Prognostic value of perfusion-weighted imaging in brain glioma: a prospective study. Acta Neurochir 148:277-285
25. Sugahara T, Korogi Y, Tomiguchi S et al (2000) Posttherapeutic intraaxial brain tumor: the value of perfusion-sensitive contrast-enhanced MR imaging for differentiating tumor recurrence from non neoplastic contrast-enhancing tissue. AJNR 21:901-909
26. Prazincola L, Steno J, Srbecky M et al (2009) MR imaging of late radiation therapy- and chemiotherapy-induced injured: a pictorial essay. Eur Radiol 19:2716-2727
27. Barajas RF, Chang JS, Segal MS et al (2009) Differentiation of recurrent glioblastoma multiforme from radiation necrosis after external beam radiation therapy with dynamic susceptibility-weighted contrast-enhanced perfusion MR imaging. Radiology 253:486-496
28. Tsien C, Galban CJ, Chenevert TL et al (2010) Parametric response map as an imaging biomarker to distinguish progression from pseudoprogression on in high-grade glioma. J Clin Oncol 28:2293-2299
29. Di Costanzo A, Scarabino T, Trojsi F et al (2006) Multiparametric 3T MR approach to the assessment of cerebral gliomas: tumor extent and malignancy. Neuroradiology 48:622-631
30. Zeng QS, Li CF, Liu H et al (2007) Distinction between recurrent glioma and radiation injury using magnetic resonance spectroscopy in combination with diffusion-weighted imaging. Int J Radiat Oncol Biol Phys 68:151-158
31. Bobek-Billewicz B, Stasik-Pres G, Majchrzak H et al (2010) Differentiation between brain tumor recurrence and radiation injury using perfusion, diffusion-weighted imaging and MR spectroscopy. Folia Neuropathol 48:81-92
32. Voglein J, Tuttenberg J, Weimer M et al (2011) Treatment monitoring in gliomas: comparisons of dynamic susceptibility-weighted contrast-enhanced and spectroscopic MRI techniques for identifying treatment failure. Invest Radiol 46:390-400
33. Kim YH, Oh SW, Lim YJ et al (2010) Differentiating radiation necrosis from tumor recurrence in high-grade gliomas: assessing the efficacy of 18F-FDG PET, 11C-methionine PET and perfusion MRI. Clin Neurol Neurosurgery. 112:758-65
34. Prat R, Galeano I, Lucas A et al (2010) Relative value of magnetic resonance spectroscopy, magnetic resonance perfusion, and 2-(18F) fluoro-2-deoxy-D-glucose positron emission tomography for detection of recurrence or grade increase in gliomas. J Clin Neurosci 17:50-53

Part D

Clinical Cases

Case 1

Early Sequelae

Postoperative CT Scan in Glioblastoma Multiforme

Ferdinando Caranci, Andrea Elefante and Arturo Brunetti

- Patient with surgically treated right frontal glioblastoma multiforme
- Postoperative CT scan performed within 24 hours

Preoperative Imaging

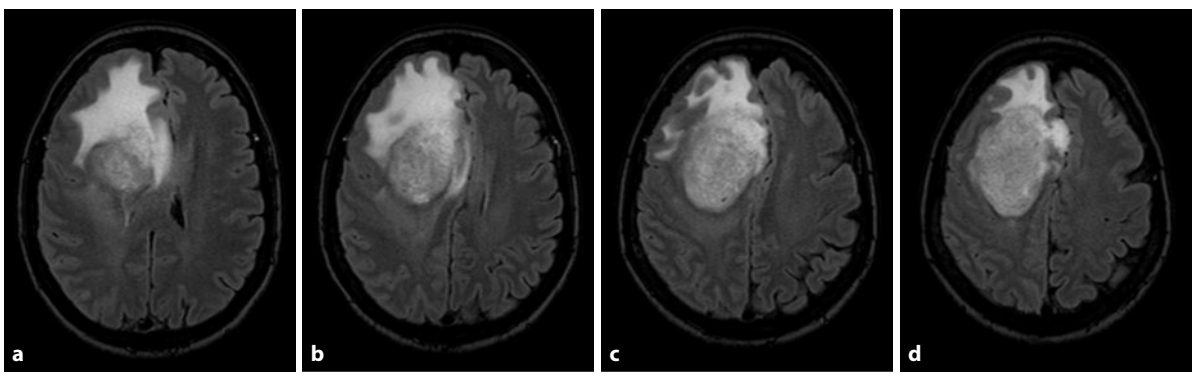

Fig. 1.1 a-d MR FLAIR sequences. A roughly oval-shaped lesion at the right frontal convexity can be seen with irregular margins and inhomogeneous structure, surrounded by a halo of edema

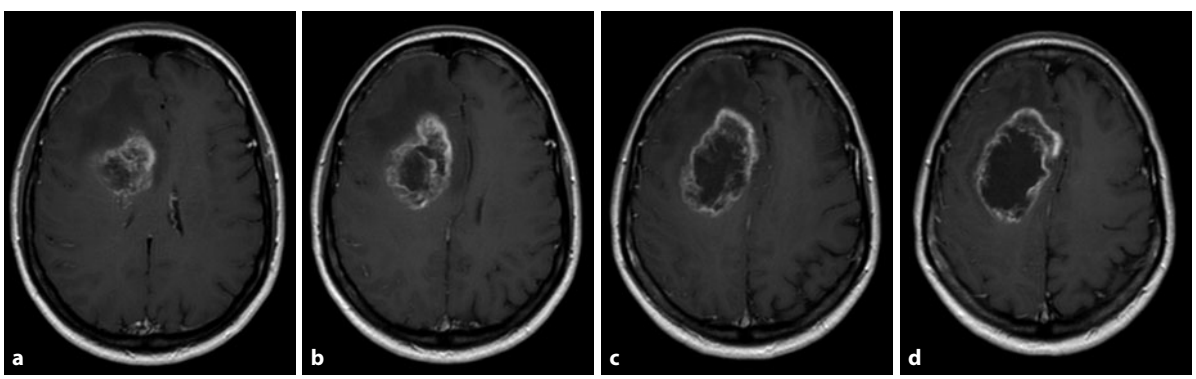

Fig. 1.2 a-d Contrast-enhanced MR SE T1-weighted images. Ring enhancement can be appreciated due to the presence of a large necrotic component within the lesion

Early Postoperative Follow-up (Within 24 Hours)

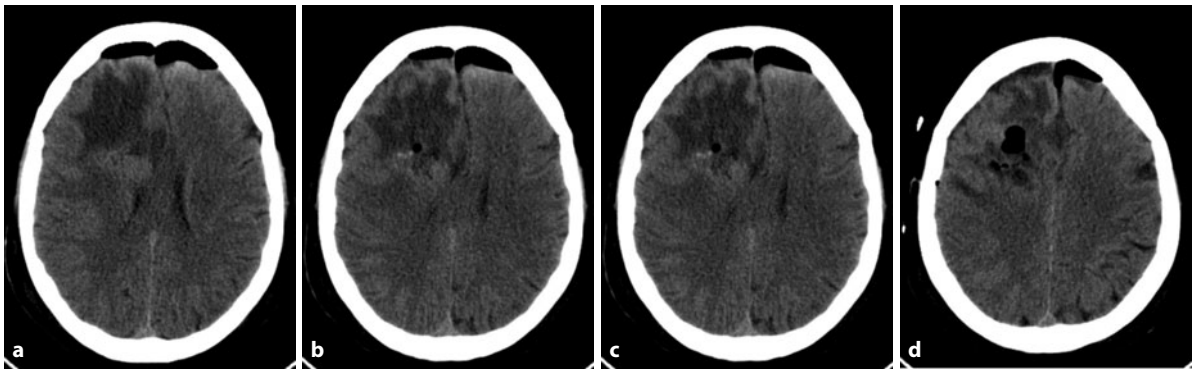

Fig. 1.3 a-d CT scan. Good repositioning of the bone flap is shown, with a small amount of extracerebral air at the surgical access site. The surgical bed in the right frontal lobe appears inhomogeneously hypodense due to the coexistence of edema, moderate blood effusion and small air bubbles. Superiorly to the ventricular roof a small amount of relatively hyperdense tissue can be appreciated, attributable to residual lesion

Case 2

Early and Late Sequelae: Evolution of Postsurgical Area

Postoperative MR Follow-up in Glioblastoma Multiforme

Ferdinando Caranci, Francesco Briganti and Arturo Brunetti

- Patient with surgically treated right temporo-occipital glioblastoma multiforme
- Postoperative MR follow-up performed early (3 days) and late (3, 6, 10 months)

Postoperative Follow-up at 3 Days

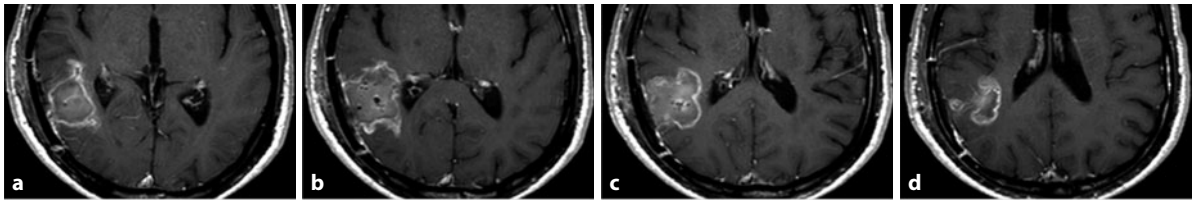

Fig. 2.1 a-d Contrast-enhanced MR SE T1-weighted images. The postoperative right temporo-occipital cavity signal is extremely inhomogeneous due to the mixture of blood-fluid components (hyperintense signal) and air. Peripheral enhancement is associated, with irregular margins and a linear morphology, produced by blood-brain barrier injury, with enhancing dura adjacent to the bone flap. The ventricular trigone appears mildly compressed

Postoperative Follow-up at 3 Months

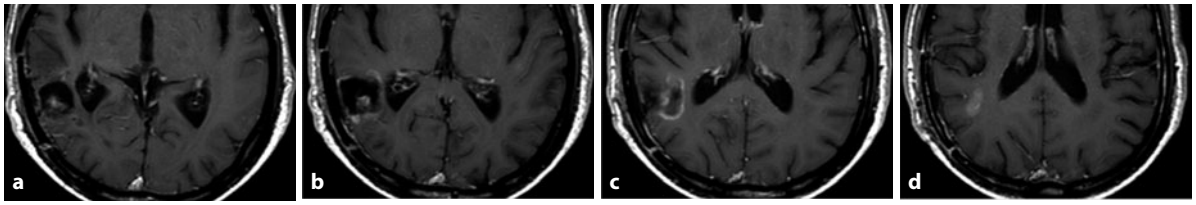

Fig. 2.2 a-d Contrast-enhanced MR SE T1-weighted images. A reduction in the size of the surgical foci is evident, with re-expansion of the ipsilateral ventricular trigone. There is evident resorption of the intralesional blood component and disappearance of the air. The lesion shows a CSF-like signal, with the presence of several internal blood clots. The peripheral enhancement produced by the blood-brain barrier injury is also still present, although reduced. The enhancing dura is also markedly reduced

Postoperative Follow-up at 6 Months

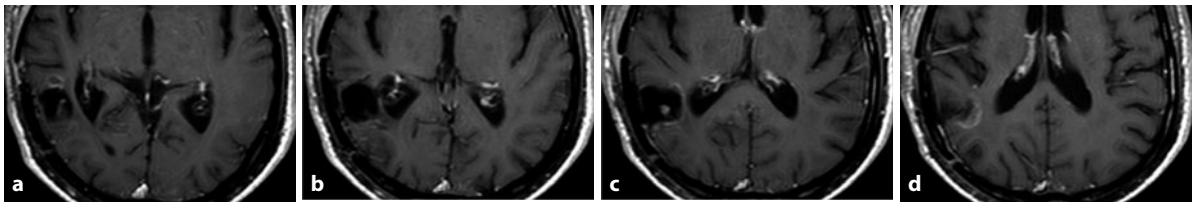

Fig. 2.3 a-d Contrast-enhanced MR SE T1-weighted images. Both the internal blood clots and the peripheral enhancement of the dura appear further reduced

Postoperative Follow-up at 10 Months

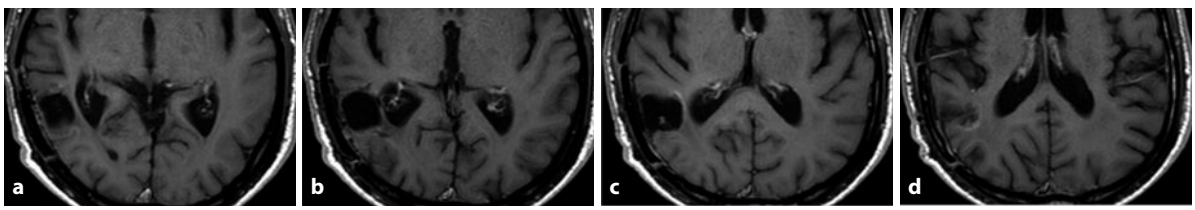

Fig. 2.4 a-d Contrast-enhanced MR SE T1-weighted images. Further progression of the phenomena described above is evident, with the formation of a cavity with a prevalent CSF content

Case 3

Late Sequelae: Gliotic Scar Formation

Postoperative MR Follow-up in Grade II Oligoastrocytoma

Bianca Cusati, Ferdinando Caranci and Alfonso Ragozzino

- Patient with surgically treated right temporo-fronto-insular grade II oligoastrocytoma
- Postoperative follow-up performed late (at 6 months) with MR morphologic sequences and spectroscopy

Preoperative Imaging

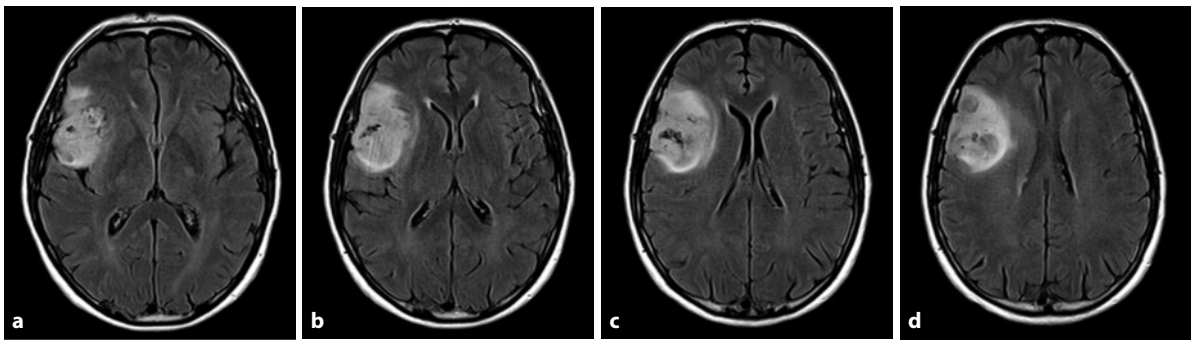

Fig. 3.1 a-d MR FLAIR sequence. An intra-axial right temporo-fronto-insular lesion can be appreciated infiltrating the cortex and extending into the white matter, with irregular margins and heterogeneous structure due to the presence of initial internal necrosis

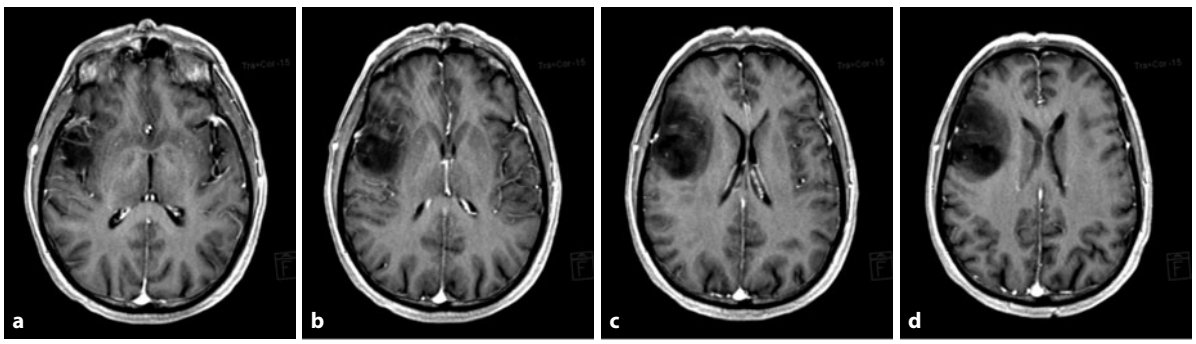

Fig. 3.2 a-d Contrast-enhanced MR SE T1-weighted images. No focal areas of pathologic enhancement can be seen within the lesion

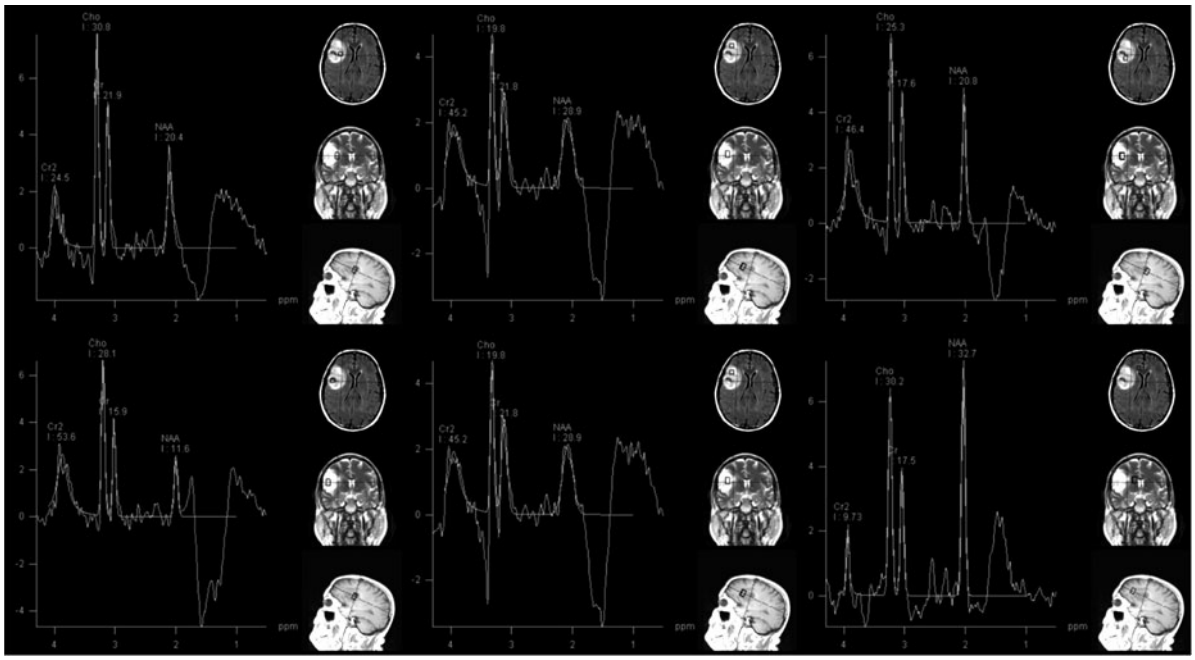

Fig. 3.3 Multi-voxel MR spectroscopy. Constant elevation in the concentration of choline can be appreciated, with reversal of the ratio with creatine

Postoperative Follow-up at 6 Months

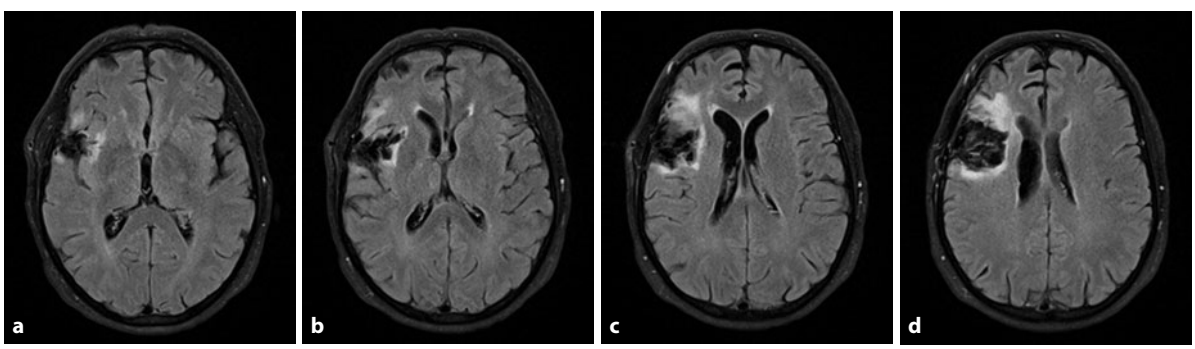

Fig. 3.4 a-d MR FLAIR sequence. The images clearly show the postsurgical cavity. A peripheral halo of high signal is associated, which does not exceed the margins of the original lesion. This may be likely due to postsurgical gliotic modifications, and should be the basis for subsequent follow-up

Case 4

Early Complications: Epidural Hematoma

Postoperative CT in Pilocytic Astrocytoma

Ferdinando Caranci, Andrea Elefante and Arturo Brunetti

- Patient with surgically treated pilocytic astrocytoma of the vermis
- Postoperative CT performed early (within 24 hours)

Early Postoperative Follow-up (Within 24 Hours)

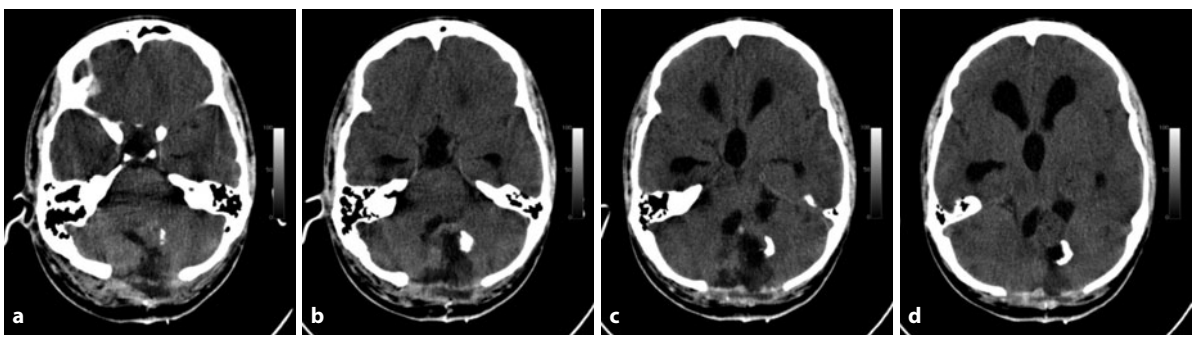

Fig. 4.1 a-d CT scan. Median suboccipital craniectomy can be appreciated and the presence of inhomogeneous tissue indicative of residual lesion is visualized in the context of the postoperative area of the vermis

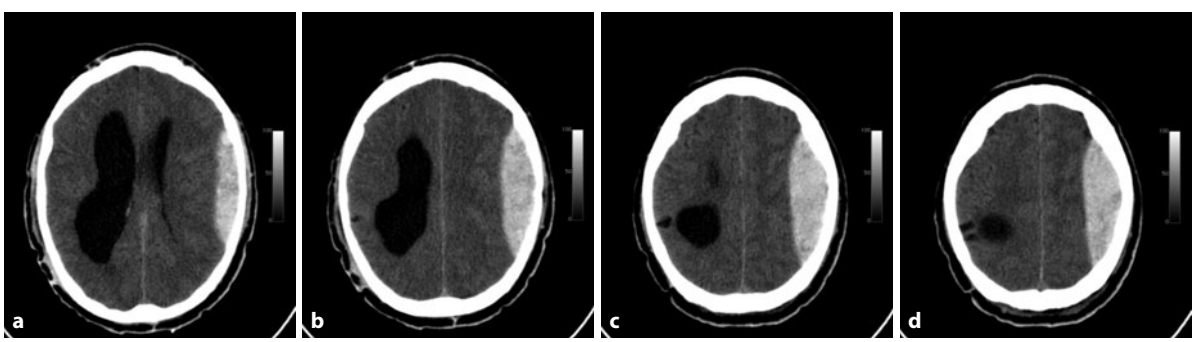

Fig. 4.2 a-d Higher sections show the presence of a biconvex hyperdense collection attributable to epidural hematoma (secondary to laceration of the middle meningeal artery by a Mayfield adaptor)

Case 5

Early Complications: Perilesional Ischemia

Postoperative MR Follow-up in Glioblastoma Multiforme

Ferdinando Caranci, Enrico Tedeschi and Arturo Brunetti

- Patient with surgically treated right temporal glioblastoma multiforme
- Postoperative MR follow-up performed early (5 days) with morphologic sequences and diffusion-weighted imaging

Preoperative Imaging

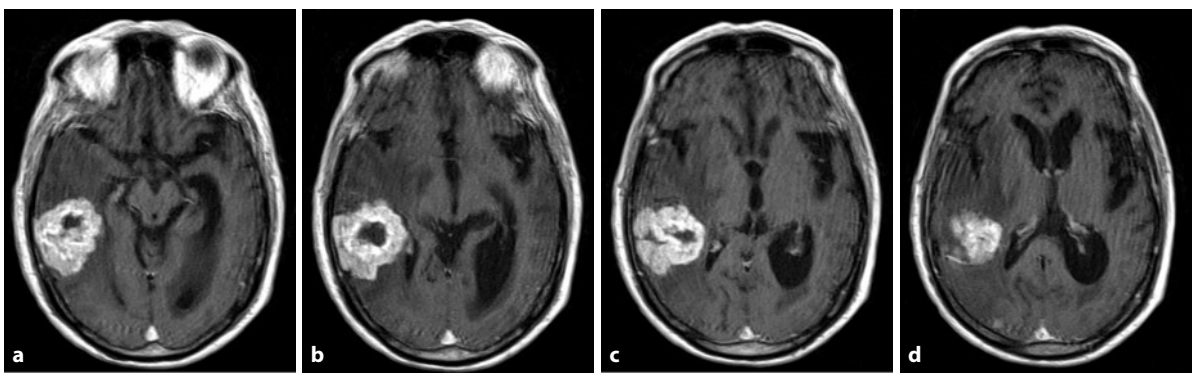

Fig. 5.1 a-d Contrast-enhanced MR SE T1-weighted images. Despite the presence of motion artifacts, an intra-axial lesion with irregular margins and heterogeneous structure due to the coexistence of a necrotic component can be appreciated in the right posterior temporal region

Early Postoperative Follow-up (at 5 Days)

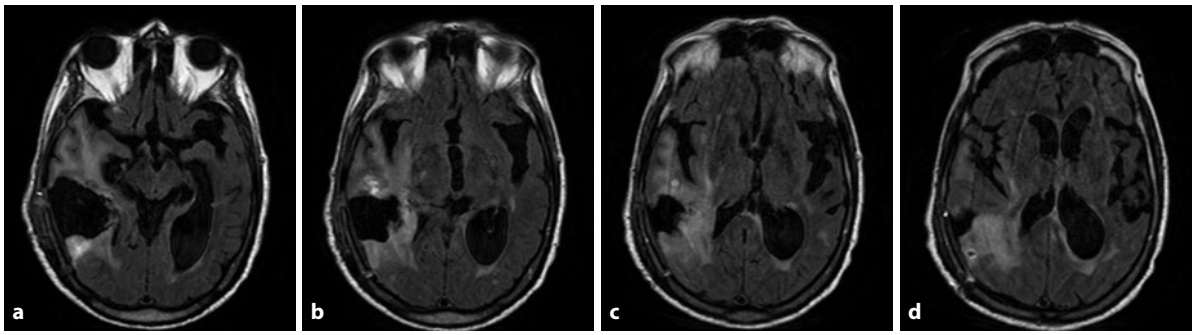

Fig. 5.2 a-d MR FLAIR sequence. The postoperative cavity filled with CSF is clearly shown, peripheral to which a diffuse signal alteration due to edema can be seen, with focal areas of partial blood effusion

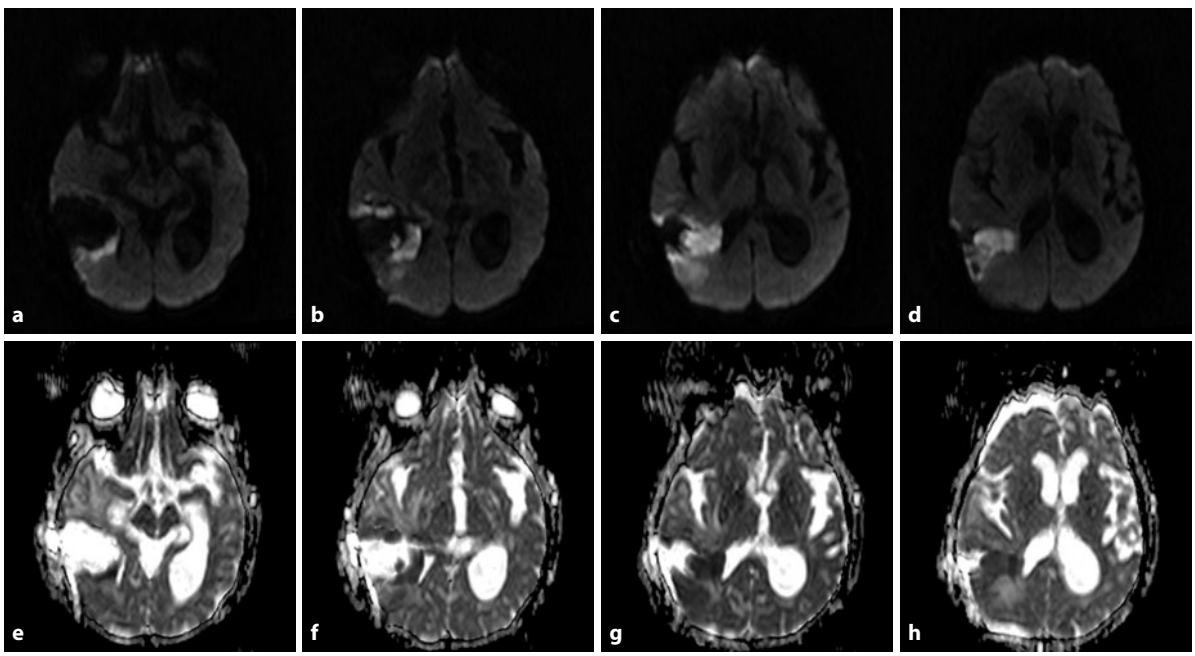

Fig. 5.3 a-h DWI with ADC maps. The postoperative cavity filled with CSF is surrounded by tissue with restricted diffusion, suggestive of ischemic changes

Case 6

Late Complications: Subdural Empyema

CT/MR Follow-up in Glioblastoma Multiforme

Alessandro Stecco, Francesco Fabbiano, Mariangela Lombardi, Sara Zizzari, Gerardo Di Nardo, Andrea Pietro Sponghini, Lucrezia Emanuela Guerra and Alessandro Carriero

- 30-year-old patient with right frontal glioblastoma multiforme treated with surgery and combined radiation therapy-chemotherapy
- Morphologic CT/MR studies performed at 5 months (following diastasis of the craniotomy bone flap with underlying purulent collection and subsequent acrylic resin cranioplasty) and at 12 months after resection

Postoperative Follow-up at 5 Months

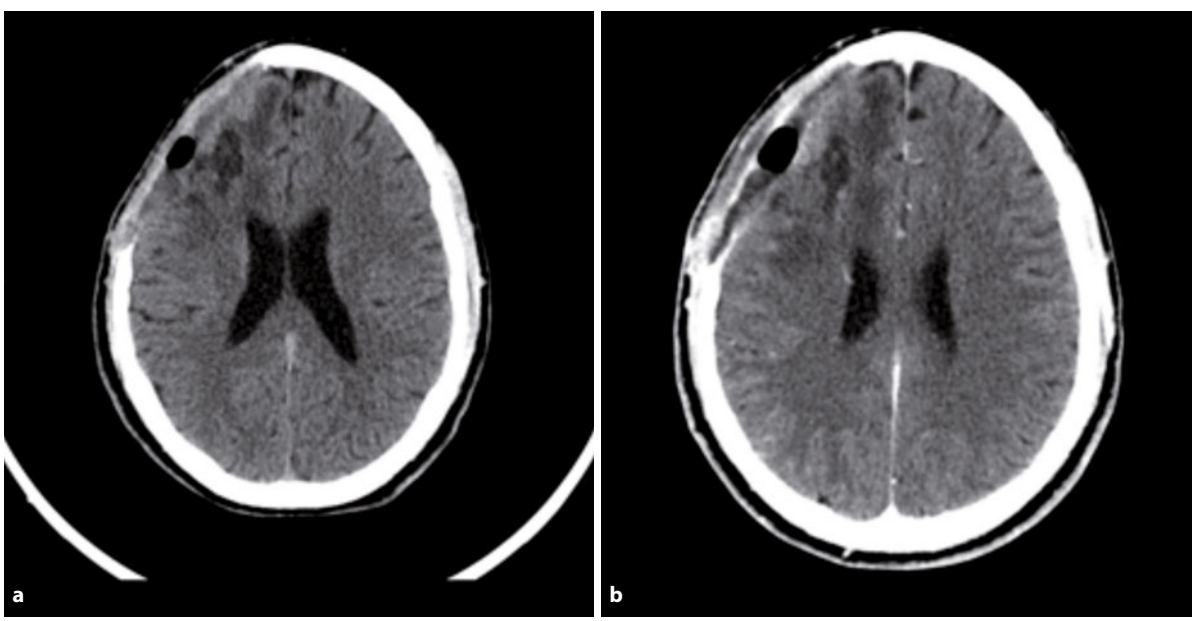

Fig. 6.1 a,b Contrast-enhanced CT scan shows craniotomy with removal of bone and the right frontal subdural postsurgical empyema

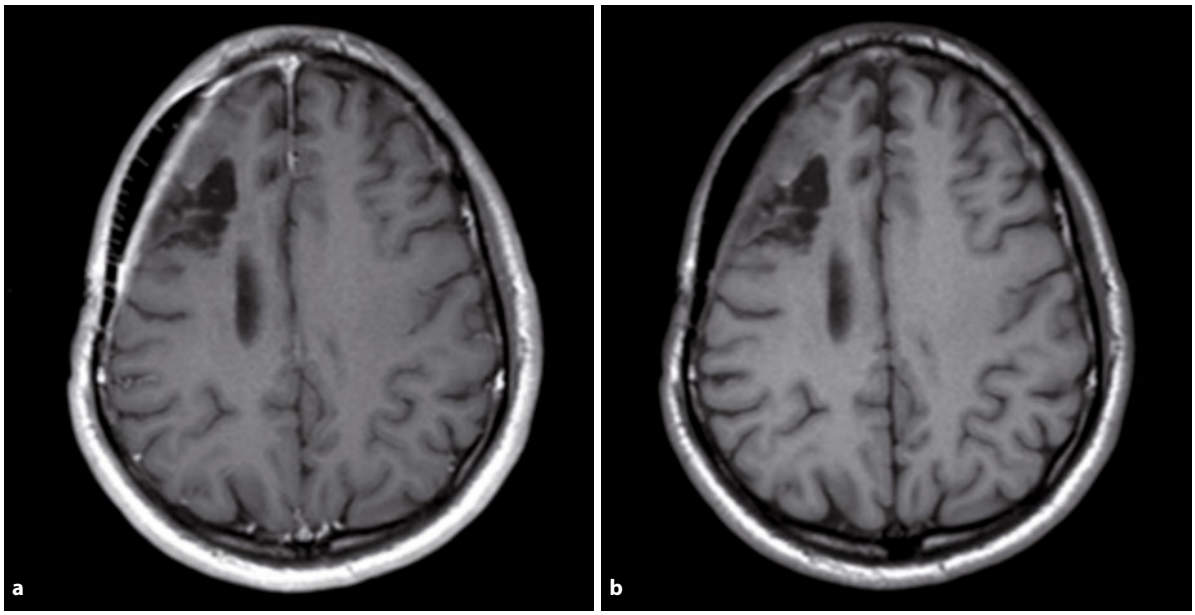

Fig. 6.2 a,b Contrast-enhanced MR SE T1-weighted sequences show the presence of pathologic epidural enhancement and more evidence of the gaseous component which compresses the soft tissue overlying the subdural empyema

Case 7

Late Complications: Abscess

Postoperative MR Follow-up in Glioblastoma Multiforme

Ferdinando Caranci, Alessandra D'Amico and Sossio Cirillo

- Patient with surgically treated right fronto-parieto-temporal glioblastoma multiforme
- Late postoperative MR imaging with morphologic sequences and diffusion-weighted imaging

Late Postoperative Follow-up

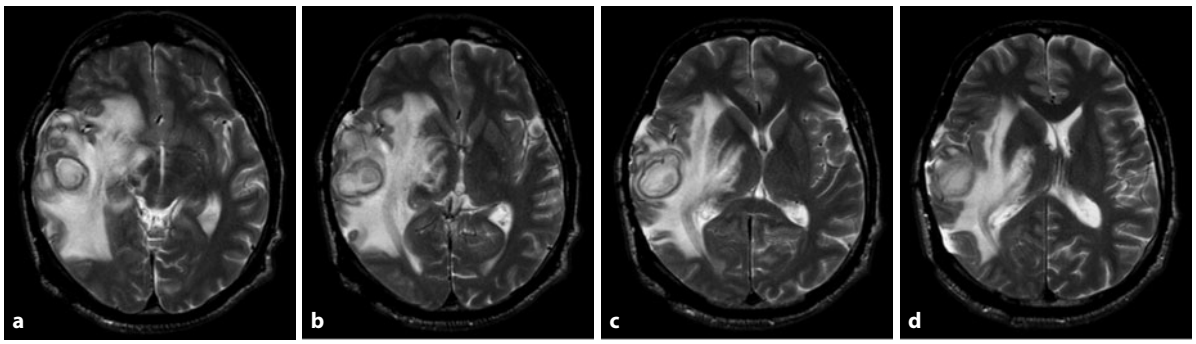

Fig. 7.1 a-d MR FSE T2-weighted sequence. The images show evidence of the previous right fronto-parieto-temporal craniotomy performed for the surgical excision of glioblastoma multiforme. Below the bone flap a lobulated structure can be appreciated, with inhomogeneously hyperintense fluid-type signal and a hypointense peripheral capsule, surrounded by a broad halo of edema

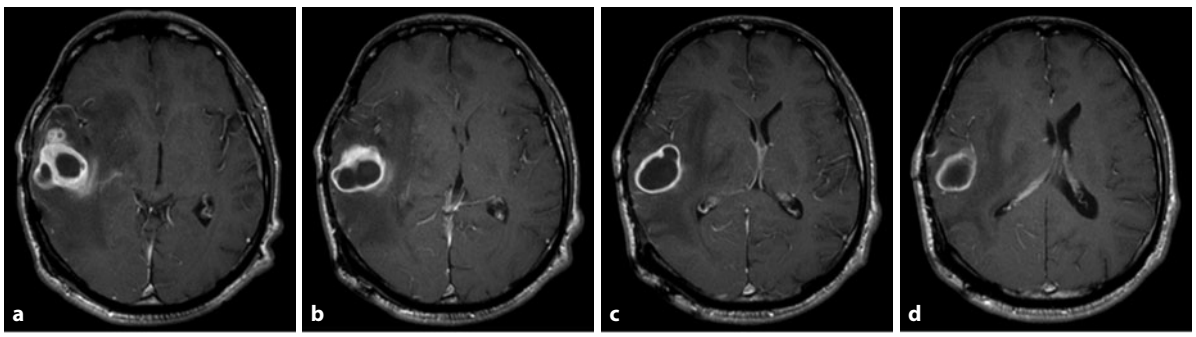

Fig. 7.2 a-d Contrast-enhanced MR SE T1-weighted images. The images show intense enhancement of the peripheral capsule

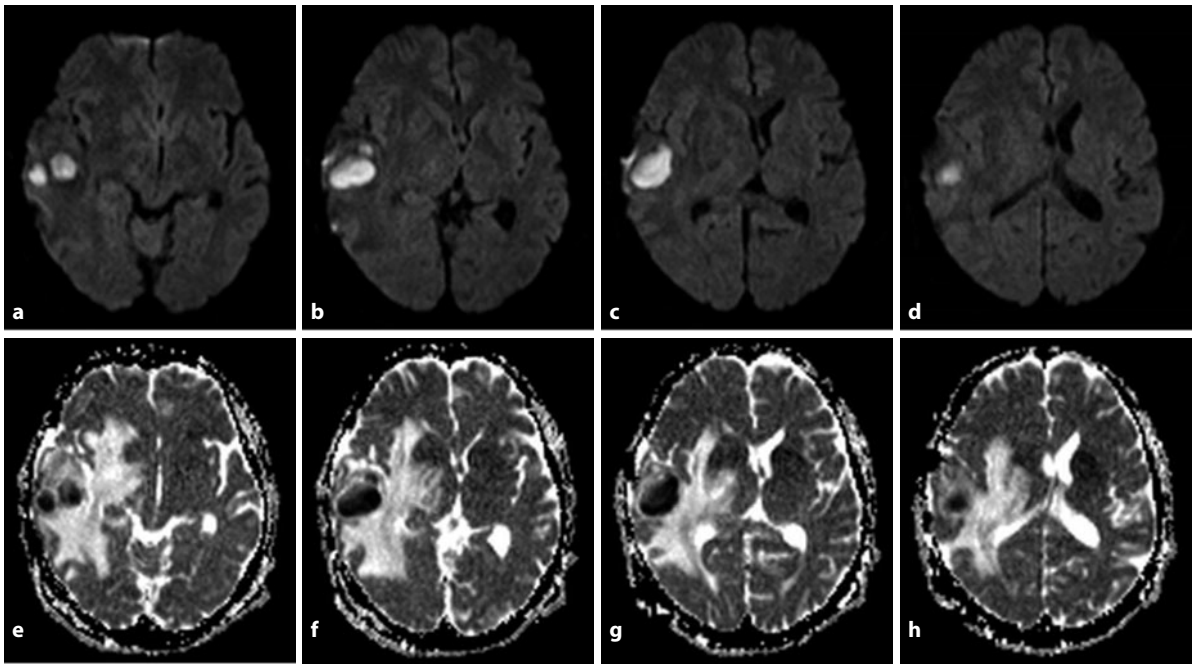

Fig. 7.3 a-h MR diffusion-weighted imaging and ADC map. The fluid content within the lesion has greatly restricted diffusion coefficients due to its high viscosity

Case 8

Early Residual Tumor

Postoperative MR Follow-up in Glioblastoma Multiforme

Luigi Cirillo, Antonella Bacci, Raffaele Agati and Marco Leonardi

- Patient with surgically treated right temporo-occipito-parietal glioblastoma multiforme
- Postoperative follow-up performed early (24 hours and 2 weeks) with MR morphologic sequences

Preoperative Imaging

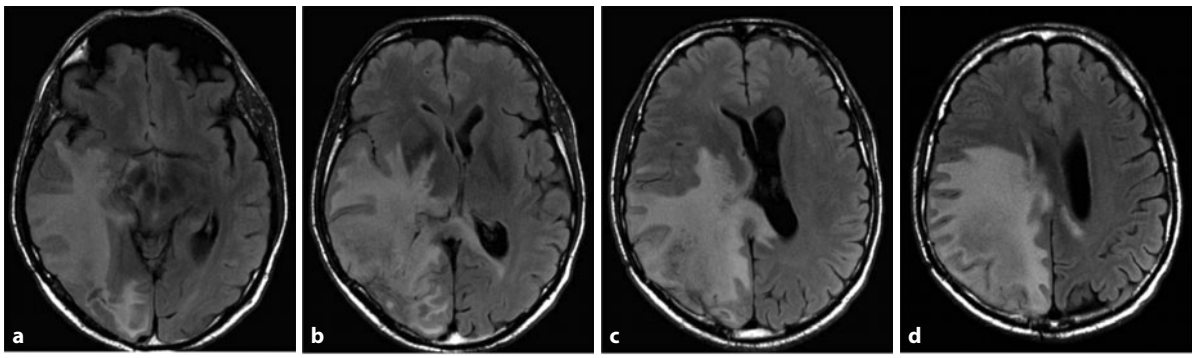

Fig. 8.1 a-d MR FLAIR sequence. A large area of high signal in the right temporo-occipito-parietal region is appreciable, with the characteristics of vasogenic edema extending contralaterally through the splenium of the corpus callosum. A relatively poorly defined hypointense tissue with infiltrating features is visualized

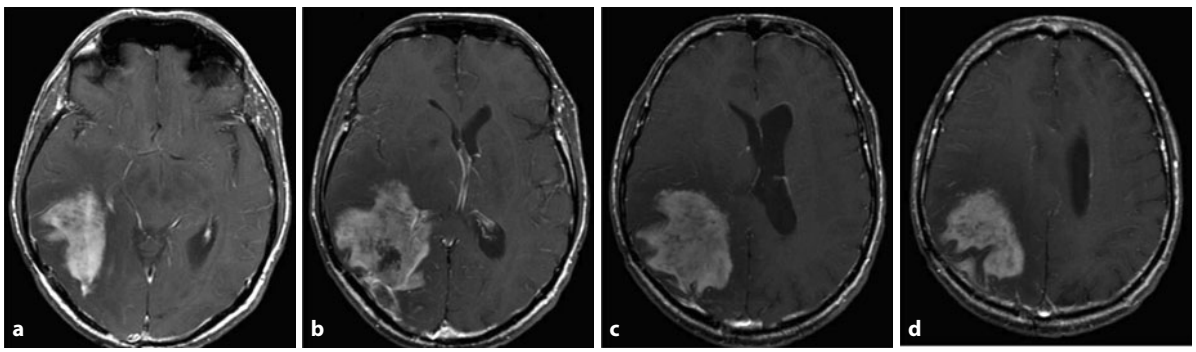

Fig. 8.2 a-d Contrast-enhanced MR SE T1-weighted images. Evidence of tissue with irregular margins, intense enhancement and an internal necrotic component

Postoperative Follow-up at 24 Hours

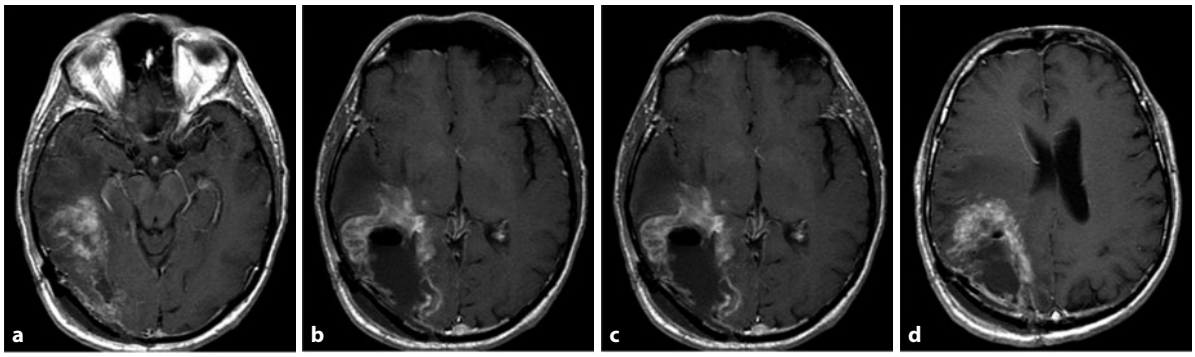

Fig. 8.3 a-d Contrast-enhanced MR SE T1-weighted images. The postsurgical cavity shows inhomogeneous fluid-like signal with air component. Peripheral to the cavity there is an intense and irregular enhancement, indicative of the residual heteroplastic tissue (at this stage there are no changes in the blood brain barrier)

Postoperative Follow-up at 2 Weeks

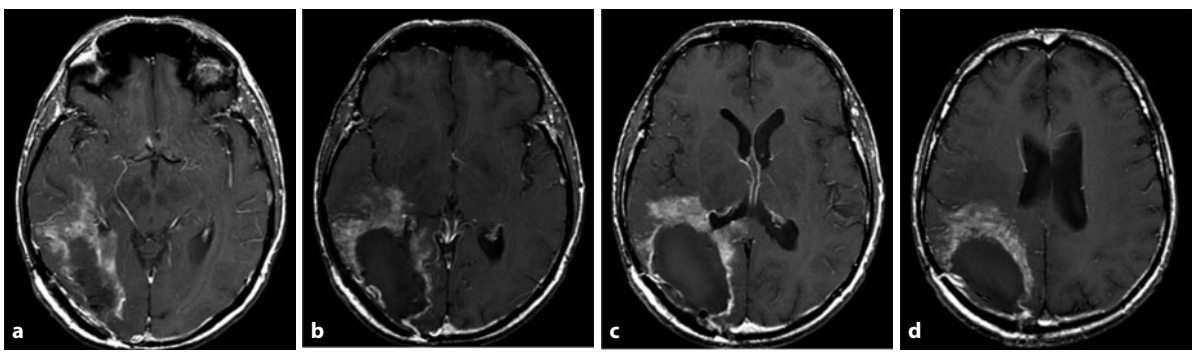

Fig. 8.4 a-d Contrast-enhanced MR SE T1-weighted images. The air component in the surgical cavity has been reabsorbed. The images confirm the presence of the peripheral heteroplastic tissue extending towards the splenium of the corpus callosum

Case 9

Late Residual Tumor

Postoperative MR Follow-up in Low-grade Astrocytoma

Ferdinando Caranci, Francesco Briganti and Arturo Brunetti

- Patient with surgically treated right temporal grade II astrocytoma
- Postoperative MR follow-up performed late (4 months) with MR morphologic sequences, spectroscopy and PET

Preoperative Imaging

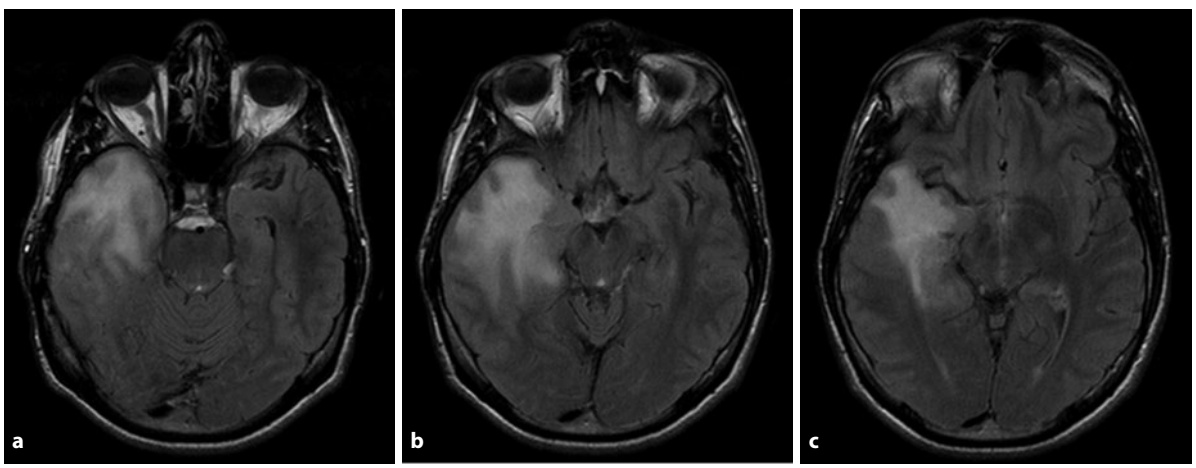

Fig. 9.1 a-c MR FLAIR sequence. Infiltrating tissue with high signal intensity can be appreciated in the right temporal region, indistinguishable from the associated edema, extending medially to the parahippocampal-hippocampal region

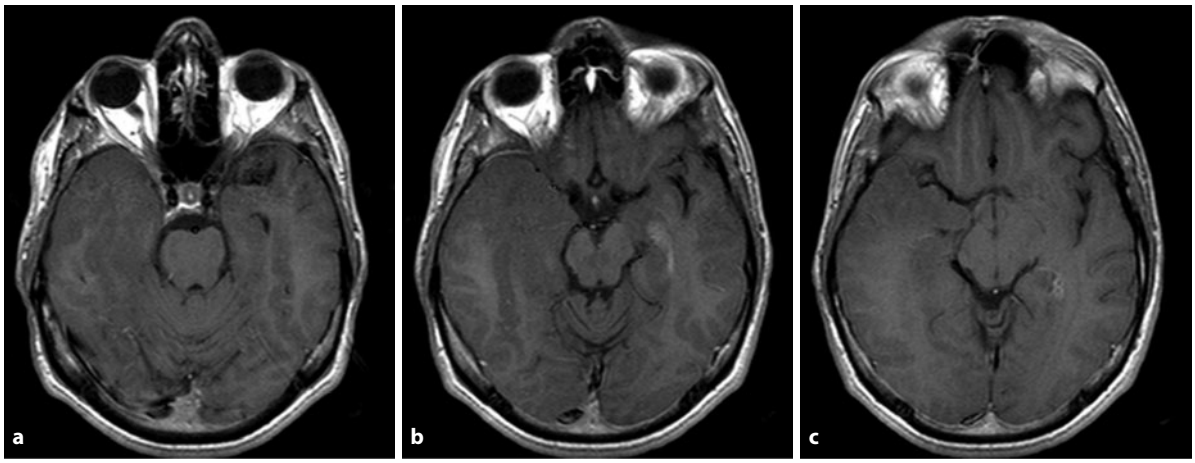

Fig. 9.2 a-c Contrast-enhanced MR SE T1-weighted images. No enhancement is appreciable after administration of contrast medium

Postoperative Follow-up at 4 Months

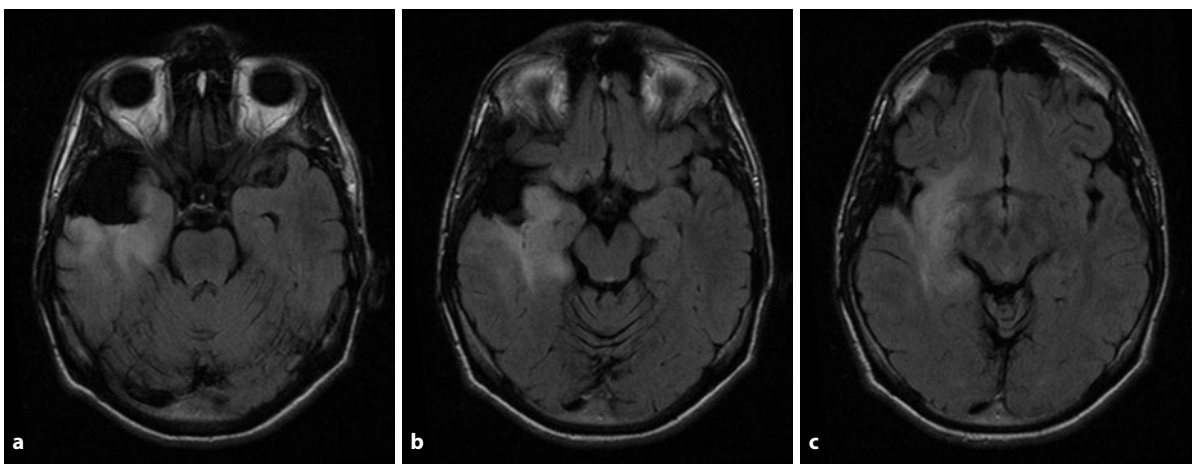

Fig. 9.3 a-c MR FLAIR sequence. Hyperintense signal indicative of residual neoplastic tissue can be appreciated peripheral to the area of CSF-like signal produced by the postsurgical cavity

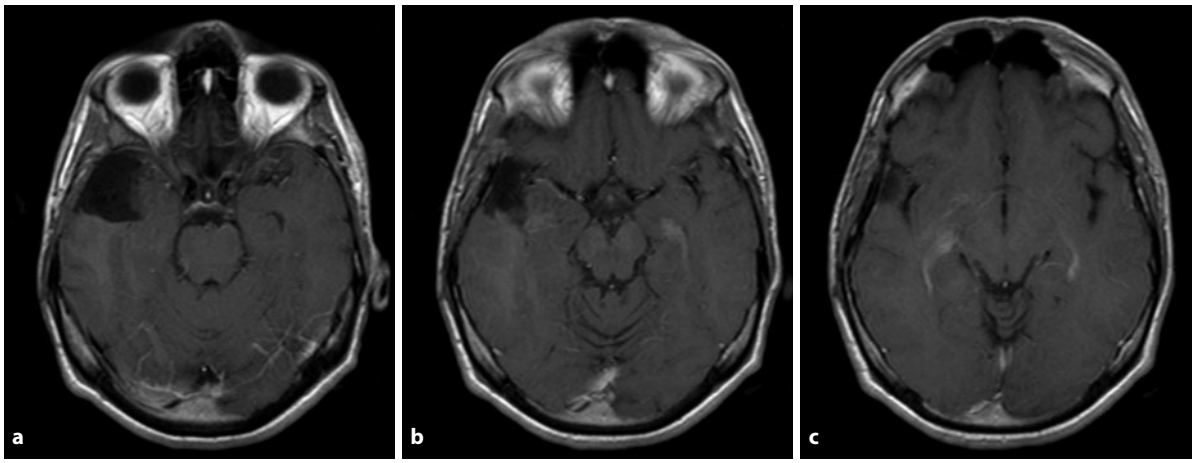

Fig. 9.4 a-c Contrast-enhanced MR SE T1-weighted images. The study confirms the absence of contrast enhancement of the residual tumor

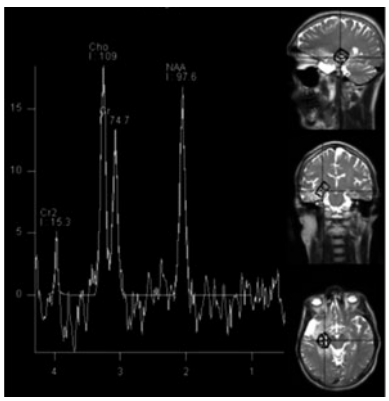

Fig. 9.5 Single-voxel MR spectroscopy. Inversion of the choline-creatine peak level in the residual tumor can be appreciated

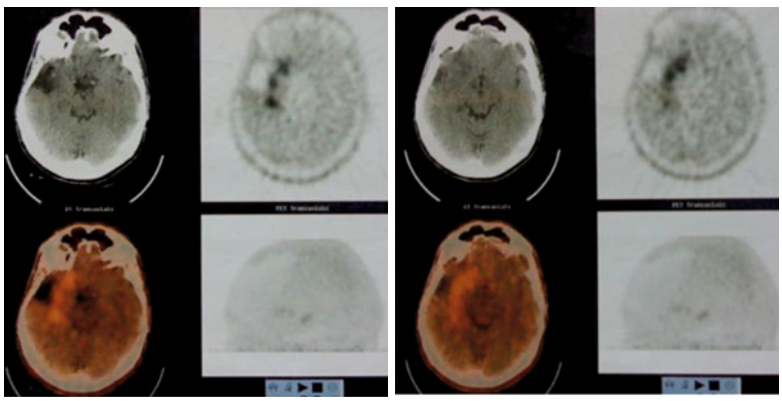

Fig. 9.6 Methionine PET study. The residual tissue shows high metabolic activity

Postoperative Follow-up at 4 Years

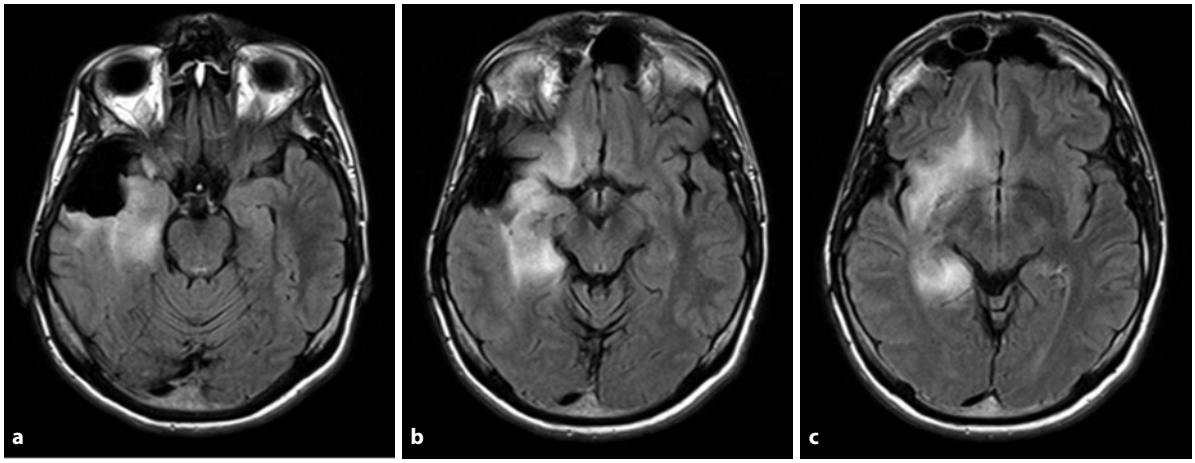

Fig. 9.7 a-c MR FLAIR sequence. The images show an increase of the infiltrating tissue, which extends to the temporal-mesial and frontal-basal region

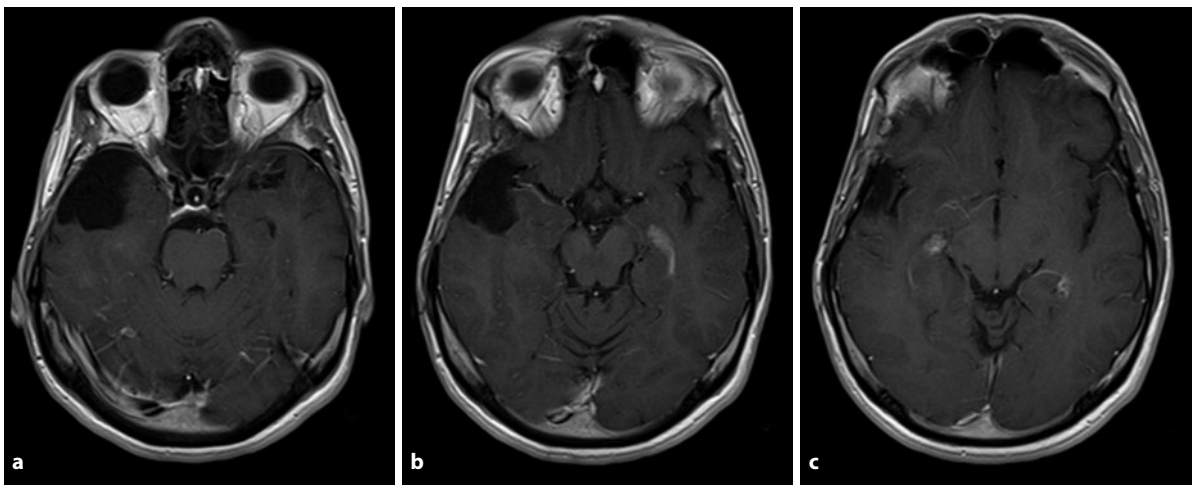

Fig. 9.8 a-c Contrast-enhanced MR SE T1-weighted images. The study confirms the absence of contrast enhancement of the residual tumor

Case 10

Low-grade Residual Tumor

Morphofunctional MR Follow-up in Anaplastic Oligoastrocytoma

Alessandro Stecco, Francesco Fabbiano, Sara Zizzari, Gerardo Di Nardo, Mariangela Lombardi, Andrea Pietro Sponghini and Alessandro Carriero

- 45-year-old patient with bilateral frontal anaplastic oligoastrocytoma treated with subtotal resection and subsequent combined radiation therapy-chemotherapy
- Morphofunctional MR follow-up performed with morphologic study, perfusion and spectroscopy preoperatively and at 3 months after surgery and radiation therapy-chemotherapy

Preoperative Imaging

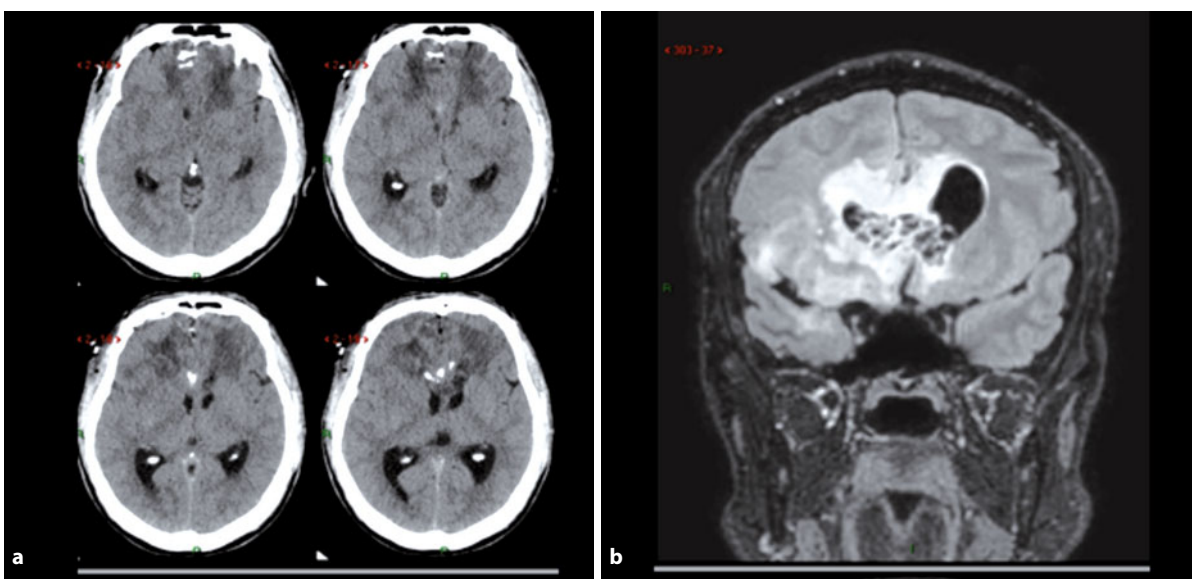

Fig. 10.1 **a** Baseline CT scan. A bilateral frontal lesion can be seen spanning the anterior genu of the corpus callosum with macrocalcifications in the frontal polar (right paramedian) region and at the level of the corpus callosum. **b** MR fluid attenuated inversion recovery with fat saturation (FLAIR FS) sequences show the hyperintense lesion extending across the corpus callosum and midline area. The presence of areas of altered signal compatible with microcalcifications in the anterior genu of the corpus callosum and diffuse perilesional hyperintensity can also be appreciated

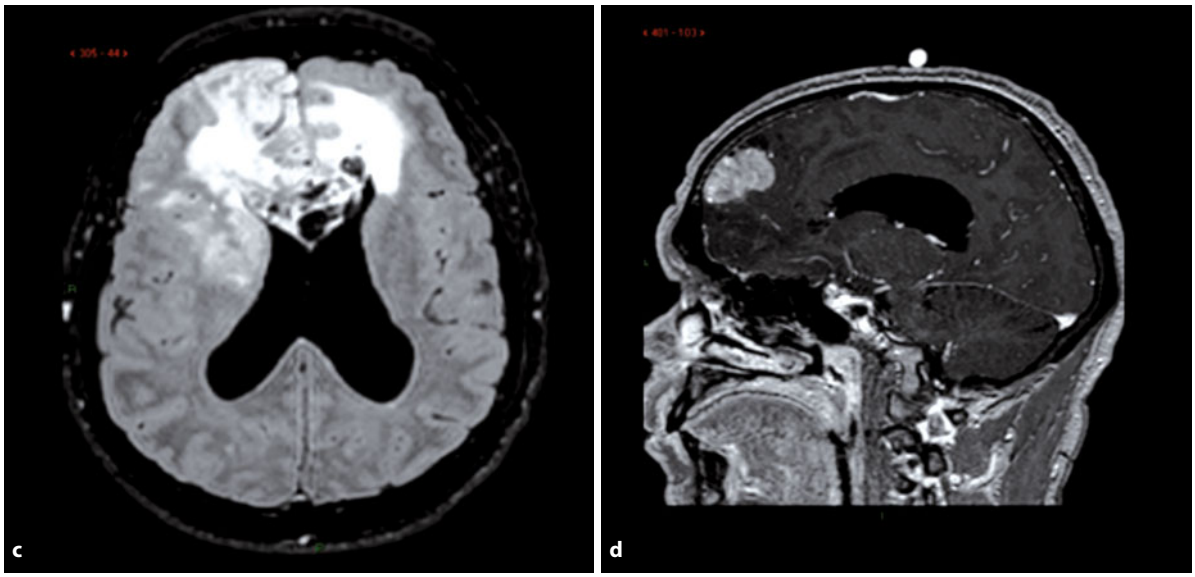

Fig. 10.1 **c** MR fluid attenuated inversion recovery with fat saturation (FLAIR FS) sequences show the hyperintense lesion extending across the corpus callosum and midline area. The presence of areas of altered signal compatible with microcalcifications in the anterior genu of the corpus callosum and diffuse perilesional hyperintensity can also be appreciated. **d** Contrast-enhanced MR SE T1-weighted sequence depicts intense pathologic enhancement of the polar component of the frontal lesion

Follow-up at 3 Months After Surgery and Radiation Therapy

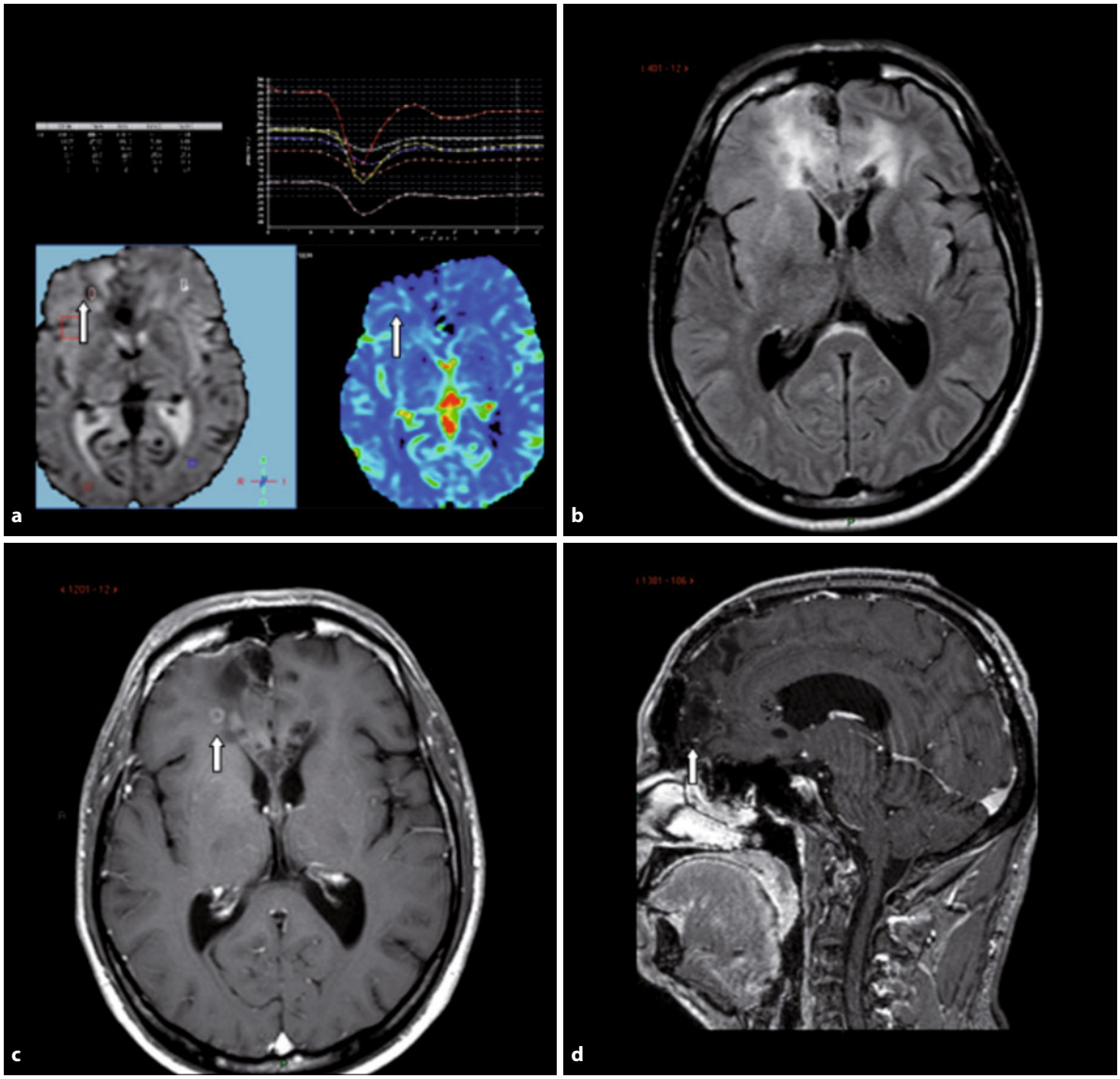

Fig. 10.2 **a** MR perfusion study with relative CBV map. An ROI (*white arrow*) is placed on a hypoperfused nodule on the CBV map (*white circle*). **b** MR FLAIR sequence shows residual alteration in the deep frontal white matter and in the anterior genu of the corpus callosum, which appears smaller than in Fig. 10.1 c, in partial response to therapy. **c,d** Contrast-enhanced MR SE T1-weighted sequences show a small nodule of rim enhancement in the context of hypointense area, partly attributable to postsurgical cavitation and in part to residual low-grade tissue

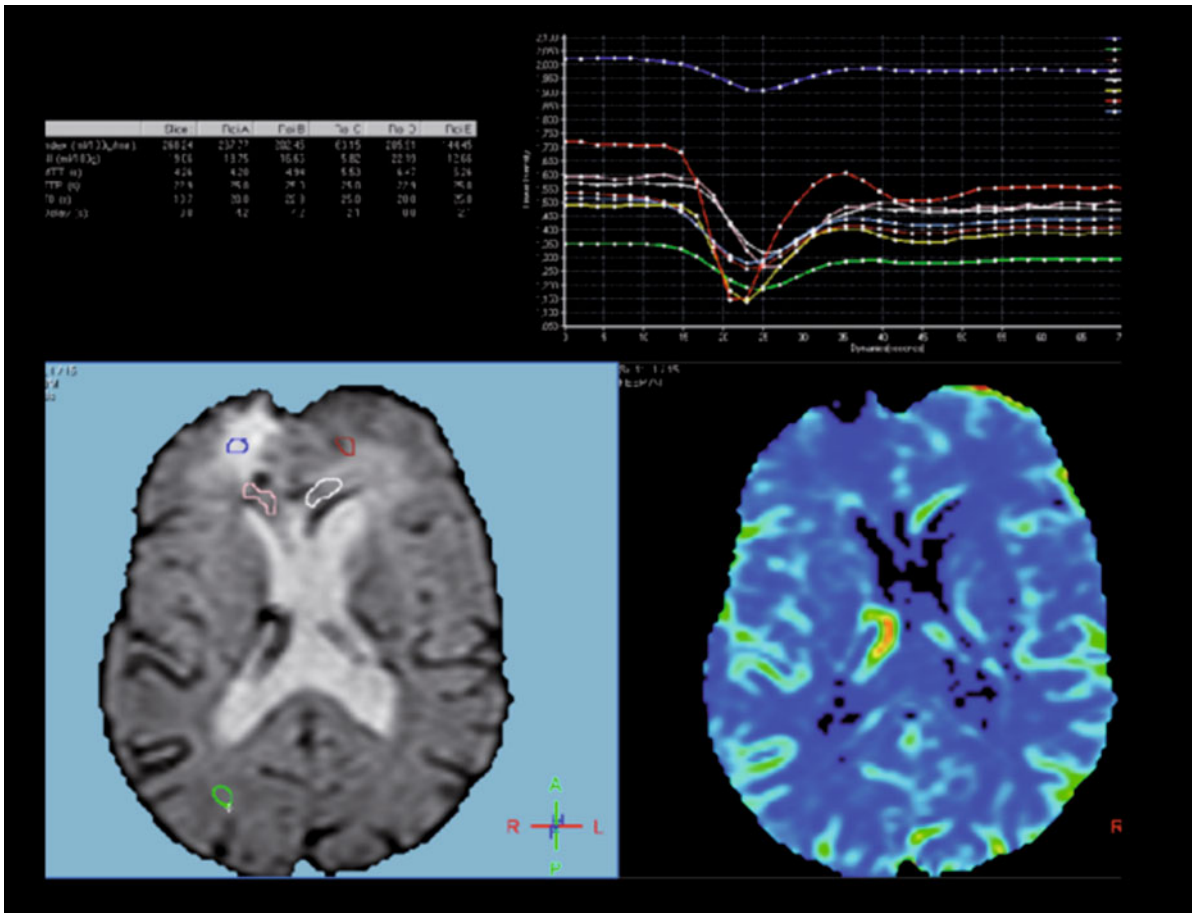

Fig. 10.3 MR perfusion study with relative CBV map. Measurement of CBV perfusion in the bilateral anterior paracallosal area (*pink and white freehand ROIs*) compared with ROIs placed in the bilateral frontal polar subcortical white matter (*blue and red freehand ROIs*) and as a reference in apparently healthy right parietal white matter (*green freehand ROI*) shows evidence of increased CBV in the anterior paracallosal area

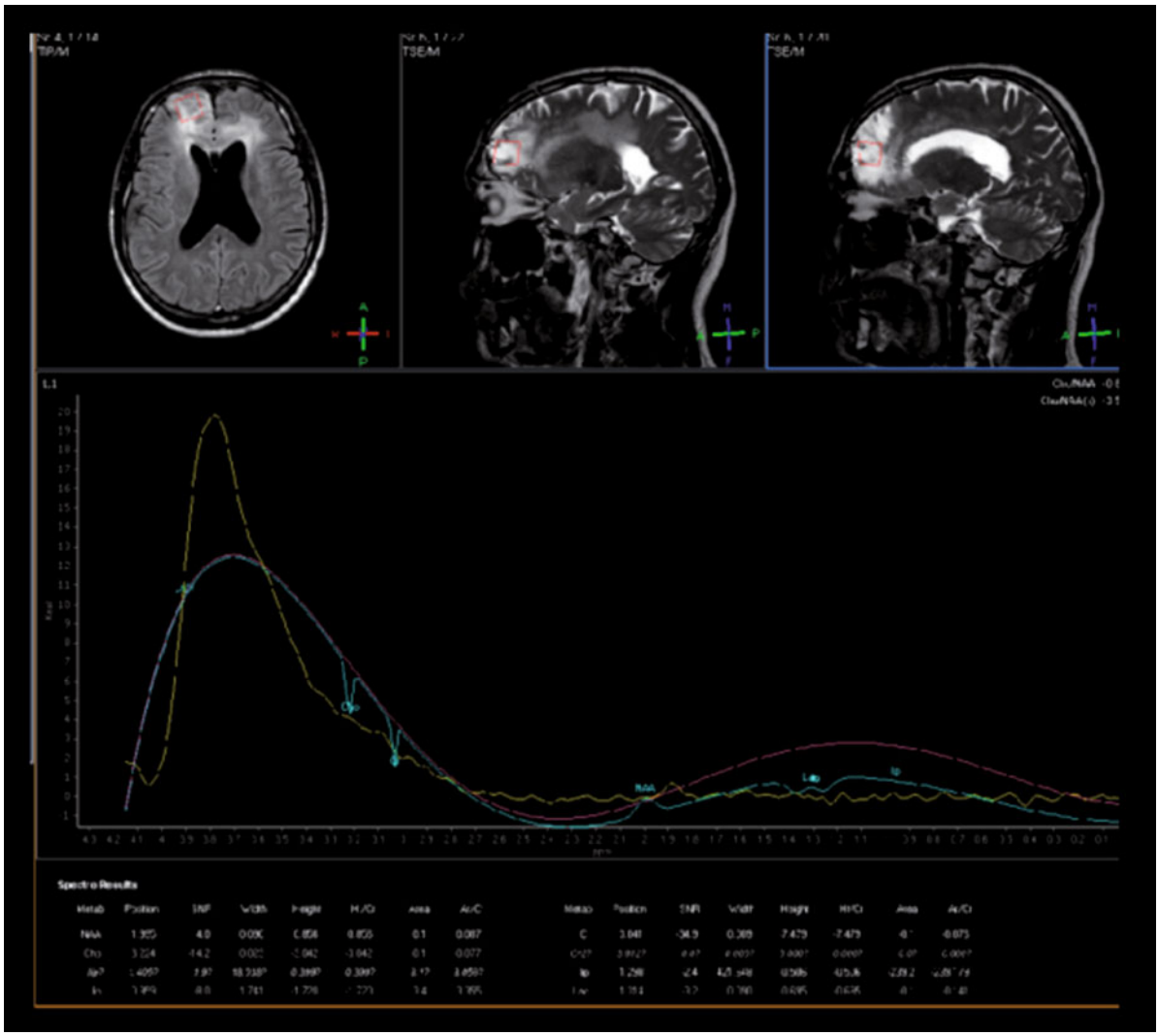

Fig. 10.4 Single-voxel MR spectroscopy. The sampling area has prevailing lesion characteristics of gliosis, cavitation and absence of neuronal metabolites

Case 11

Medium-low-grade Residual Tumor

Morphofunctional MR Follow-up in Astrocytoma

Alessandro Stecco, Sara Zizzari, Francesco Fabbiano, Gerardo Di Nardo, Mariangela Lombardi, Emanuele Malatesta and Alessandro Carriero

- 45-year-old patient with low-grade astrocytoma of the right temporal lobe treated with subtotal excision and subsequent chemotherapy
- Morphofunctional MR follow-up performed with morphologic study, perfusion and spectroscopy at 36 months after surgery and combined chemotherapy

Follow-up at 36 Months After Surgery and Combined Chemotherapy

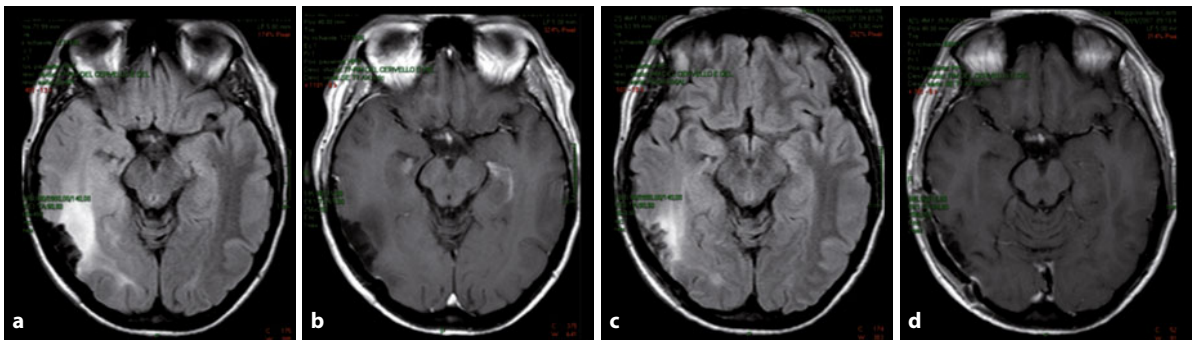

Fig. 11.1 a-d MR FLAIR and contrast-enhanced SE T1-weighted sequences on two contiguous sections. A cavitary cystic area can be seen accompanied by a solid residual portion appearing hyperintense in FLAIR and hypointense in T1 without pathologic enhancement, located in the deep white matter of the right temporal lobe

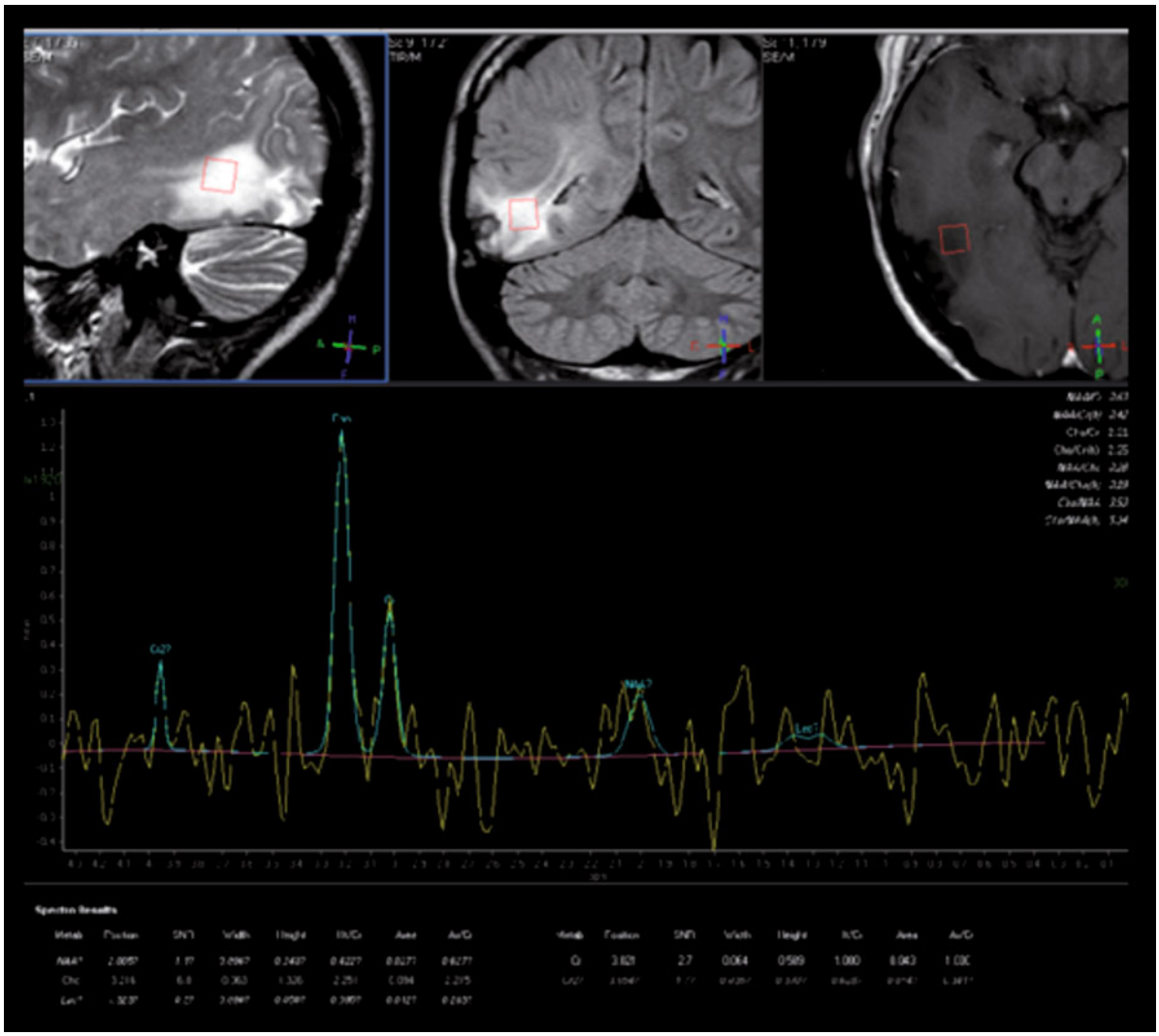

Fig. 11.2 Single-voxel MR spectroscopy. The ROI placed in the residual solid tissue in the temporal lobe shows a reduction in NAA and an increase in Cho with metabolic ratios compatible with low-medium grade residual disease, in the context of the perilesional hyperintense area in FLAIR

Case 12

Medium-low-grade Residual Tumor

Morphofunctional MR Follow-up in Fibrillar Astrocytoma

Alessandro Stecco, Sara Zizzari, Francesco Fabbiano, Gerardo Di Nardo, Mariangela Lombardi, Giuseppe Fiscer and Alessandro Carriero

- 58-year-old patient with low-grade astrocytoma of the left frontal lobe treated with surgery and first-line chemotherapy
- Morphofunctional MR follow-up performed with morphologic study, perfusion and spectroscopy preoperatively and at 5 and 10 months after surgery and combined chemotherapy

Preoperative Imaging

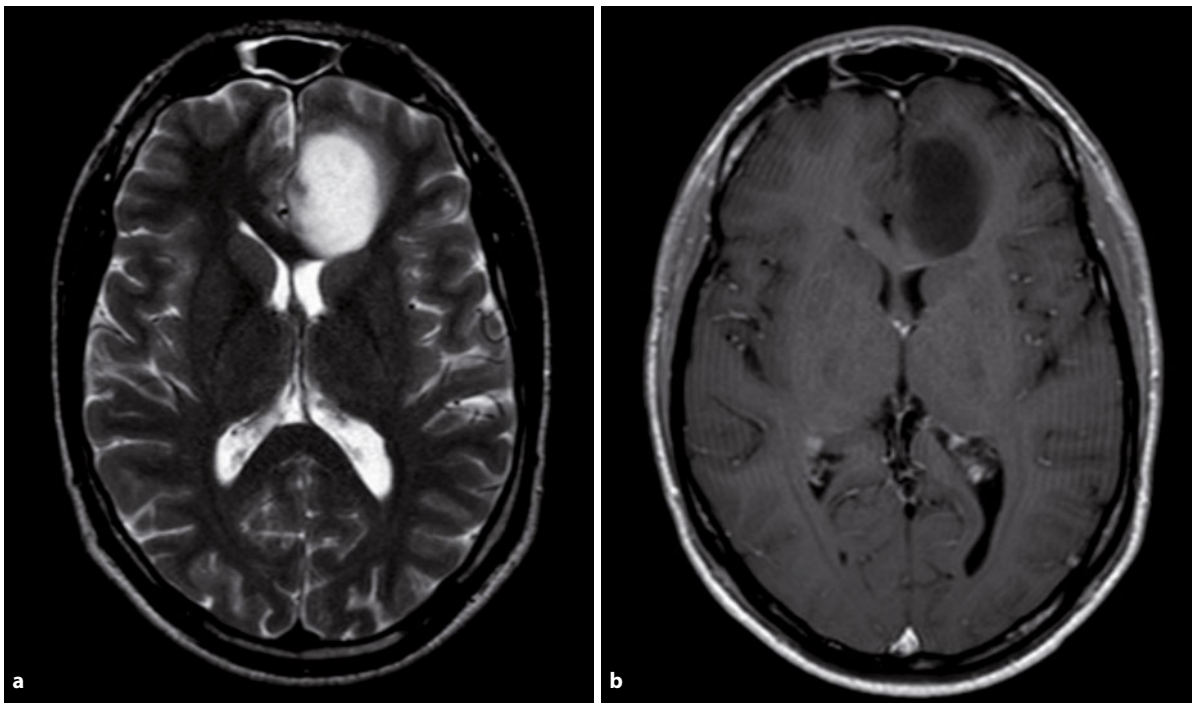

Fig. 12.1 **a** MR FSE T2-weighted sequence shows intra-axial deep left frontal lesion with involvement of the rostrum of the corpus callosum and mass effect on neighboring structures. **b** Contrast-enhanced MR SE T1-weighted sequence. No pathologic enhancement is evident at the lesion site

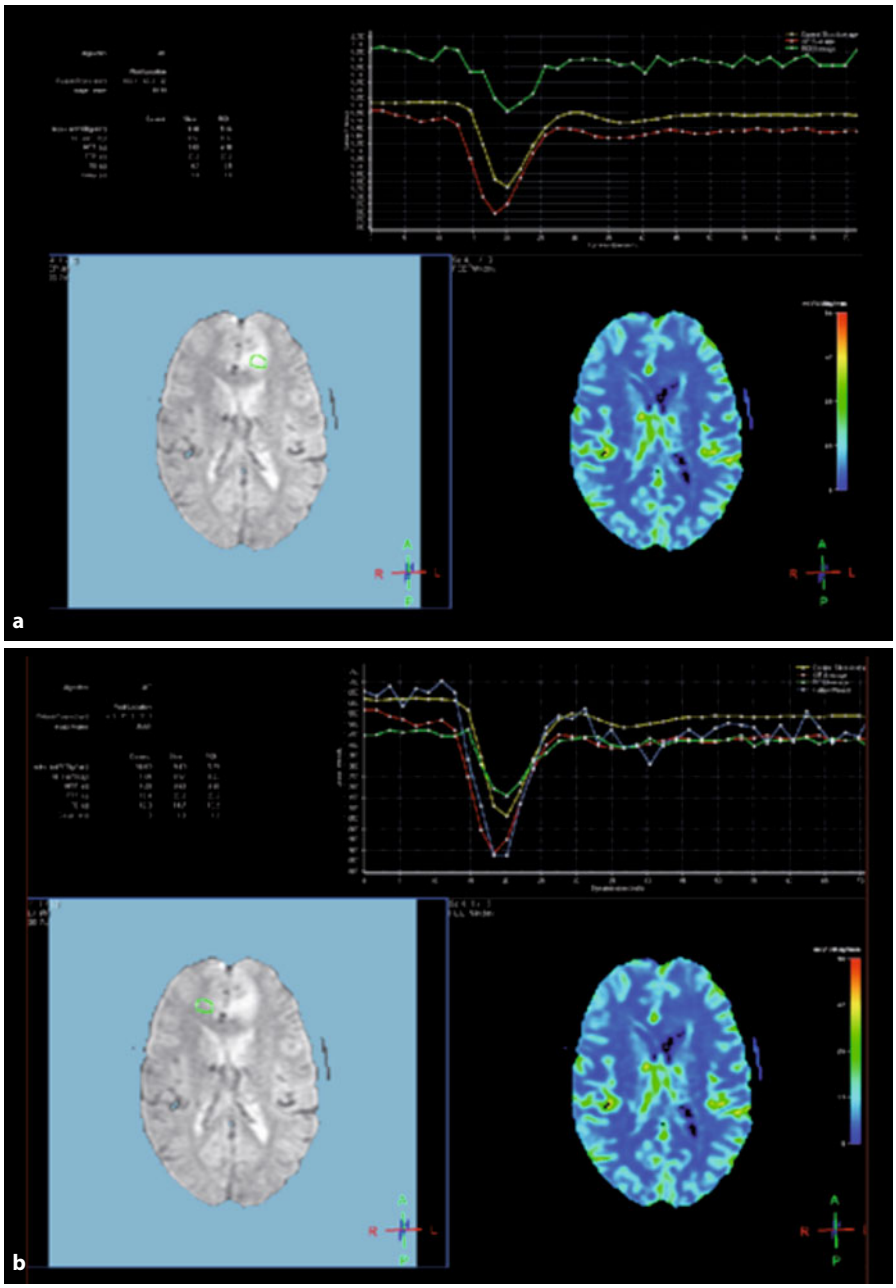

Fig. 12.2 MR perfusion study with relative CBV map showing an ROI placed on the lesion (**a**) and on an apparently healthy contralateral area (**b**). The comparison shows the lower CBV in the lesion area than in the healthy contralateral tissue, thus indicating weak neovascularization

Follow-up at 5 Months After Surgery

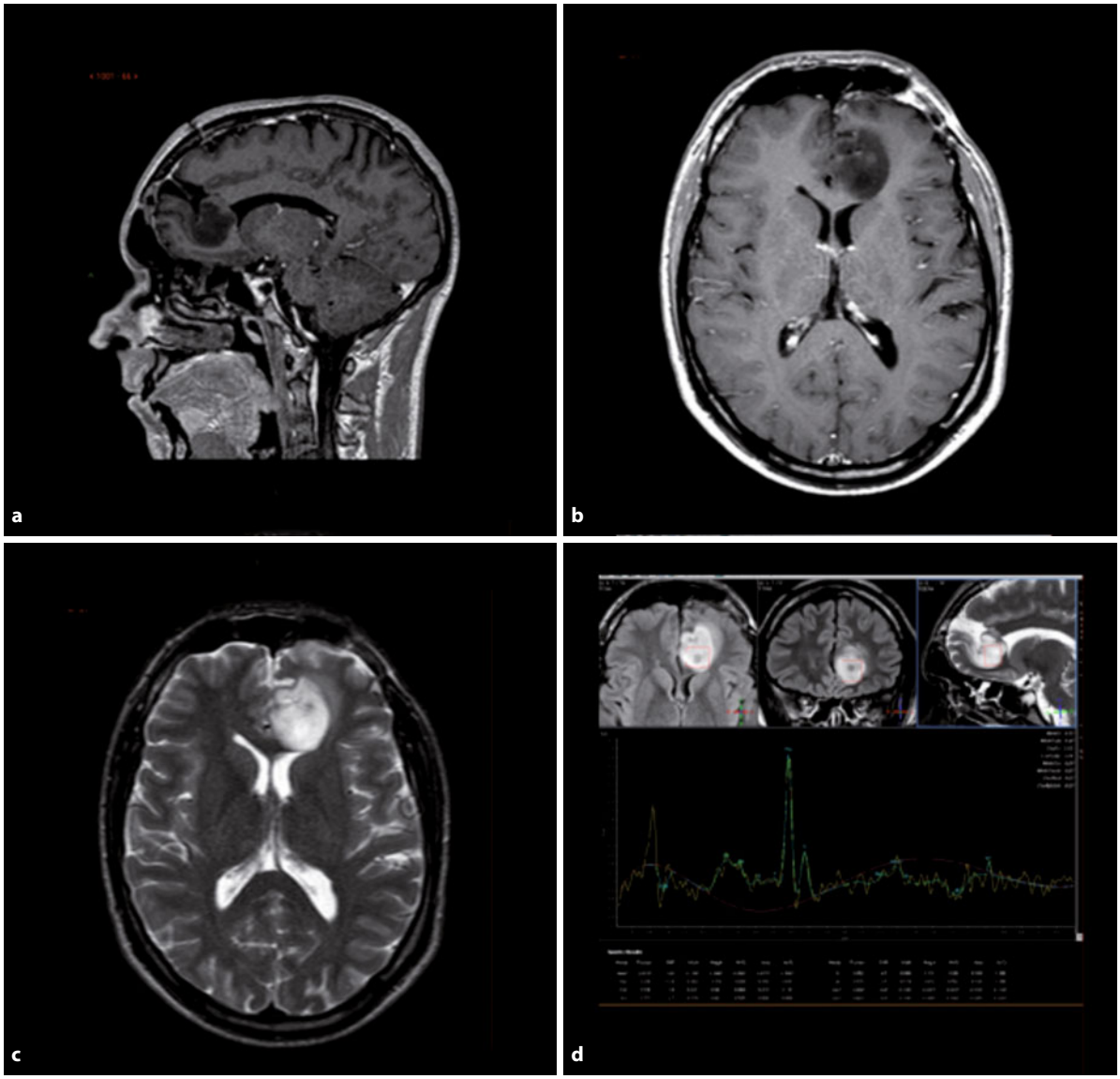

Fig. 12.3 **a-c** Contrast-enhanced MR SE T1-weighted and FSE T2-weighted sequences show postsurgical findings of partial resection at 1 month with residual disease. **d** Single-voxel MR spectroscopy. Sampling of the residual lesion shows a metabolic pattern consistent with low-to-medium grade lesion

Follow-up at 10 Months

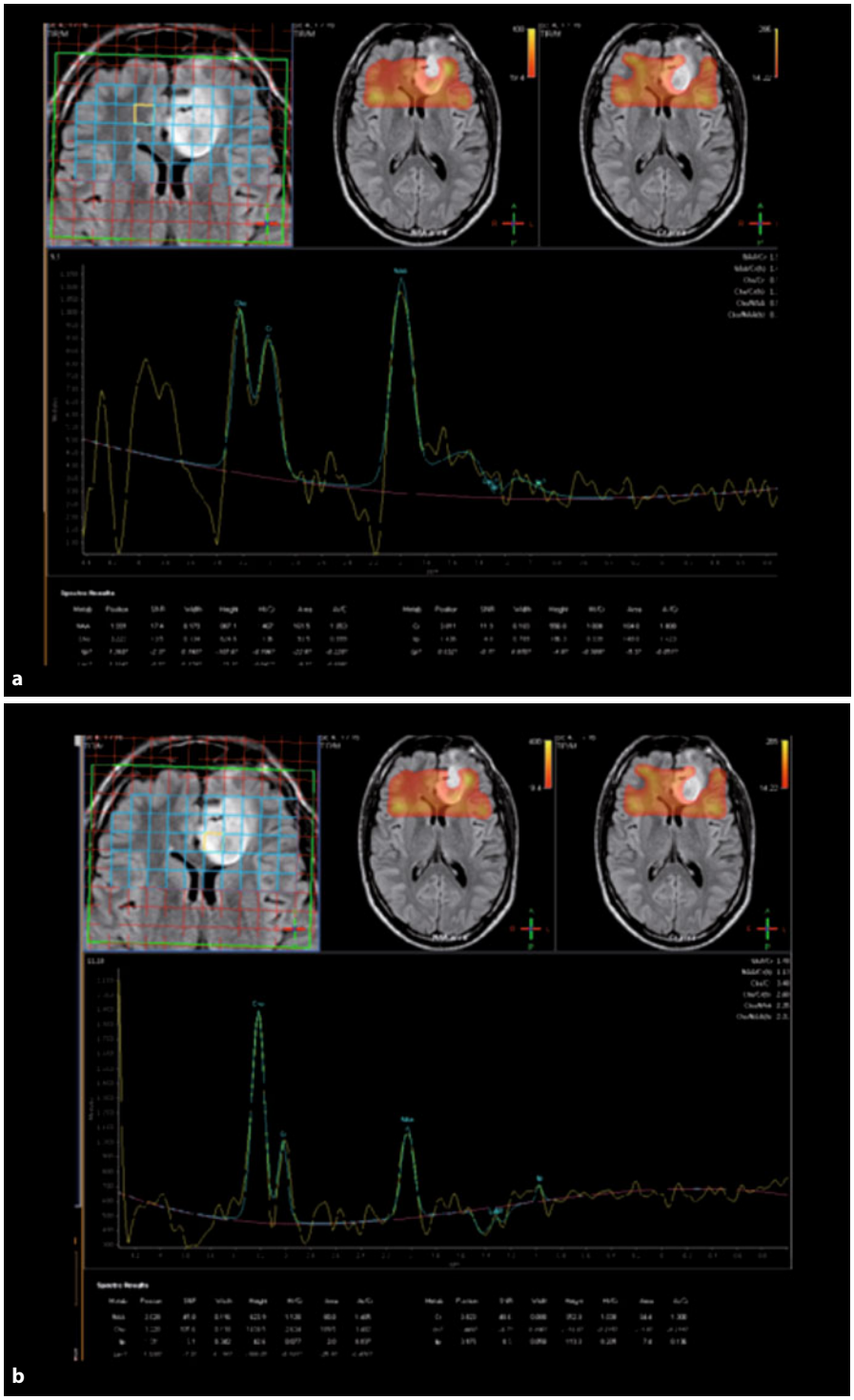

Fig. 12.4 Multivoxel MR spectroscopy. The apparently healthy sampling area (**a**) and pathologic tissue (**b**) show at that level a pattern of metabolites consistent with the presence of low-to-medium grade residual cancer

Case 13

Medium-low-grade Residual Tumor

Morphofunctional MR Follow-up in Anaplastic Oligodendroglioma

Alessandro Stecco, Francesco Fabbiano, Sara Zizzari, Gerardo Di Nardo, Mariangela Lombardi, Lorenzo Fortunelli and Alessandro Carriero

- 58-year-old patient with right frontal-temporal-parietal-insular anaplastic oligodendroglioma treated with surgery and subsequent combined radiation therapy-chemotherapy and second-line chemotherapy
- Morphofunctional MR follow-up performed with morphologic study, perfusion and spectroscopy preoperatively and at 10, 15 and 19 months after surgery and combined chemotherapy

Preoperative Imaging

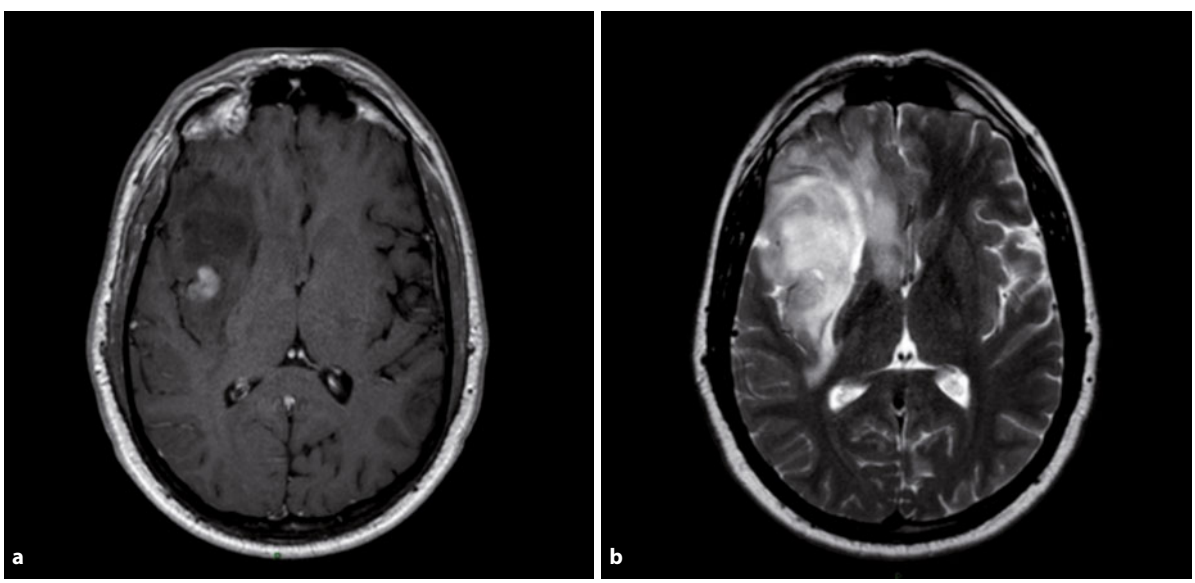

Fig. 13.1 Contrast-enhanced MR SE T1-weighted (**a**), FSE T2-weighted (**b**) and diffusion-weighted (**c**) sequences. A primary intra-axial neoplasm can be appreciated in the right frontal-insular lobe with diffuse perilesional signal alterations at the level of the white matter and in the frontal basal ganglia, with associated mass effect on neighboring structures. After contrast medium administration a pseudonodular enhancement can be appreciated in the subcortical right insular region. **d** Multi-voxel MR spectroscopy shows a Cho peak within the lesion (*cont.* →)

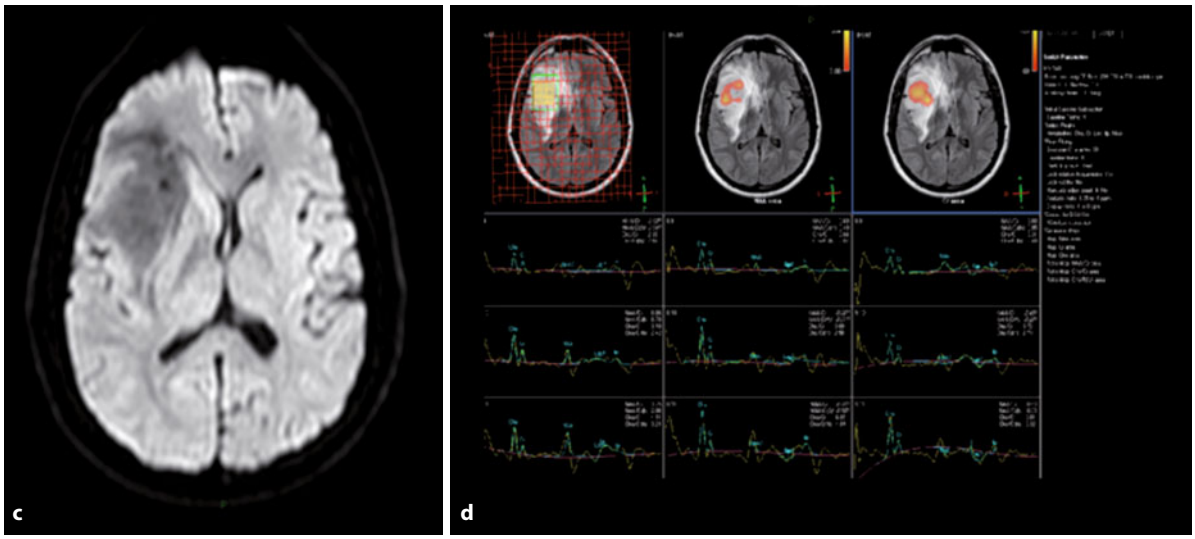

Fig. 13.1 (*continued*)

Follow-up at 10 Months After Surgery, Radiation Therapy and Chemotherapy

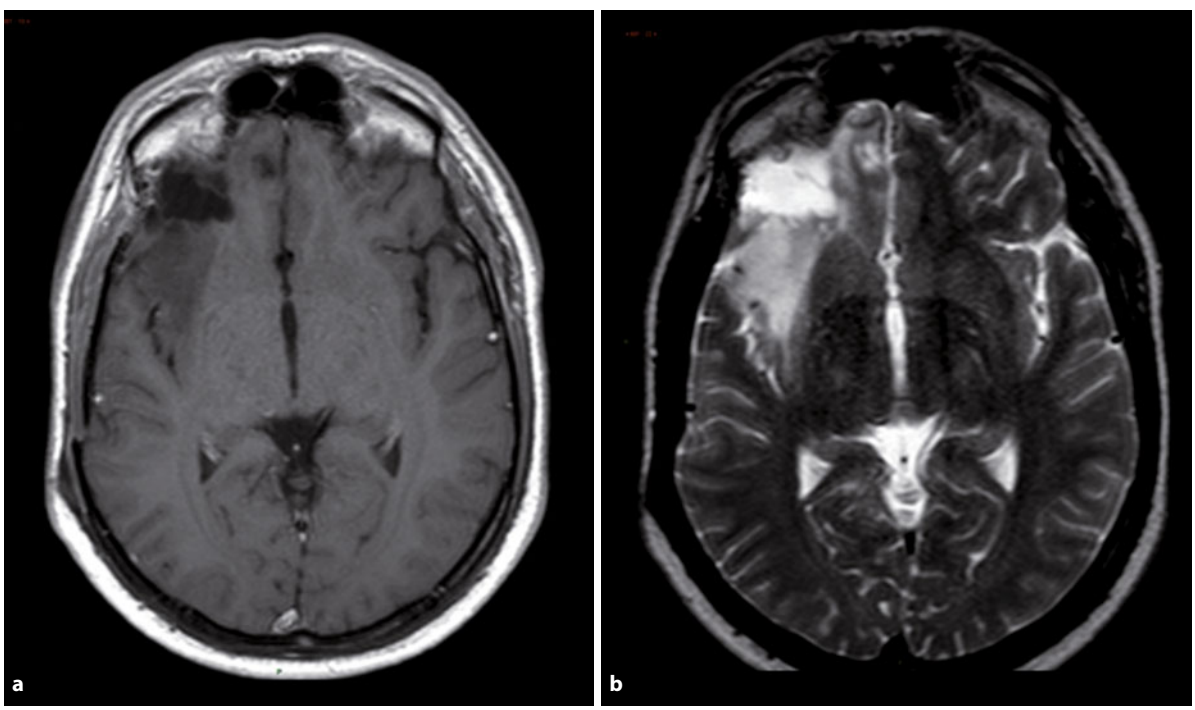

Fig. 13.2 **a** Contrast-enhanced MR SE T1-weighted sequence shows nonenhancing residual tumor in inferior frontal location and postsurgical cavity in anteroinferior location at the level of the upper right orbital gyrus. **b** Contrast-enhanced MR SE T1-weighted sequence. The residual signal alteration appears to extend to the insula and external capsule

Follow-up at 15 Months

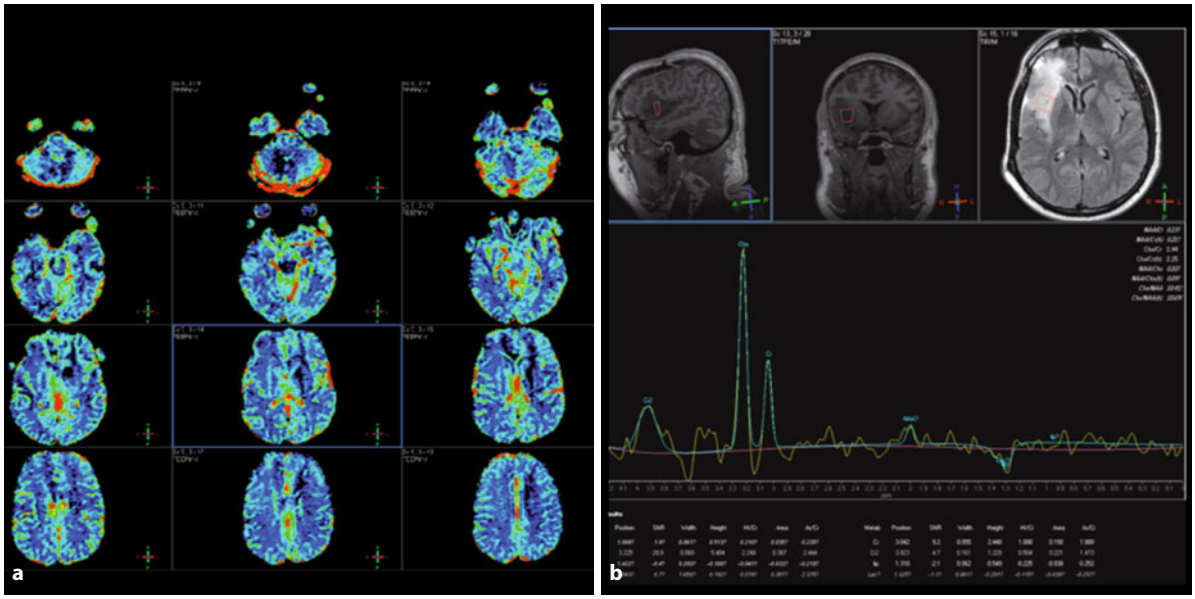

Fig. 13.3 **a** MR perfusion study with relative CBV map shows no significant increase in perfusion in the lesion. **b** Single-voxel MR spectroscopy confirms the findings of residual cancer without disease progression

Follow-up at 19 Months

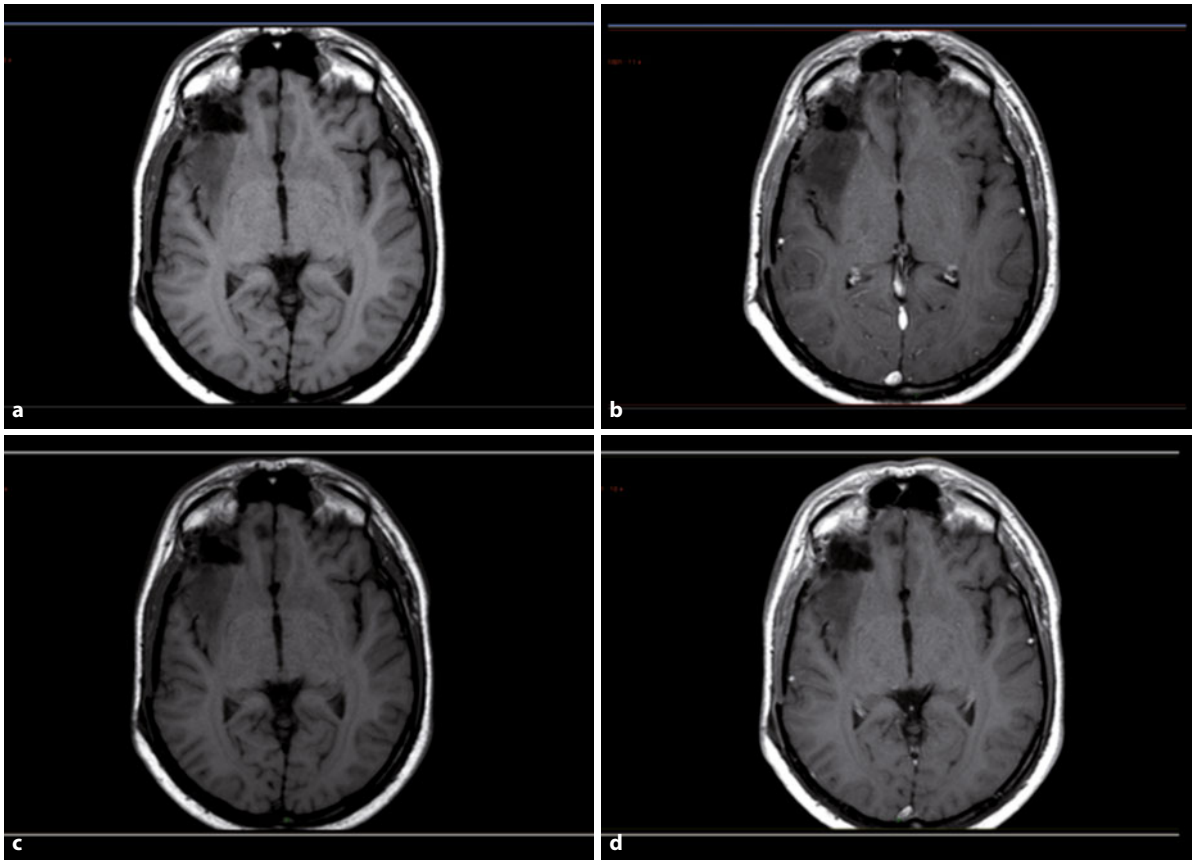

Fig. 13.4 Comparison between contrast-enhanced MR SE T1-weighted sequences at 5 months after surgery and prior to chemotherapy and radiation therapy (**a,b**) and post-chemotherapy images at 19 months postoperatively (**c,d**). The post-chemotherapy images show less hypointensity at the level of residual tissue with increasing amplitude of the cavitary cyst in response to therapy

Case 14

High-grade Residual Tumor

Morphofunctional MR Follow-up in Gemistocytic Astrocytoma

Francesco Fabbiano, Alessandro Stecco, Sara Zizzari, Gerardo Di Nardo, Anthony Azubuike Obaze, Mariangela Lombardi and Alessandro Carriero

- 71-year-old patient affected by right parietal gemistocytic astrocytoma treated with subtotal resection and subsequent combined radiation therapy-chemotherapy
- Morphofunctional MR follow-up performed with morphologic study, perfusion and spectroscopy preoperatively and at 3 months after surgery and radiation therapy-chemotherapy

Preoperative Imaging

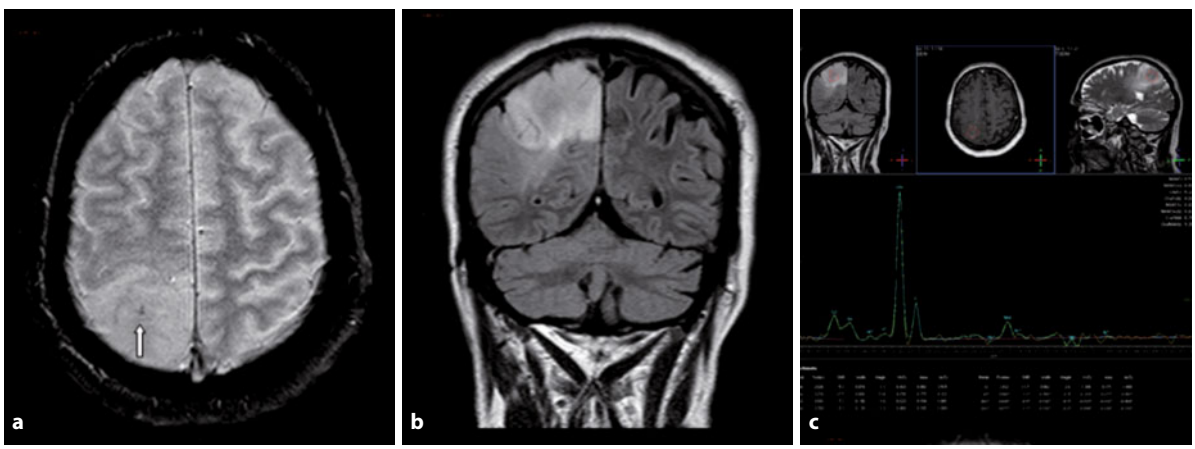

Fig. 14.1 a MR FFE T2*-weighted sequence shows small focal inhomogeneities induced by microcalcification (*white arrow*) within the lesion in the right parietal lobe. **b** Morphologic MR FLAIR images show right parietal cortical-subcortical pathologic tissue and perilesional signal alteration. **c** Single-voxel MR spectroscopy. The metabolic ratios are consistent with the presence of a high-grade glial lesion

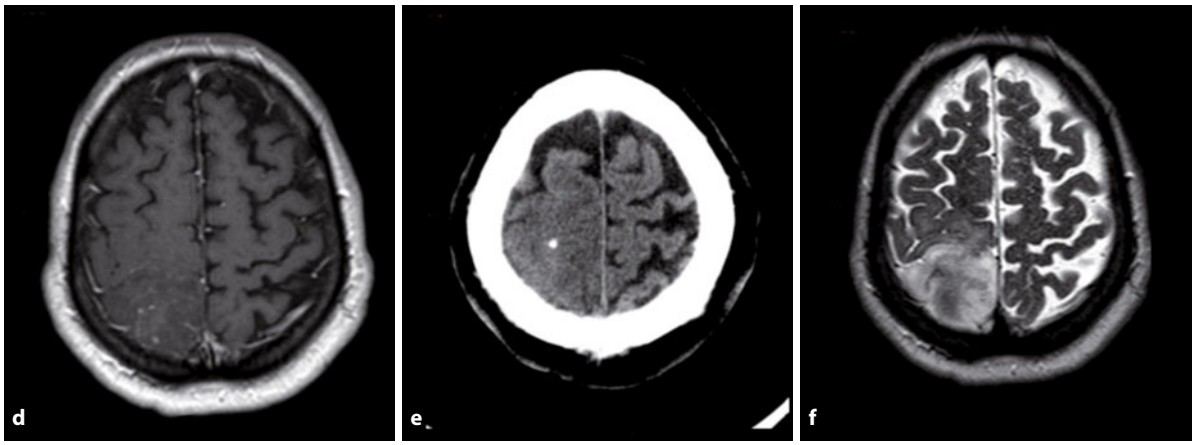

Fig. 14.1 d Contrast-enhanced MR SE T1-weighted sequence shows a slight pathologic enhancement in the right parietal cortical-subcortical lobe. **e** Baseline CT scan shows microcalcification in the lesion in the right parietal lobe. **f** MR FSE T2-weighted sequence. The right parietal cortical-subcortical pathologic tissue is visible with low signal in T2 accompanied by perilesional changes

Follow-up at 3 Months After Subtotal Resection and Radiation Therapy-chemotherapy

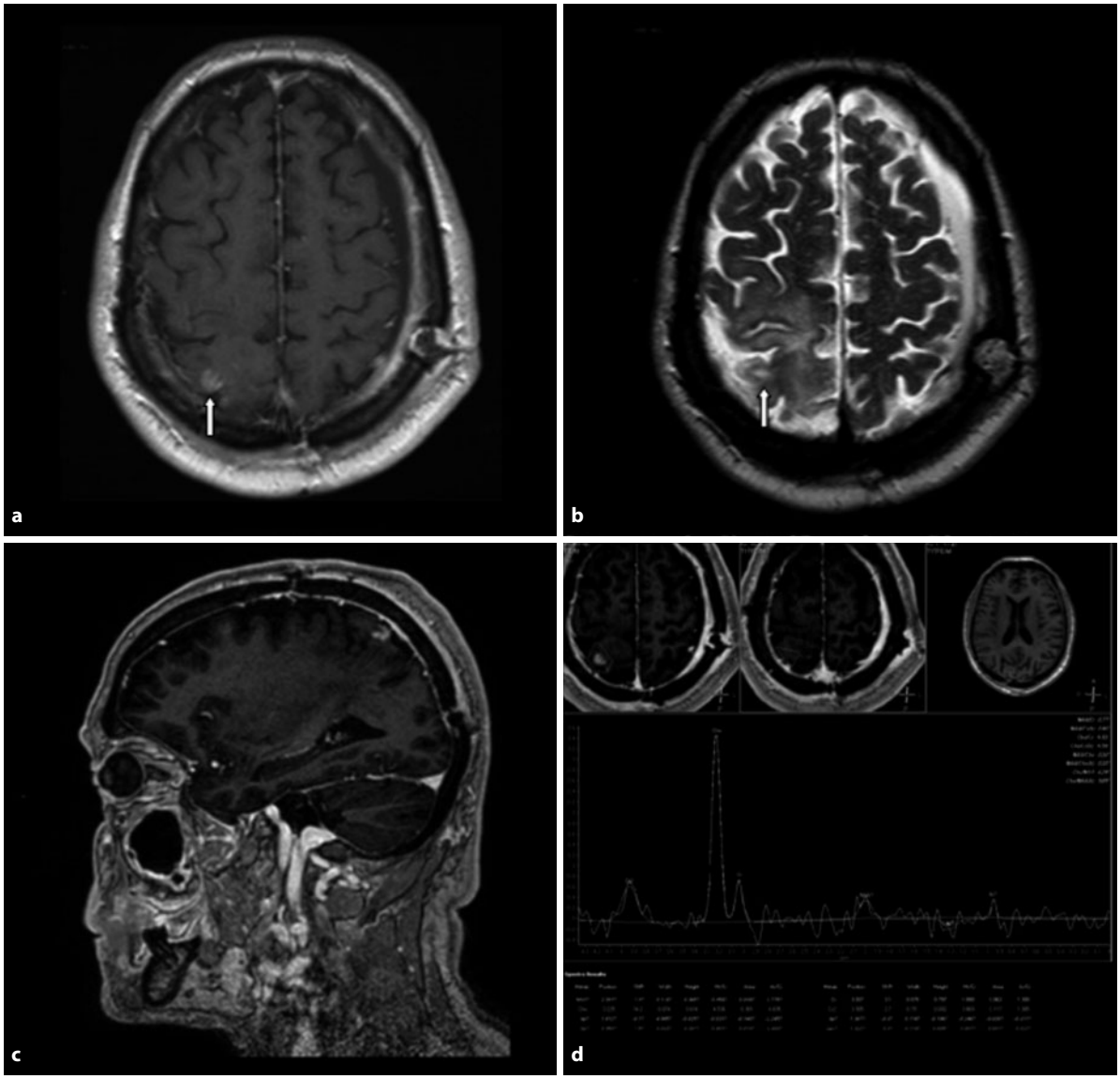

Fig. 14.2 **a** Contrast-enhanced MR SE T1-weighted sequence shows slight pathologic enhancement with the presence of a more notable enhancing nodule in the cortical-subcortical area (*white arrow*). **b** MR FSE T2-weighted sequence visualizes the area of pathologic enhancement corresponding to tissue with low signal in T2 (*white arrow*). **c** Contrast-enhanced MR SE T1-weighted sequence shows the residual tumor with enhancement in the right parietal cortical-subcortical lobe. **d** Single-voxel MR spectroscopy. Sampling on the enhancing lesion shows marked elevation of the Cho peak and reduced NAA with metabolic ratios consistent with a high-grade lesion

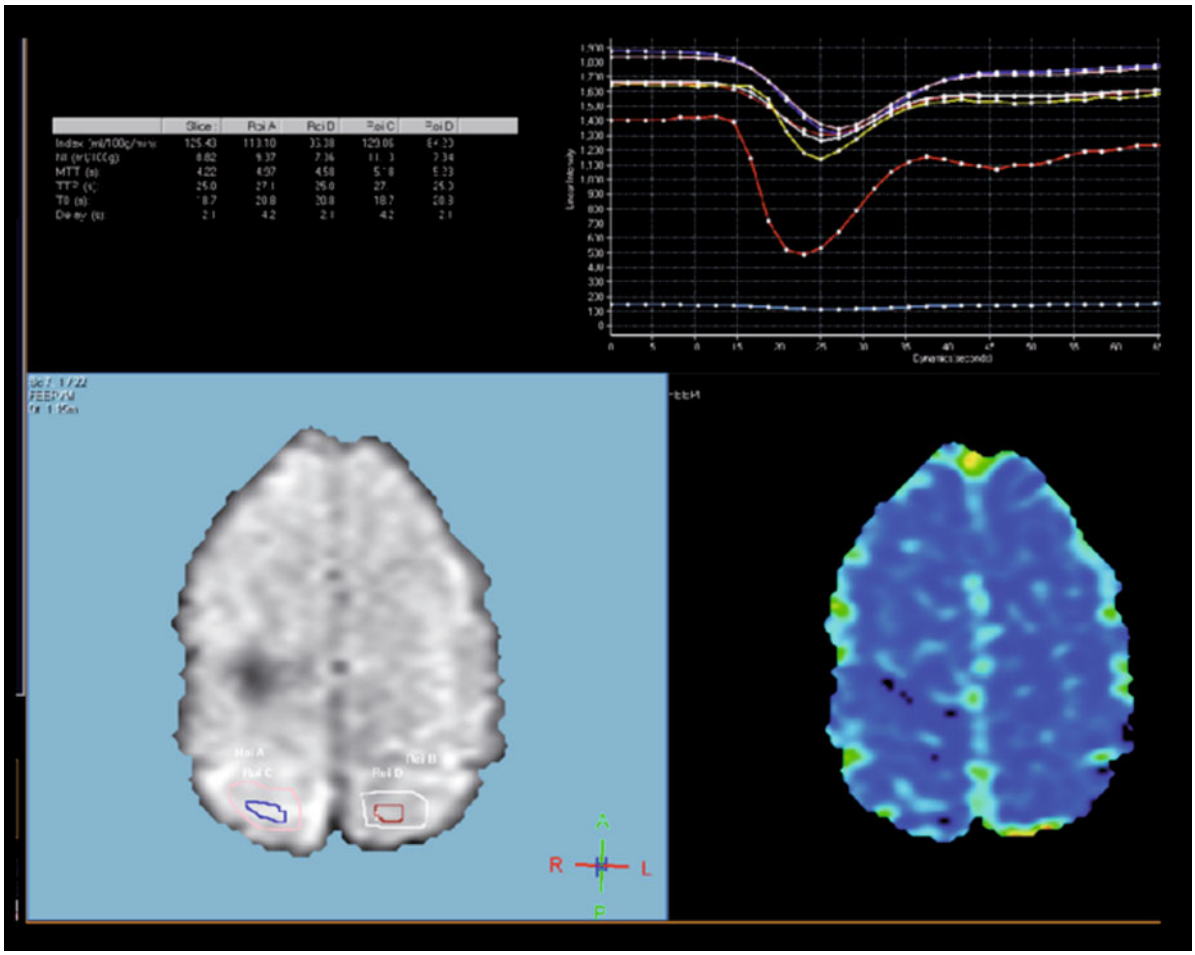

Fig. 14.3 MR perfusion study with relative CBV map shows a blue ROI placed on the residual tumor and a red ROI on apparently normal contralateral area. The elevated CBV is compatible with high-grade residual tumor

Case 15

High-grade Residual Tumor

Morphofunctional MR Follow-up in Low-grade Oligoastrocytoma and Following Anaplastic Transformation

Alessandro Stecco, Sara Zizzari, Francesco Fabbiano, Gerardo Di Nardo, Mariangela Lombardi, Ignazio Divenuto and Alessandro Carriero

- Patient with right frontal low-grade oligoastrocytoma treated with partial excision surgery and subsequent combined radiation therapy-chemotherapy following anaplastic transformation
- Morphofunctional MR follow-up performed with morphologic study, perfusion and spectroscopy at 24 months after surgery and combined chemotherapy

Follow-up at 24 Months After Surgery and Radiation Therapy-chemotherapy

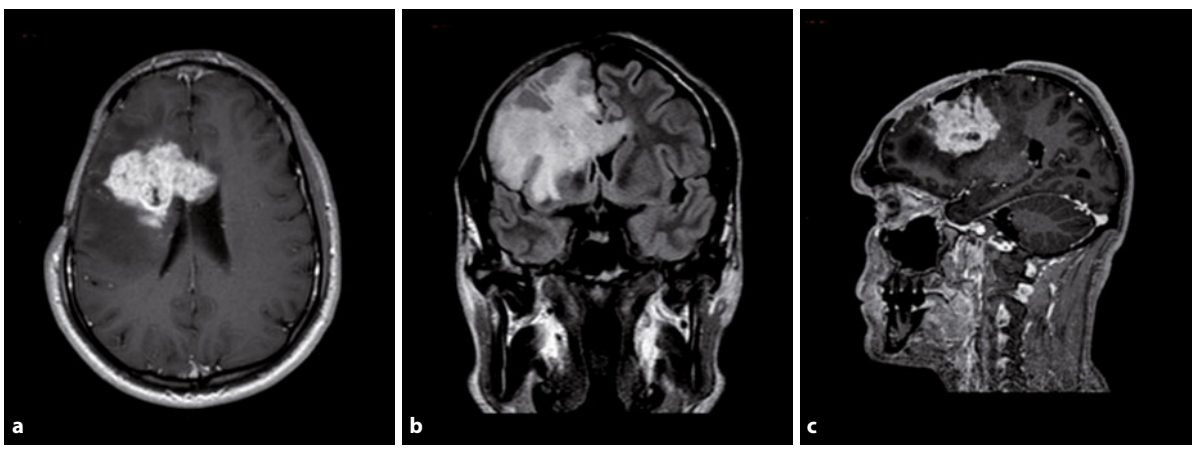

Fig. 15.1 a-c Contrast-enhanced MR SE T1-weighted and FLAIR sequences show massive recurrence of disease in the right deep frontal region involving the basal ganglia, the corpus callosum and extending across the midsagittal line. The FLAIR sequence shows the extension of pathologic tissue in the midline and contralateral area

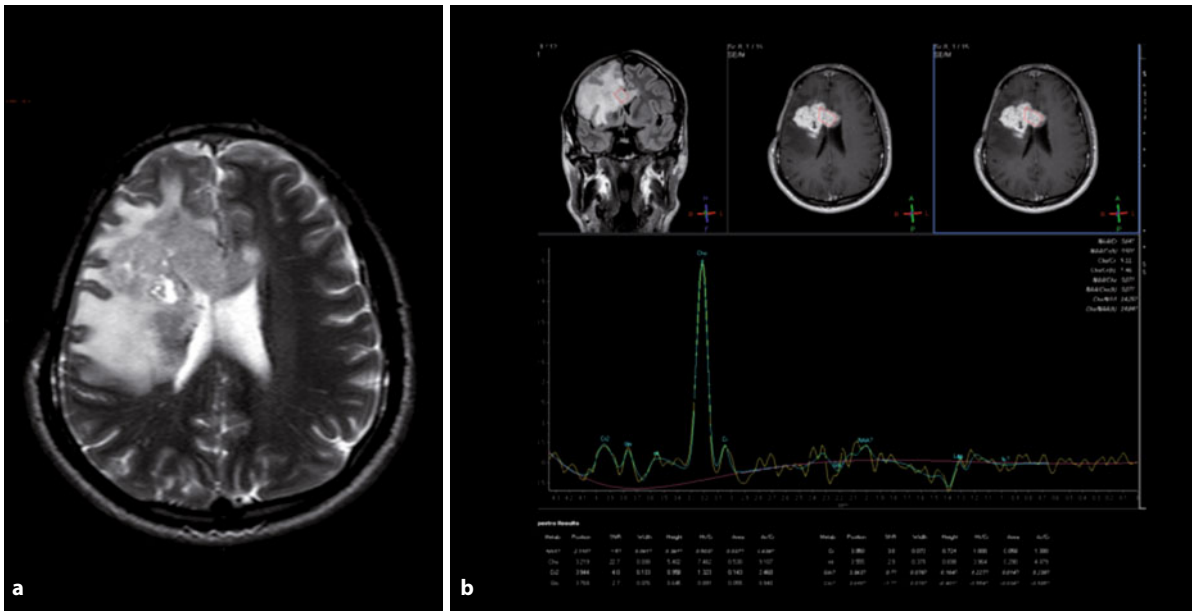

Fig. 15.3 **a** MR FSE T2-weighted sequence shows pathologic tissue with low signal on T2 indicating a high ratio of nucleus-cytoplasm. **b** Single-voxel MR spectroscopy. NAA is almost completely absent and there is marked elevation of Cho with metabolic ratios compatible with the presence of residual high-grade cancer. The presence of small Lac peak indicates necrosis

Case 16

Stable Disease

Multimodal CT/MR Follow-up in Glioblastoma Multiforme

Sara Zizzari, Alessandro Stecco, Mariangela Lombardi, Gerardo Di Nardo, Francesco Fabbiano, Andrea Pietro Sponghini and Alessandro Carriero

- 45-year-old patient with left parietal-occipital glioblastoma multiforme treated with surgery and combined radiation therapy-chemotherapy and subsequent second-line adjuvant chemotherapy
- Multimodal CT (morphologic and perfusion) and morphologic MR follow-up at 3, 5 and 8 months after surgery and combined radiation therapy-chemotherapy

Follow-up at 3 Months After Surgery

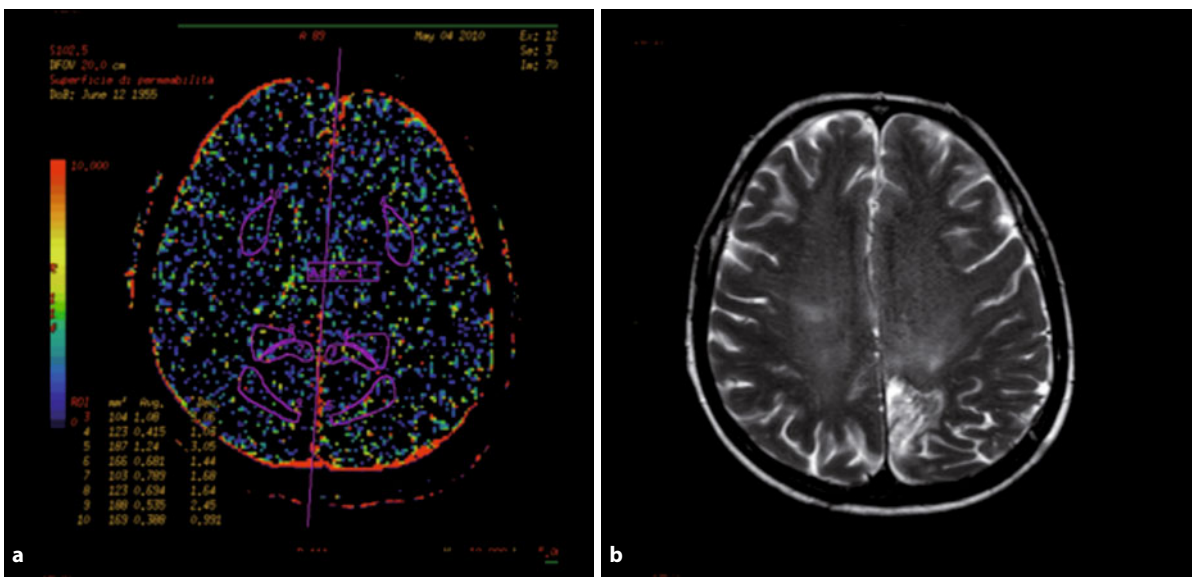

Fig. 16.1 **a** CT perfusion map of permeability surface (PS) shows an absence of significant residual tumor around the surgical cavity. **b** MR FSE T2-weighted sequence depicting the postsurgical cavity

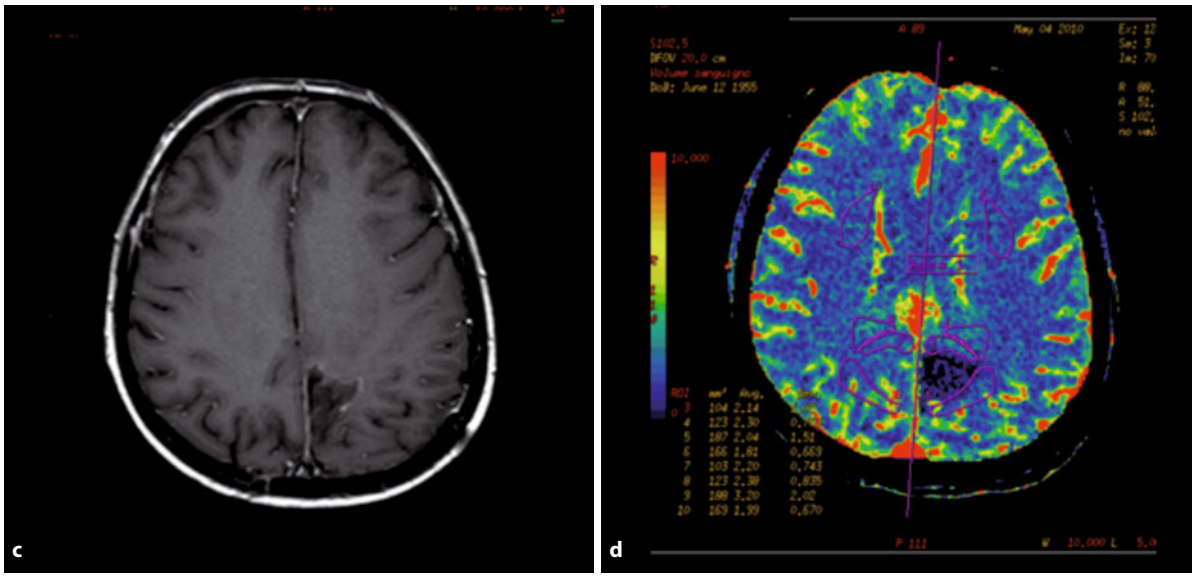

Fig. 16.1 **c** Contrast-enhanced MR SE T1-weighted image. Postsurgical cavitation with non-neoplastic fine rim enhancement visualized shortly after the surgical procedure. **d** CT perfusion study with relative CBV map shows an absence of elevated tissue parameters

Follow-up at 5 Months After Surgery and Subsequent Radiation Therapy-chemotherapy

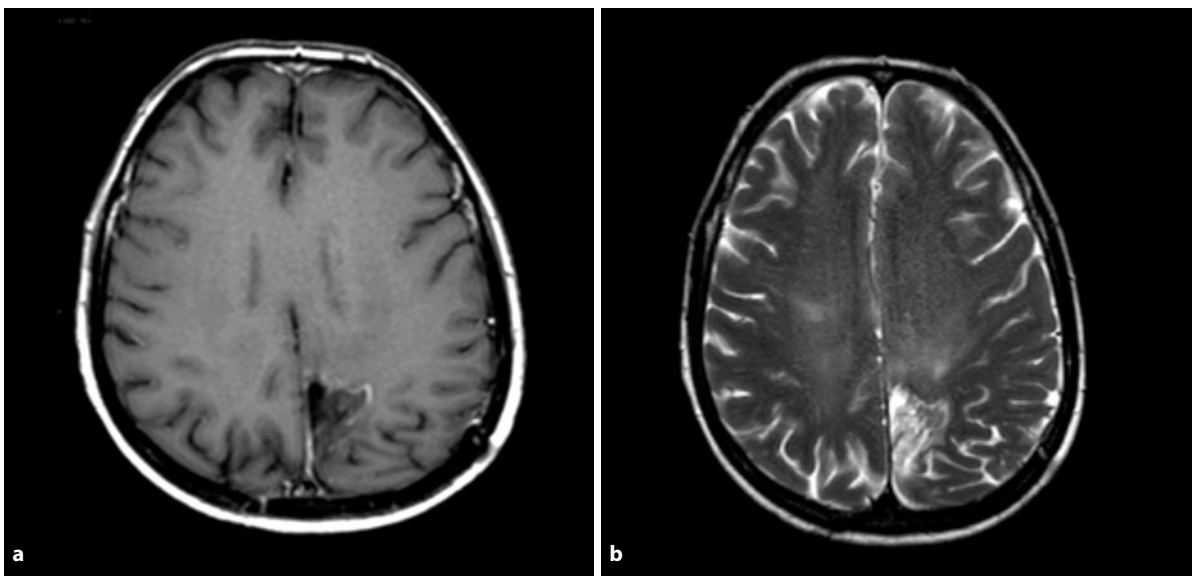

Fig. 16.2 Contrast-enhanced MR SE T1-weighted (**a**) and FSE T2-weighted (**b**) sequences depict an absence of disease progression and reduction in the solid tissue component at the surgical site in response to treatment with associated enlargement of the cavity compared to Fig. 16.1 c

Follow-up at 8 Months

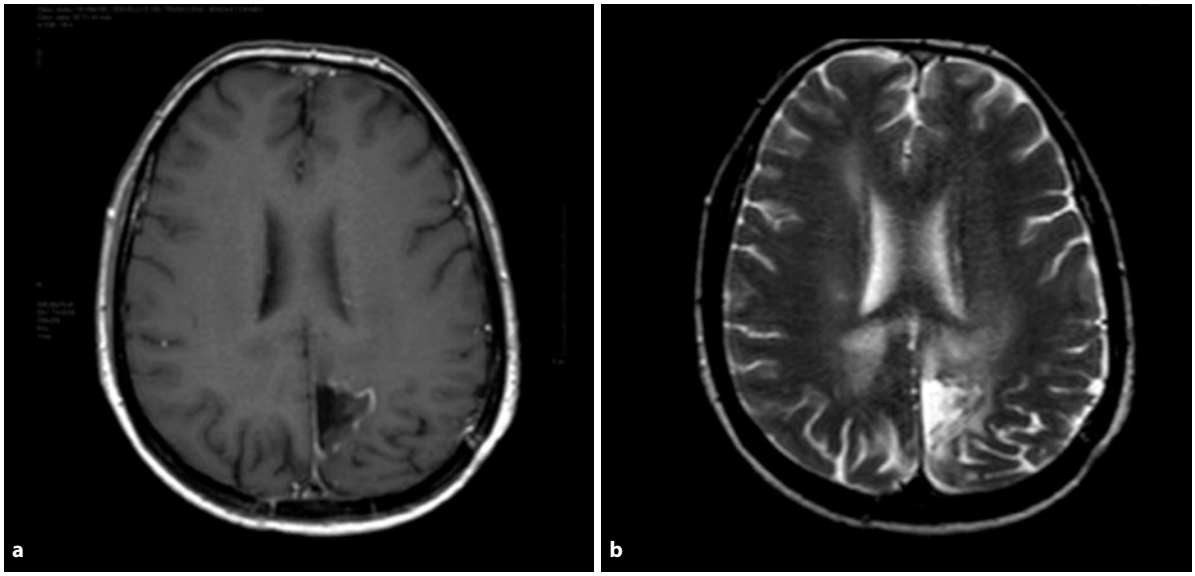

Fig. 16.3 Contrast-enhanced MR SE T1-weighted (**a**) and FSE T2-weighted (**b**) sequences show further enlargement of the cavity in response to therapy

Case 17

Stable Disease

Morphofunctional MR Follow-up in Glioblastoma Multiforme

Gabriele Polonara, Lorenzo Alvaro and Nathalie Herber

- 66-year-old patient with (methylated MGMT gene promoter) temporal-insular glioblastoma multiforme treated with surgery and subsequent radiotherapy and concomitant adjuvant chemotherapy
- Morphofunctional MR follow-up performed with morphologic study, diffusion-weighted imaging, perfusion and spectroscopy preoperatively, at 48 hours, 4, 7, 9 and 12 months after surgery

Preoperative Imaging

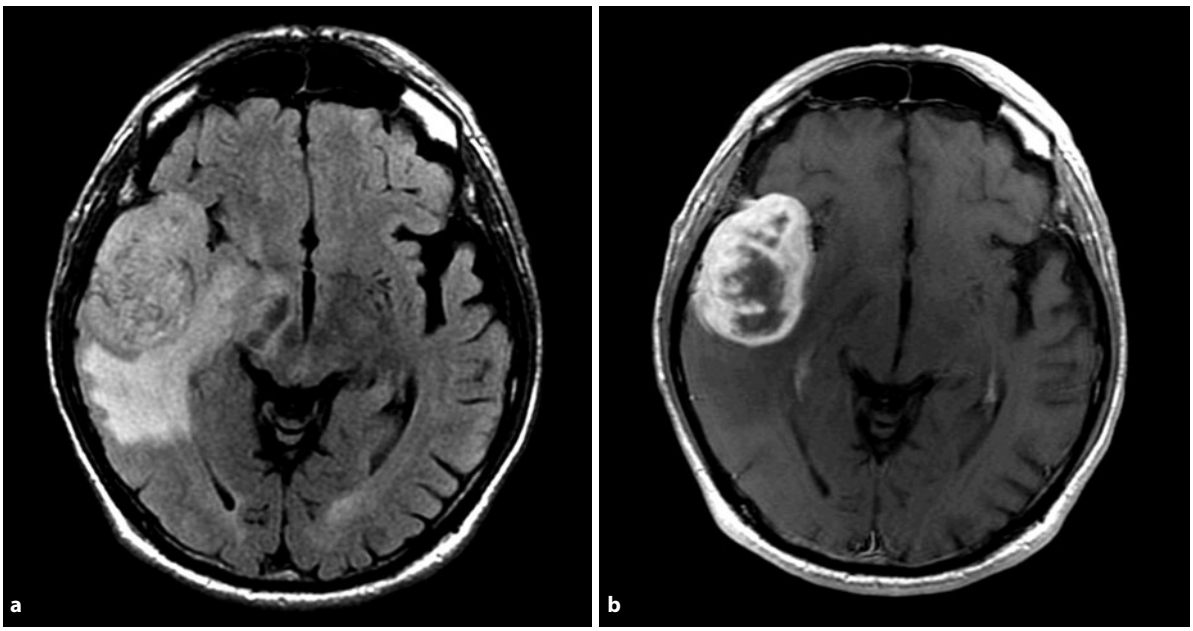

Fig. 17.1 **a** MR FLAIR sequence shows massive intra-axial right temporal-insular lesion, with maximum antero-posterior diameter of 5.5 cm and heterogeneous signal. The lesion is associated with white matter signal hyperintensity in the temporal lobe and right capsular-insular region with signs of compression on the right lateral ventricle. A slight midline shift to the left can also be seen. **b** Contrast-enhancement MR SE T1-weighted sequence displays an intensely enhancing nodule with ill-defined margins and central necrosis

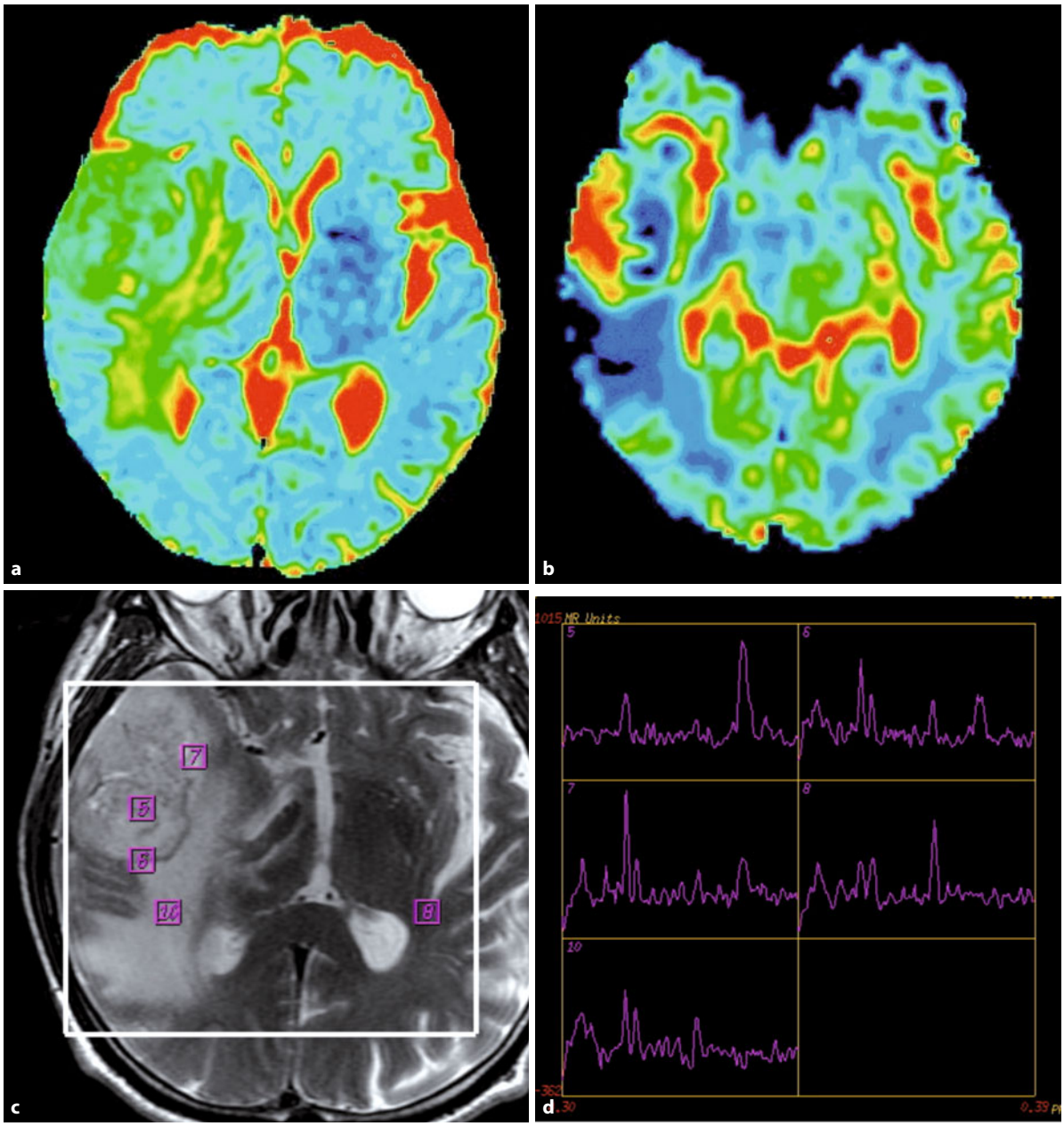

Fig. 17.2 **a** MR diffusion-weighted image shows an increase in the apparent diffusion coefficient at the infiltrative-expansive mass with perilesional signal alteration. **b** MR perfusion study shows an increase in perfusion more evident at the margins, in the right inferolateral region. **c,d** MR spectroscopy. In the center of the lesion there is an increase in the lipid peak (necrosis) and choline peak (cell proliferation), whereas choline is high and lipids are low at the margins. The choline is still high and NAA is low at about one centimeter from the macronodular lesion, a finding suggestive of neoplastic infiltration in the peripheral area

Early Postoperative Follow-up (at 48 Hours)

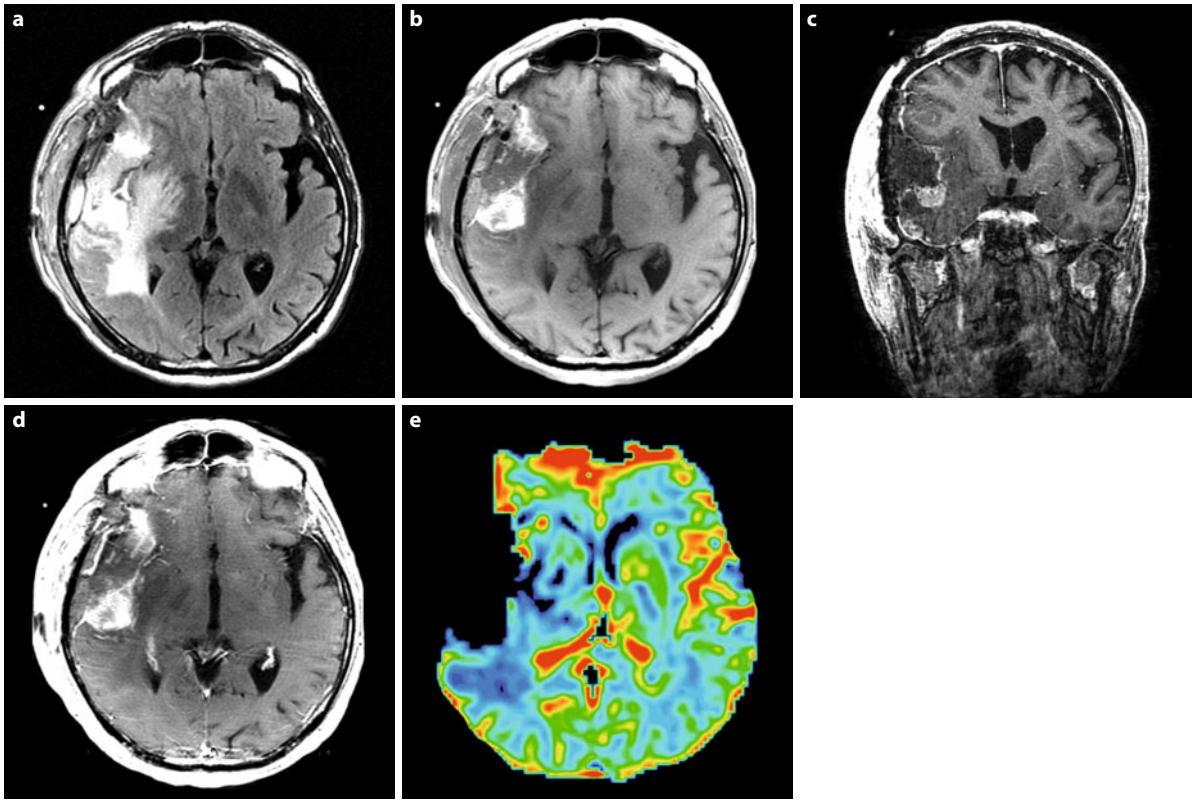

Fig. 17.3 **a** MR FLAIR sequence shows evidence of the frontal-parietal craniotomy and surgical removal of the right temporal-insular lesion. Signs of bleeding can be seen in the surgical cavity, as well as re-expansion of the frontal horn right ventricle and a reduction in the compression on the right lateral ventricle and the left lateral shift of the midline structures. A thin layer of fluid can be appreciated below the bone flap. **b** MR SE T1-weighted sequence shows hyperintense tissue at the margins of the surgical cavity suggestive of blood and tamponade material. **c,d** Contrast-enhanced MR SE T1-weighted sequences show enhancing tissue in the temporal lobe at the anterior-inferior-medial margin of the surgical cavity possibly compatible with a small residual of the resected lesion. **e** MR perfusion study shows no sign of increased perfusion at the margins of the surgical cavity

Follow-up Performed at 4 Months After Surgery, Radiotherapy and Concomitant Adjuvant Chemotherapy

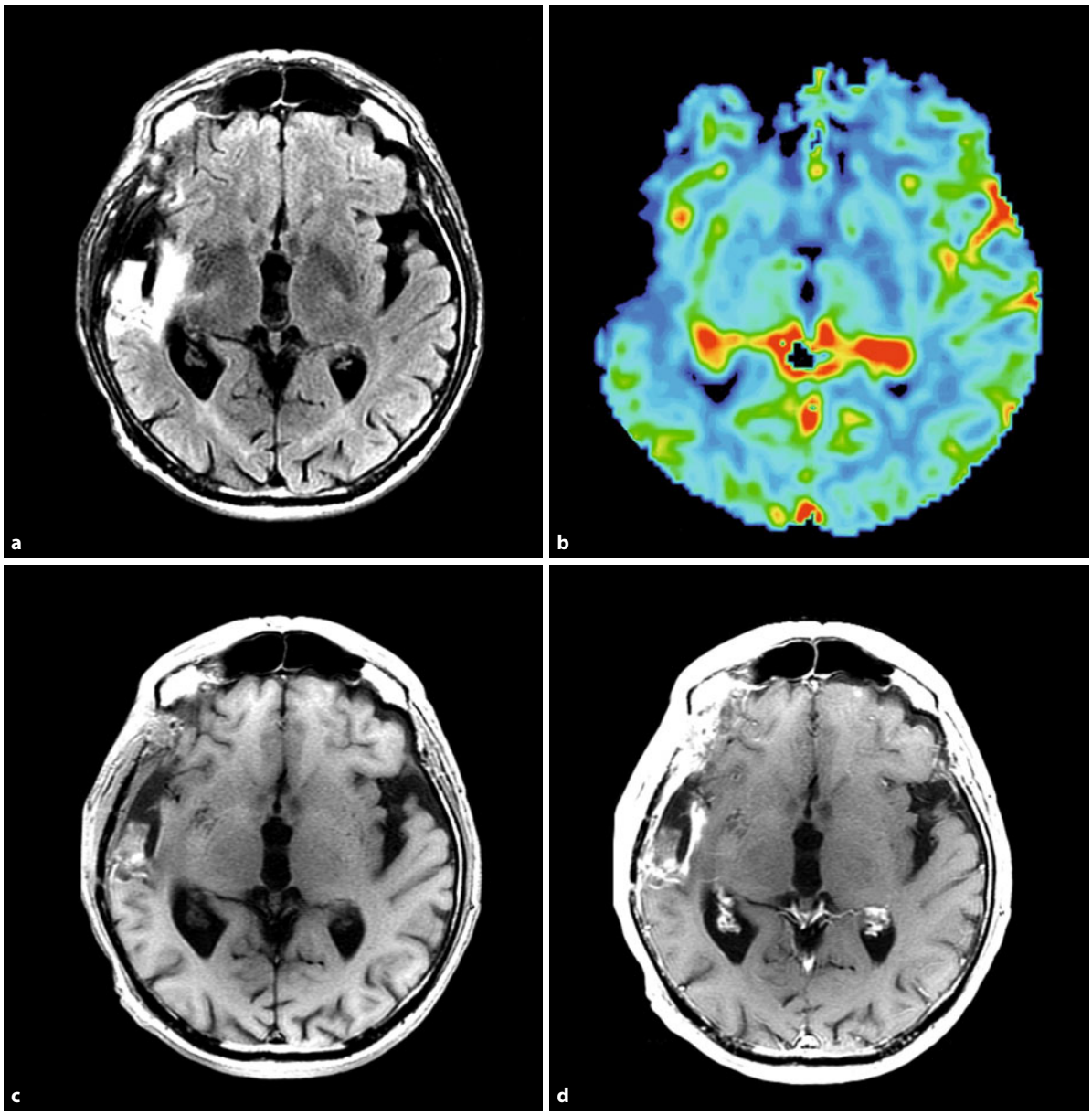

Fig. 17.4 **a** MR FLAIR sequence shows a reduction in the signs of bleeding within the right temporal-insular surgical cavity, the perilesional edema and the size of the surgical cavity, with dilation of the temporal horn and right ventricular trigone. The thin fluid layer beneath the bone flap is no longer appreciable and the midline structures appear completely realigned. **b** MR perfusion study shows no sign of increased perfusion at the margins of the surgical cavity. MR SE T1-weighted sequences before (**c**) and after contrast media injection (**d**) show a marked reduction in the signs of altered BBB at the surgical margins, which remained more pronounced posteriorly

Follow-up Performed at 7 Months

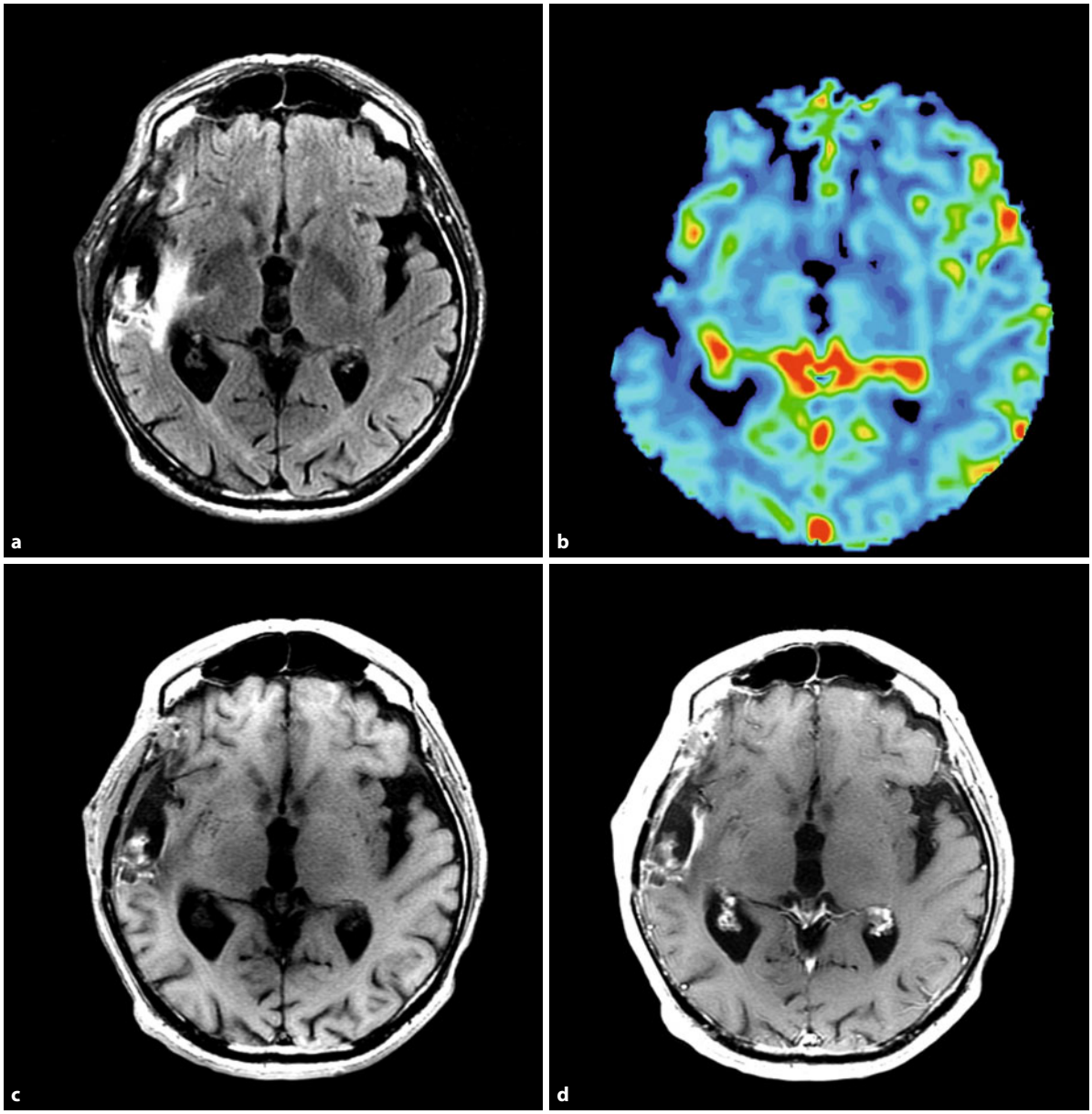

Fig. 17.5 MR FLAIR sequence (**a**), perfusion study (**b**) and SE T1-weighted sequences before (**c**) and after gadolinium-based contrast agent injection (**d**) show a reduction in T1 signal enhancement after contrast medium administration at the level of the dura and the margins of the surgical cavity correlated with the findings of the previous surgery. No other appreciable changes compared to the previous study can be seen

Follow-up Performed at 9 Months After Surgery and Further Adjuvant Chemotherapy

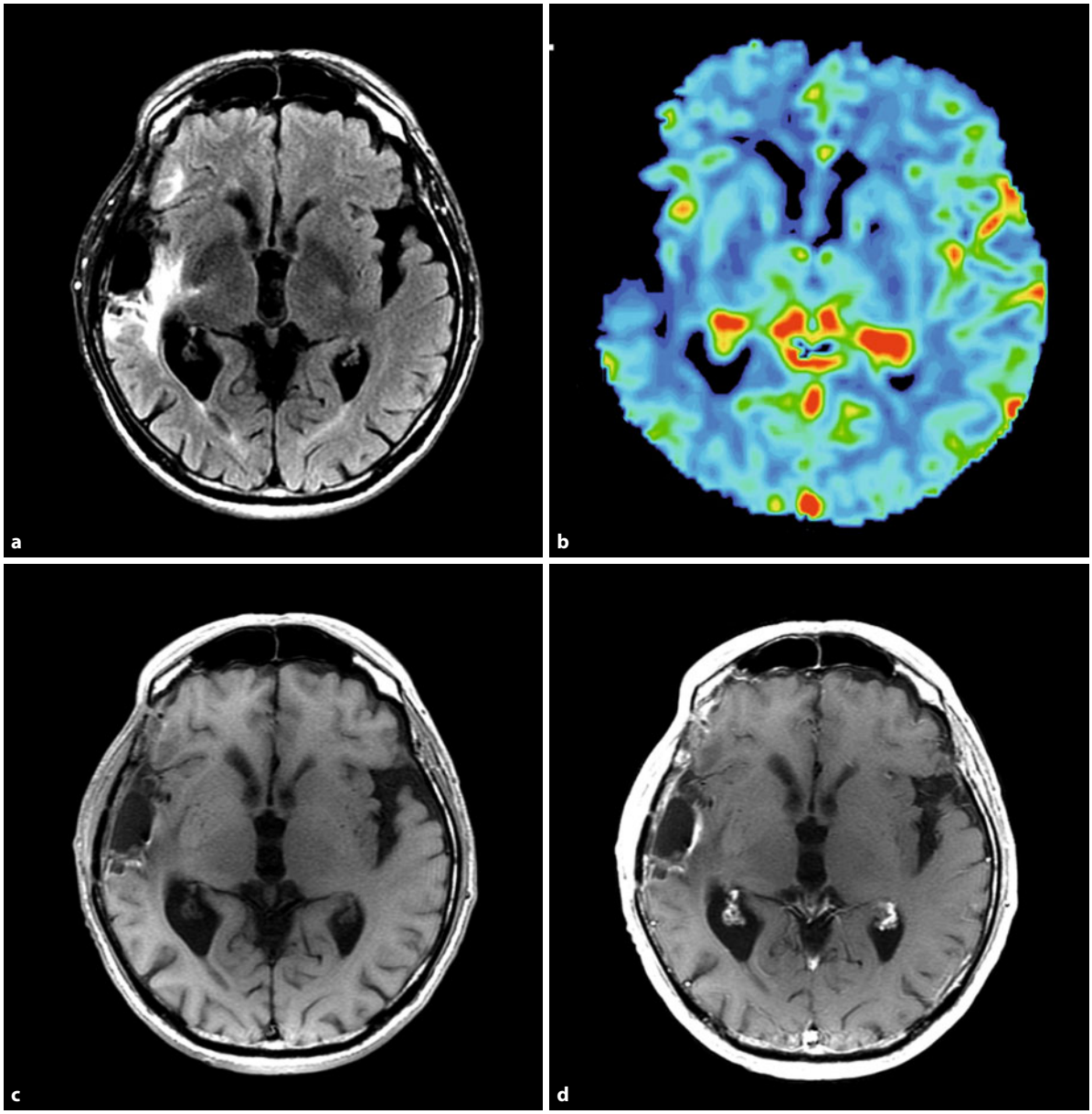

Fig. 17.6 MR FLAIR sequence (**a**), perfusion study (**b**) and SE T1-weighted sequences before (**c**) and after gadolinium-based contrast agent injection (**d**) show a reduction in T1 signal enhancement after contrast medium administration at the level of the dura and the margins of the surgical cavity correlated with the findings of the previous surgery. No other appreciable changes compared to the previous study can be seen

Follow-up Performed at 12 Months

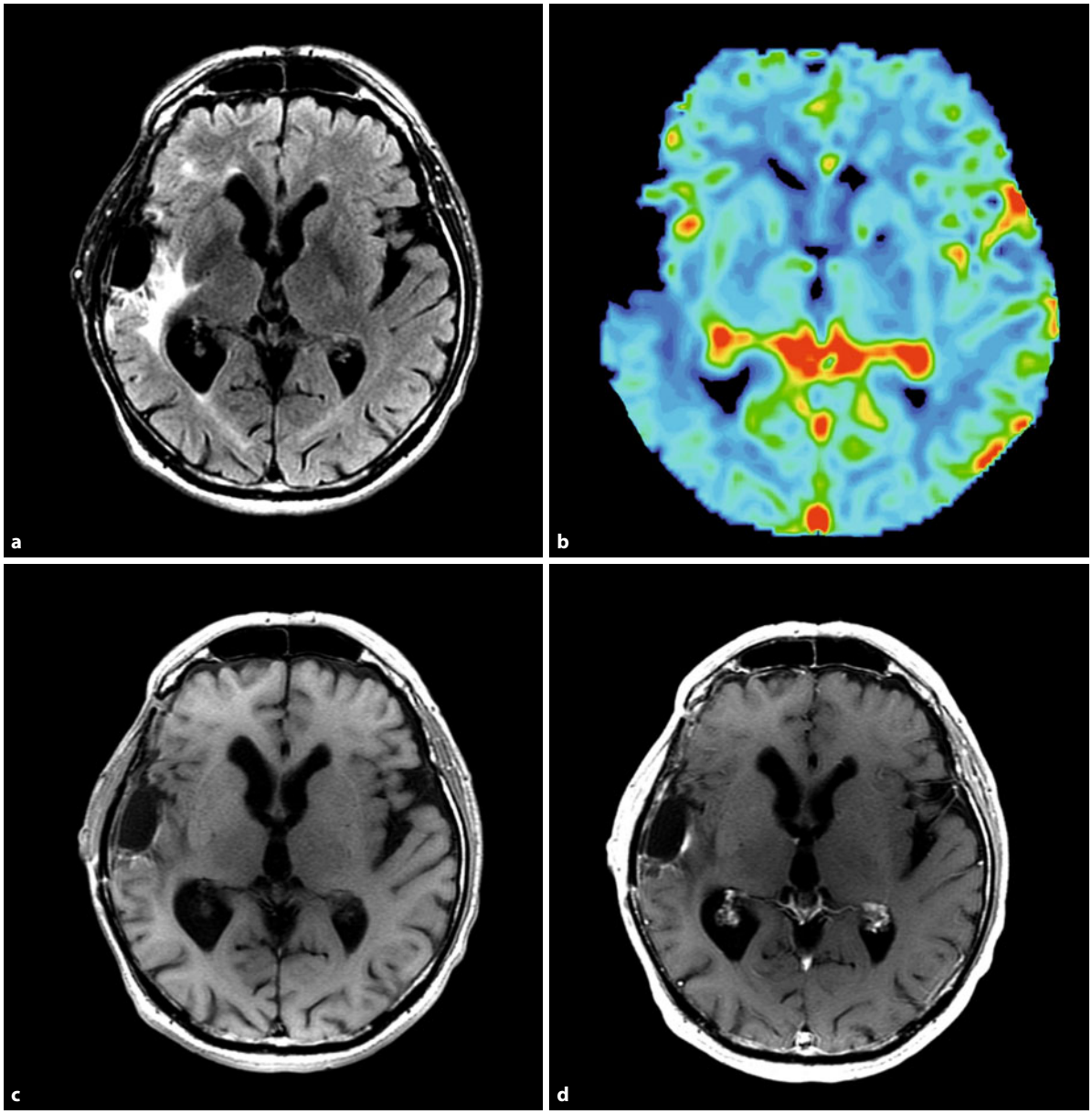

Fig. 17.7 MR FLAIR sequence (**a**), perfusion study (**b**) and SE T1-weighted sequences before (**c**) and after gadolinium-based contrast agent injection (**d**) show a reduction in T1 signal enhancement after contrast medium administration at the level of the dura and the margins of the surgical cavity correlated with the findings of the previous surgery. No other appreciable changes compared to the previous study can be seen

Case 18

Stable Disease

3T Multimodal MR Follow-up in Glioblastoma Multiforme

Tommaso Scarabino, Teresa Popolizio, Saverio Pollice, Vincenzo D'Angelo and Alfonso Di Costanzo

- 45-year-old patient with left frontal-insular glioblastoma multiforme treated with subtotal resection and combined radiation therapy-chemotherapy
- 3T multimodal MR follow-up performed with morphologic imaging, diffusion, perfusion and spectroscopy preoperatively and at 6 and 12 months after surgery and combined radiation therapy-chemotherapy

T. Scarabino (ed.), *Imaging Gliomas After Treatment,* © Springer-Verlag Italia 2012

Preoperative Imaging

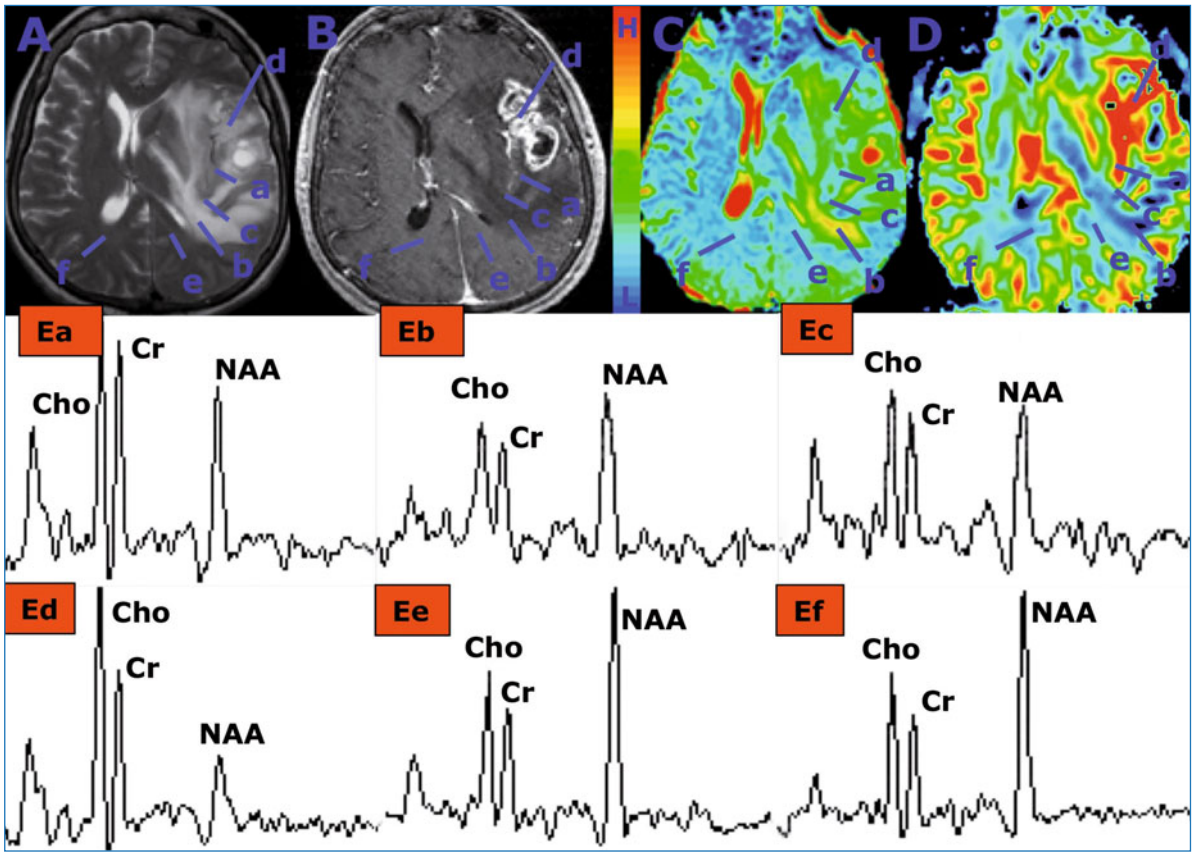

Fig. 18.1 MR FSE T2-weighted (**a**) and contrast-enhanced SE T1-weighted (**b**) sequences show a large mass with heterogeneous signal and enhancement due to the presence of large components of central necrosis, with abundant edema and moderate mass effect on the midline structures which appear shifted laterally. The MR multimodal study with diffusion-weighted imaging and ADC map (**c**), perfusion study with CBV map (**d**) and single-voxel spectroscopy with multiple ROIs (**e**) show spectra relative to the areas with enhancing tumor and immediately behind the lesion with the typical pattern of high Cho and inversion of the Cho/NAA ratio. In these ROIs, the ADC is reduced and the CBV increased; the opposite happens in the necrotic-colliquative area. The spectra in the apparently edematous area beyond the enhancing margins have overall reduced levels of all metabolites but with spectroscopic patterns indicating tumor-infiltrated edema. In these locations, ADC is reduced while CBV is high. Moving away from the lesion the metabolic pattern along with ADC and CBV values return to normal as in the contralateral hemisphere

Follow-up Performed at 6 Months After Surgery and Combined Radiation Therapy-chemotherapy

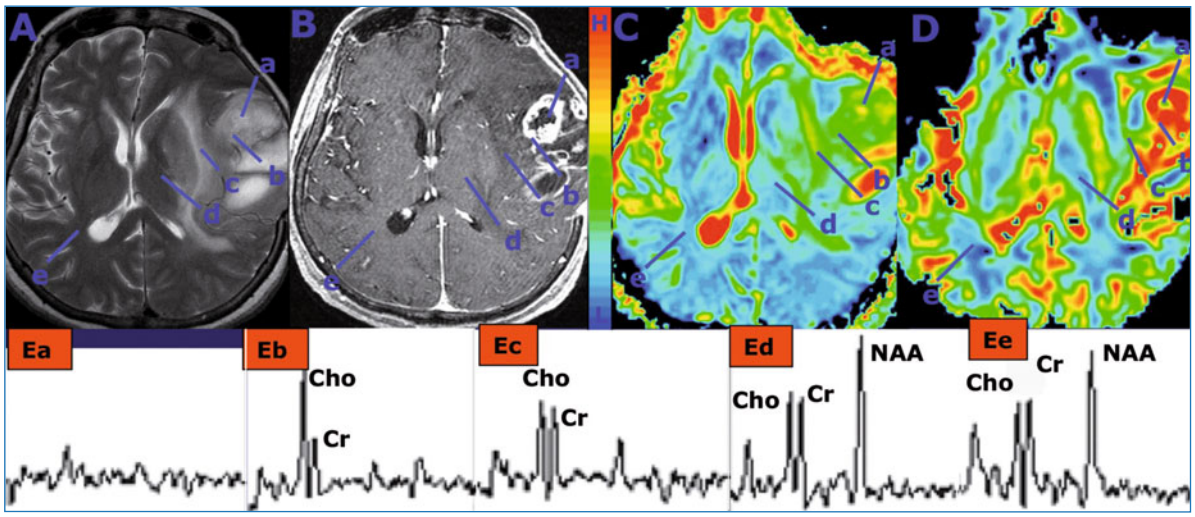

Fig. 18.2 Morphofunctional MR with FSE T2-weighted (**a**) and contrast-enhanced SE T1-weighted (**b**) sequences, diffusion-weighted imaging with ADC map (**c**), perfusion study with CBV map (**d**) and multivoxel spectroscopy with multiple ROIs (**e**). The imaging findings following treatment show an increase in the necrotic component, characterized by a reduction in the spectral levels of all metabolites, increased ADC and decreased CBV. These indices instead retain the tumor pattern in the enhancing areas and those immediately adjacent to the lesion

Follow-up Performed at 12 Months

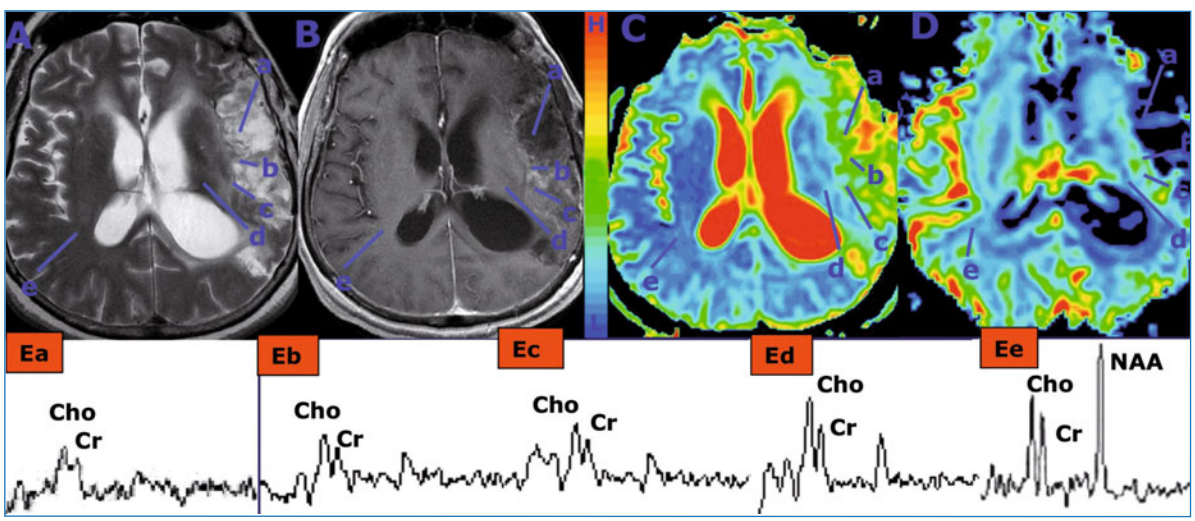

Fig. 18.3 Multimodal MR with FSE T2-weighted (**a**) and contrast-enhanced SE T1-weighted (**b**) sequences, diffusion-weighted imaging with ADC map (**c**), perfusion study with CBV map (**d**) and multi-voxel spectroscopy with multiple ROIs (**e**). The results obtained by radiation therapy and chemotherapy show an almost complete necrotic transformation of the lesion with no sign of significant enhancement and with associated retraction dilatation of the adjacent lateral ventricle. There is a concomitant reduction in the spectra of all metabolites, an increase in ADC and a reduction in CBV. These indices can also be appreciated in the surrounding tissue

Case 19

Stable Disease

3T Morphofunctional MR Follow-up in High-grade Oligodendroglioma

Massimo Caulo, Chiara Briganti, Valentina Panara, Simone Salice, Domenico Tortora and Armando Tartaro

- 54-year-old patient with right parietal high-grade oligodendroglioma treated with subtotal surgery and combined radiation therapy-chemotherapy
- 3T morphofunctional MR follow-up performed with morphologic sequence and spectroscopy at 2 years after surgery and combined radiation therapy-chemotherapy

Follow-up Performed at 2 Years After Surgery and Combined Radiation Therapy-chemotherapy

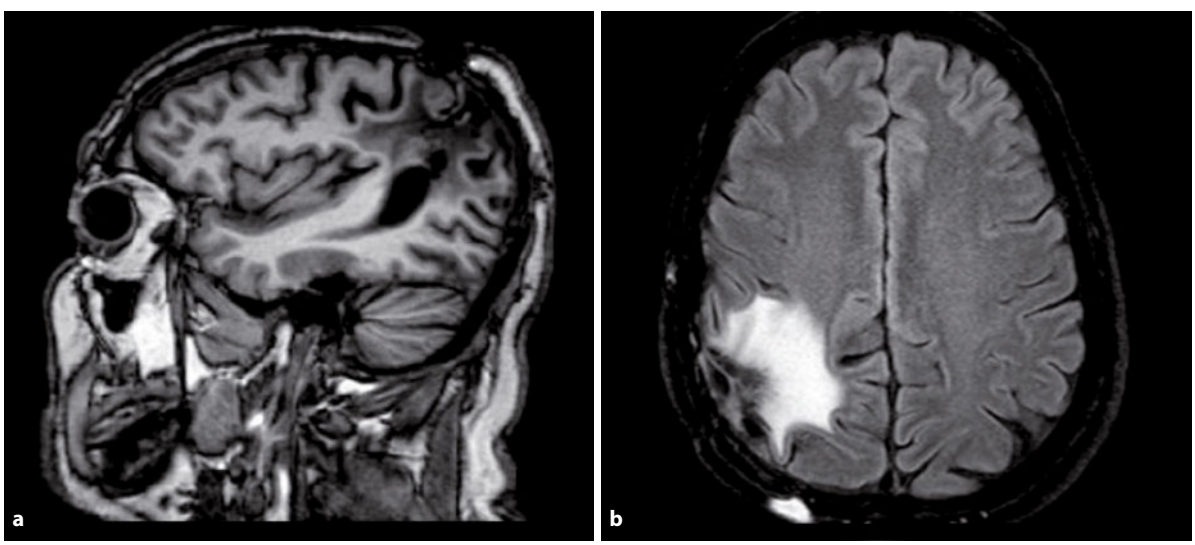

Fig. 19.1 Contrast-enhanced MR SE T1-weighted (**a**) and FLAIR (**b**) sequences show the surgical site in the right parietal region characterized by cavitation surrounded by diffuse signal alteration of the white matter

T. Scarabino (ed.), *Imaging Gliomas After Treatment,* © Springer-Verlag Italia 2012

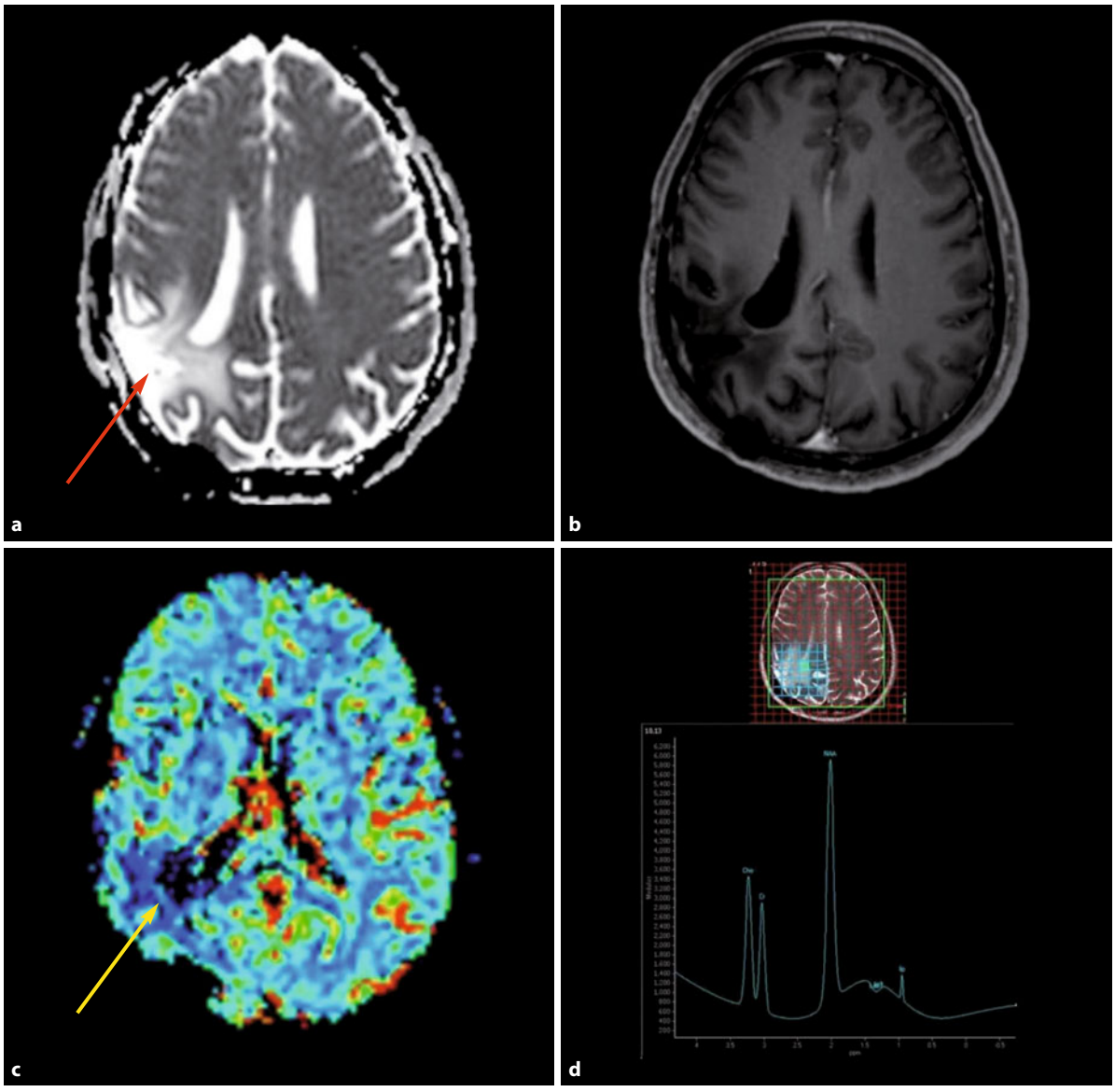

Fig. 19.2 **a** MR diffusion-weighted imaging with ADC map shows increased ADC values (1.832±0.832 mm²/s) at the surgical cavity (*red arrow*). **b** Contrast-enhanced MR SE T1-weighted sequence. Contrast enhancement is absent. **c** MR perfusion study with CBV map. The value of rCBV [CBV lesions/contralateral white matter CBV] is 0.78 close to the surgical cavity (*yellow arrow*). **d** Multi/single-voxel spectroscopy shows no increase in the concentration of Cho, which indicates low cell turnover and thus the absence of disease progression

Case 20

Tumor Recurrence

Postoperative MR Follow-up in Grade III Oligodendroglioma

Ferdinando Caranci, Alessandra D'Amico and Sossio Cirillo

- Patient with surgically treated grade III left fronto-parietal oligodendroglioma
- Postoperative follow-up performed late (9 months) with MR morphologic sequences

Preoperative Imaging

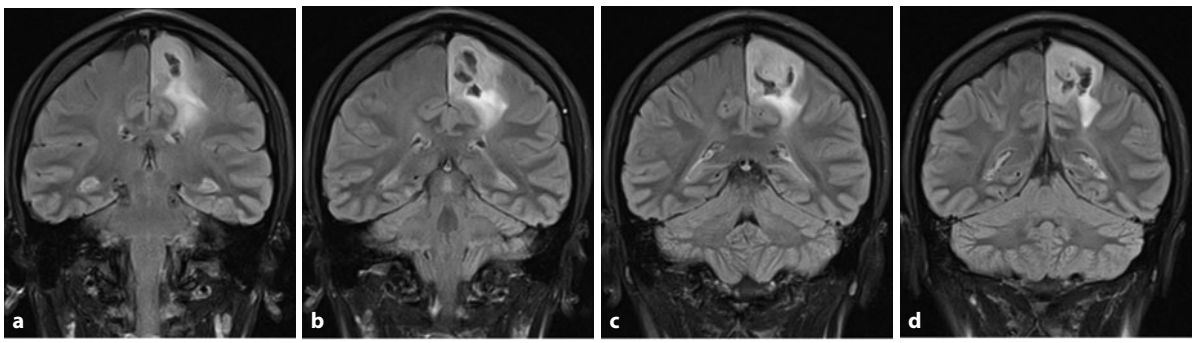

Fig. 20.1 a-d MR FLAIR sequence. Images show an infiltrating lesion at the left parasagittal fronto-parietal convexity, extending from the cortical profile to the deep white matter, with inhomogeneous structure due to internal areas of necrosis

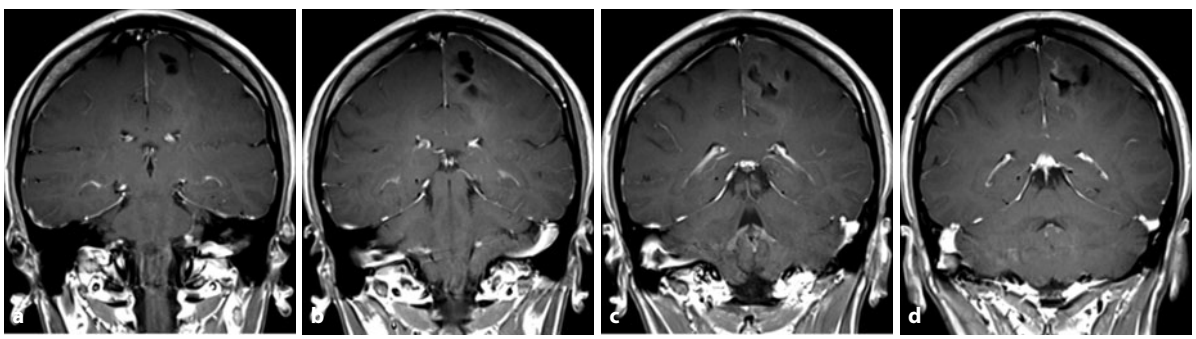

Fig. 20.2 a-d Contrast-enhanced MR SE T1-weighted images. Thin linear streaks of enhancement can be appreciated in the posterior portion of the lesion

Postoperative Follow-up at 9 Months

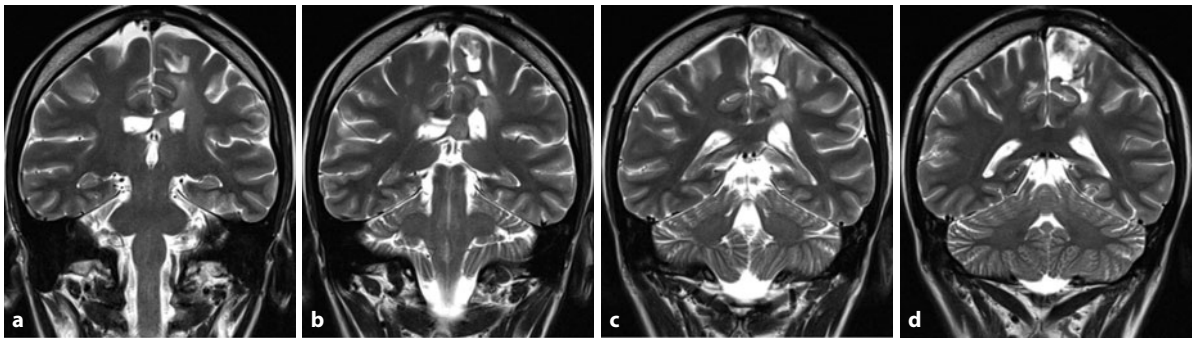

Fig. 20.3 a-d MR FSE T2-weighted sequence. The inhomogeneous appearance of the surgical cavity resulting from partial resection of the lesion is associated with evident heteroplastic pseudonodular thickening of the ipsilateral fornix

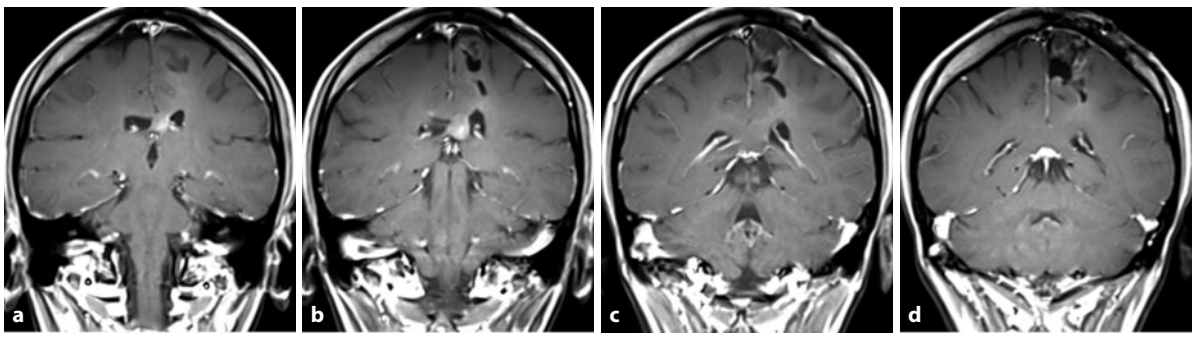

Fig. 20.4 a-d Contrast-enhanced MR SE T1-weighted images. Peripheral linear enhancement of the surgical cavity is appreciable, in part caused by blood brain barrier injury. Enhancement of the tumor component at the fornix is also evident

Case 21

Tumor Recurrence

Postoperative MR Follow-up in Gliosarcoma

Ferdinando Caranci, Antonio Volpe and Arturo Brunetti

- Patient with surgically treated left temporo-occipital gliosarcoma
- Postoperative follow-up performed late (6 and 9 months) with MR morphologic sequences

Preoperative Imaging

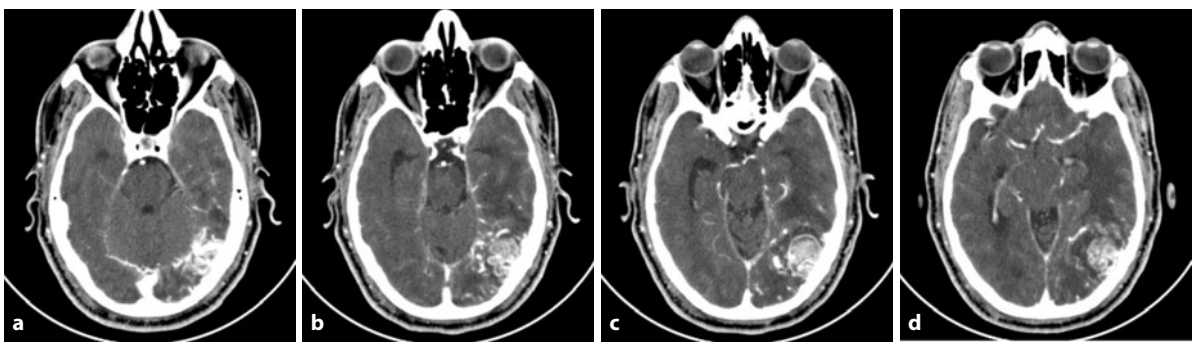

Fig. 21.1 a-d Contrast-enhanced CT scan. Left temporo-occipital lesion characterized by intense enhancement associated with high vascularity

Postoperative Follow-up at 6 Months

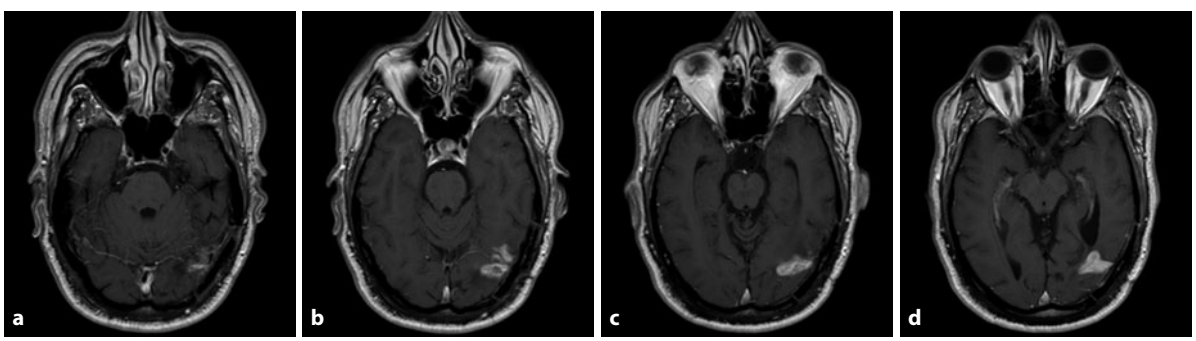

Fig. 21.2 a-d Contrast-enhanced MR SE T1-weighted images. A nodular pattern of enhancement is appreciable at the site of the previously removed lesion indicating tumor recurrence

Postoperative Follow-up at 9 Months

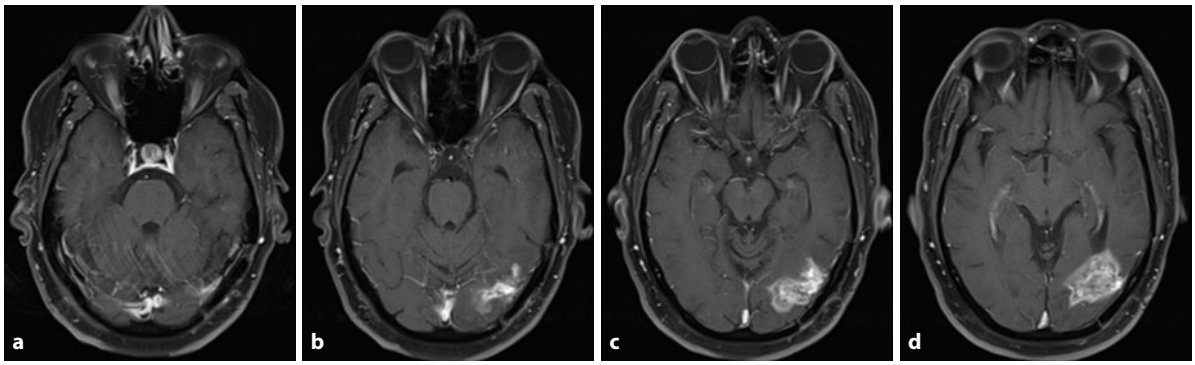

Fig. 21.3 a-d Contrast-enhanced MR SE T1-weighted images. Further expansion of tumor recurrence

Case 22

Tumor Recurrence

Postoperative MR Follow-up in Low-grade Astrocytoma

Ferdinando Caranci, Antonio Volpe and Arturo Brunetti

- Patient with surgically treated grade II left frontal astrocytoma
- Postoperative follow-up performed late (at 9 and 24 months) with MR morphologic sequences

Postoperative Follow-up at 9 Months

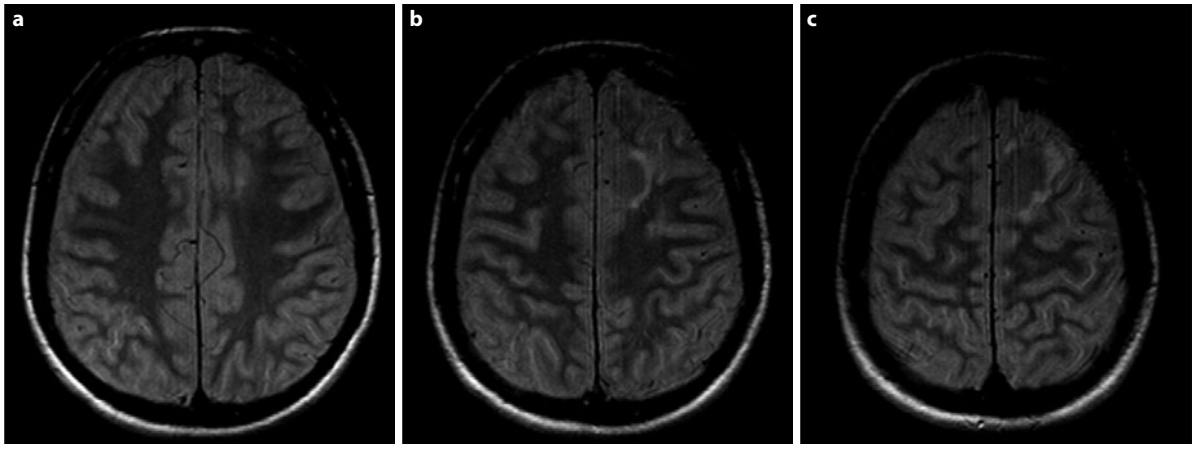

Fig. 22.1 a-c MR DP sequence. A CSF-like area indicating the postsurgical cavity can be appreciated in the white matter of the left frontal convexity surrounded by a halo of high signal

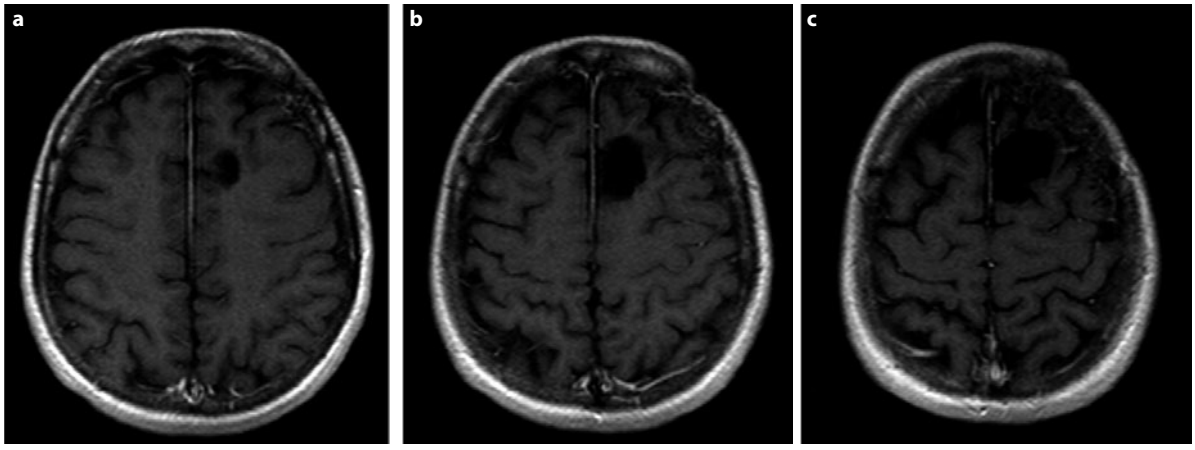

Fig. 22.2 a-c Contrast-enhanced MR SE T1-weighted images. No areas of pathologic enhancement can be appreciated

Postoperative Follow-up at 24 Months

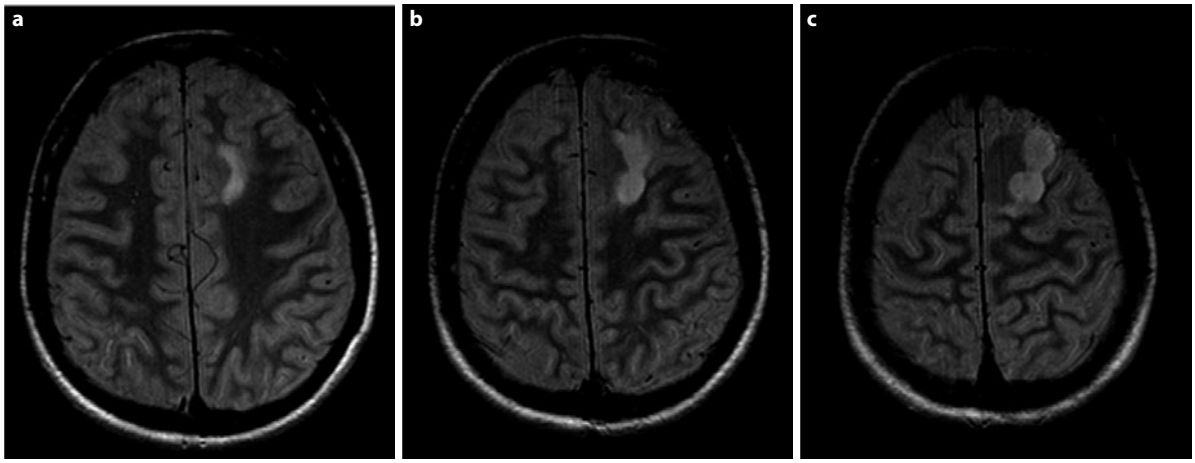

Fig. 22.3 a-c MR DP sequence. The images show an increase of the tissue with pseudonodular characteristics at the lateral margins of the postsurgical cavity (tumor recurrence)

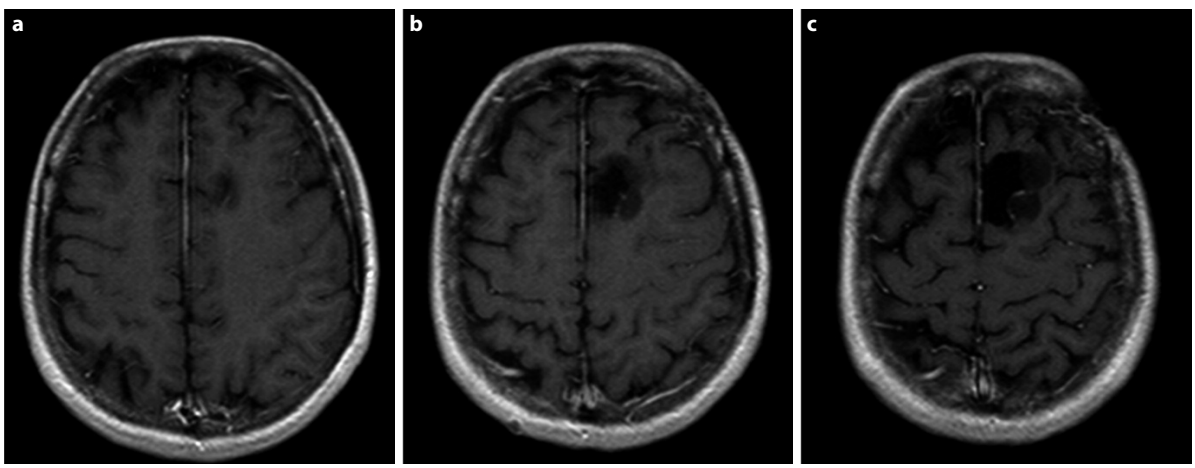

Fig. 22.4 a-c Contrast-enhanced MR SE T1-weighted images. The appearance of slight enhancement corresponding to the recurrence can be seen

Case 23

Tumor Recurrence

Postoperative MR Follow-up in Anaplastic Oligoastrocytoma

Ferdinando Caranci and Sossio Cirillo

- Patient with posterior left temporal anaplastic oligoastrocytoma treated with surgery and subsequent radiation
- Postoperative and post-radiation therapy follow-up performed late (6, 15, and 24 months) with MR morphologic and perfusion sequences

Postoperative Follow-up at 6 Months

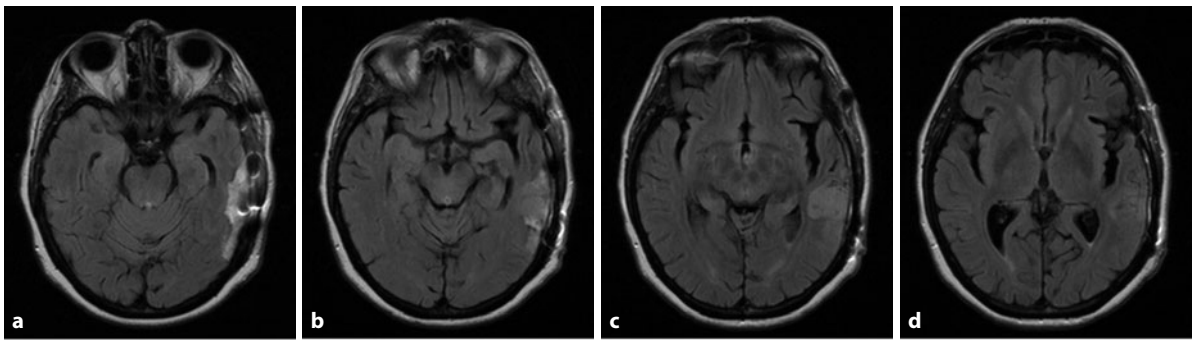

Fig. 23.1 a-d MR FLAIR sequence. Nodular neoplastic residual is visualized in the left posterior temporal region (**c**) and associated with a cortical blood effusion (**a, b**)

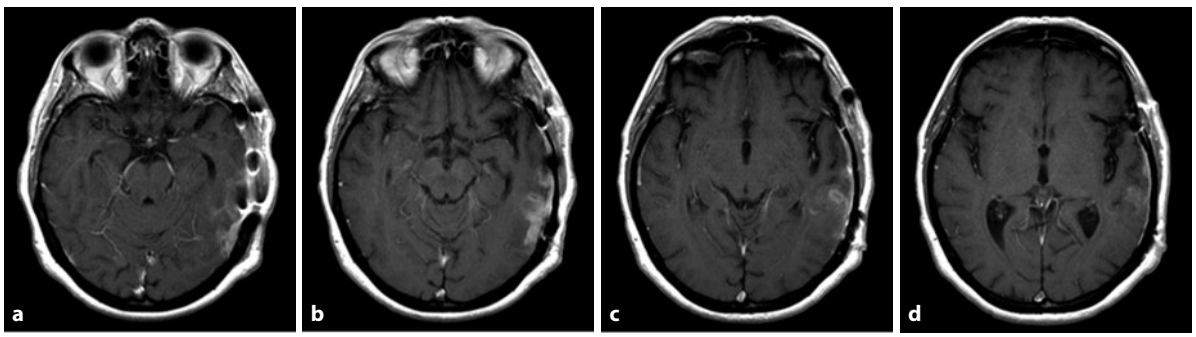

Fig. 23.2 a-d Contrast-enhanced MR SE T1-weighted images. Cortical-subcortical enhancement can be appreciated in the left posterior temporal region, in part caused by blood brain barrier injury, with reactive enhancing dura adjacent to the bone flap

Postoperative Follow-up (Post-radiation) at 15 Months

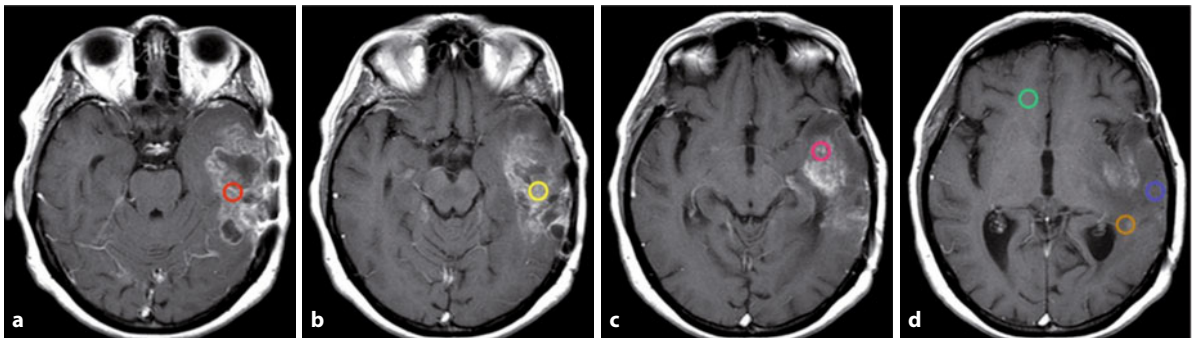

Fig. 23.3 a-d Contrast-enhanced MR SE T1-weighted images. The area of pathologic enhancement in the left temporal region appears increased, with irregular margins and internal necrotic components. The colored rings denote several regions of interest in the context of the lesion

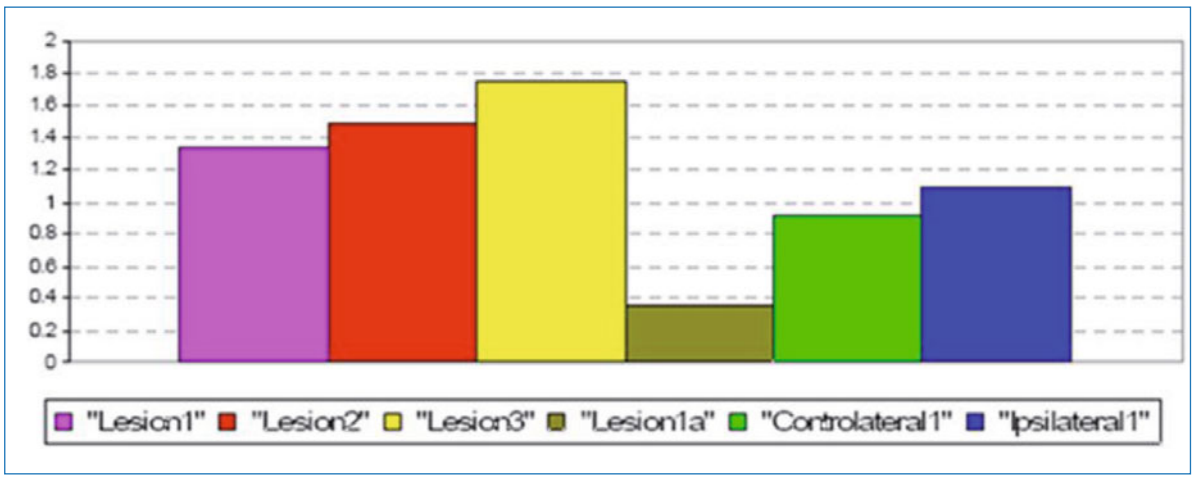

Fig. 23.4 MR perfusion study with CBV values. Compared to white matter (*green*) which is taken as a reference value, the graph shows multiple areas of increased CBV (*yellow, red, pink and blue*) which indicate heteroplastic tissue. Reduced CBV (*brown*) in the left paratrigonal region indicates an area free from neoplastic infiltration

Postoperative Follow-up at 24 Months

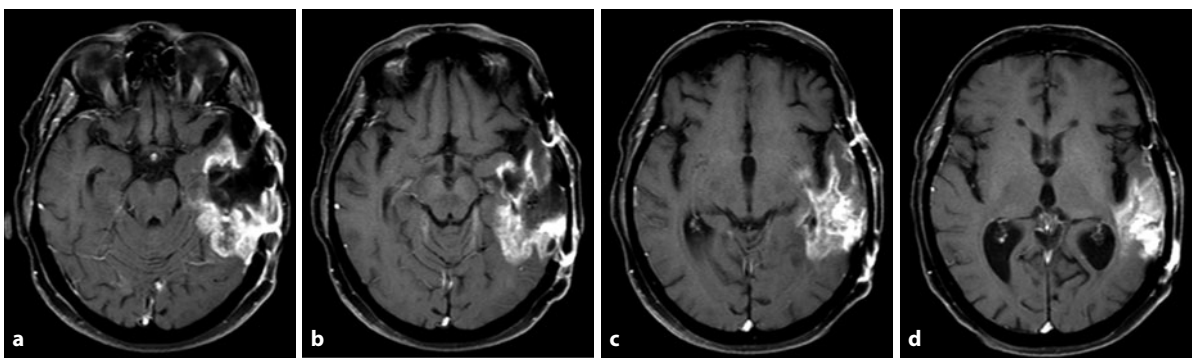

Fig. 23.5 a-d Contrast-enhanced MR SE T1-weighted images. An increase in the tissue with pathologic enhancement is evident

Case 24

Tumor Progression/Recurrence

Multimodal CT/MR Follow-up in Glioblastoma Multiforme

Alessandro Stecco, Sara Zizzari, Francesco Fabbiano, Gerardo Di Nardo, Andrea Pietro Sponghini, Mariangela Lombardi and Alessandro Carriero

- 58-year-old patient with left temporal glioblastoma multiforme treated with subtotal surgery, combined radiation therapy-chemotherapy and second-line adjuvant chemotherapy
- Multimodal CT (morphologic and perfusion study) follow-up performed at 5 and 9 months after surgery and combined radiation therapy-chemotherapy

Follow-up at 5 Months After Surgery and Combined Radiation Therapy-chemotherapy

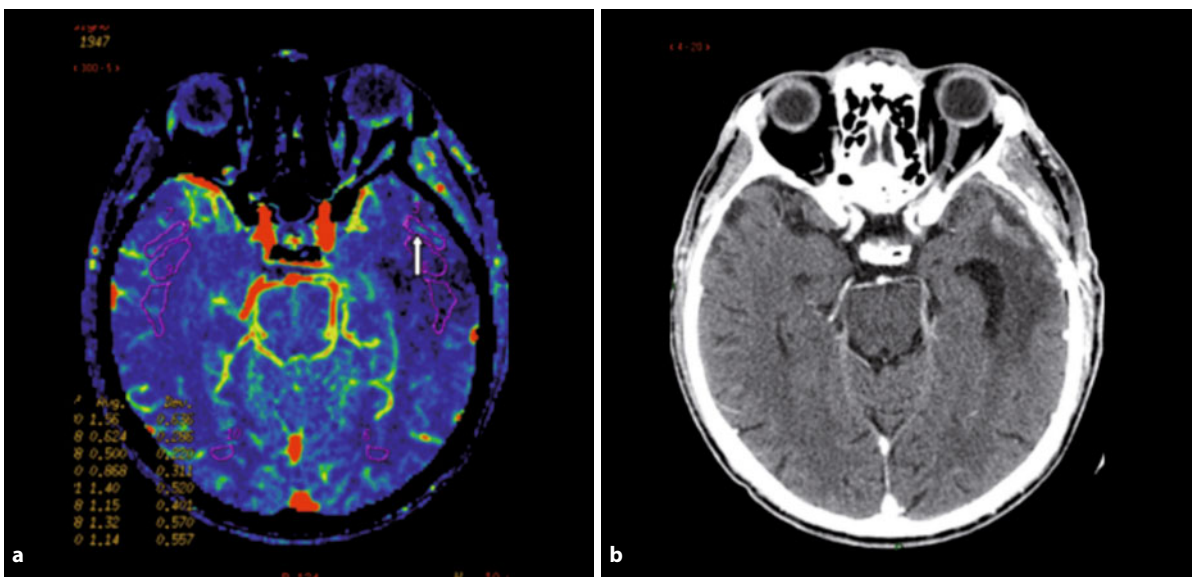

Fig. 24.1 **a** CT perfusion study with relative CBV map shows a small nodular area with the highest levels of CBV (*white arrow*). **b** Contrast-enhanced CT scan. An enhancing area is visible corresponding to the area of elevated CBV

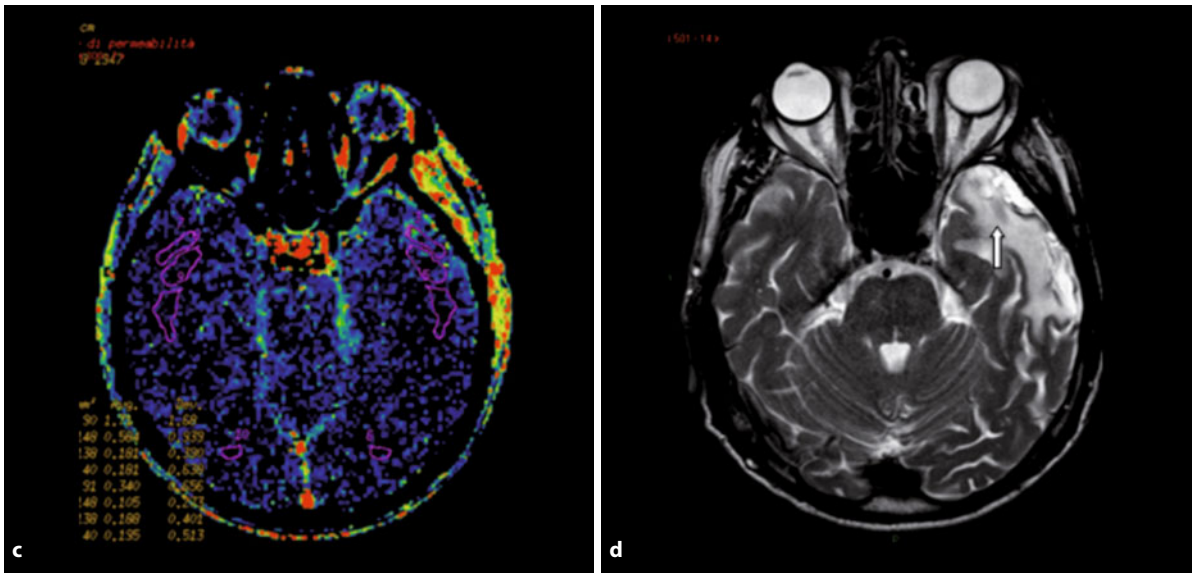

Fig. 24.1 **c** CT permeability surface (PS) perfusion map confirms the findings reported in the CBV map. **d** MR FSE T2-weighted sequence shows evidence of residual tissue with low signal in T2 (*white arrow*) accompanied by widespread perilesional alteration

Follow-up at 9 Months

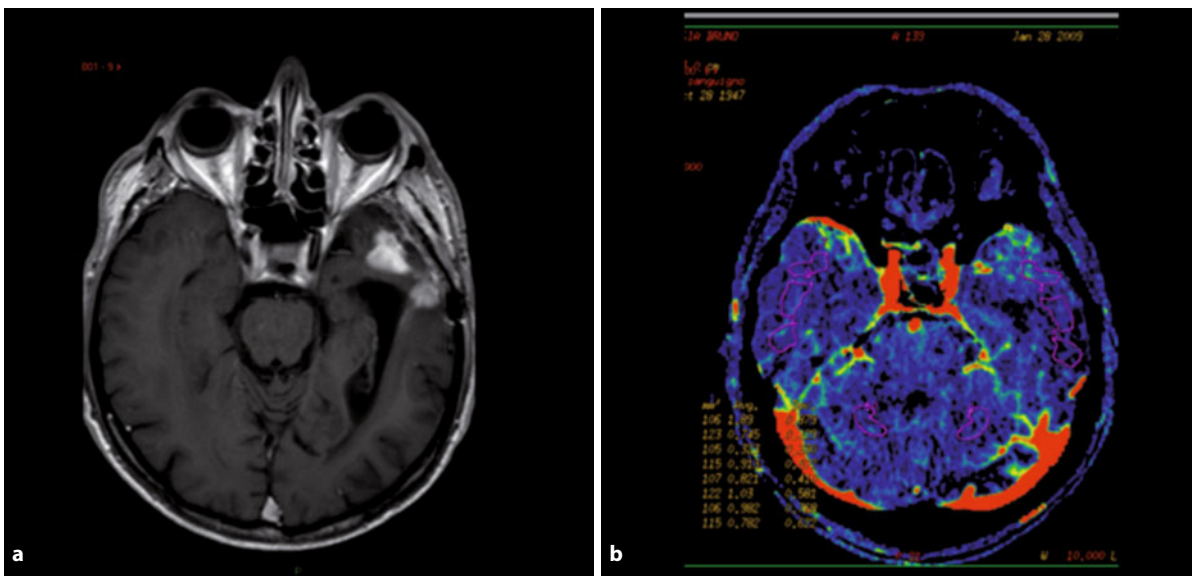

Fig. 24.2 **a** Contrast-enhanced MR SE T1-weighted sequence shows increased size and enhancement of the pathologic tissue. **b** CT perfusion study with relative CBV map. Higher CBV values can be appreciated at the site of the lesion than in the surrounding and contralateral parenchyma

Case 25

Tumor Progression/Recurrence

Multimodal CT/MR Follow-up in Anaplastic Astrocytoma

Alessandro Stecco, Francesco Fabbiano, Sara Zizzari, Gerardo Di Nardo, Mariangela Lombardi, Ignazio Divenuto and Alessandro Carriero

- 58-year-old patient with left frontal anaplastic astrocytoma treated with surgery and subsequent combined radiation therapy-chemotherapy
- Multimodal CT/MR (morphologic and perfusion study) follow-up performed in the early and late postoperative phase at 1, 9 and 12 months after surgery and combined radiation therapy-chemotherapy

Early Postoperative Imaging in Patient Candidate for Radiation Therapy and Chemotherapy

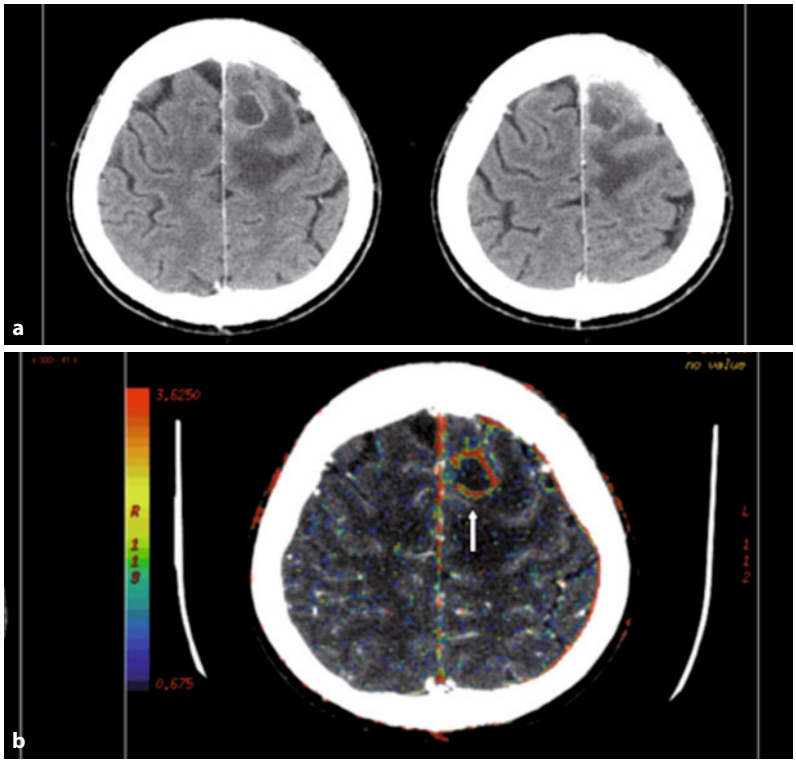

Fig. 25.1 a Contrast-enhanced CT scan shows a left parafalcal enhancing ring lesion accompanied by perilesional hypodensity of white matter. **b** Postoperative CT perfusion study with permeability surface (PS) map. The fusion image shows high PS values along the lesion margins (*white arrow*)

Follow-up at 1 Month After Surgery During Radiation Therapy

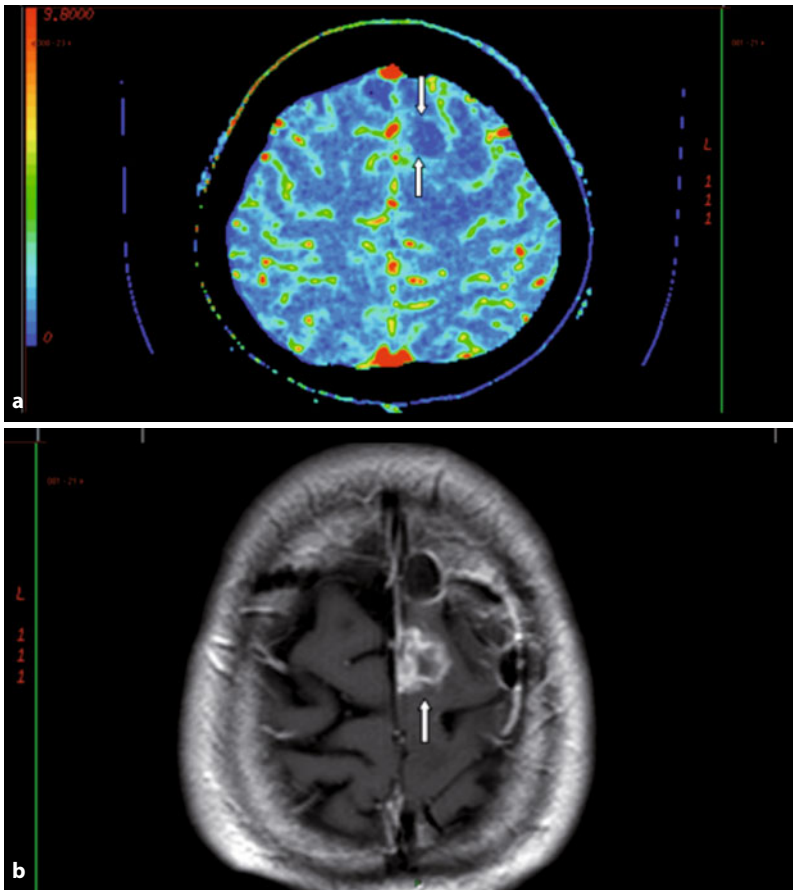

Fig. 25.2 a MR perfusion study with relative CBV map. The highest values of CBV are seen along the peripheral margins of the lesion (*white arrows*). **b** Contrast-enhanced MR SE T1-weighted sequence shows peripheral enhancement of the lesion (*white arrow*)

Follow-up at 9 Months After Surgery Following Combined Radiation Therapy-chemotherapy

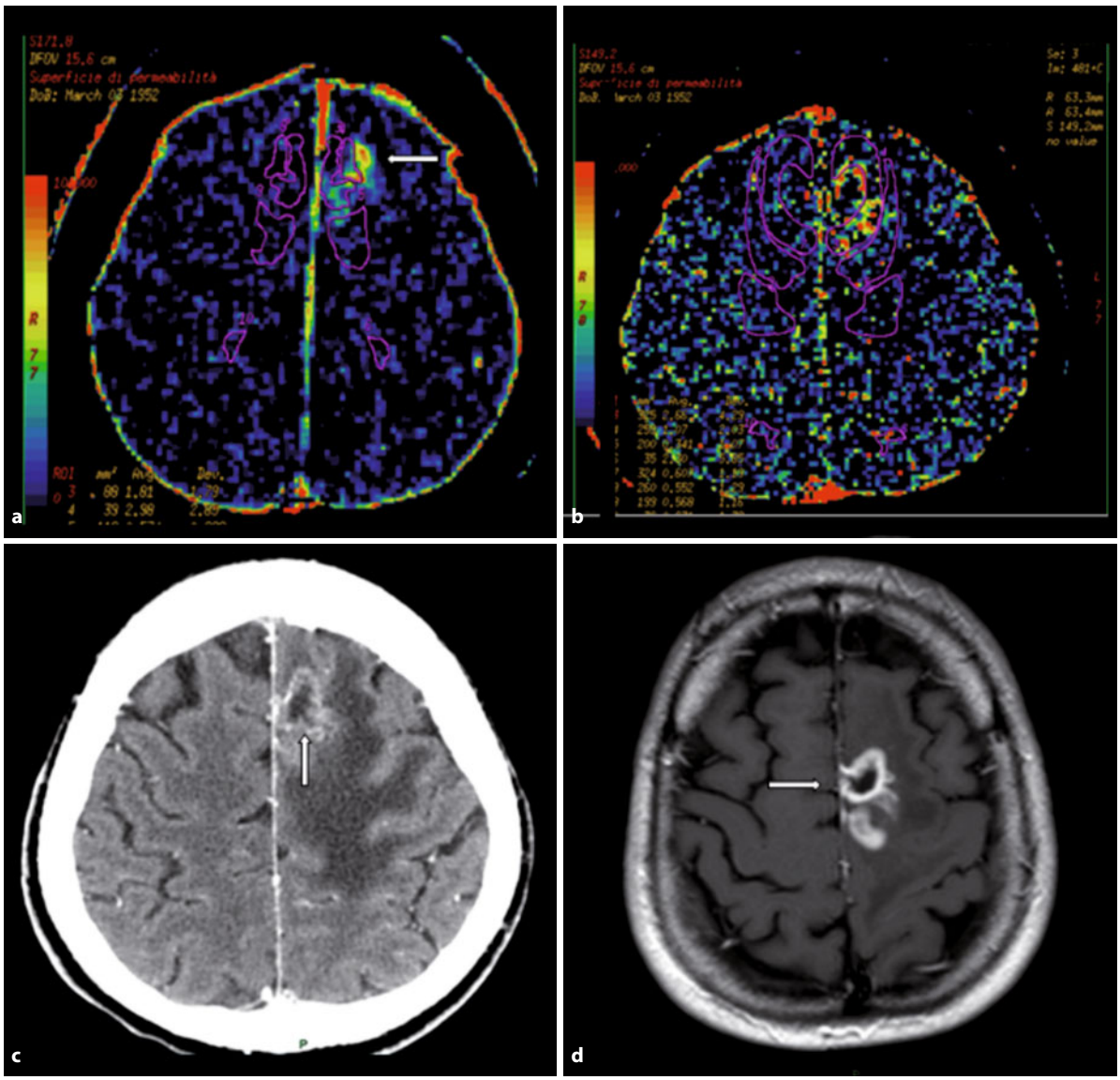

Fig. 25.3 **a** CT perfusion study shows focal elevation of PS in the lateral portion of the neurosurgical cavity, resulting from resection (*white arrow*). **b** Greater extension of the pathologic increase in PS than in the previous examination (Fig. 8.1 b), with rim appearance along the margins of the surgical resection. **c** Contrast-enhanced CT scan depicts evidence of recurrence with irregular enhancement of surgical margins with less extent than the corresponding PS map in **b** (*white arrow*). **d** Contrast-enhanced MR SE T1-weighted sequence confirms the CT morphologic and perfusion findings (*white arrow*)

Follow-up at 12 Months

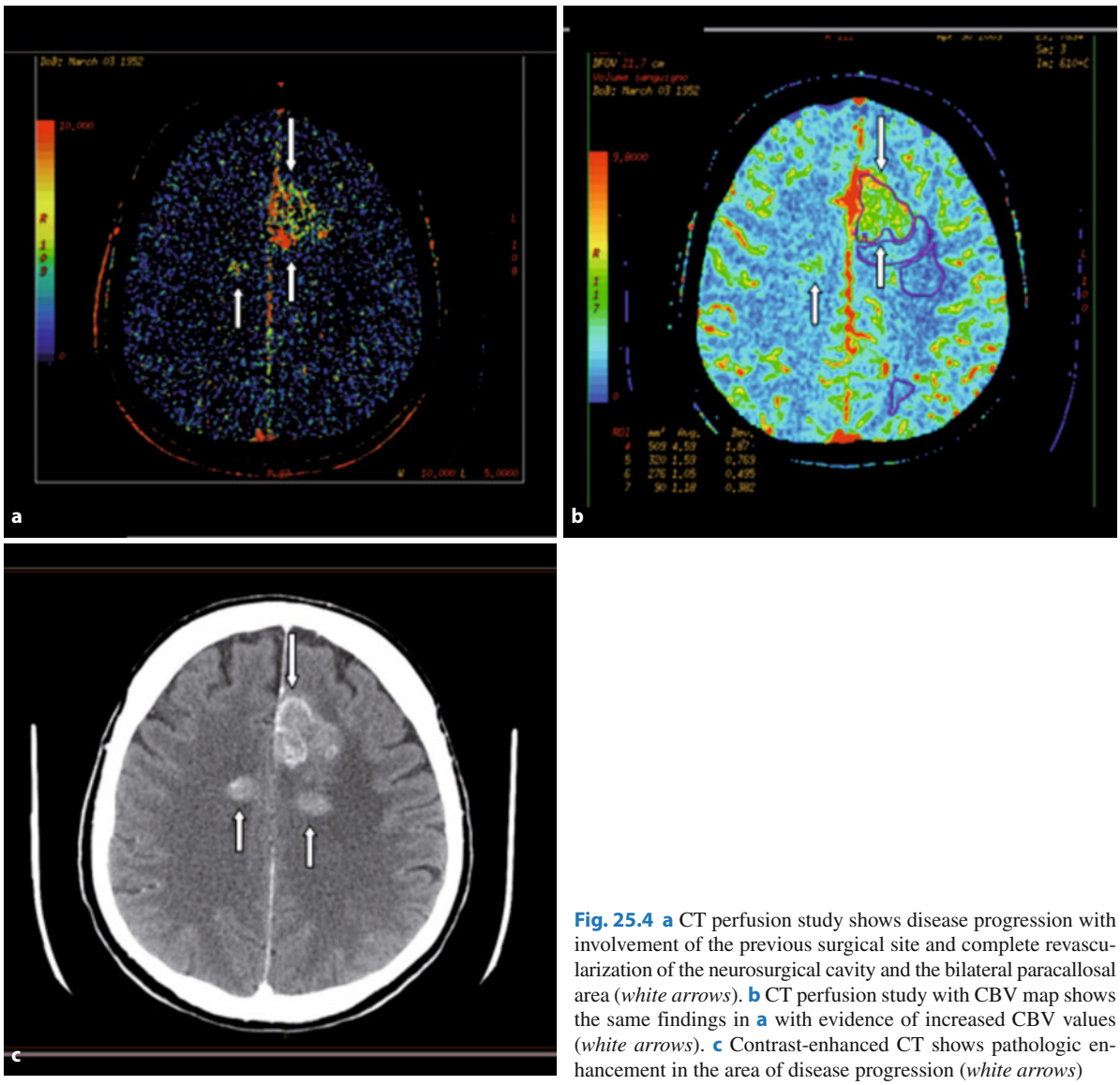

Fig. 25.4 **a** CT perfusion study shows disease progression with involvement of the previous surgical site and complete revascularization of the neurosurgical cavity and the bilateral paracallosal area (*white arrows*). **b** CT perfusion study with CBV map shows the same findings in **a** with evidence of increased CBV values (*white arrows*). **c** Contrast-enhanced CT shows pathologic enhancement in the area of disease progression (*white arrows*)

Case 26

Tumor Progression/Recurrence

Multimodal CT/MR Follow-up in Glioblastoma Multiforme

Alessandro Stecco, Mariangela Lombardi, Francesco Fabbiano, Gerardo Di Nardo, Sara Zizzari, Andrea Pietro Sponghini and Alessandro Carriero

- 53-year-old patient affected by right temporal glioblastoma multiforme treated with subtotal surgery, combined radiation therapy-chemotherapy, and second- and third-line adjuvant chemotherapy
- Multimodal CT/MR follow-up with morphologic and perfusion studies performed preoperatively and at 1, 4 and 8 months after surgery and combined radiation therapy-chemotherapy

Preoperative Imaging

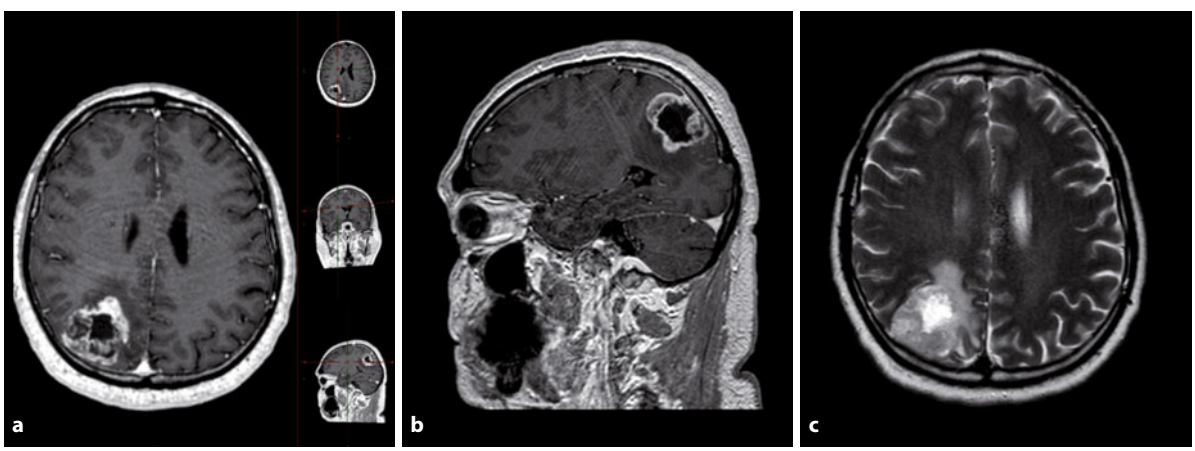

Fig. 26.1 Contrast-enhanced MR SE T1-weighted (**a**), FSE T2-weighted (**b**) and FLAIR (**c**) sequences show a right parietal lesion with irregular peripheral enhancement and central necrosis, findings consistent with high-grade lesion

Follow-up at 1 Month After Surgery

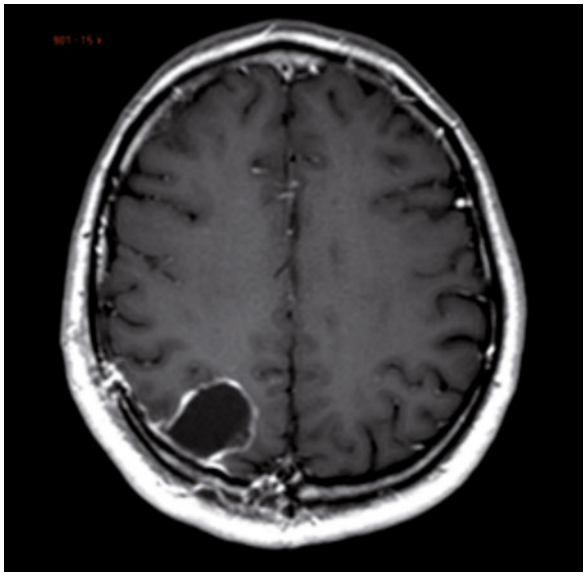

Fig. 26.2 Contrast-enhanced MR SE T1-weighted sequence shows wide surgical cavity with enhancing surgical margins

Follow-up at 4 Months After Surgery and Radiation Therapy

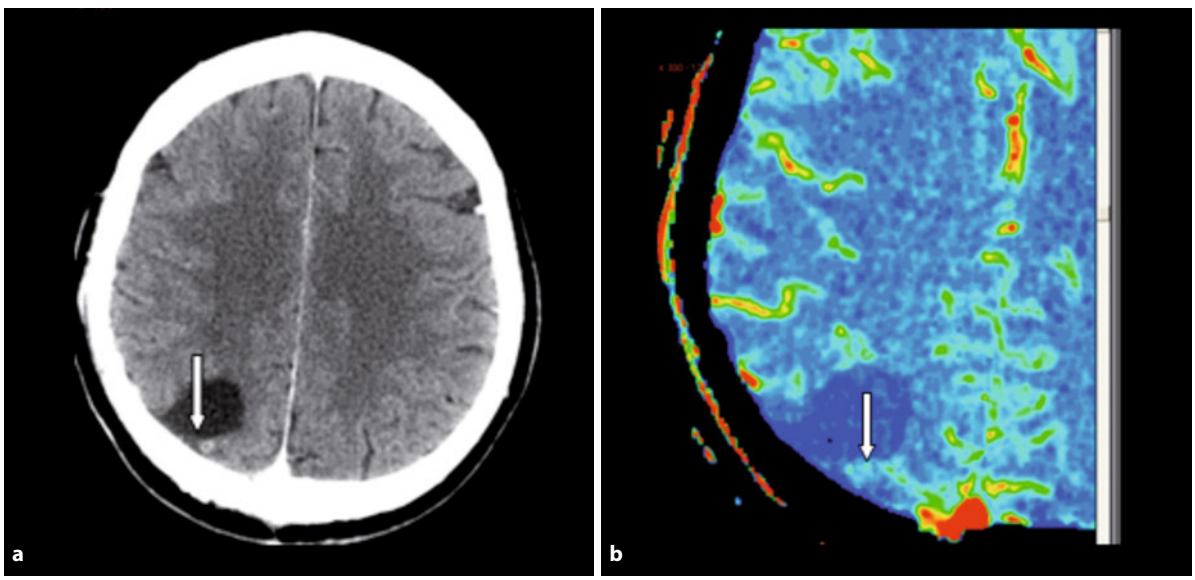

Fig. 26.3 **a** Contrast-enhanced CT scan. A millimetric nodular rim enhancement can be seen on the posterior edge of the surgical cavity (*white arrow*). **b** MR perfusion study with relative CBV map shows elevated CBV nodule at the site of nodular enhancement shown on CT (*white arrow*)

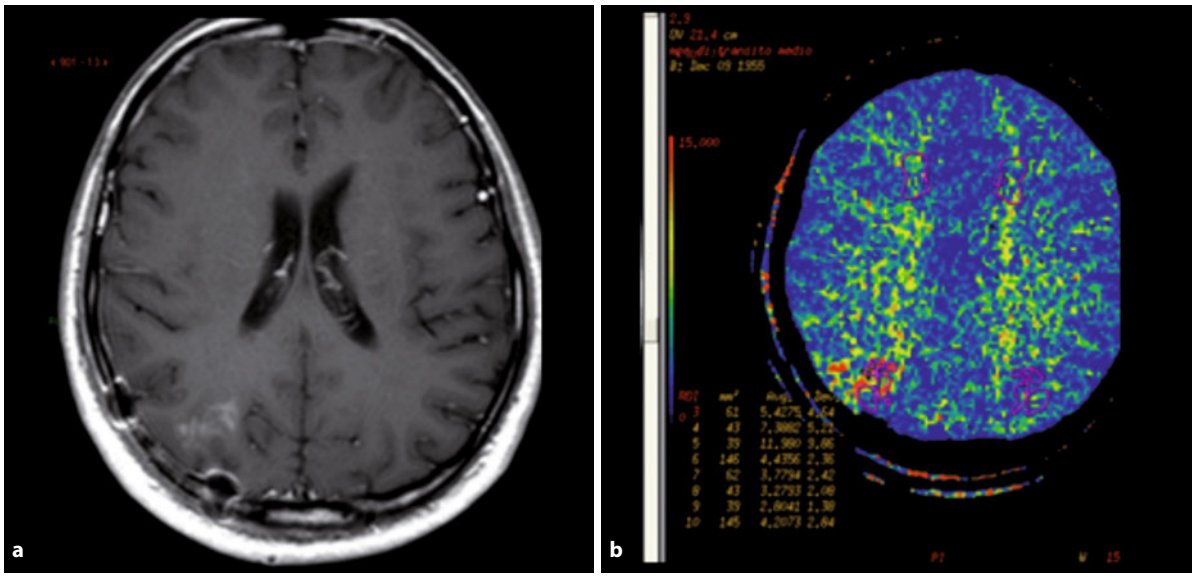

Fig. 26.4 **a** Contrast-enhanced MR SE T1-weighted image. This lower section shows revascularization of the cavity by newly formed tissue with inhomogeneous pattern of enhancement. **b** CT perfusion map of permeability surface (PS). This lower section shows marked elevation of the PS coefficient at the surgical site

Follow-up at 8 Months After Surgery and Radiation Therapy-chemotherapy

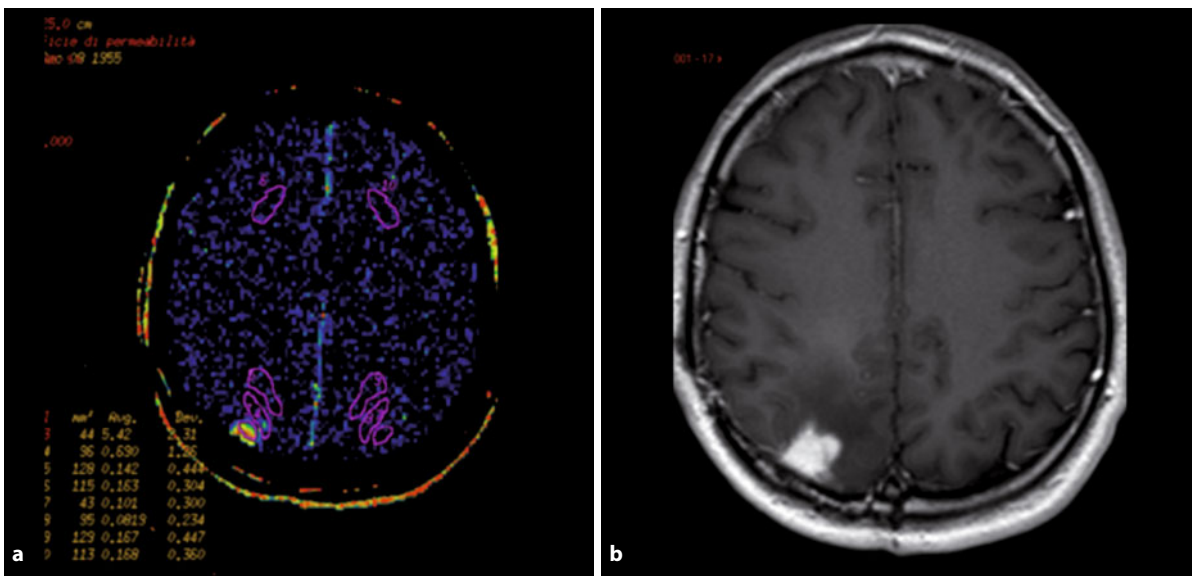

Fig. 26.5 **a** CT perfusion study. This higher section shows another area of disease recurrence with marked elevation of the permeability coefficient. **b** Contrast-enhanced MR SE T1-weighted sequence shows marked enhancement at the site of recurrence

Case 27

Local and Distant Recurrence

3T Multimodal MR Follow-up in Glioblastoma Multiforme

Tommaso Scarabino, Teresa Popolizio, Saverio Pollice, Vincenzo D'Angelo and Alfonso Di Costanzo

- 46-year-old patient with right frontal-insular glioblastoma multiforme treated with subtotal excision and combined radiation therapy-chemotherapy and subsequent second-level adjuvant chemotherapy
- 3T multimodal MR follow-up performed with morphologic imaging, diffusion, perfusion and spectroscopy preoperatively and at 6, 9 and 12 months after surgery and combined radiation therapy-chemotherapy

T. Scarabino (ed.), *Imaging Gliomas After Treatment,* © Springer-Verlag Italia 2012

Preoperative Imaging

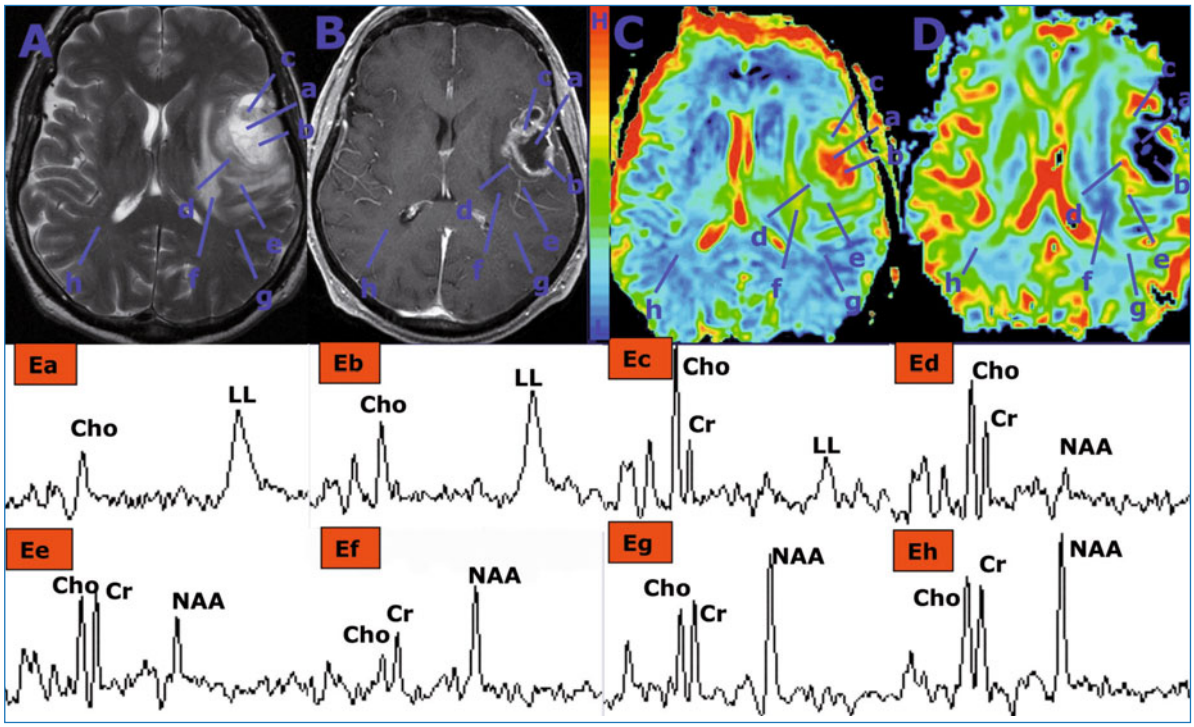

Fig. 27.1 MR FSE T2-weighted (**a**) and contrast-enhanced SE T1-weighted (**b**) sequences show a large mass with significant central necrotic component, moderate edema with mild mass effect on midline structures which appear shifted contralaterally. The MR multimodal study with diffusion-weighted imaging and ADC map (**c**), perfusion study with CBV map (**d**) and single-voxel spectroscopy with multiple ROIs (**e**) show spectra relative to the enhancing areas and those immediately adjacent to the lesion with the typical biologic behavior of an aggressive tumor, characterized by high Cho, inversion of the Cho/NAA ratio and the presence of Lac/Lip (LL). In these ROI, ADC is reduced and CBV increased. In the large necrotic-colliquative area there is a reduction in the spectral levels of all metabolites with a minimum Cho peak, the presence of LL, an increase in ADC and reduction in CBV. The spectra associated with apparently edematous areas outside the enhancement have reduced levels of all metabolites, but different patterns, i.e. normal Cho/NAA in the non-infiltrated vasogenic edema and tumor pattern (high Cho/NAA) in the infiltrated edema. ADC and CBV in these locations have the opposite behavior, with the former being elevated and the latter reduced in the area of pure edema and vice versa in the infiltrated edema. Moving away from the lesion the metabolic pattern along with the ADC and CBV values return to normal as in the contralateral hemisphere

Follow-up Performed at 6 Months After Surgery and Combined Radiation Therapy-chemotherapy

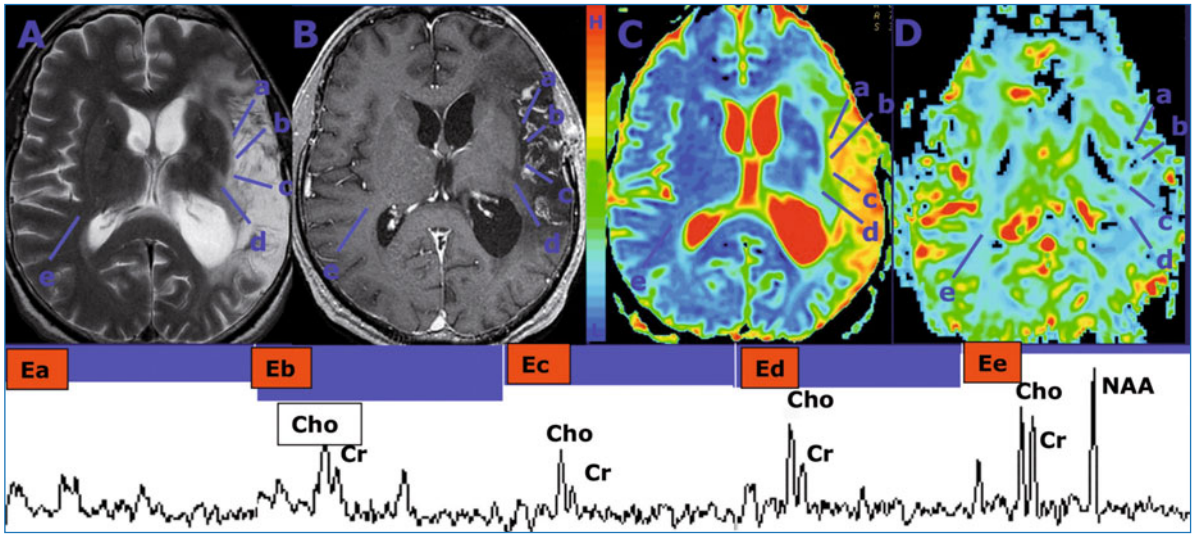

Fig. 27.2 Morphofunctional MR with FSE T2-weighted (**a**) and contrast-enhanced SE T1-weighted (**b**) sequences, diffusion-weighted imaging with ADC map (**c**), perfusion study with CBV map (**d**) and multivoxel spectroscopy with multiple ROIs (**e**). The imaging findings after treatment show an almost complete necrotic transformation of the lesion free from significant pathologic enhancement with associated retraction dilatation of the adjacent lateral ventricle. At that level there is spectral reduction of the levels of all metabolites, an increase in ADC and reduction in CBV. These indicators are also appreciable in the surrounding tissue with the exception of a small area of high CBV lesion located posterior to the tumor (distant recurrence)

Follow-up Performed at 9 Months

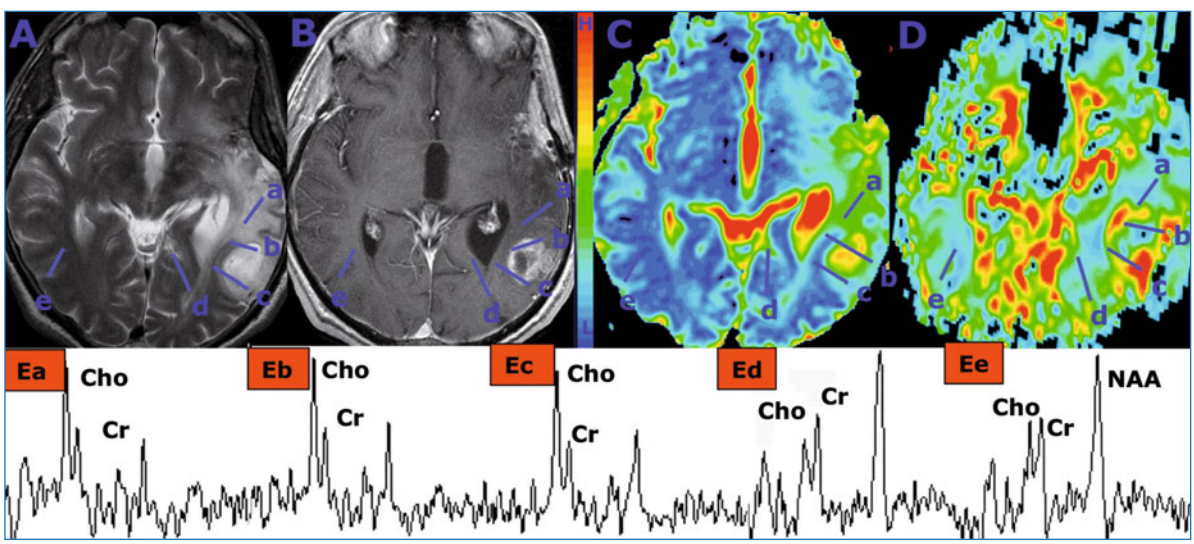

Fig. 27.3 MR with FSE T2-weighted (**a**) and contrast-enhanced SE T1-weighted (**b**) sequences. The images show distant recurrence posterior to the main surgical site which appears free from persistence/recurrence with the exception of mild peripheral thickening with pathologic enhancement. Multimodal MR with diffusion-weighted imaging and ADC map (**c**), perfusion study with CBV map (**d**) and multivoxel spectroscopy with multiple ROIs (**e**). The recurrence has morphofunctional characteristics similar to the original lesion with a large component of central tumor necrosis and typical pattern of the spectra in the areas with enhancing tumor immediately behind the lesion (high Cho and inversion of the Cho/NAA ratio), of ADC (low) and CBV (increased); the opposite can be seen in the necrotic-colliquative area

Follow-up Performed at 12 Months

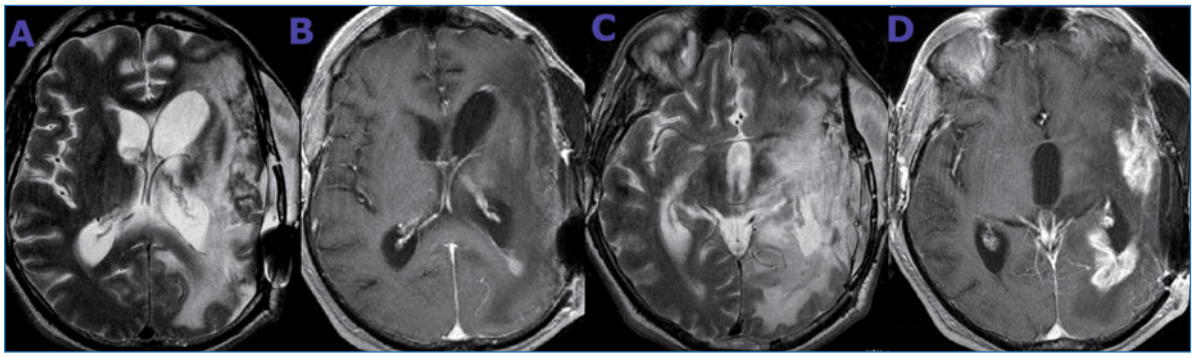

Fig. 27.1 MR FSE T2-weighted (**a,c**) and contrast-enhanced SE T1-weighted (**b,d**) sequences show not only the distant recurrence but also the recurrence of the lesion in the original sites. In both cases, apart from the extensive surrounding edema, there is the presence of a solid lesion with irregular margins

Case 28

Tumor Recurrence

3T Morphofunctional MR Follow-up in Low-grade Astrocytoma with Anaplastic Appearance

Massimo Caulo, Chiara Briganti, Valentina Panara, Simone Salice, Domenico Tortora and Armando Tartaro

- 46-year-old patient with right frontal lowgrade astrocytoma treated with subtotal surgery and combined radiation therapy-chemotherapy
- 3T morphofunctional MR follow-up performed with morphologic imaging, diffusion, perfusion, and spectroscopy at 4 years after surgery and combined radiation therapy-chemotherapy

Follow-up Performed at 4 Years After Surgery and Combined Radiation Therapy-chemotherapy

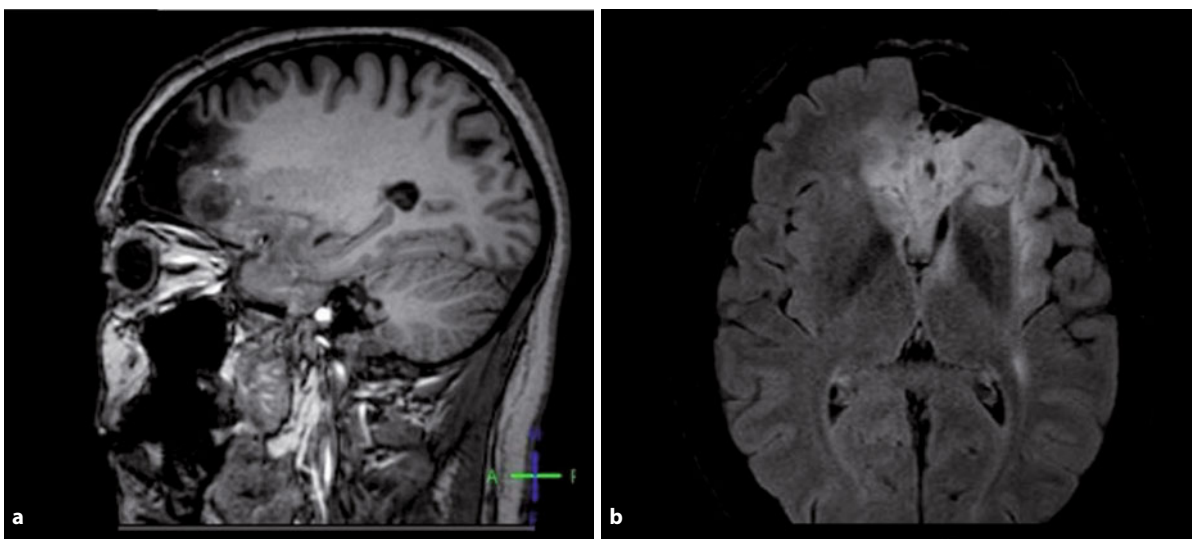

Fig. 28.1 **a** Contrast-enhanced MR SE T1-weighted sequence shows a nodular lesion with thick and irregular walls and necrotic-hemorrhagic content. **b** MR FLAIR sequence visualizes the tumor almost completely infiltrating the polar and basal portions of the frontal lobes, the genu of the corpus callosum and the left temporal lobe

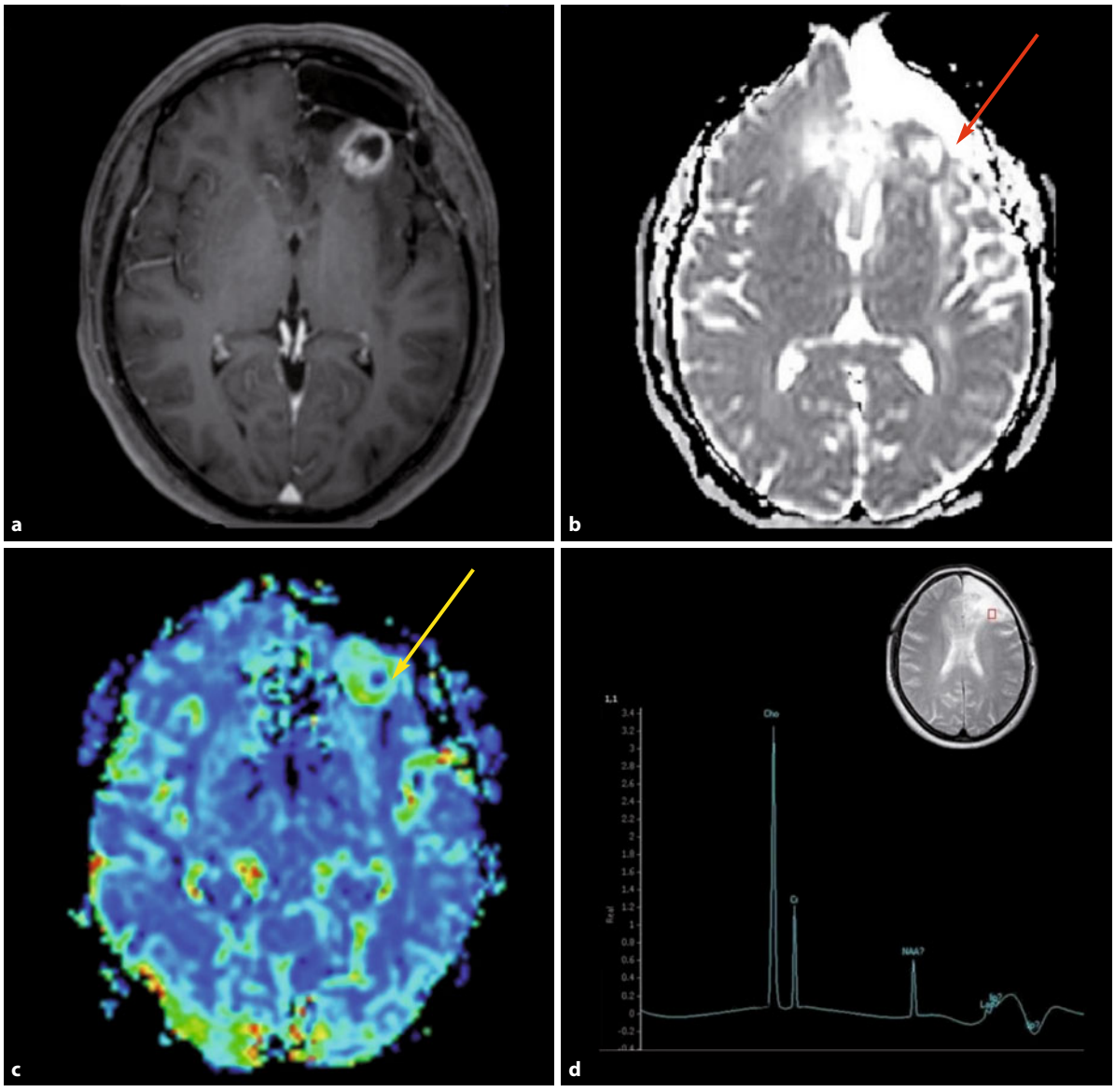

Fig. 28.2 **a** Contrast-enhanced MR SE T1-weighted sequence shows nodular contrast enhancement of the surgical cavity indicative of disease progression. **b** MR diffusion-weighted imaging with ADC map is characterized by a low ADC mean value of 0.672±0.122 mm^2/s in the nodule (*arrow*). **c** MR perfusion study with CBV map. The high value of the rCBV of 4.1 [CBV lesion/contralateral white matter CBV sound] corresponds to the areas of enhancement adjacent to the surgical cavity (*yellow arrow*). **d** MR single/multivoxel spectroscopy shows a reversal of the Cho/Cr (3.1) and Cho/NAA (4.2) ratios corresponding to the areas of tumor recurrence, indicative of recurrence with anaplastic appearance

Case 29

Tumor Progression

Morphofunctional MR Follow-up in Glioblastoma Multiforme

Mario Muto and Alessandra D'Amico

- 56-year-old patient with right frontal-temporal glioblastoma multiforme treated with surgical removal and combined radiation therapy-chemotherapy
- Morphofunctional MR follow-up at 24 hours, 2, 6, 8, 13 and 15 months after surgery and combined radiation therapy-chemotherapy in glioblastoma multiforme

Preoperative Imaging

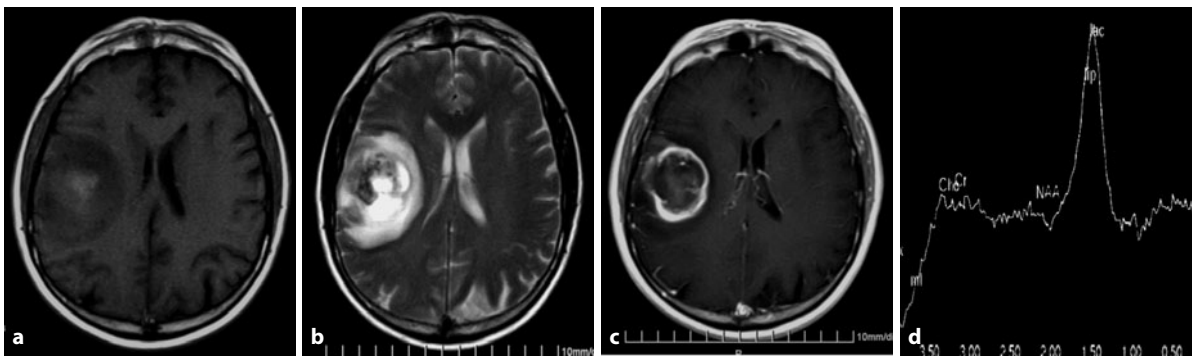

Fig. 29.1 MR morphofunctional study performed with SE T1-weighted (**a**), FSE T2-weighted (**b**), contrast-enhanced SE T1-weighted (**c**) sequences and single voxel spectroscopy (**d**). A right frontal-temporal lesion can be appreciated with edema and inhomogeneous signal due to the presence of central hemorrhagic areas, more peripheral cystic-necrotic areas and peripheral pathologic rim enhancement. Compression of the adjacent sulcuses and slight compression of the lateral ventricle below are also evident. Spectroscopic analysis shows reduction of all metabolites and increased Lip/Lac peak, indicative of necrosis within the infiltrating lesion

Early Postoperative Follow-up (Within 24 Hours)

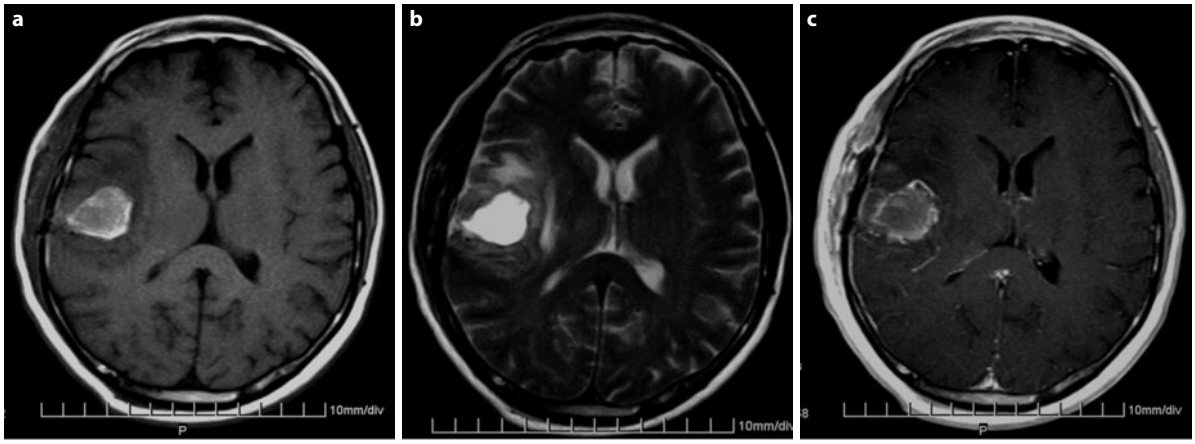

Fig. 29.2 MR SE T1-weighted (**a**), FSE T2-weighted (**b**) and contrast-enhanced SE T1-weighted (**c**) sequences. The right frontal-temporal craniotomy with well positioned bone flap and the underlying surgical cavity with hyperintense blood signal are visualized. A reduction in perifocal edema can be seen and consequent slight residual compression on the underlying lateral ventricle. After contrast medium administration, faint marginal enhancement of the surgical cavity is visible caused by blood-brain barrier injury (normal early postoperative finding)

Postoperative Follow-up at 2 Months

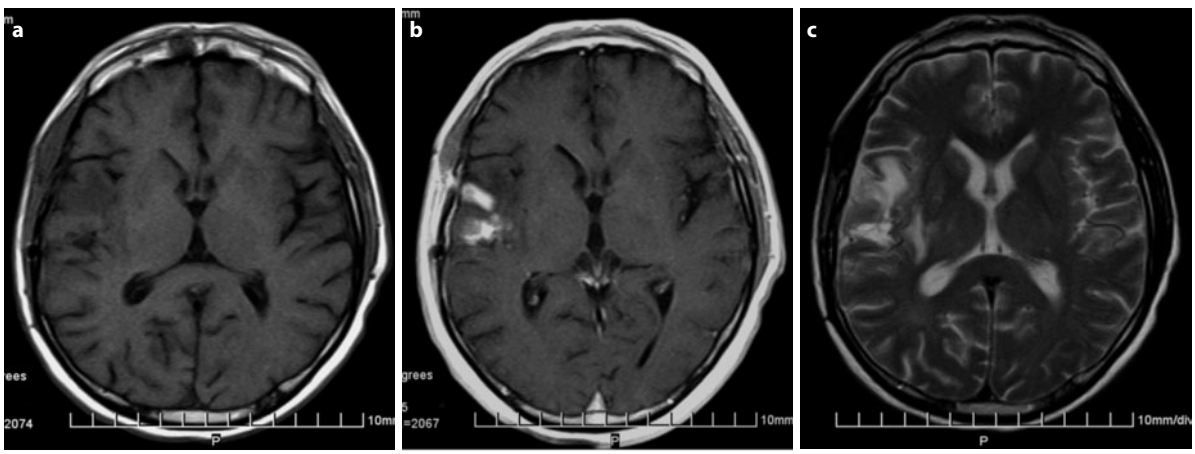

Fig. 29.3 MR SE T1-weighted (**a**), FSE T2-weighted (**b**) and contrast-enhanced SE T1-weighted (**c**) sequences. A slight signal alteration can be appreciated within the surgical cavity and the subcortical areas with re-expansion of the lateral ventricle of the same side. After contrast medium administration some marginal enhancement can be seen

Follow-up at 6 Months After Surgery and Combined Radiation Therapy-chemotherapy

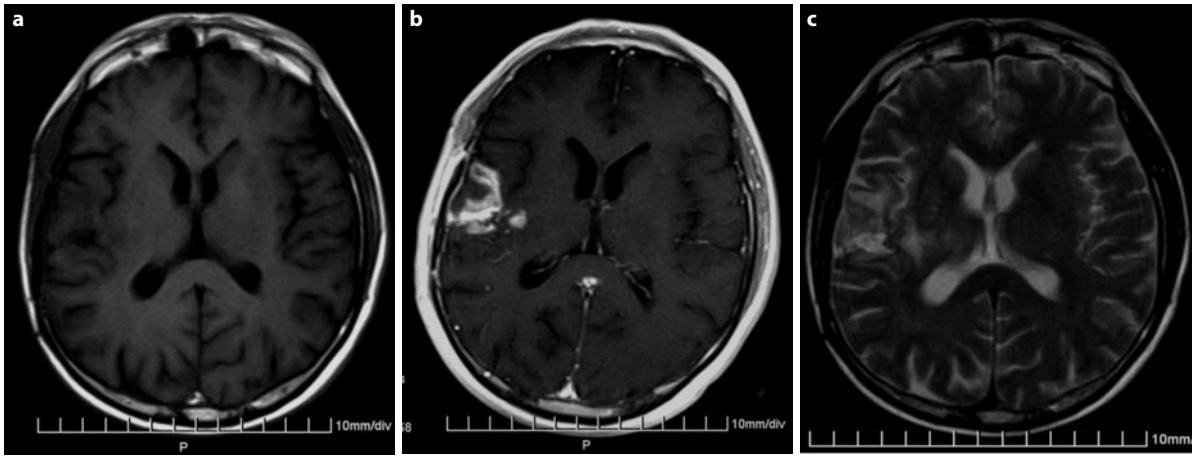

Fig. 29.4 MR SE T1-weighted (**a**), contrast-enhanced SE T1-weighted (**b**) and FFSE T2-weighted (**c**) sequences. The postsurgical gliotic findings are more pronounced than in the previous examination. After contrast medium administration a slight increase in the size of the enhancing foci is appreciable

Follow-up at 8 Months

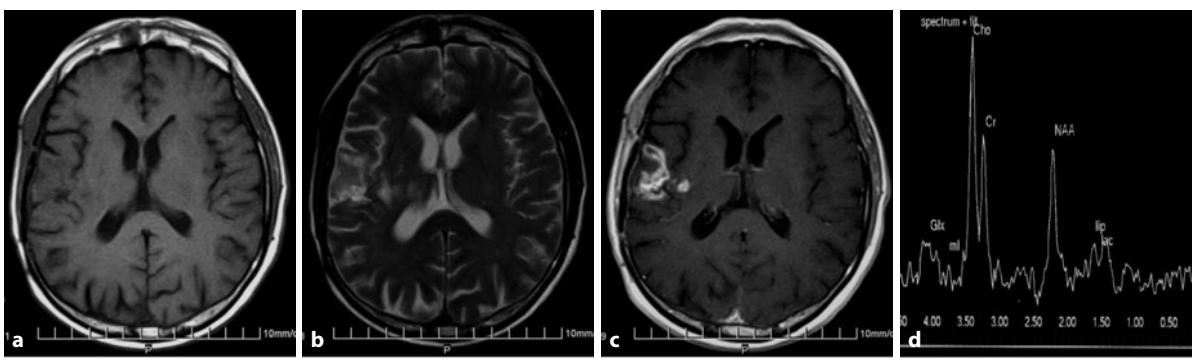

Fig. 29.5 MR morphofunctional study performed with SE T1-weighted (**a**), FSE T2-weighted (**b**) and contrast-enhanced SE T1-weighted (**c**) sequences and single-voxel spectroscopy (**d**). There are no major changes to the findings already known, with enhancing foci substantially unchanged in size and signal characteristics. Spectroscopic analysis with a voxel placed in the previous surgical site shows a reversal of the Cho/NAA peak (indicating altered turnover of the cell membrane and neuronal loss) and a small Lip\Lac peak (initial index of necrotic changes)

Follow-up at 13 Months

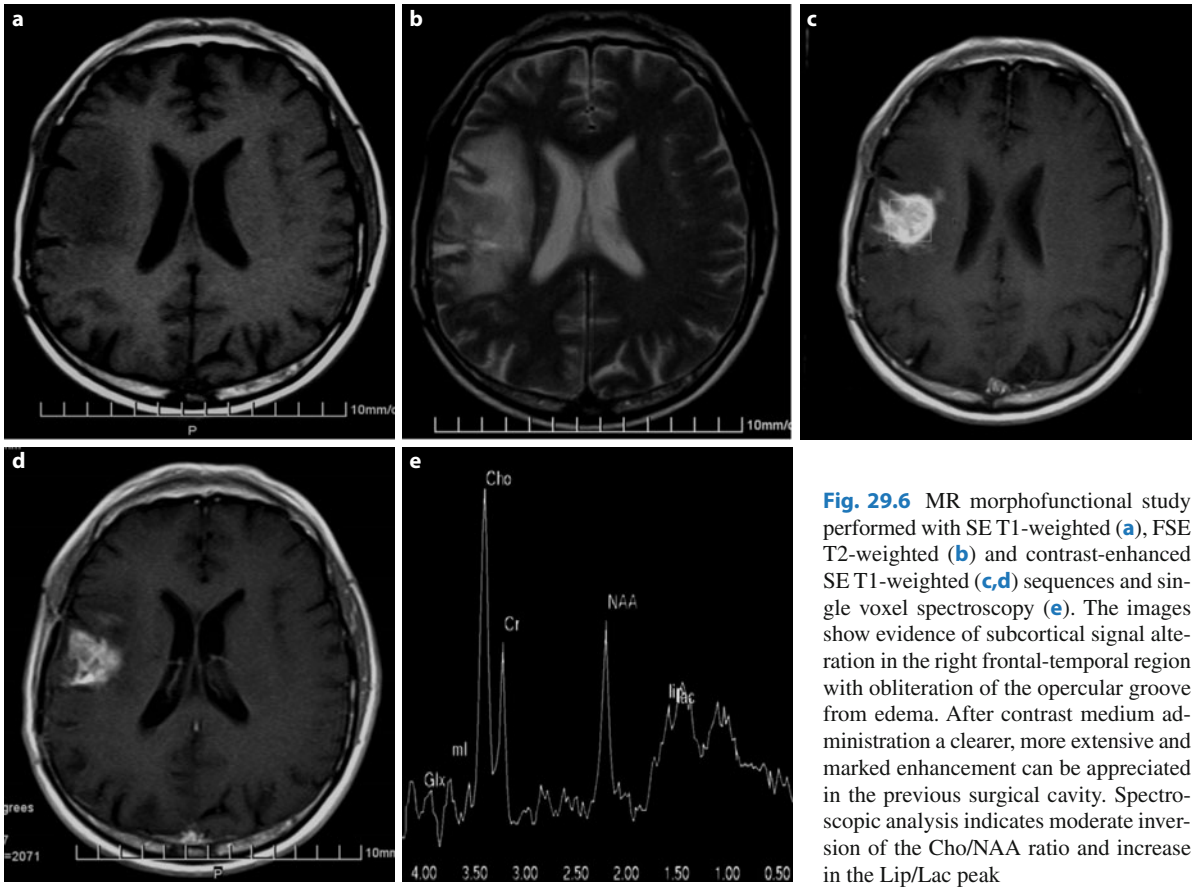

Fig. 29.6 MR morphofunctional study performed with SE T1-weighted (**a**), FSE T2-weighted (**b**) and contrast-enhanced SE T1-weighted (**c,d**) sequences and single voxel spectroscopy (**e**). The images show evidence of subcortical signal alteration in the right frontal-temporal region with obliteration of the opercular groove from edema. After contrast medium administration a clearer, more extensive and marked enhancement can be appreciated in the previous surgical cavity. Spectroscopic analysis indicates moderate inversion of the Cho/NAA ratio and increase in the Lip/Lac peak

Follow-up at 15 Months

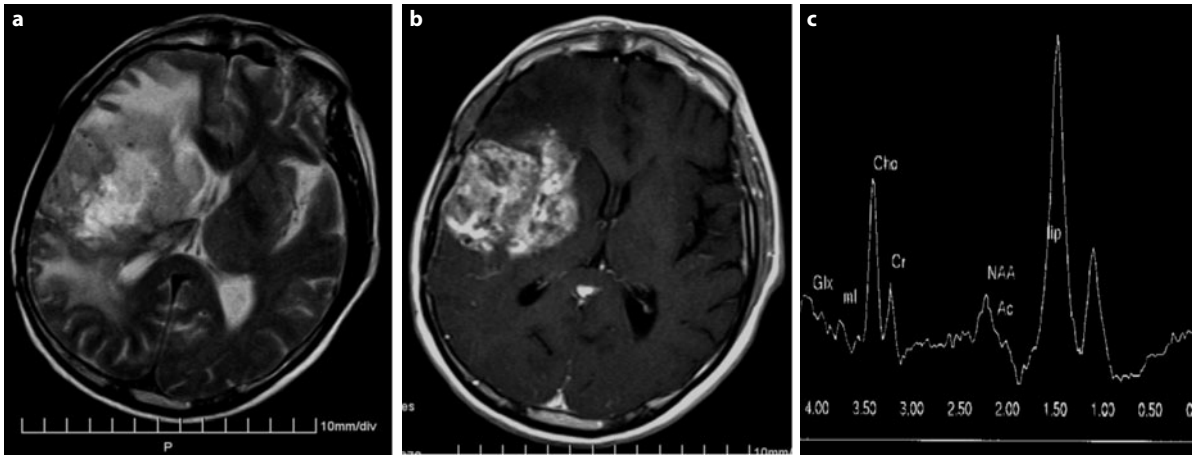

Fig. 29.7 MR morphofunctional study performed with SE T1-weighted (**a**), FSE T2-weighted (**b**) and contrast-enhanced SE T1-weighted (**c**) sequences and single voxel spectroscopy (**d**). The images document a worsening of the previous situation with a noticeable extension of signal abnormalities in the right frontal-temporal region, which appears inhomogeneous due to the presence of necrosis. Perilesional edema extends to the ipsilateral frontal-polar and peritrigonal regions, with mass effect on adjacent structures and the underlying contralateral lateral ventricle with a mild midline shift. After contrast medium administration there is irregular enhancement of the surgical cavity extending to the frontal-temporal cortex and temporal-insular infiltration of the basal ganglia (lenticular nucleus and internal capsule). Spectroscopic analysis shows a further net inversion of the Cho/NAA ratio and marked increase in the Lip/Lac peak

Case 30

Tumor Progression

Morphofunctional MR Follow-up in Glioblastoma Multiforme

Gabriele Polonara, Lorenzo Alvaro and Francesco Sessa

- 44-year-old patient with right frontal-parietal pararolandic anaplastic astrocytoma (WHO III) treated with surgery, radiotherapy, chemotherapy and subsequent co-adjuvant level II chemotherapy
- Morphofunctional MR follow-up performed with morphologic imaging, diffusion, perfusion and spectroscopy preoperatively and at 48 hours, 4 (contrast-enhanced CT scan), 7, 10, 12 and 14 months after surgery

Preoperative Imaging

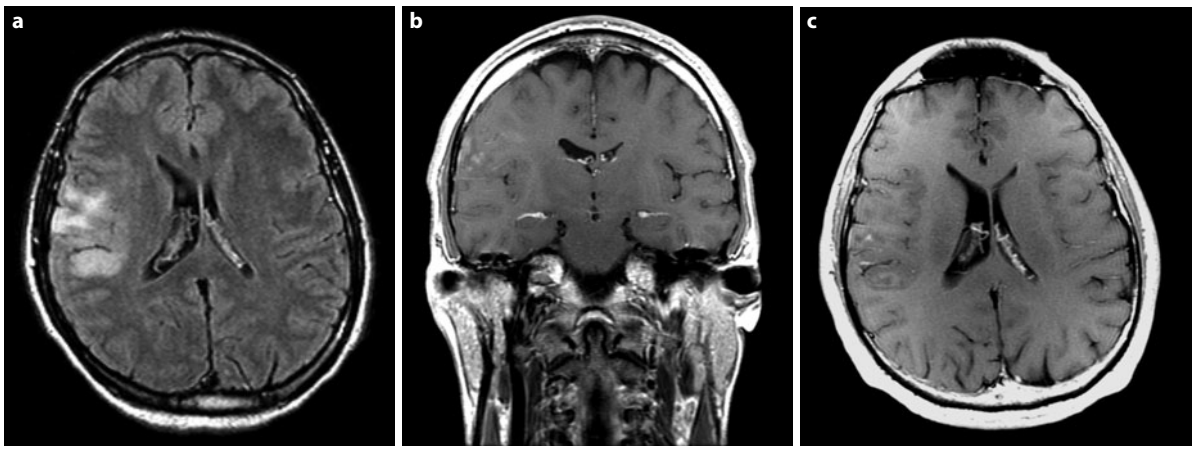

Fig. 30.1 **a** MR FLAIR sequence shows a cortical-subcortical area of altered signal with poor visualization of the corresponding cortical sulci in the right frontal-parietal pararolandic region, at the level of the frontal-parietal opercular area and the right insular region. **b,c** Contrast-enhanced MR SE T1-weighted sequences show minimal signs of altered BBB in the context of the lesion, mainly located in the cortical and immediately subcortical regions at the level of the parietal operculum and ascending parietal gyrus

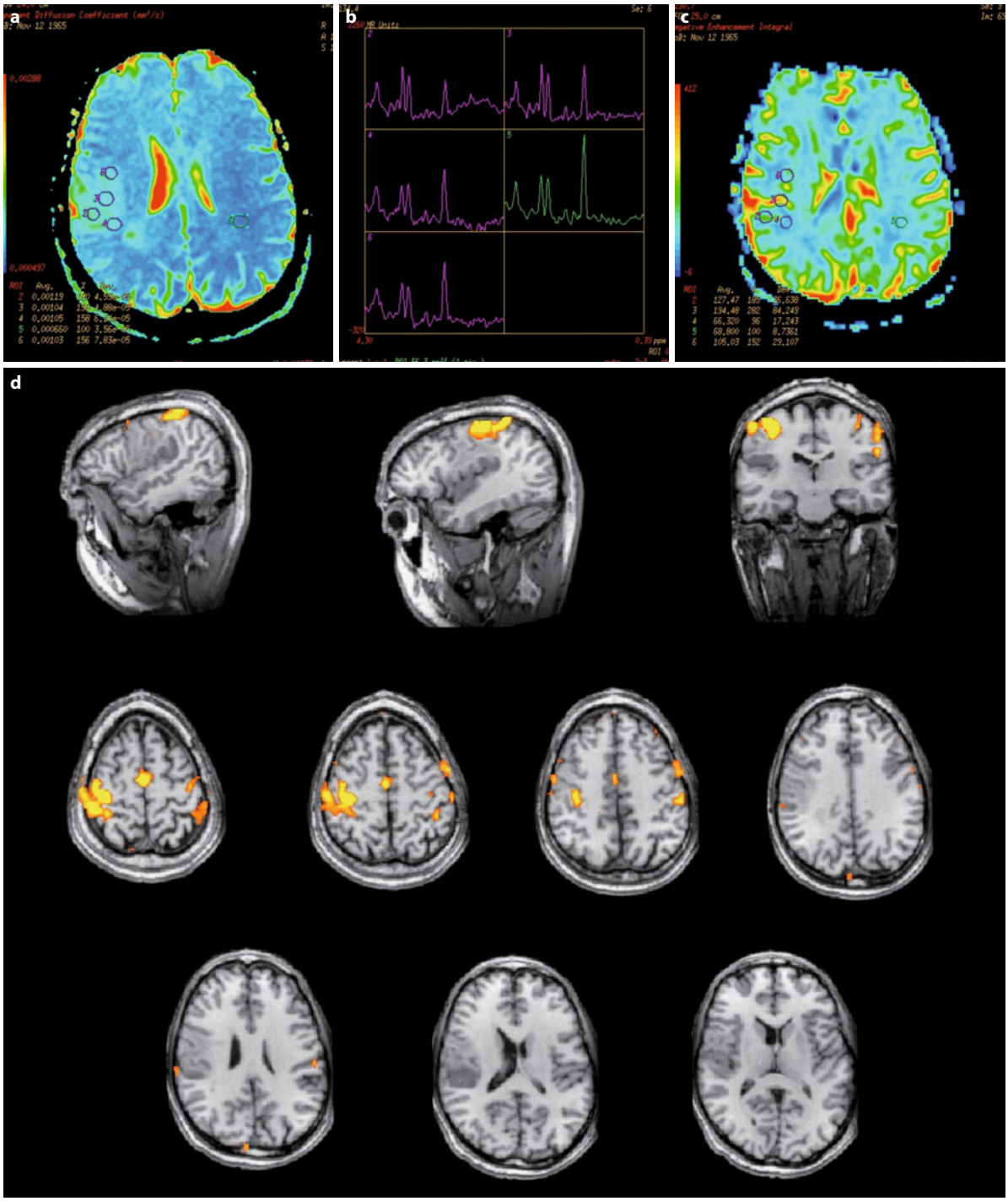

Fig. 30.2 **a** MR diffusion-weighted imaging shows moderate increase in the apparent diffusion coefficient in the right frontal-parietal lesion. **b** MR multivoxel and long TE spectroscopy. A decrease in the NAA/Cr ratio, a slight increase in the Cho/Cr and Cho/NAA ratios (indices of increased proliferative activity) are shown and an absence of lactic acid or lipid peaks. **c** MR perfusion study shows a moderate increase in perfusion of the lesion compared with the apparently healthy contralateral brain parenchyma. **d** MR study mapping functional areas shows areas that are activated during the opening and closing movements of the left hand

Early (48 hours) Postoperative Follow-up

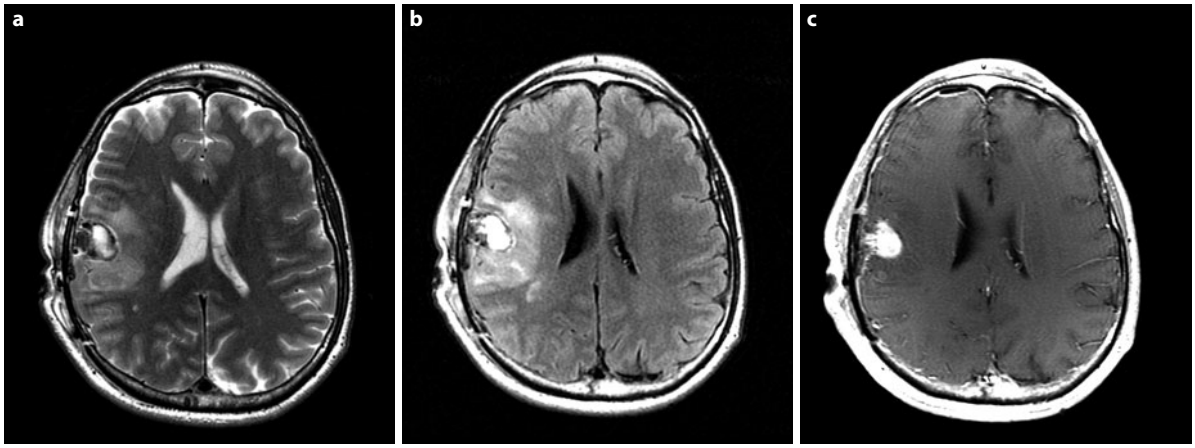

Fig. 30.3 MR FSE T2-weighted (**a**) and FLAIR (**b**) sequences display the right parietal-temporal craniotomy (with repositioned bone flap) and postsurgical evidence of partial removal of a right frontal-parietal lesion. In particular, a postsurgical area of loss of white matter can be appreciated at the level of the inferior portion of the right postcentral gyrus. A small amount of hyperintense perilesional edema and minimal signs of expansion can also be seen. **c** Contrast-enhanced MR SE T1-weighted sequence shows evidence in the right frontal-parietal lobe of a slight accentuation of the CSF spaces, a slight thickening of the dura and probably a residual lesion

Follow-up Performed at 4 Months After Surgery, Radiotherapy and Concomitant Chemotherapy

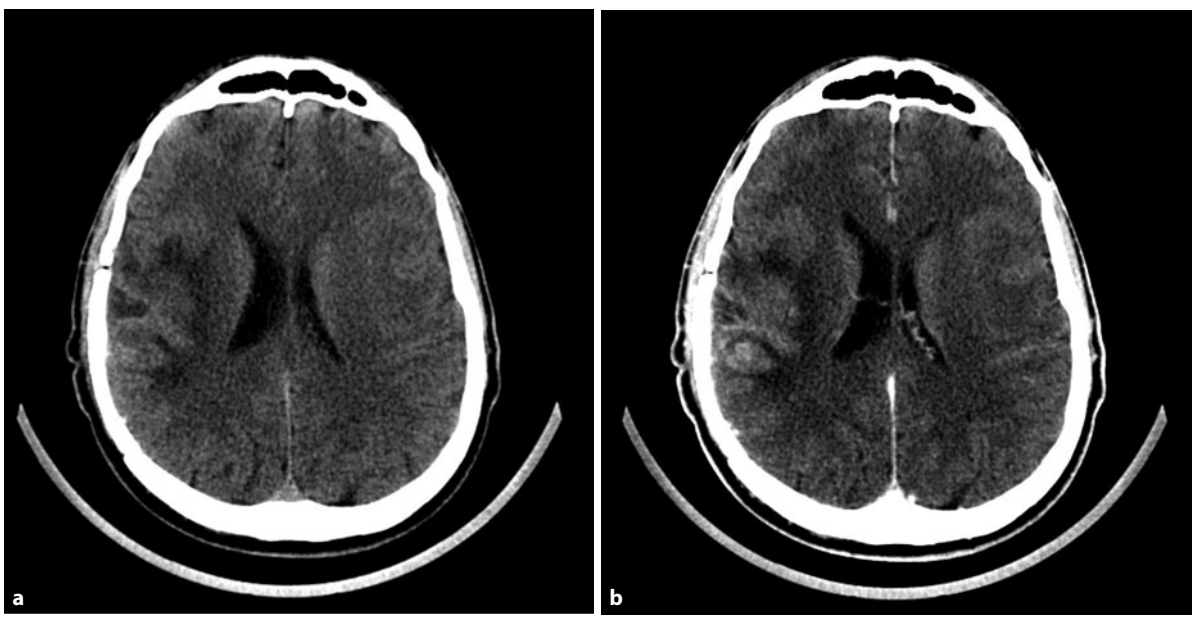

Fig. 30.4 CT scan without (**a**) and with (**b**) administration of contrast medium. Regrowth of the tumor can be seen in the right cortical-subcortical inferior parietal region, with associated peripheral hypodensity indicating infiltration/edema, and mild signs of locoregional expansion. After administration of contrast medium there is an irregular enhancement of the tumor

Follow-up Performed at 7 Months After Surgery and 3 Cycles Of Adjuvant Chemotherapy

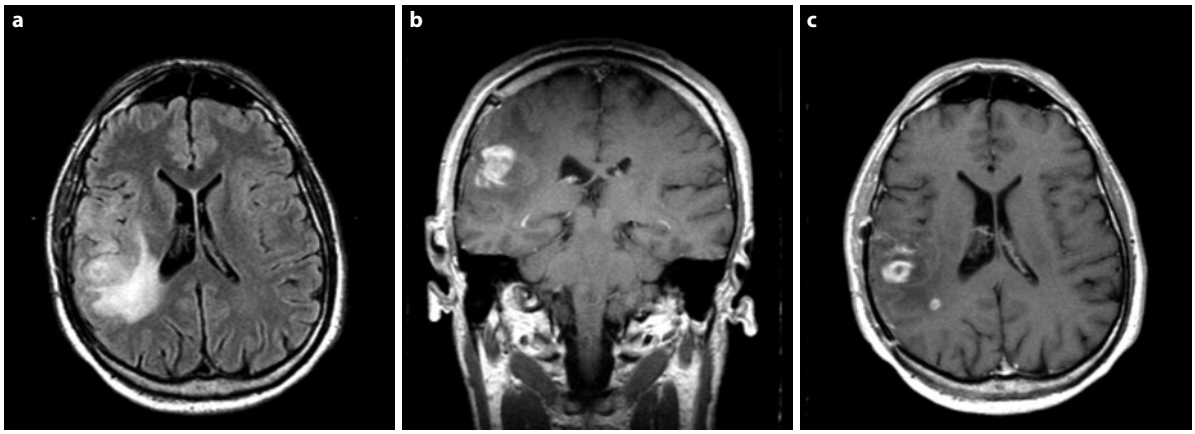

Fig. 30.5 **a** MR FLAIR sequence shows inhomogeneous increase in size of infiltrating lesion with ill-defined margins located in the right frontal-parietal pararolandic region, surrounded by slight perilesional edema extending in the right subependymal paratrigonal region. Increased signs of compression on the right frontal-parietal cortex and mild compression of the ipsilateral ventricular trigone can also be seen. **b,c** Contrast-enhanced MR SE T1-weighted sequences show considerable enhancement of the infiltrating lesion in the right frontal-parietal pararolandic region associated with micronodular lesions in the right subcortical parietal region adjacent to and above the trigone

Follow-up Performed at 10 Months After Surgery, Two Conventional Cycles and Other Intensified Cycles of Chemotherapy

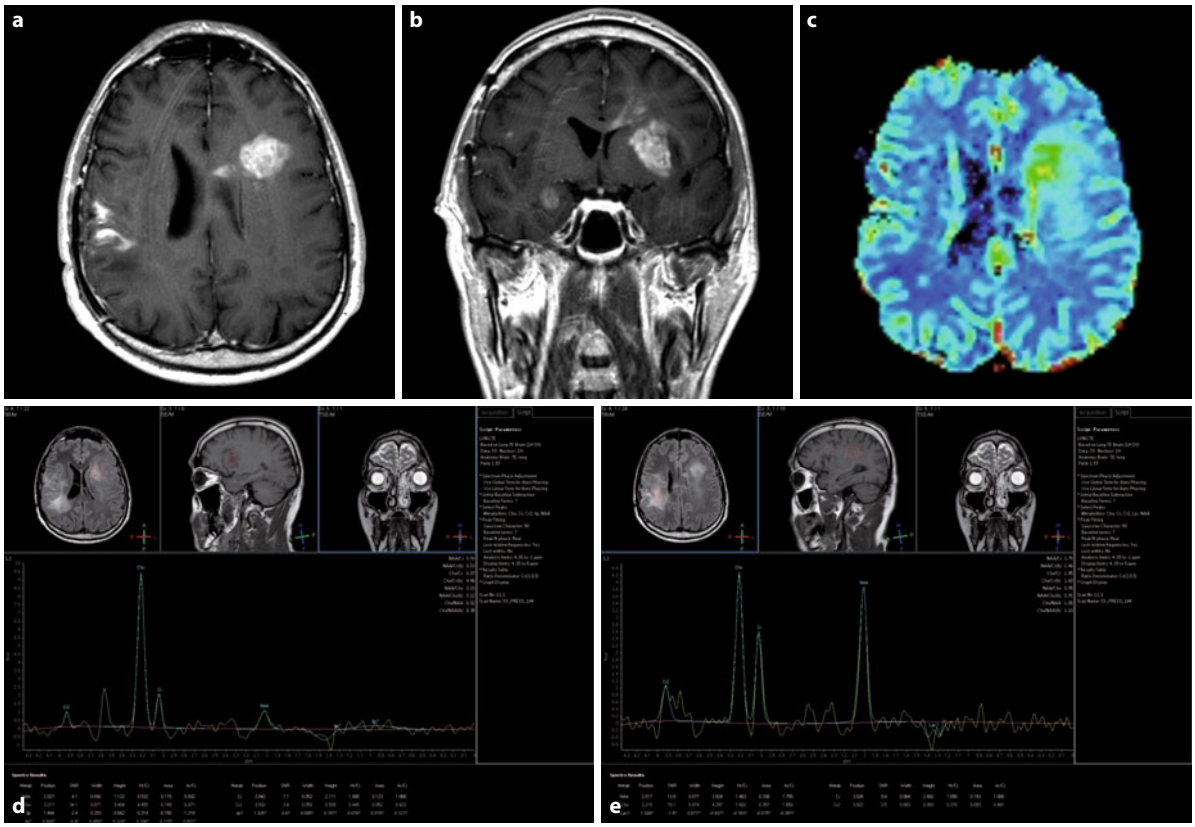

Fig. 30.6 a,b Contrast-enhanced MR SE T1-weighted sequence identifies the appearance of new expansive-infiltrative lesions in the left anterior frontal-insular region, with partial infiltration of the adjacent corpus callosum. Less evident changes can be seen in the contralateral residual lesion-recurrence at the site of previous surgery. On the left increased enhancement of the entire lesion is evident, whereas enhancement on the right appears more heterogeneous and appreciable mainly in the portion of right cortical-subcortical frontal-parietal region. Enhancement can also be seen in the right parauncal region which was absent in the previous study. MR study performed with perfusion imaging (**c**) and spectroscopy (**d,e**) seem to confirm a possible increased aggressiveness of the new-onset lesions on the left, which tend to appear hyperperfused (**c**), unlike the contralateral lesions. On the left there is also a marked increase in the Cho peak (**d**), associated with a marked reduction in the principal metabolites and appearance of a lactate peak, likely due to a poorly differentiated lesion with high cell turnover and initial necrosis. On the right the spectroscopic changes (**e**), despite a clearly pathologic appearance of infiltration-proliferation, appear less marked, with the exception of the right cortical-subcortical frontal-parietal portion immediately below the bone flap, which appears comparable to those on the left

Follow-up Performed at 12 Months After Surgery and After Starting Level II Chemotherapy

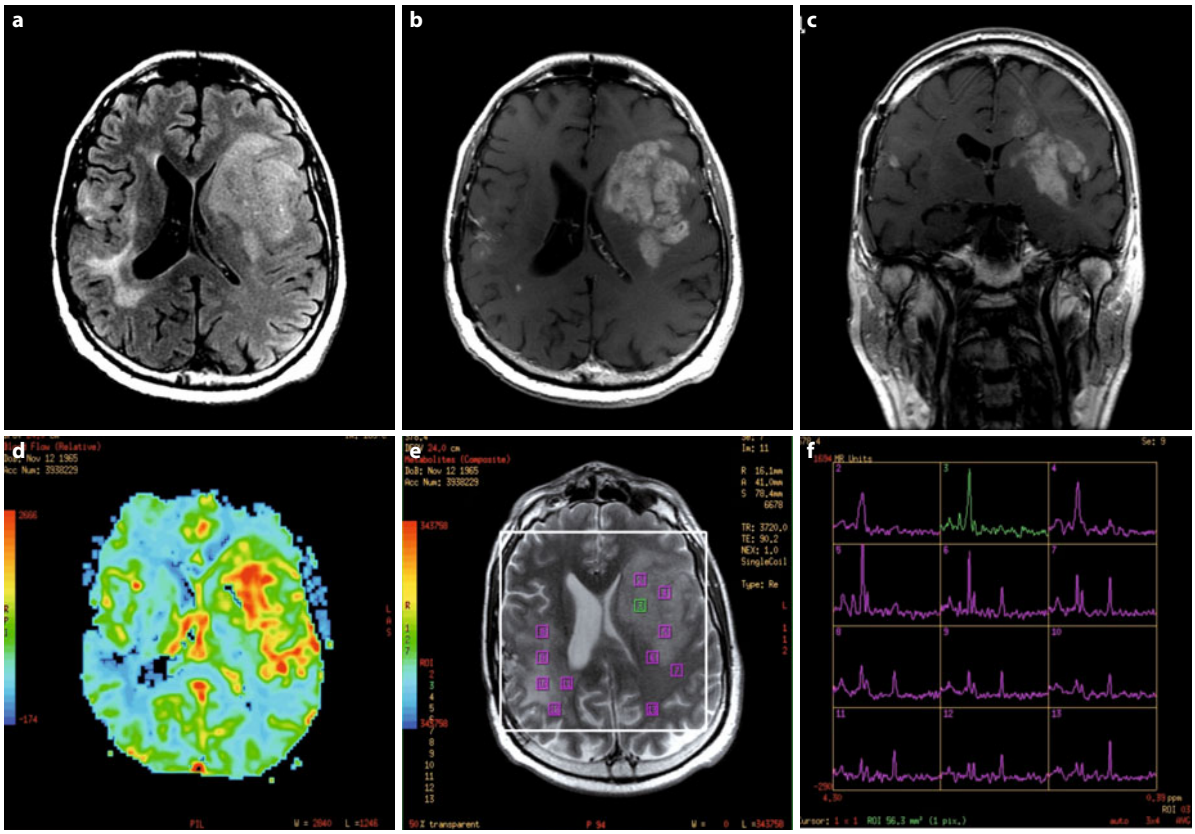

Fig. 30.7 **a** MR FLAIR sequence shows an overall extension of the expansive/infiltrating lesions. The increase is much more evident on the left with overall increase in the size of the known lesion. A concomitant increase in signs of expansion can also be seen characterized by increased compression of the ipsilateral ventricle and initial midline shift to the right. Contrast-enhanced MR SE T1-weighted sequences (**b,c**) and perfusion study (**d**). A slight reduction in the enhancement of the lesion on the right can be appreciated, while there is an extension of the hyperperfused area (**d**) and enhancement of the lesion on the left. **e,f** MR multivoxel spectroscopy with long TE shows a marked increase in the Cho/Cr and Cho/NAA ratios (indices of increased proliferation), while no lactic acid or lipid peaks are observed in relation to the lesions located in the left hemisphere. Only a slight increase in the Cho/Cr and Cho/NAA ratios can be seen on the right

Follow-up Performed at 14 Months After Surgery and After Continuing Level II Chemotherapy

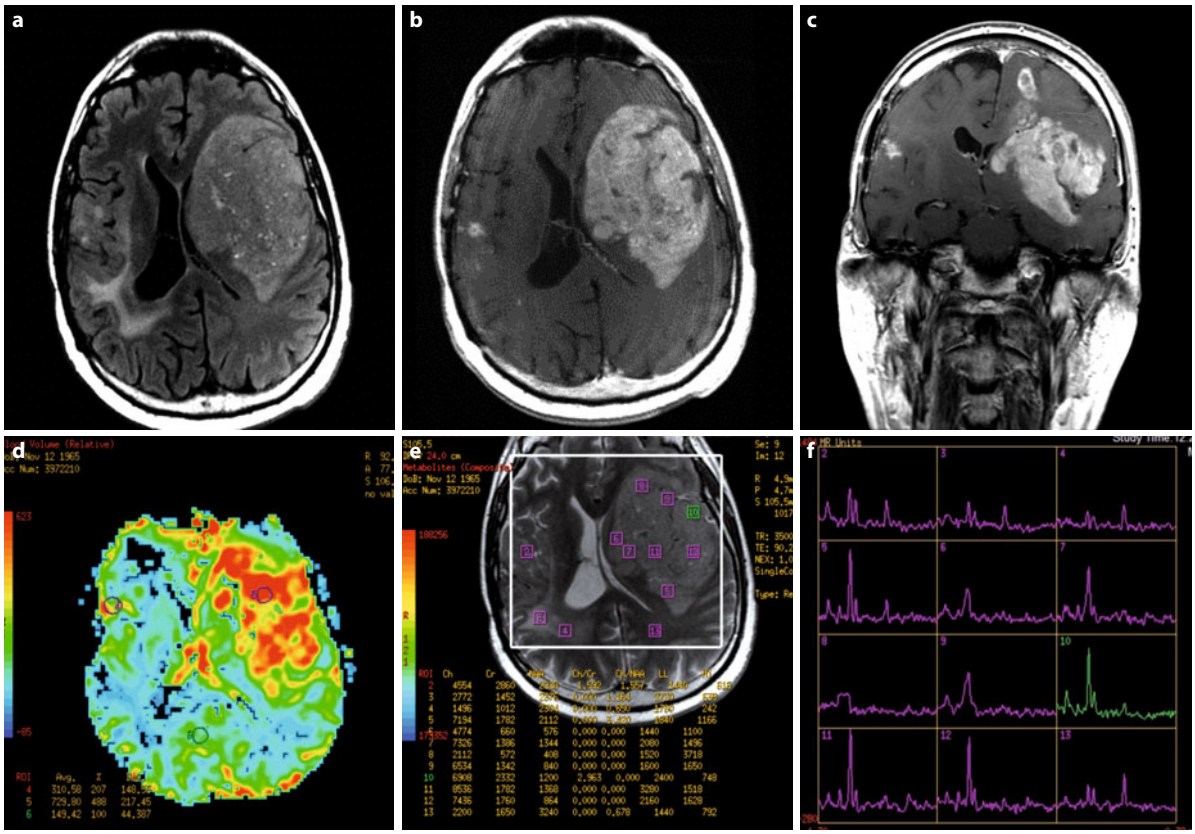

Fig. 30.8 MR FLAIR (**a**) and contrast-enhanced SE T1-weighted (**b,c**) sequences show further marked increase in the overall size of the left expansive/infiltrative lesion and the associated signs of expansion. The changes are characterized by the near complete disappearance of the frontal CSF spaces and compression/displacement of the supratentorial ventricular system and midline shift to the right. **d** MR perfusion study show high perfusion associated with the lesion in the left hemisphere. **e,f** MR spectroscopy shows a marked increase in the Cho/Cr and Cho/NAA ratios in the progressive neoplastic lesions in the left hemisphere

Case 31

Tumor Progression

Morphofunctional MR Follow-up in Glioblastoma Multiforme

Gabriele Polonara, Lorenzo Alvaro and Luana Regnicolo

- 66-year-old patient with (unmethylated MGMT gene promoter) left posterior temporal glioblastoma multiforme treated with surgery and subsequent radiotherapy and concomitant adjuvant chemotherapy
- Morphofunctional MR follow-up performed with morphologic study, diffusion, perfusion and spectroscopy preoperatively, at 48 hours, 4, 7 and 9 months after surgery

Preoperative Imaging

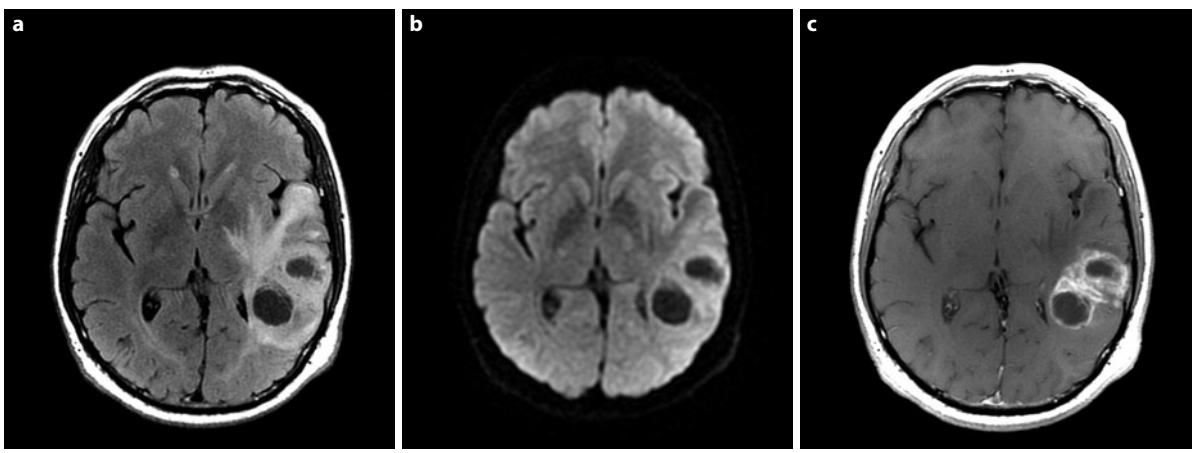

Fig. 31.1 **a** MR FLAIR sequence shows a partly cystic voluminous heterogeneous expansive lesion infiltrating the left temporal cortical-subcortical region, with extensive perilesional hyperintense signal indicating edema-infiltration that extends forward to the posterior arm of the internal capsule and the posterior portion of the external capsule. The lesion extends deep to the temporal horn, trigone and occipital horn of the left ventricle ependyma. A reduction of CSF spaces, compression of the ipsilateral ventricle and mild right-deviation of the midline can also be appreciated. **b** MR diffusion-weighted image confirms the presence of two large cysts with higher intralesional diffusion coefficient suggestive of necrotic-cystic nature. **c** Contrast-enhanced MR SE T1-sequence shows intense enhancement with the presence of two inhomogeneous areas of rim enhancement with cystic-like areas indicating necrosis

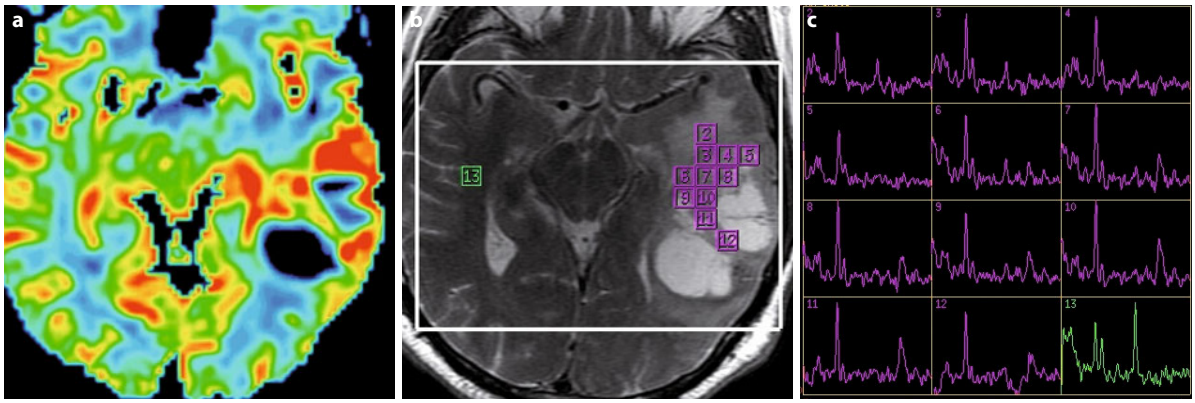

Fig. 31.2 **a** MR perfusion study shows inhomogeneous increase in perfusion with hypoperfused areas in the context of the expansive/infiltrative lesion. **b,c** Multi-voxel MR spectroscopy with long echo times shows an increase in the Cho/Cr and Cho/NAA ratios (indices of increased proliferative activity), with a high lipid peak compatible with the presence of necrosis

Early (48 Hours) Postoperative Follow-up

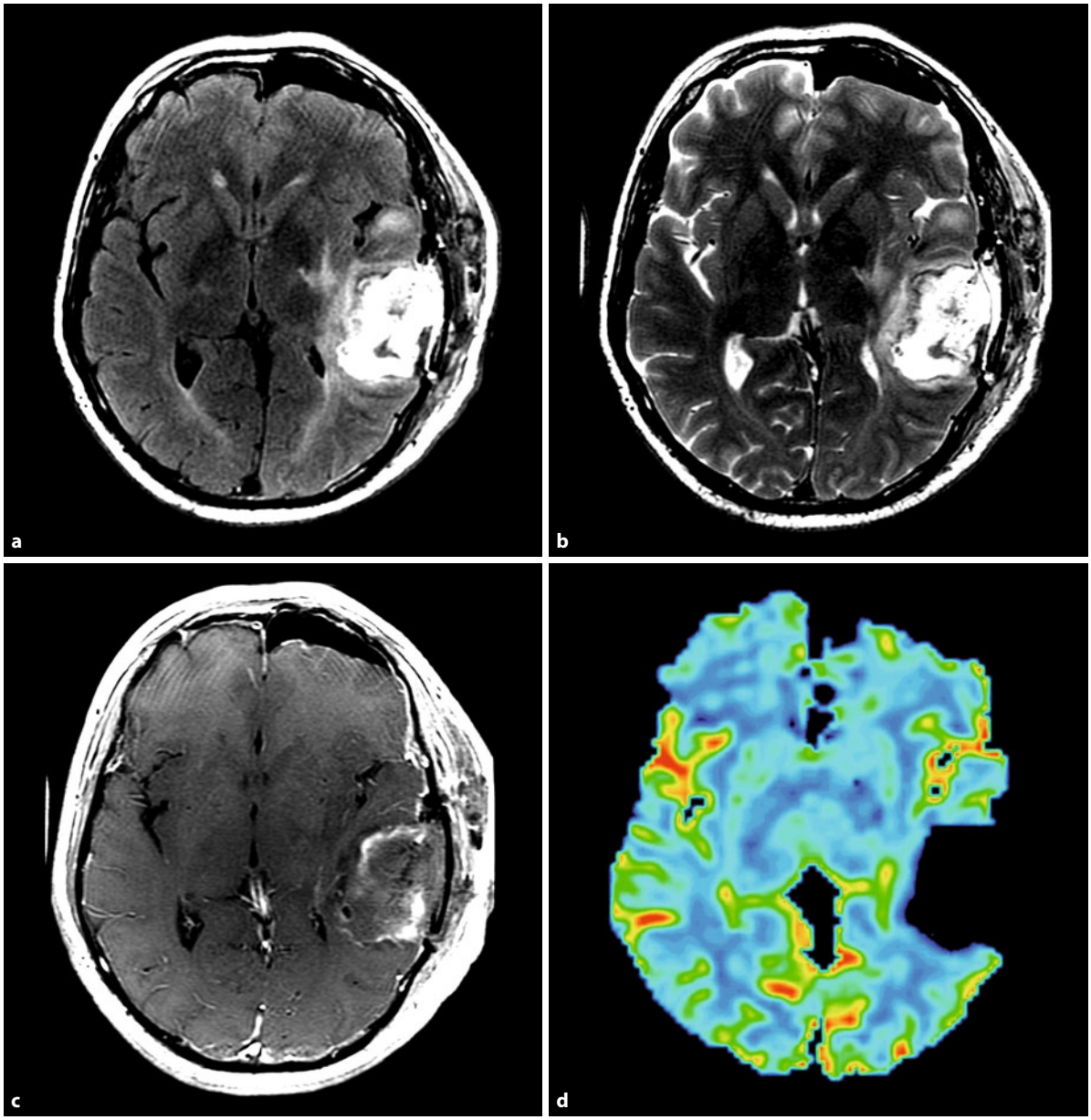

Fig. 31.3 MR FLAIR (**a**), FSE T2-weighted (**b**) and contrast-enhanced SE T1-weighted (**c**) sequences visualize the left temporal-parietal craniotomy and partial removal of the expansive/infiltrative lesion previously documented. Some air bubbles and blood can be seen within the surgical cavity. At the edge of the cavity signs of injured BBB and traces of blood in the anterior region can be appreciated. A reduction in perilesional edema, persistent signs of lesion expansion as visualized in the preoperative images, the appearance of a layer of air in the frontal-polar region and moderate diastasis of the repositioned bone flap can also be appreciated. **d** MR perfusion study shows no appreciable signs of high perfusion at the margins of the surgical cavity

Follow-up Performed at 4 Months After Surgery, Radiotherapy and Concomitant Chemotherapy

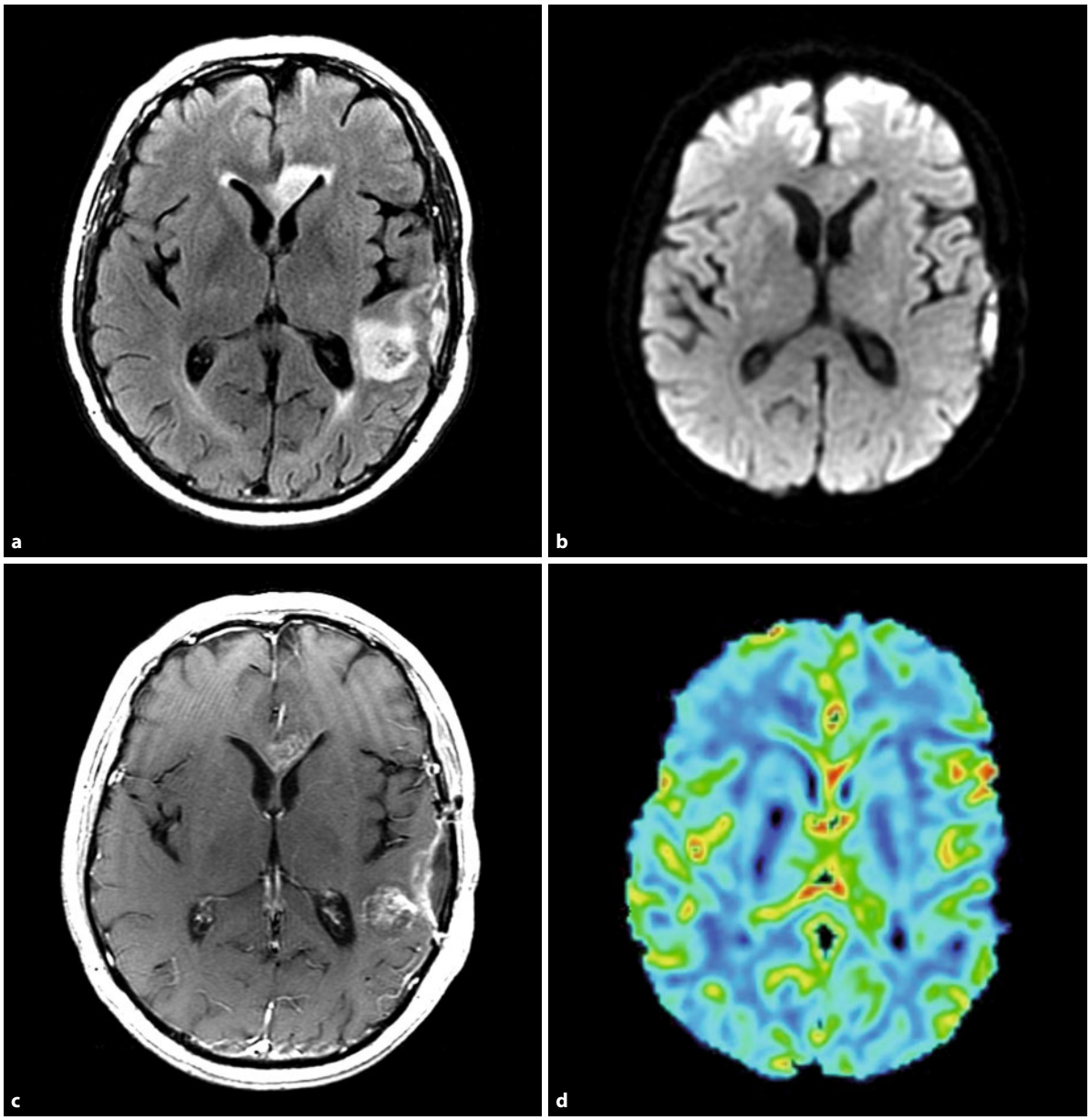

Fig. 31.4 MR FLAIR (**a**) and diffusion-weighted (**b**) sequences show a reduction in size of the surgical cavity, with air and blood no longer appreciable. The air layer in the frontal-temporal regions and the signs of expansion are also no longer visible. **c** Contrast-enhanced MR SE T1-weighted sequence displays an increase in the thickness of the marginal zone with signs of altered BBB, the presence of some tissue with neoplastic appearance extending into the brain parenchyma. Another area with signs of altered BBB not shown in the previous examination can be seen in the genu of the corpus callosum, in the left parasagittal region. **d** MR perfusion study shows a slight increase in perfusion indices near the margins of the surgical cavity and at the genu of the corpus callosum

Follow-up Performed at 7 Months After Surgery and Adjuvant Chemotherapy

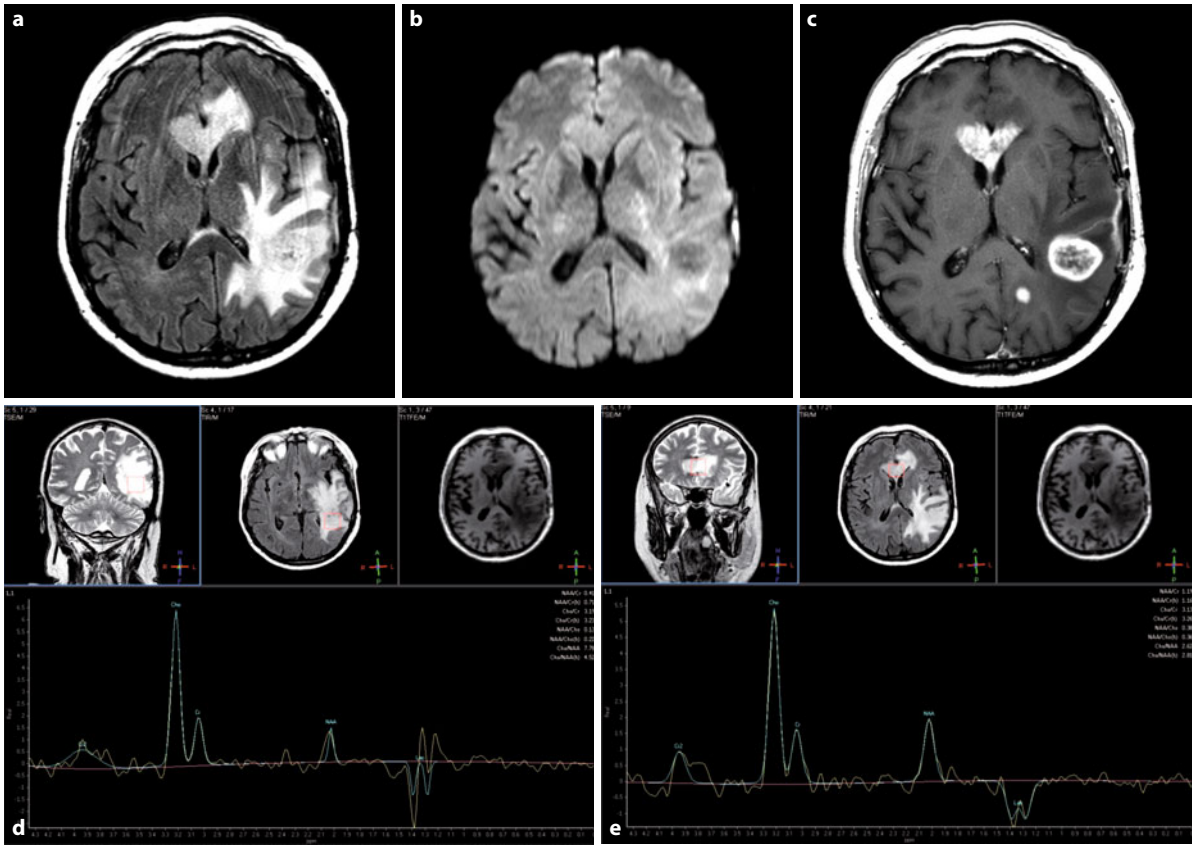

Fig. 31.5 MR FLAIR sequence (**a**) and diffusion-weighted imaging (**b**) show an increase in size of the expansive/infiltrative lesion peripherally in the left parietal-temporal surgical cavity. An increase in signal hyperintensity can also be seen indicating edema-infiltration peripheral to the lesion extending anteriorly in the left temporal-polar region, posteriorly in the retroparatrigonal area and deep to involve the capsules/nuclei. Signs of expansion are associated, with a reduction in the visualization of the CSF spaces and compression/shift of the left lateral ventricle. **c** Contrast-enhanced MR SE T1-weighted sequence shows an increase in the size of the lesion located at the genu of the corpus callosum, the appearance of another small area of disease in the left retrotrigonal region and increase in nodular enhancement at the surgery site. MR spectroscopy performed at the surgical margins (**d**) and at the genu of the corpus callosum (**e**) shows strong signs of tumor proliferation (high Cho/Cr and Cho/NAA ratios), and intense replacement/infiltration of the parenchyma from high-grade recurrence/progression (low ratio of NAA/Cr) primitive brain tumor

Follow-up Performed at 9 Months After Surgery and Further Cycles of Adjuvant Chemotherapy

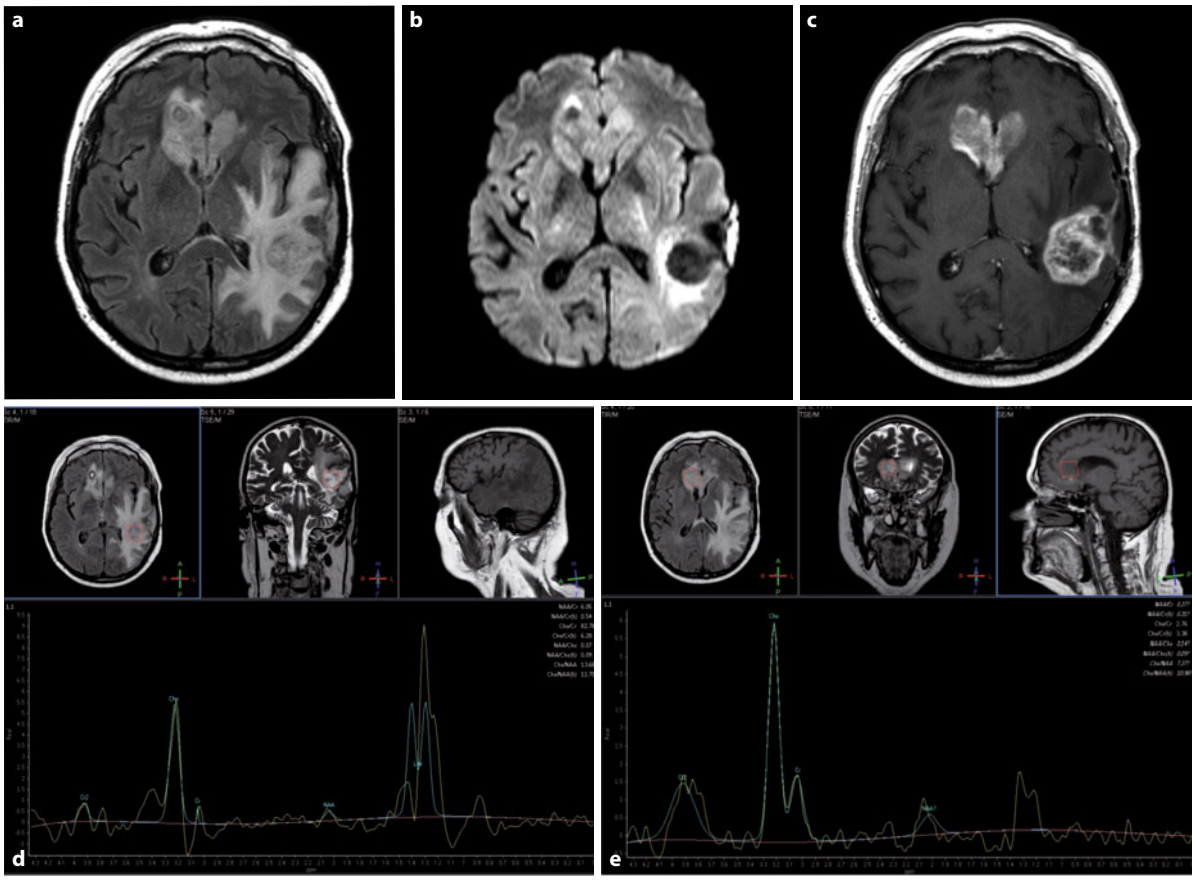

Fig. 31.6 MR FLAIR sequence (**a**), diffusion-weighted imaging (**b**) and contrast-enhanced SE T1-weighted sequence (**c**) show further increased size of the expansive/infiltrative lesions located in left temporal-parietal region and at the genu of the corpus callosum, the latter having extended to the right hemisphere. MR spectroscopy at the surgical margins (**d**) and at the corpus callosum (**e**) show a further reduction in the NAA/Cr peak and increased lipid peak indicative of tumor necrosis

Case 32

Radionecrosis

MR Follow-up in Metastasis From Breast Cancer

Mario Muto and Fabio Zeccolini

- 14-year-old patient with a history of meningeal spread of leukemia treated with whole brain radiation therapy
- Follow-up MR morphologic study without and with contrast medium administration performed after whole brain radiation therapy

Follow-up at 15 Months

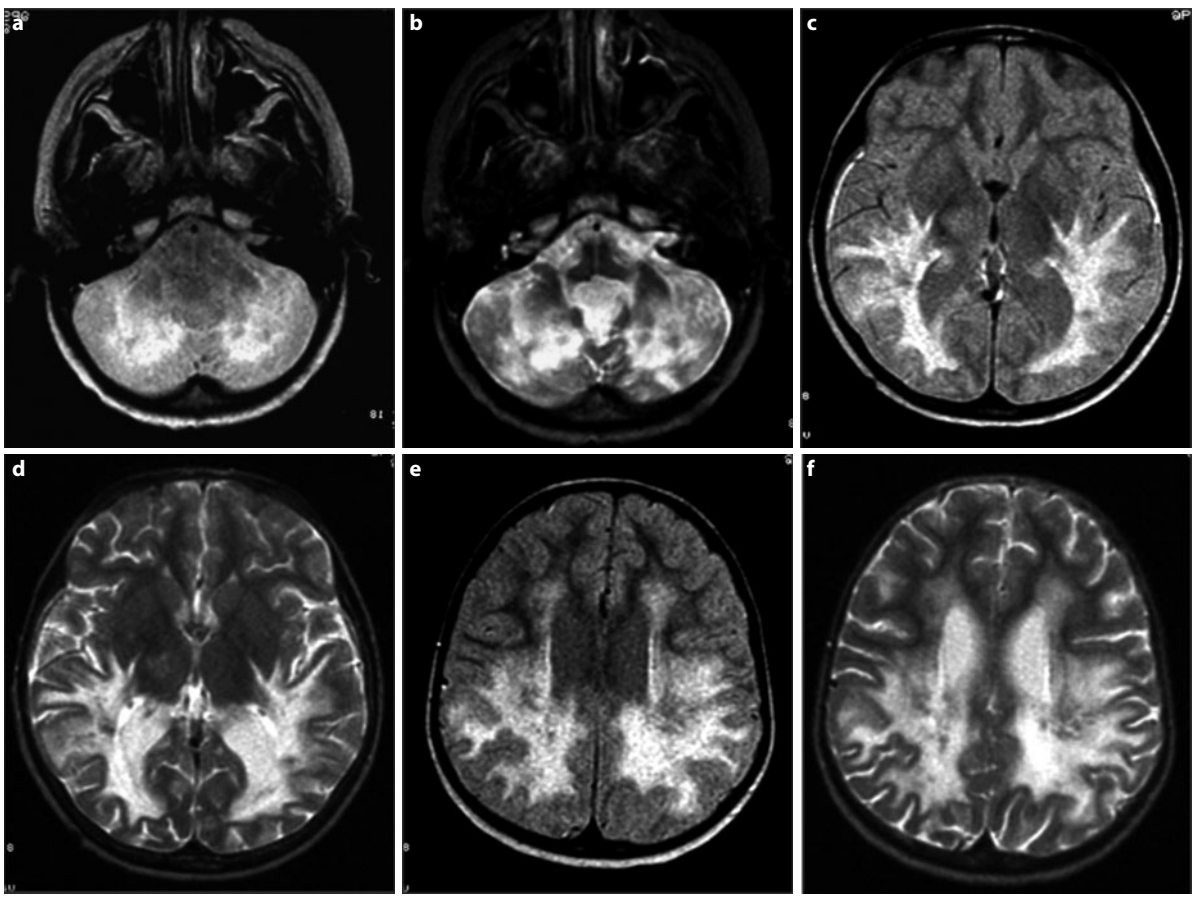

Fig. 32.1 MR performed with SE-DP (**a,c,e**), FSE (**b,d,f**) and contrast-enhanced SE T1-weighted (**g,h,i**) sequences. The images depict widespread signal alteration (hyperintensity in T2) in the white matter (acute leukoencephalopathy) with enhancement after contrast medium administration in the periventricular white matter (radionecrosis) (*cont.* →)

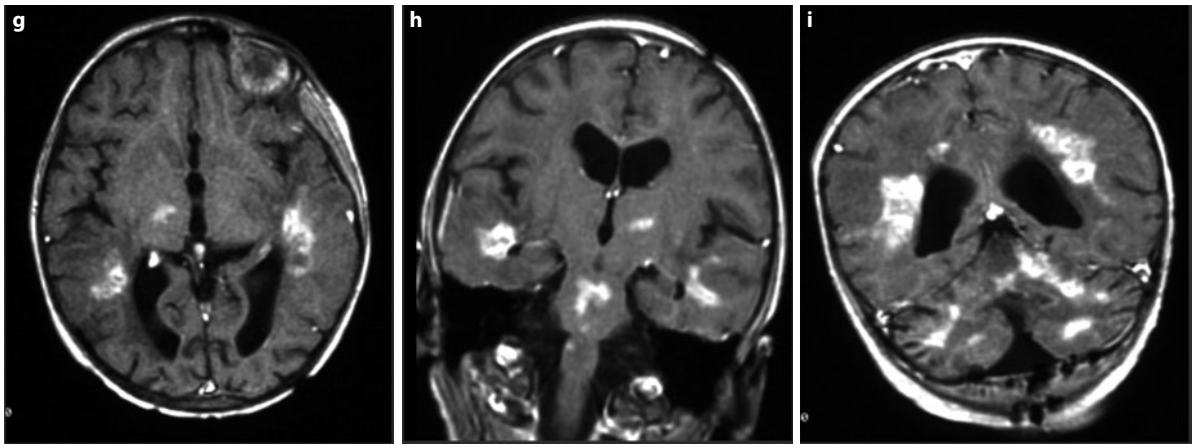

Fig. 32.1 (*continued*)

Case 33

Radionecrosis

Morphofunctional MR Follow-up in Metastasis from Breast Cancer

Teresa Popolizio, Maria Teresa Cascavilla, Nicola Sforza, Antonio Casillo and Alessandra Stranieri

- 48-year-old patient with breast lesion secondary to previous breast cancer
- Morphofunctional MR follow-up performed with morphologic imaging, diffusion and spectroscopy at 1 year from stereotactic therapy of metastasis from breast cancer

Follow-up 1 at Year From Surgery of Breast Cancer in Symptomatic Patient

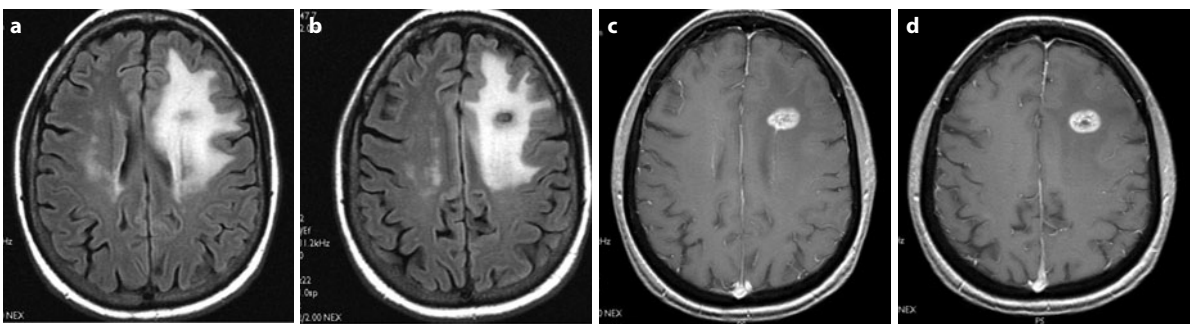

Fig. 33.1 MR FLAIR (**a,b**) and contrast-enhanced SE T1-weighted (**c,d**) sequences show a nodular lesion surrounded by edema in the left frontal region with iso-hypointensity in FLAIR and thick enhancing ring in the contrast enhanced images

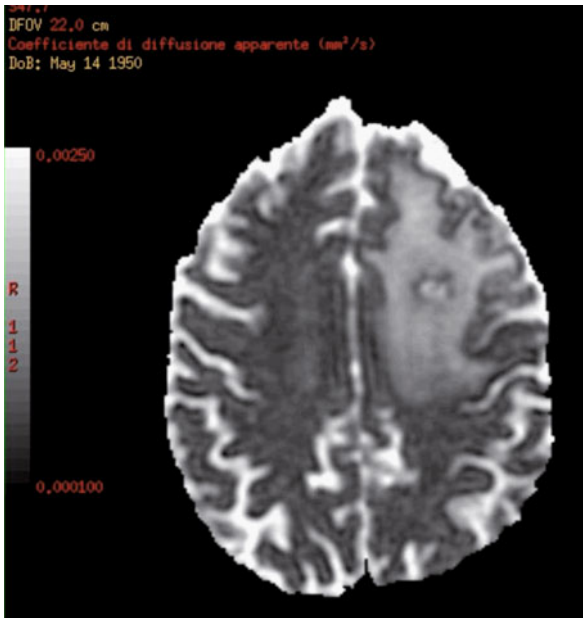

Fig. 33.2 MR diffusion-weighted image with ADC map shows high restriction of diffusion within the lesion

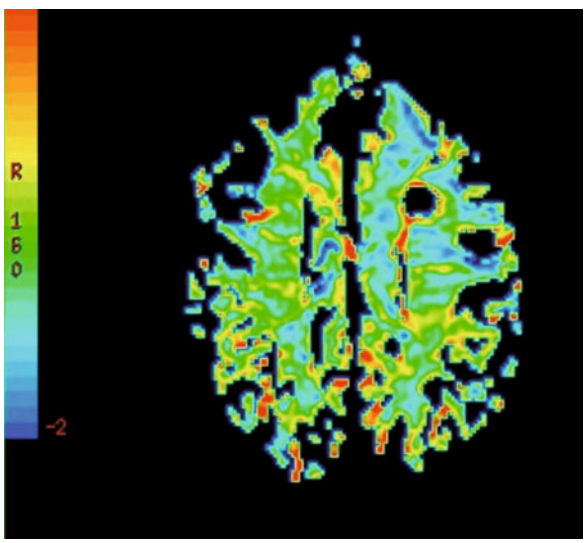

Fig. 33.3 MR perfusion study with CBV map shows the lesion devoid of perfusion

Case 34

Radionecrosis

Morphofunctional MR Follow-up in Glioblastoma

Teresa Popolizio, Maria Teresa Cascavilla, Nicola Sforza, Antonio Casillo and Alessandra Stranieri

- 53-year-old patient with glioblastoma
- Morphofunctional MR follow-up performed with morphologic imaging, diffusion-weighted imaging and spectroscopy 9 months after surgery and radiation therapy in a patient with glioblastoma

Follow-up at 9 Months After Surgery and Radiation Therapy

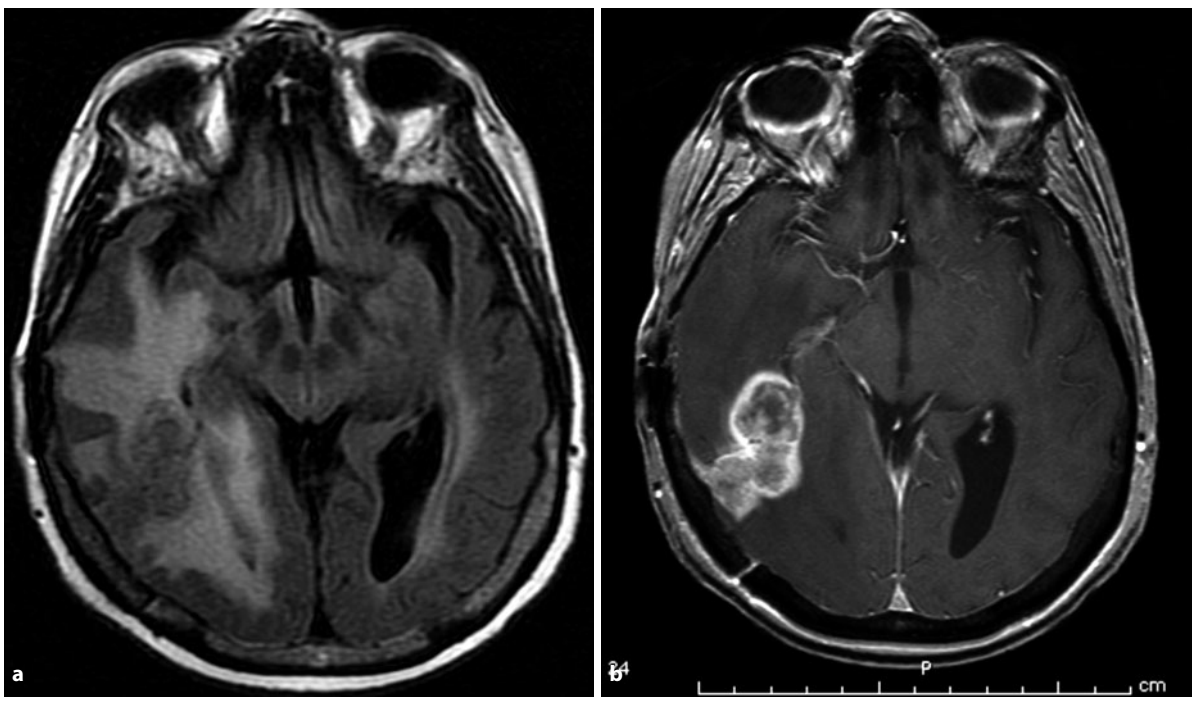

Fig. 34.1 MR FSE T2-weighted (**a**) and contrast-enhanced SE T1-weighted (**b**) sequences. A right temporal-occipital lesion with moderate edema and patchy enhancement due to the presence of a necrotic component can be seen. There is also a significant mass effect on the adjacent midline structures, particularly with obliteration of the ventricular junction

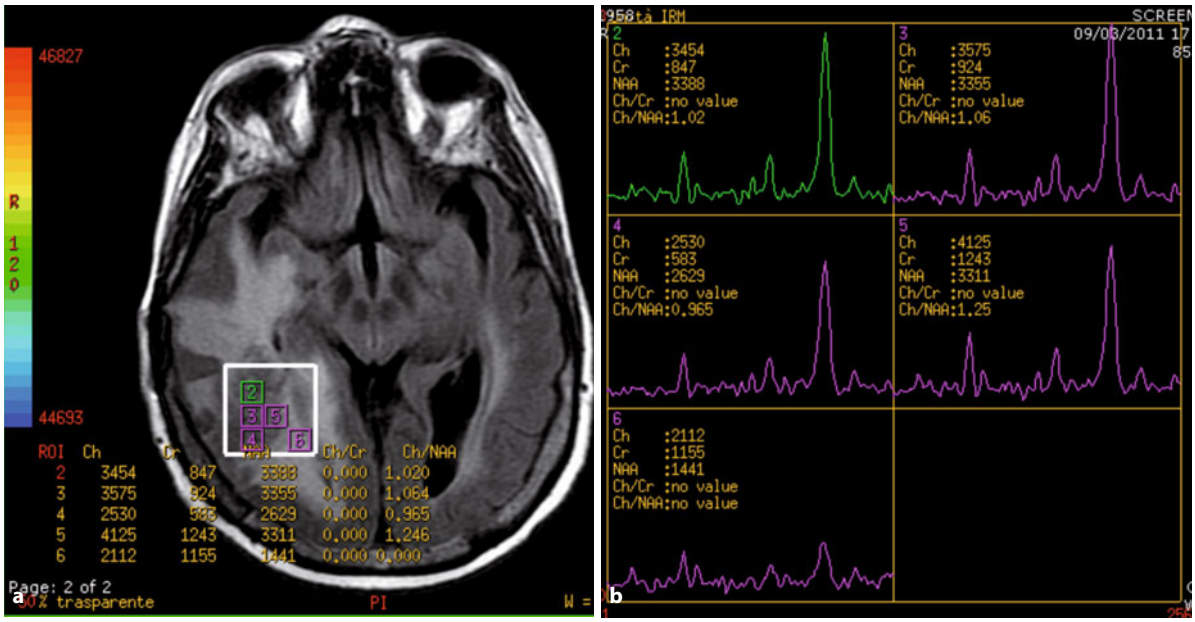

Fig. 34.2 a,b MR single-voxel spectroscopy with ROI placed in the lesion shows a high Lac/Lip peak indicating necrosis and a low component of NAA and Cho

Case 35

Late Radionecrosis

CT/MR Performed in Nasopharyngeal Carcinoma

Tommaso Scarabino, Saverio Pollice, Gilda Morlino, Michela Capuano, Angela Lorusso and Alberto Maggialetti

- 60-year-old patient with previous radiation therapy in undifferentiated nasopharyngeal carcinoma
- CT/MR follow-up performed at 3 and 4 years after radiation therapy

Follow-up Performed at 3 Years After Radiation Treatment

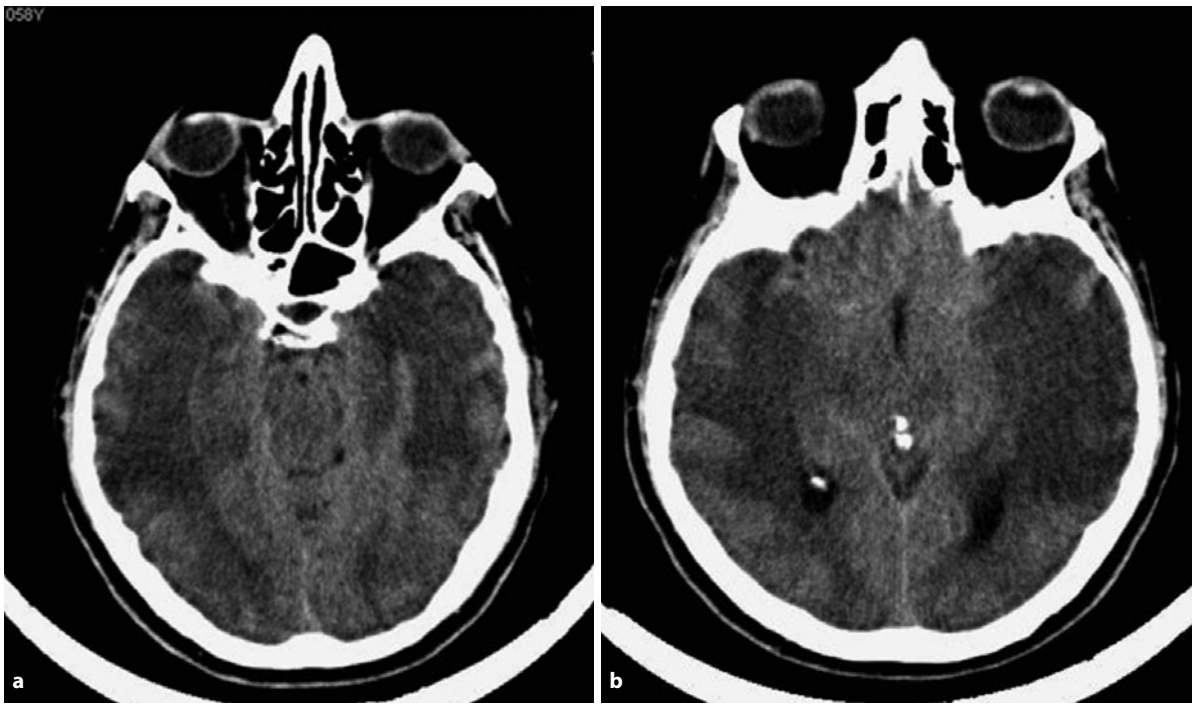

Fig. 35.1 a,b Emergent morphologic CT scan shows an ill-defined cortical-subcortical hypodensity in the bilateral temporal area extending cranially and involving the frontal and parietal lobes

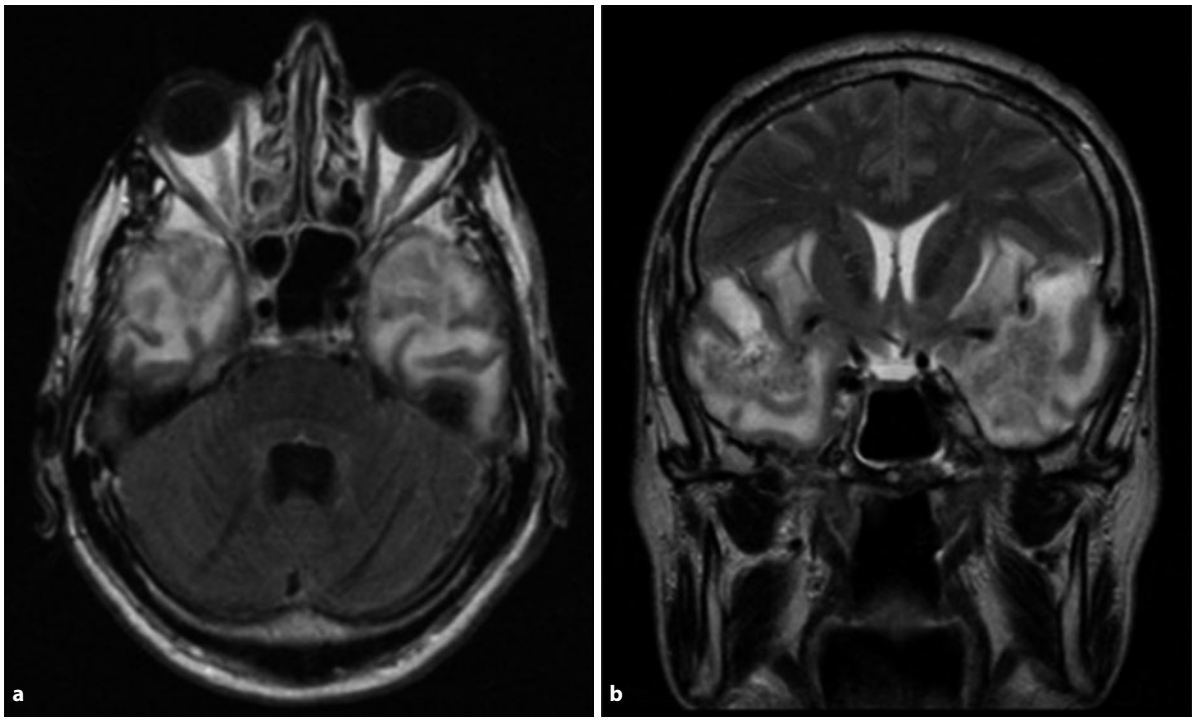

Fig. 35.2 Axial (**a**) and sagittal (**b**) MR FLAIR sequences show bilateral temporal-polar cortical-subcortical heterogeneous hyperintensity extending cranially into the parietal lobe. Coexisting atrophy of the nasopharyngeal mucosa can also be appreciated

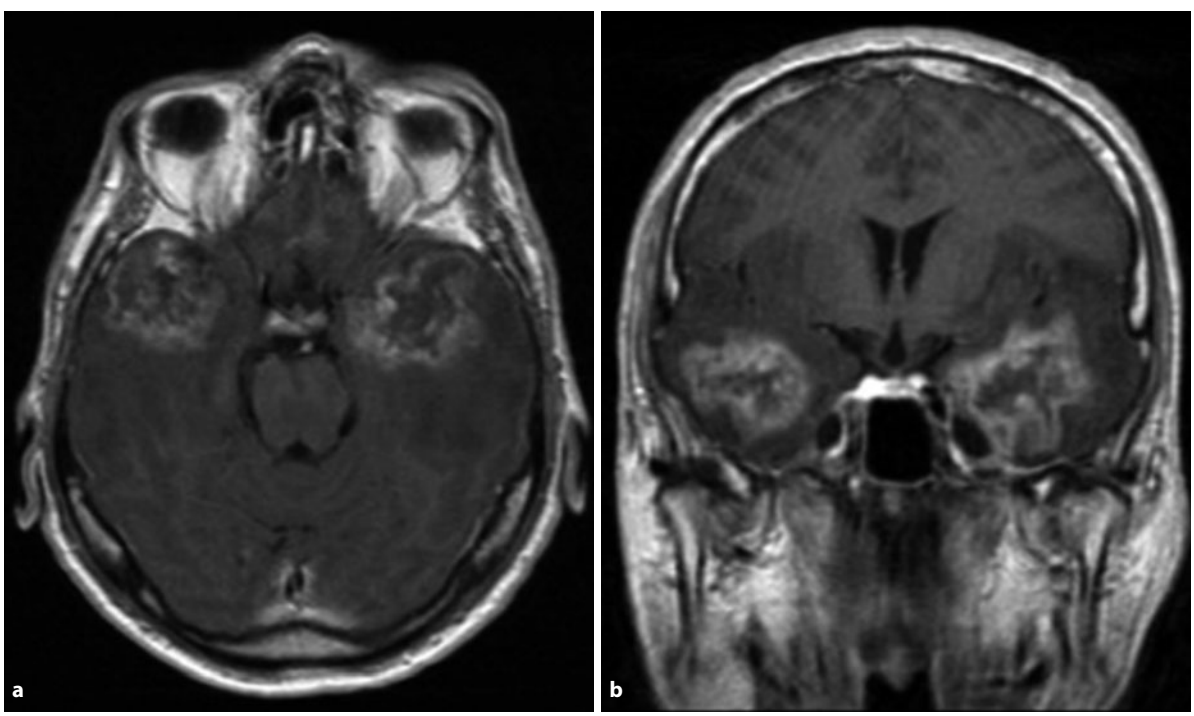

Fig. 35.3 Contrast-enhanced axial (**a**) and coronal (**b**) MR SE T1-sequences show thick and irregular enhancement of the margins of the lesion described above with central hypointensity attributable to necrosis, surrounded by a wide area of hypointensity indicating perilesional edema

Follow-up Performed at 4 Years

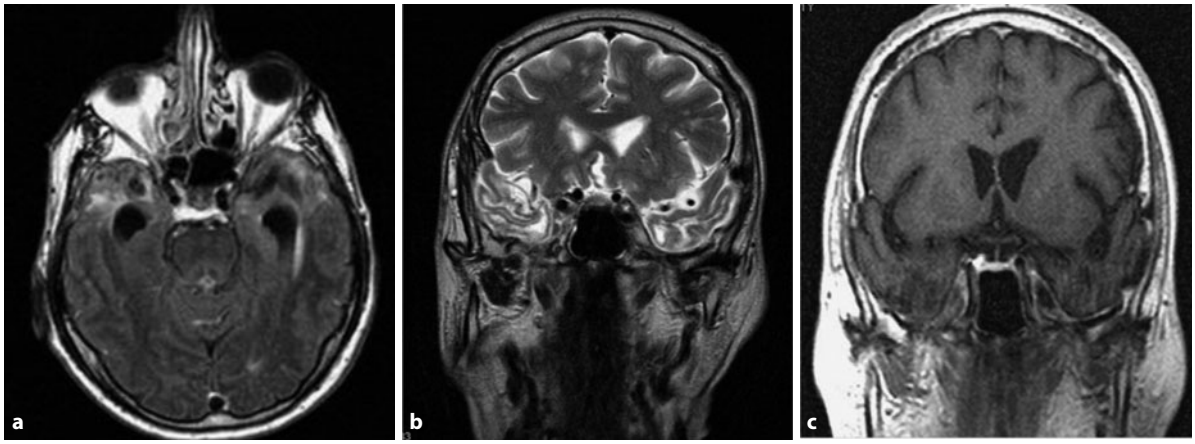

Fig. 35.4 MR FLAIR (**a**), FSE T2-weighted (**b**) and contrast-enhancement SE T1-weighted (**c**) sequences show moderate and irregular residual alteration of the cortical-subcortical signal in the temporal-polar region bilaterally, slight edema and no significant pathologic enhancement. Mild traction dilatation of the adjacent ventricular temporal horns can also be appreciated

Case 36

Late Radionecrosis

CT/MR Follow-up in Nasopharyngeal Carcinoma

Teresa Popolizio, Maria Teresa Cascavilla, Nicola Sforza, Antonio Casillo and Alessandra Stranieri

- 54-year-old patient with previous radiation therapy in nasopharyngeal carcinoma
- MR and CT follow-up performed with morphologic imaging, diffusion and spectroscopy 2 years after radiation treatment in nasopharyngeal carcinoma

Follow-up at 2 Years After Radiation Therapy

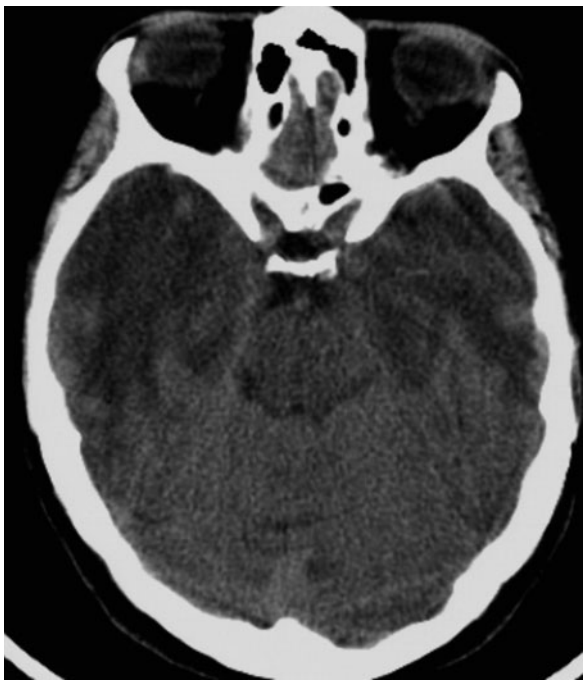

Fig. 36.1 CT scan in emergency shows a slight cortical-subcortical hypodensity in the temporal region bilaterally

Preoperative Imaging

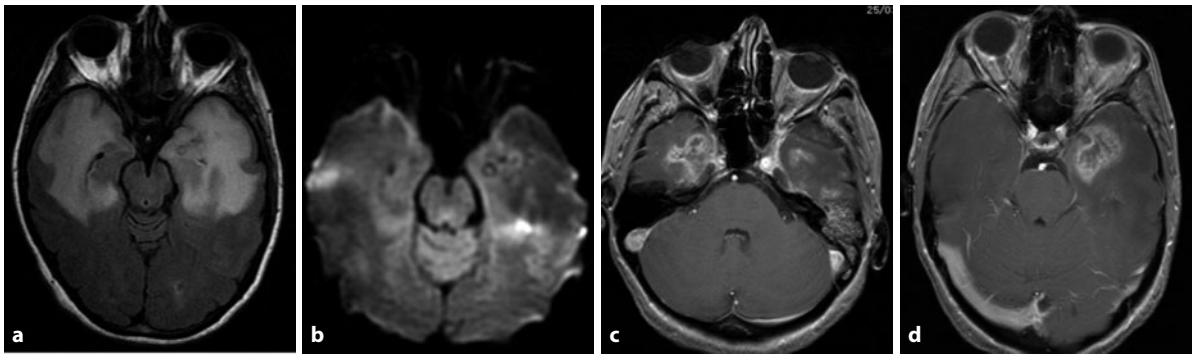

Fig. 36.2 MR FLAIR (**a**), diffusion-weighted (**b**) and contrast-enhanced SE T1-weighted (**c,d**) sequences. Patchy hyperintensity can be seen in the cortical-subcortical temporal-polar region bilaterally (**a,b**). After administration of contrast medium thick and irregular enhancement of the margins of the lesions are visualized with central hypointensity attributable to necrosis, surrounded by large area of hypointensity indicating perilesional edema (**c,d**)

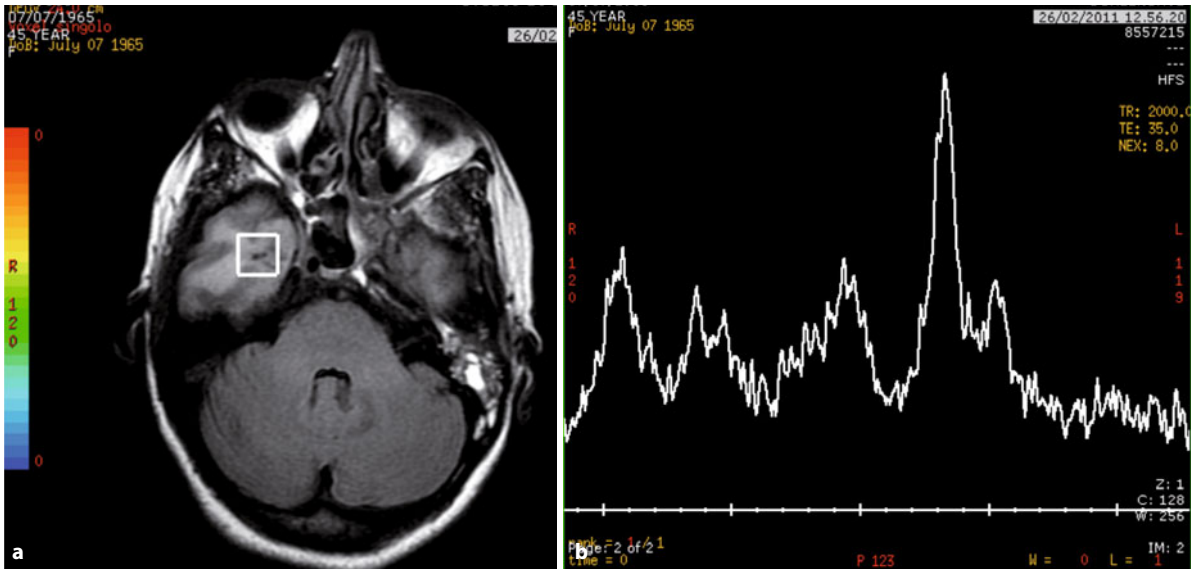

Fig. 36.3 **a,b** MR single-voxel spectroscopy with ROI placed on right temporal lesion shows a high peak of the Lac/Lip ratio indicating necrosis and a low component of NAA and Cho

Case 37

Late Radionecrosis

Postoperative and Post-radiation Therapy Follow-Up in Meningioma

Ferdinando Caranci and Sossio Cirillo

- Patients with previous surgery of a right frontal meningioma subsequently irradiated
- Postoperative and post-radiation therapy follow-up performed late (3 and 4 years) with MR morphologic and perfusion sequences

Postoperative and Post-Radiation Therapy Follow-up at 3 Years

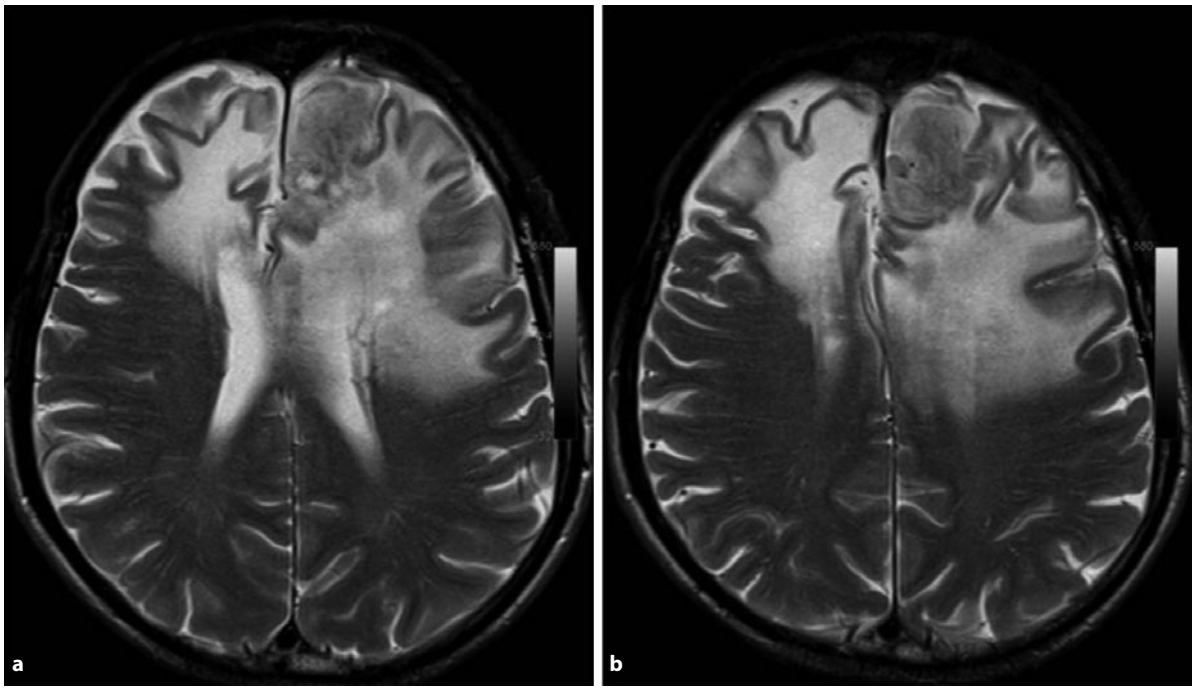

Fig. 37.1 a,b MR FSE T2-weighted sequence. An extended halo of high signal in the bilateral frontal region and extending more on the left indicates vasogenic edema. At that level in the parasagittal area some relatively hypointense tissue with irregular margins can be seen

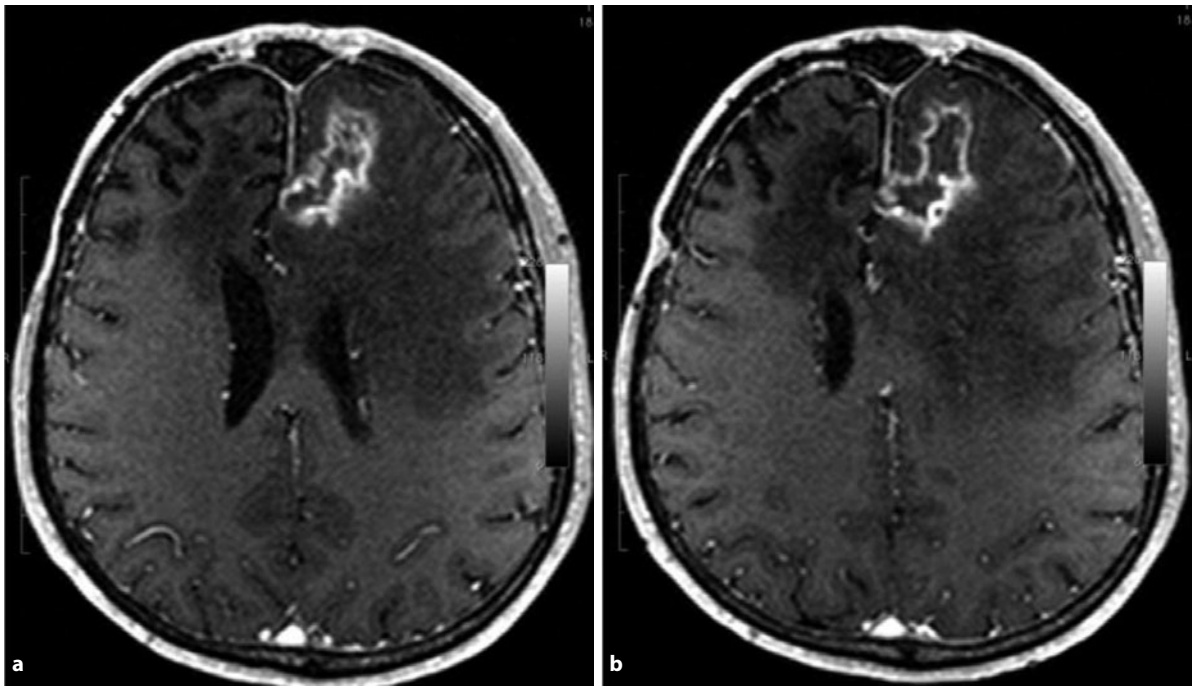

Fig. 37.2 a,b Contrast-enhanced MR SE T1-weighted images. The tissue in the left frontal area shows necrotic component and peripheral enhancement

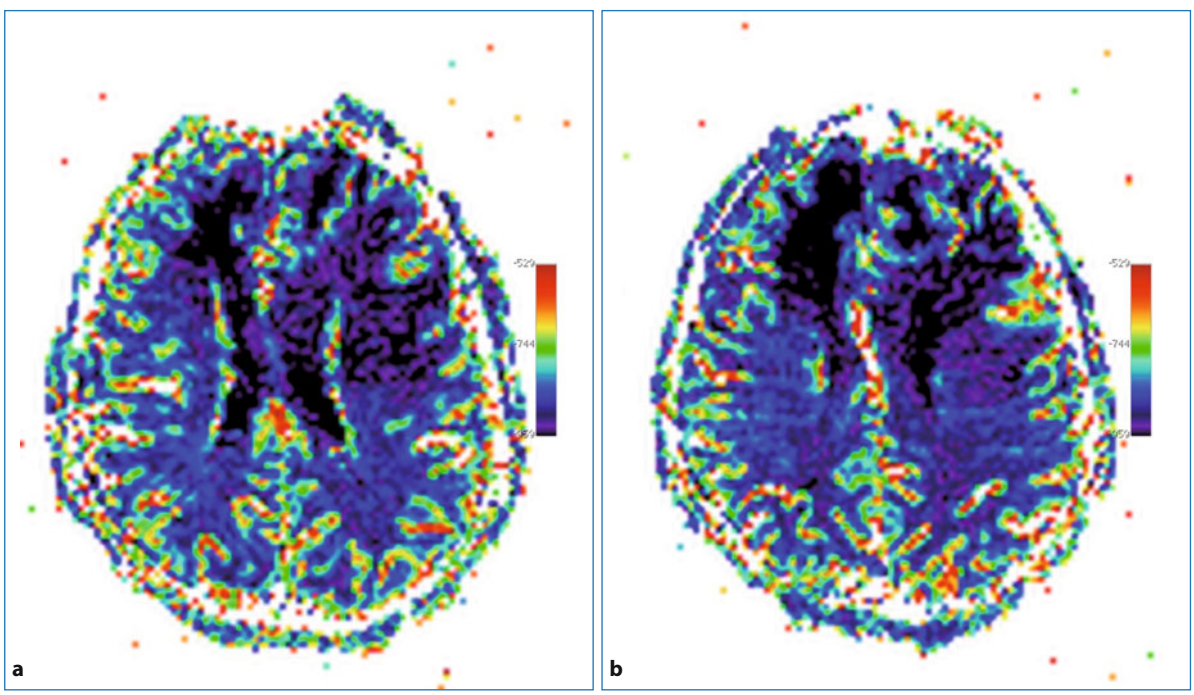

Fig. 37.3 a,b MR perfusion with CBV map. The lesion shows a clear reduction in cerebral blood volume values (CBV)

Postoperative and Post-Radiation Therapy Follow-up at 4 Years

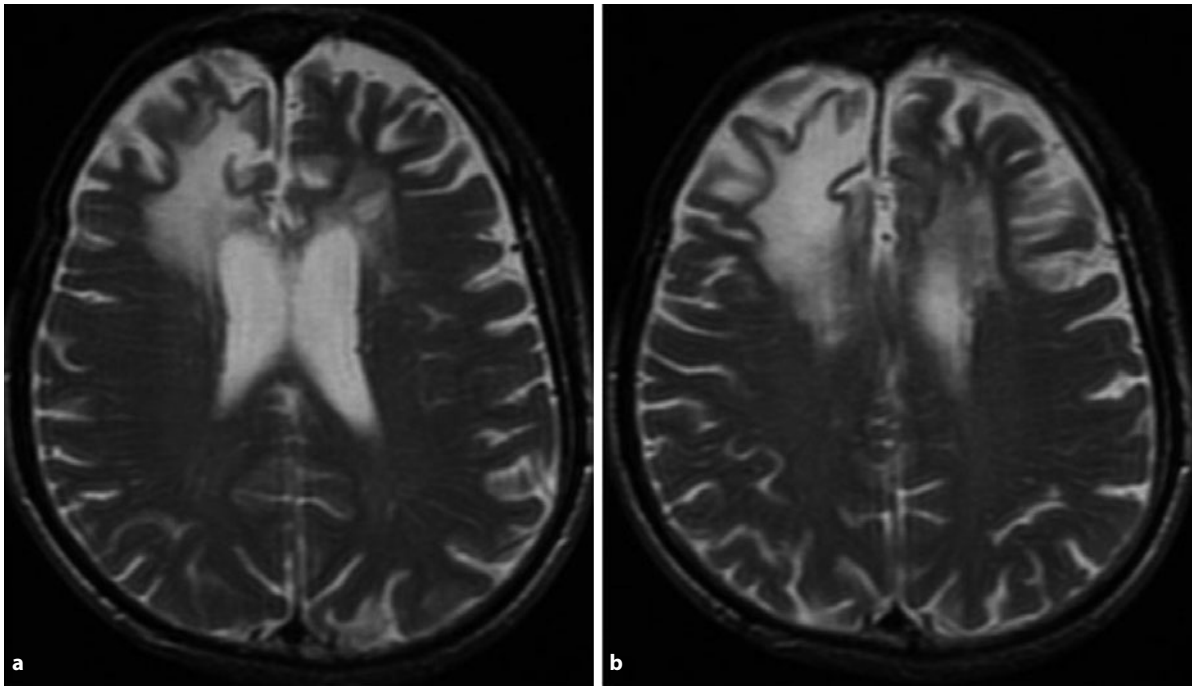

Fig. 37.4 a,b MR FSE T2-weighted sequence. Subtotal disappearance of the vasogenic edema can be appreciated, along with the remaining right-sided gliotic changes resulting from the previous surgery

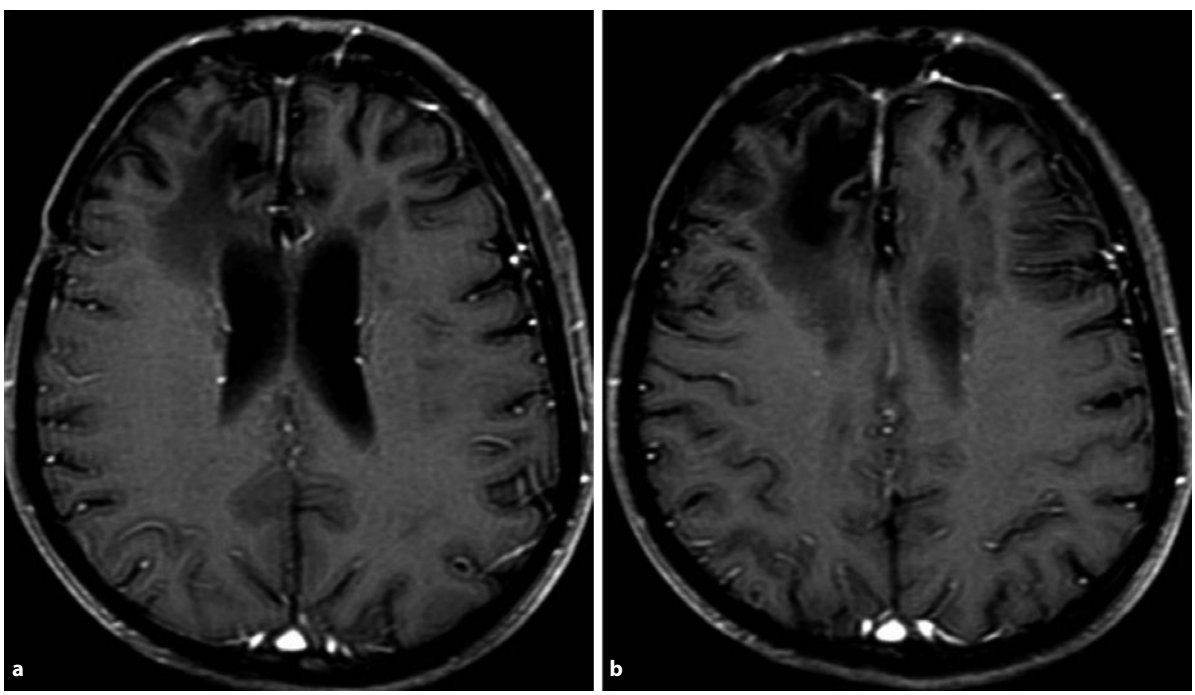

Fig. 37.5 a,b Contrast-enhanced MR SE T1-weighted images. The images show the disappearance of radiation necrosis changes described in the left frontal region

Case 38

Radionecrosis

3T Multimodal MR Follow-up in Anaplastic Astrocytoma

Tommaso Scarabino, Teresa Popolizio, Saverio Pollice, Vincenzo D'Angelo and Alfonso Di Costanzo

- 46-year-old patient with left frontal-opercular anaplastic astrocytoma and subsequent anaplastic transformation treated with surgery and partial excision and combined radiation therapy-chemotherapy and subsequent adjuvant second-level chemotherapy
- 3T multimodal MR follow-up performed with morphologic sequences, diffusion and perfusion imaging and spectroscopy preoperatively and at 6 and 12 months after surgery and combined radiation therapy-chemotherapy

Preoperative Imaging

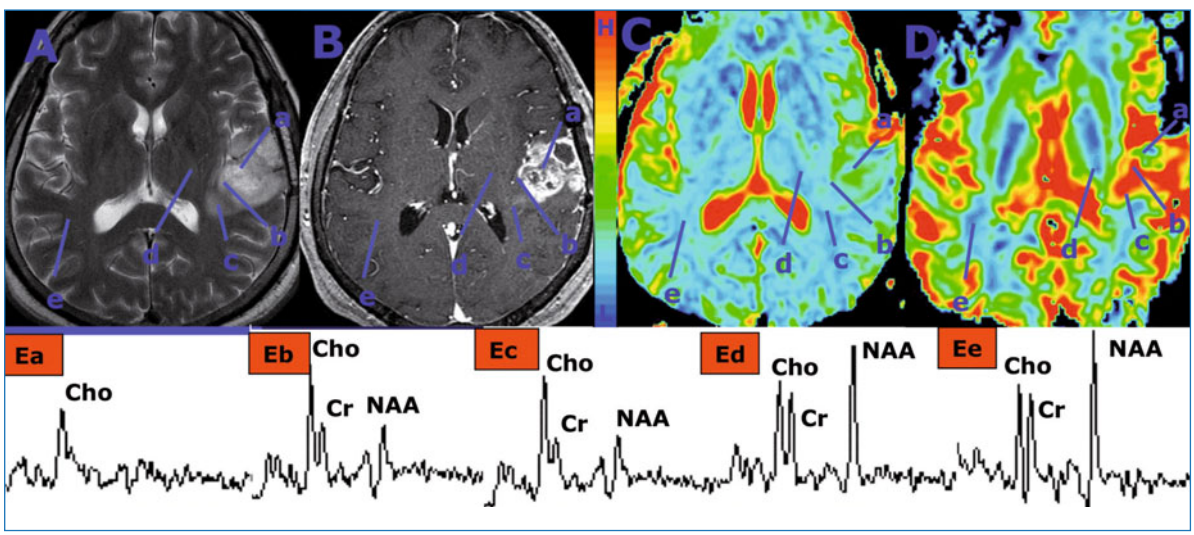

Fig. 38.1 MR FSE T2-weighted (**a**) and contrast-enhanced SE T1-weighted (**b**) sequences show an almost completely solid lesion with heterogeneous enhancement, moderate edema and with a slight mass effect on midline structures. Multimodal MR with diffusion-weighted imaging and ADC map (**c**), perfusion study with CBV map (**d**) and single-voxel spectroscopy with multiple ROIs (**e**). The spectra placed over and immediately behind the almost completely solid enhancing lesion have the typical tumor pattern, with high Cho peak and inversion of the Cho/NAA ratio. In these ROIs, the ADC is reduced and the CBV increased. The spectra in the apparently edematous area beyond the enhancing margins have overall reduced levels of all metabolites but with a pattern indicating tumor infiltrated edema. In these areas ADC is reduced and CBV is increased. Moving away from the lesion the metabolic pattern along with the ADC and CBV values return to normal as in the contralateral hemisphere

Follow-up Performed at 6 Months After Surgery and Combined Radiation Therapy-chemotherapy

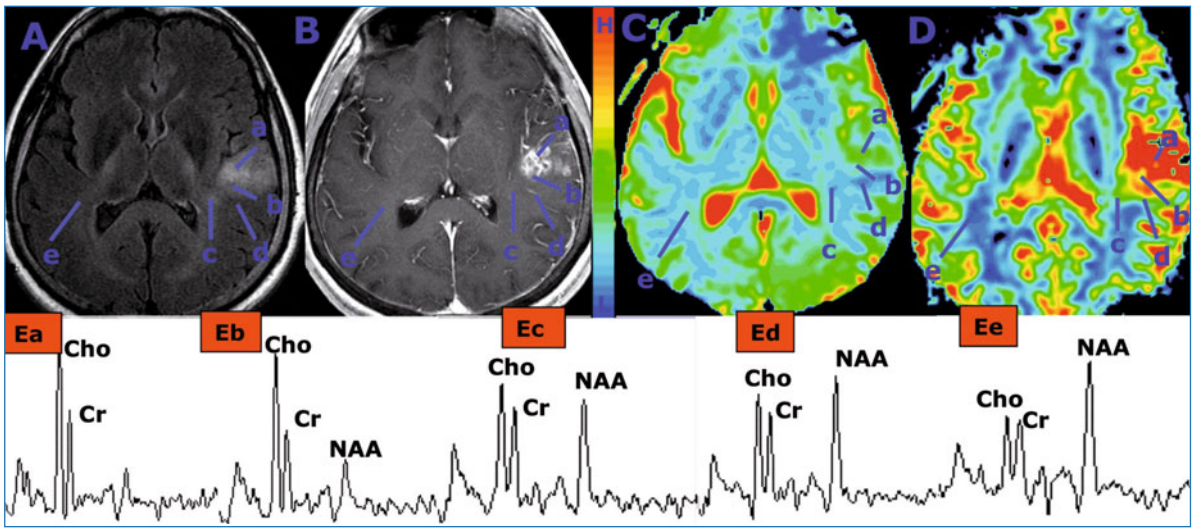

Fig. 38.2 a,b MR FSE T2-weighted and contrast-enhanced SE T1-weighted sequences. The appearance of the lesions suggests a worsening, with progression towards a probable glioblastoma multiforme. The lesion appears larger, with heterogeneous enhancement due to central necrotic components and increased surrounding edema and little mass effect on the midline structures. Multimodal MR with diffusion-weighted imaging and ADC map (**c**), perfusion study with CBV map (**d**) and single-voxel spectroscopy with multiple ROIs (**e**). The treatment performed have led to the appearance of a necrotic component characterized by increased ADC and decreased CBV. These indicators instead retain the tumor pattern in the enhancing areas and immediately adjacent to the lesion

Follow-up Performed at 12 Months After Surgery and Combined Radiation

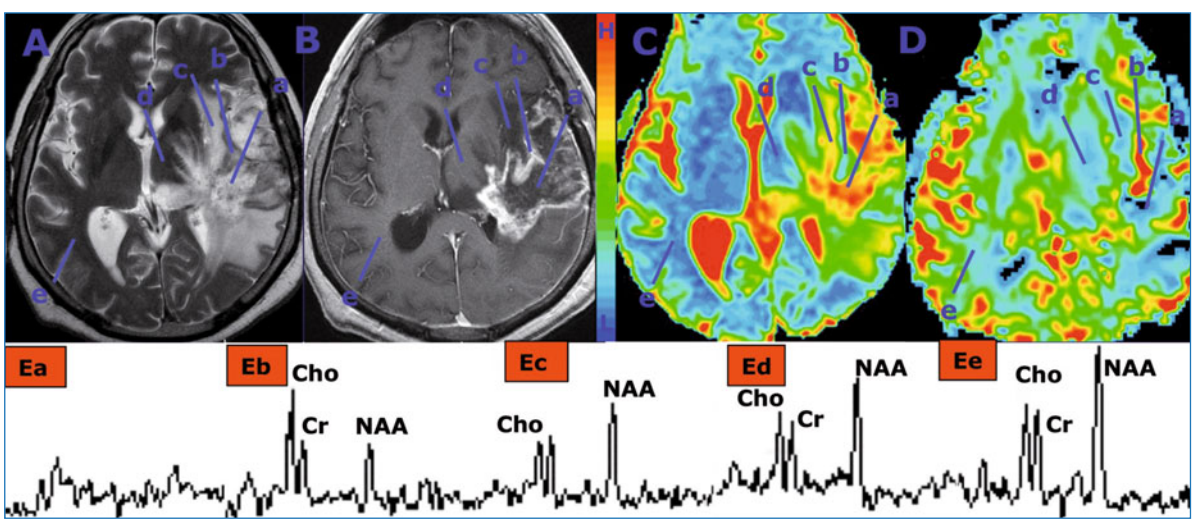

Fig. 38.3 Morphofunctional MR with FSE T2-weighted (**a**), contrast-enhanced SE T1-weighted (**b**) sequences, diffusion-weighted imaging with ADC map (**c**), perfusion study with CBV map (**d**) and multivoxel spectroscopy with multiple ROIs (**e**). The results obtained by radiation therapy and chemotherapy show a further significant increase in the size of the tumor surrounded by abundant edema and moderate mass effect on the midline structures. The lesion displays an almost complete radioinduced necrotic transformation with irregular peripheral enhancement. Consequently the spectra show a reduction in the levels of all metabolites, with a corresponding increase in ADC and reduction in CBV. These indices are inverted in the areas of healthy tissue and in the surrounding tissue adjacent to the lesion

Case 39

Radiation-induced Leukoencephalopathy

MR Follow-up After Whole Brain Radiation Therapy

Mario Muto and Alessandra D'Amico

- 56-year-old patient with secondary lesion from previous breast cancer
- MR follow-up at 1, 3 and 6 years after stereotactic radiation therapy for metastatic brain lesion from breast cancer

Follow-up at 1 Year After Breast Cancer Surgery in Symptomatic Patient

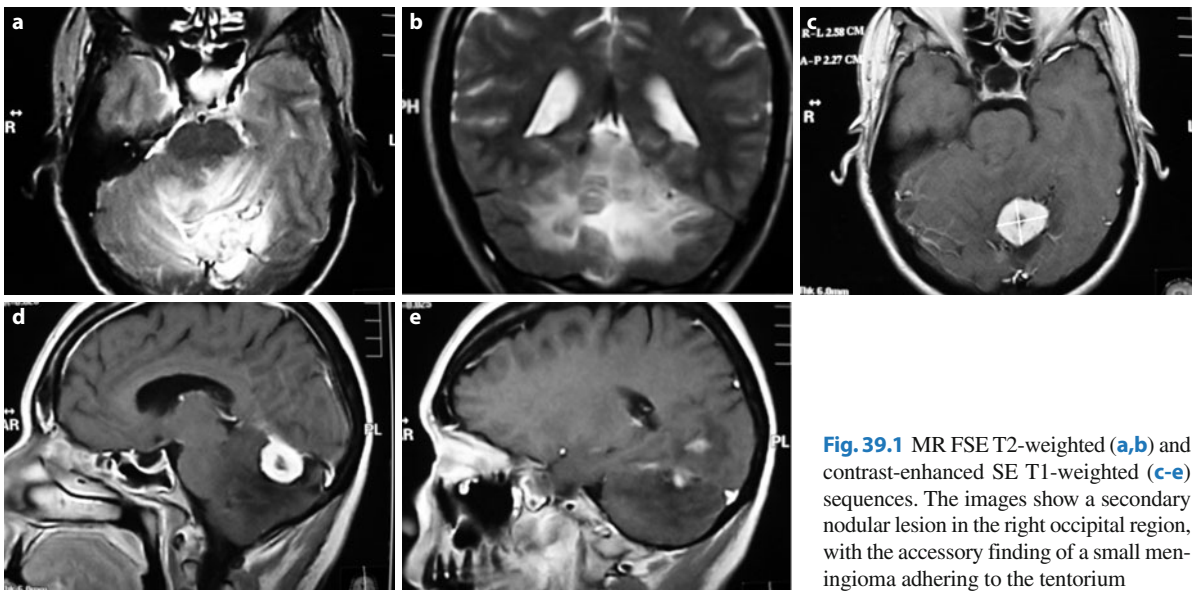

Fig. 39.1 MR FSE T2-weighted (**a**,**b**) and contrast-enhanced SE T1-weighted (**c**-**e**) sequences. The images show a secondary nodular lesion in the right occipital region, with the accessory finding of a small meningioma adhering to the tentorium

Follow-up at 1 Year After Stereotactic Radiation Therapy for Metastasis

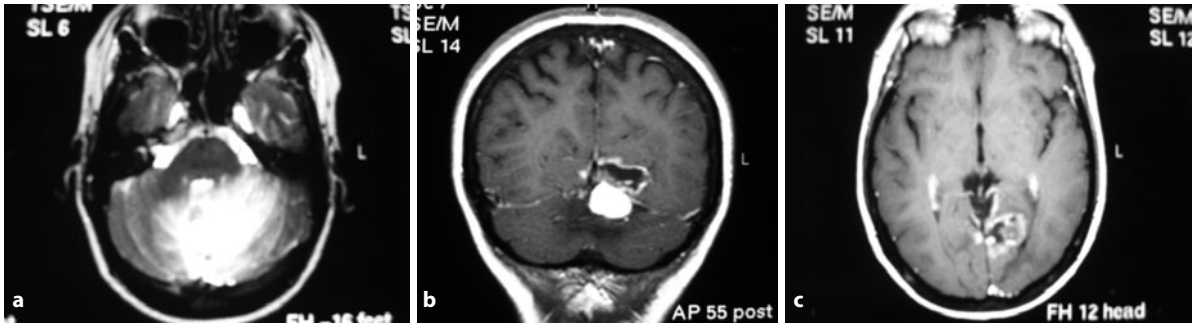

Fig. 39.2 MR FSE T2-weighted (**a**) and contrast-enhanced SE T1-weighted (**b,c**) sequences. Signal alteration and enhancement typical of radionecrosis can be appreciated in the left occipital region, with persistence of the tentorial meningioma, which appears unchanged in size with abundant surrounding edema

Follow-up at 3 Years

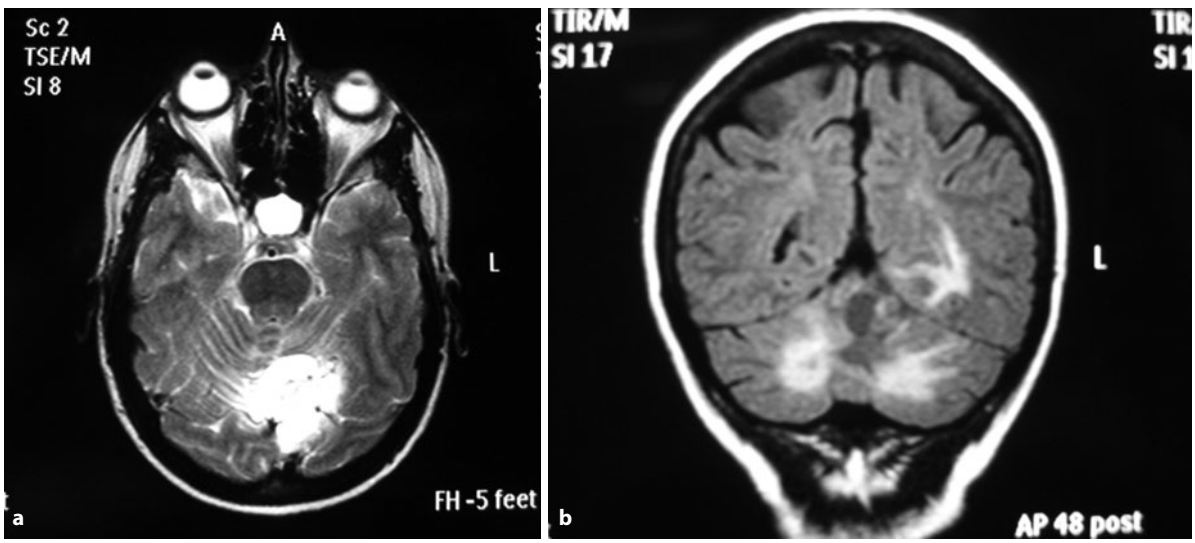

Fig. 39.3 MR FSE T2-weighted (**a**) and FLAIR (**b**) sequences. A modest reduction in the size of the tentorial lesion and the appearance of an area of softening with post-irradiation atrophy both in the cerebellar and occipital region are shown. A related allergic diathesis hindered the completion of the study with contrast agents

Follow-up at 6 Years

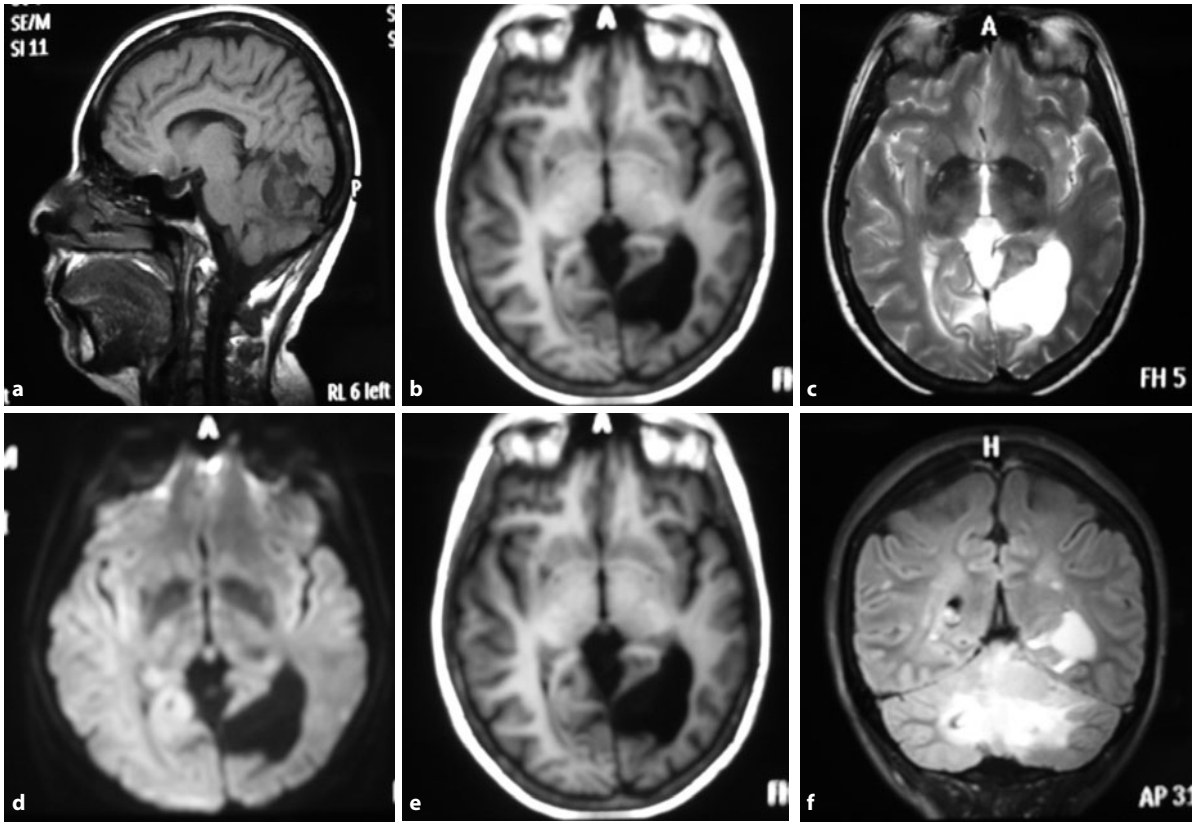

Fig. 39.4 MR SE T1-weighted (**a,b**), FSE T2-weighted (**c**), SE DP (**d**) and FLAIR (**e**) sequences. The images show softening with further extension of the left occipital and cerebellar atrophy and reduction in the size of the tentorial lesion

Case 40

Radiation Therapy-induced Tumor Pseudoprogression

MR Follow-up in Pilocytic Astrocytoma

Teresa Popolizio, Maria Teresa Cascavilla, Nicola Sforza, Antonio Casillo and Alessandra Stranieri

- 18-year-old patient with pilocytic astrocytoma
- MR follow-up at 1, 4 and 7 months after surgery and radiotherapy

Preoperative Imaging

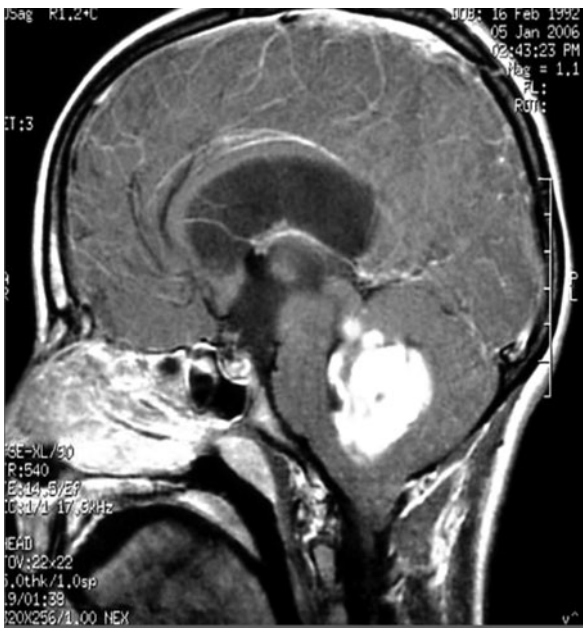

Fig. 40.1 Contrast-enhanced MR SE T1-weighted sequence shows a voluminous vermian mass obliterating the IV ventricle with intense and homogeneous enhancement

Early Postoperative Imaging

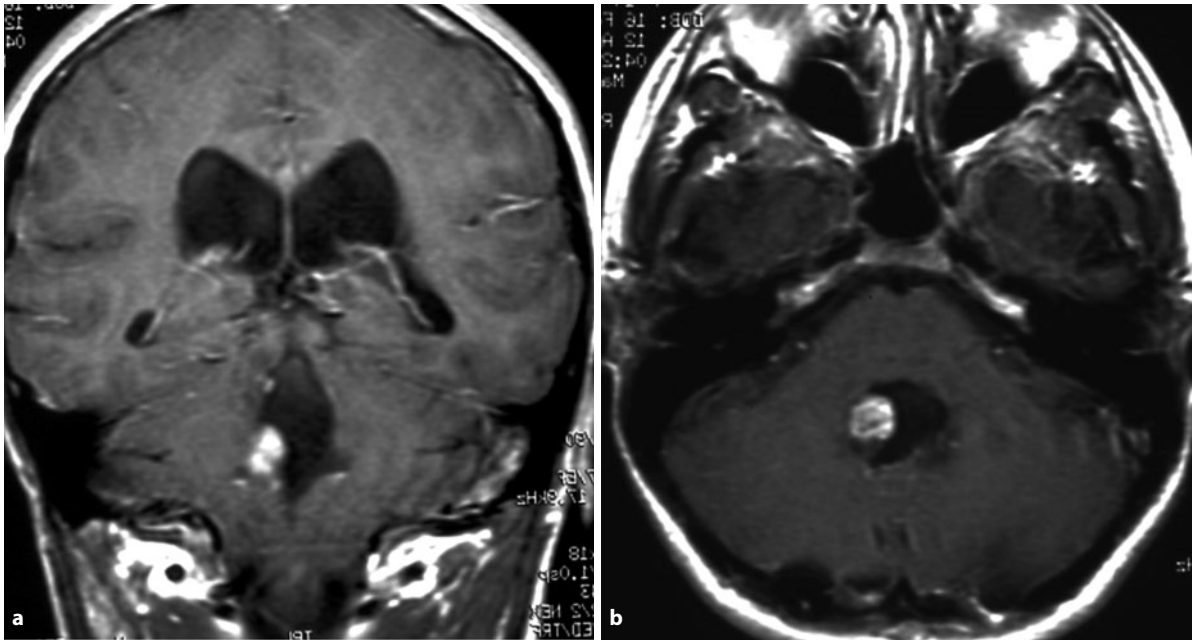

Fig. 40.2 a,b MR contrast-enhanced SE T1-weighted sequences shows residual neoplastic tissue occupying the right portion of the IV ventricle

Imaging at 1 Month After Surgery and Radiation Therapy

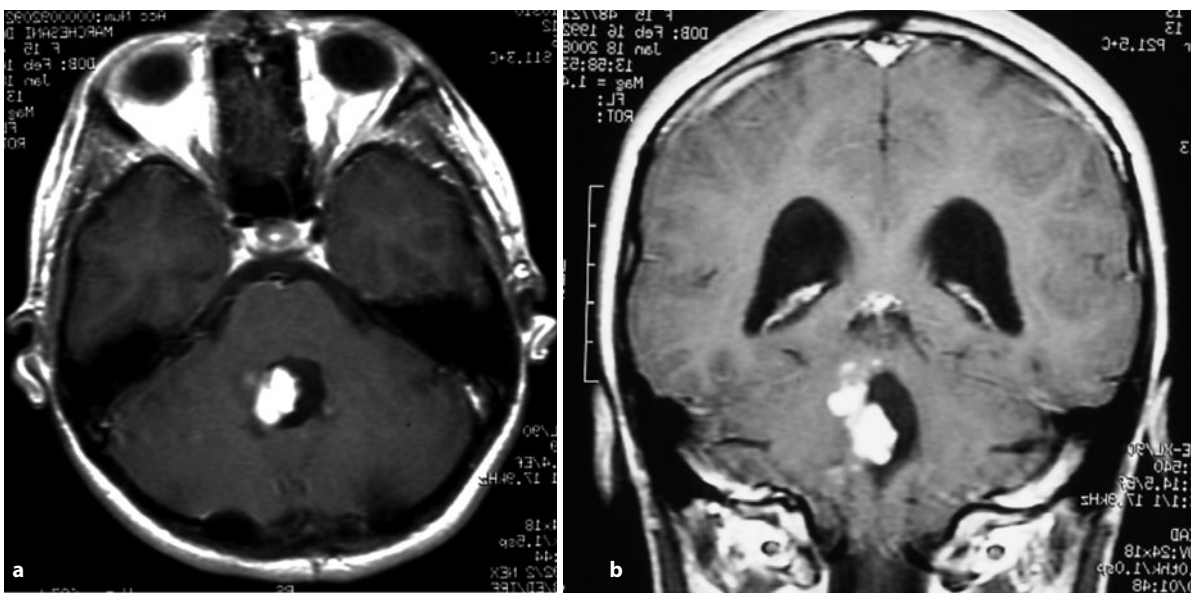

Fig. 40.3 a,b Contrast-enhanced MR SE T1-weighted sequences show an increase in the volume of the residual cancer

Imaging at 4 Months

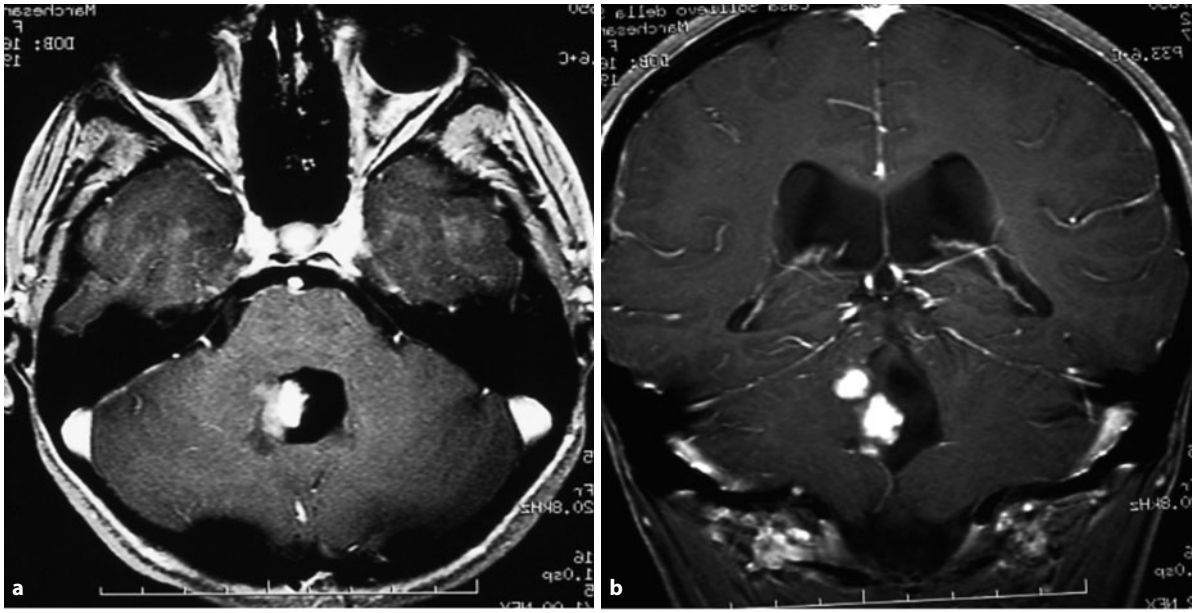

Fig. 40.4 a,b Contrast-enhanced MR SE T1-weighted sequences. There has been a moderate reduction in the volume of the residual cancer

Imaging at 7 Months

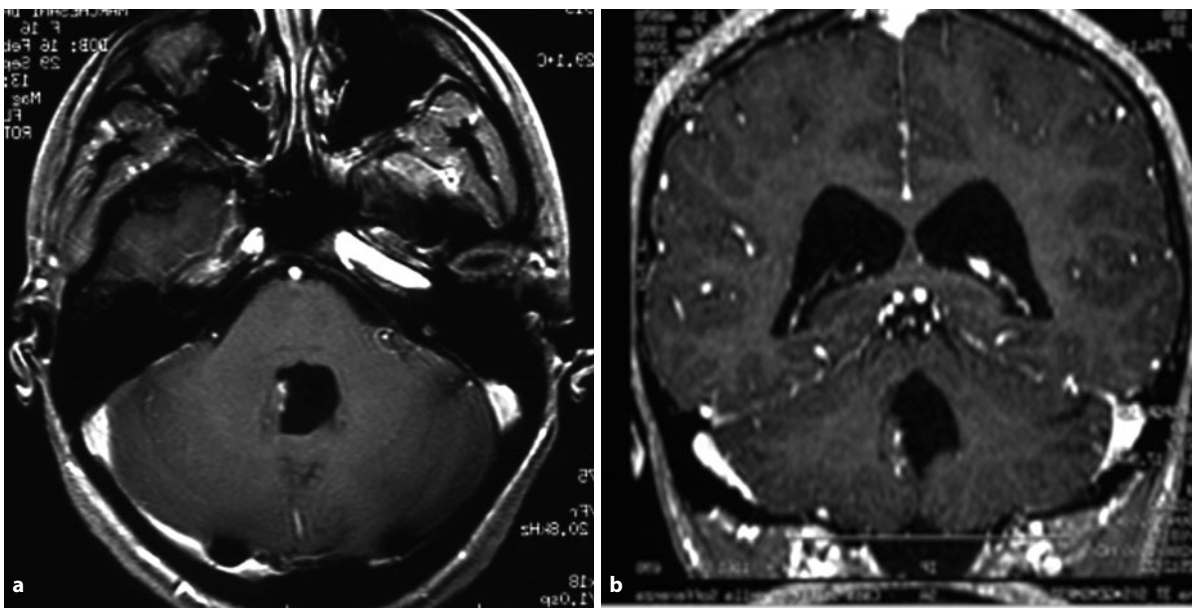

Fig. 40.5 a,b Contrast-enhanced MR SE T1-weighted sequence. There has been a significant reduction in the volume of residual cancer

Case 41

Chemotherapy-induced Tumor Pseudoprogression

3T MR Follow-up in Glioblastoma

Teresa Popolizio, Maria Teresa Cascavilla, Nicola Sforza, Antonio Casillo and Alessandra Stranieri

- 73-year-old patient with right temporal glioblastoma treated with partial surgical excision and combined radiation therapy-chemotherapy
- 3T MR follow-up performed at 1, 3, 9 and 12 months after surgery and combined radiation therapy-chemotherapy

Preoperative Imaging

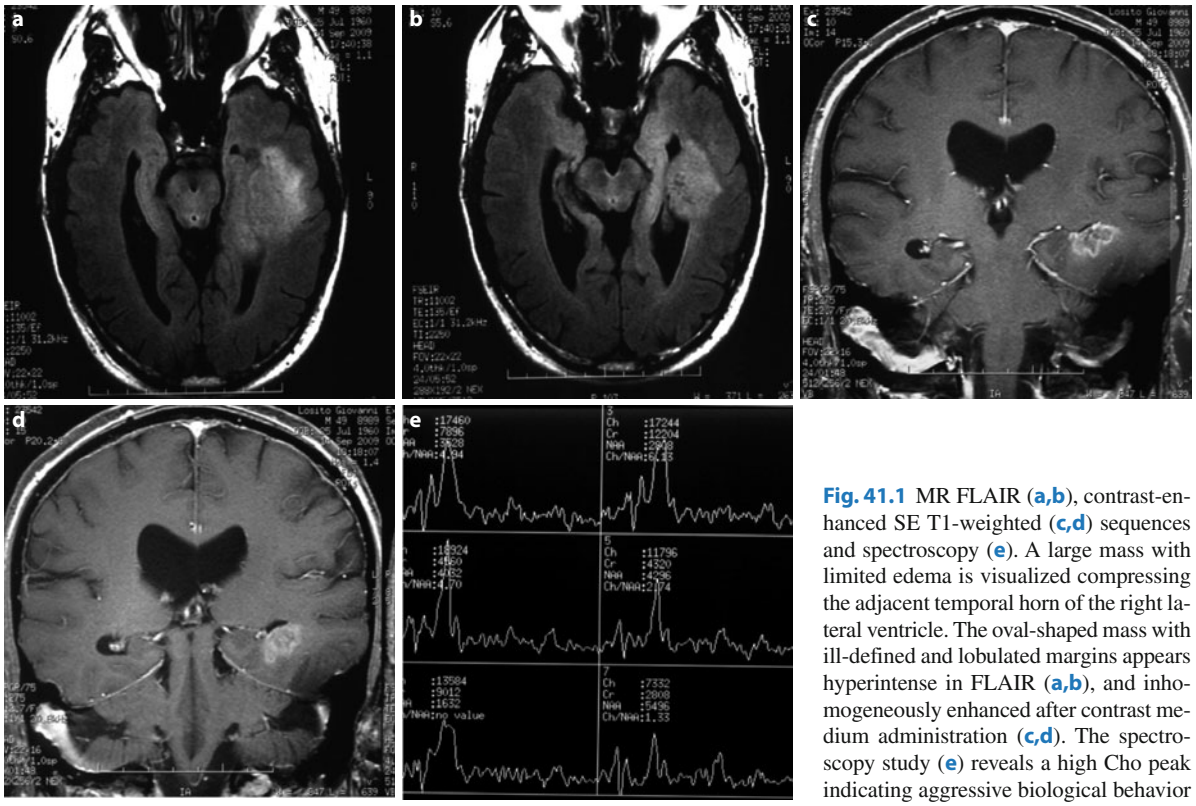

Fig. 41.1 MR FLAIR (**a,b**), contrast-enhanced SE T1-weighted (**c,d**) sequences and spectroscopy (**e**). A large mass with limited edema is visualized compressing the adjacent temporal horn of the right lateral ventricle. The oval-shaped mass with ill-defined and lobulated margins appears hyperintense in FLAIR (**a,b**), and inhomogeneously enhanced after contrast medium administration (**c,d**). The spectroscopy study (**e**) reveals a high Cho peak indicating aggressive biological behavior

Follow-up at 1 Month After Surgery

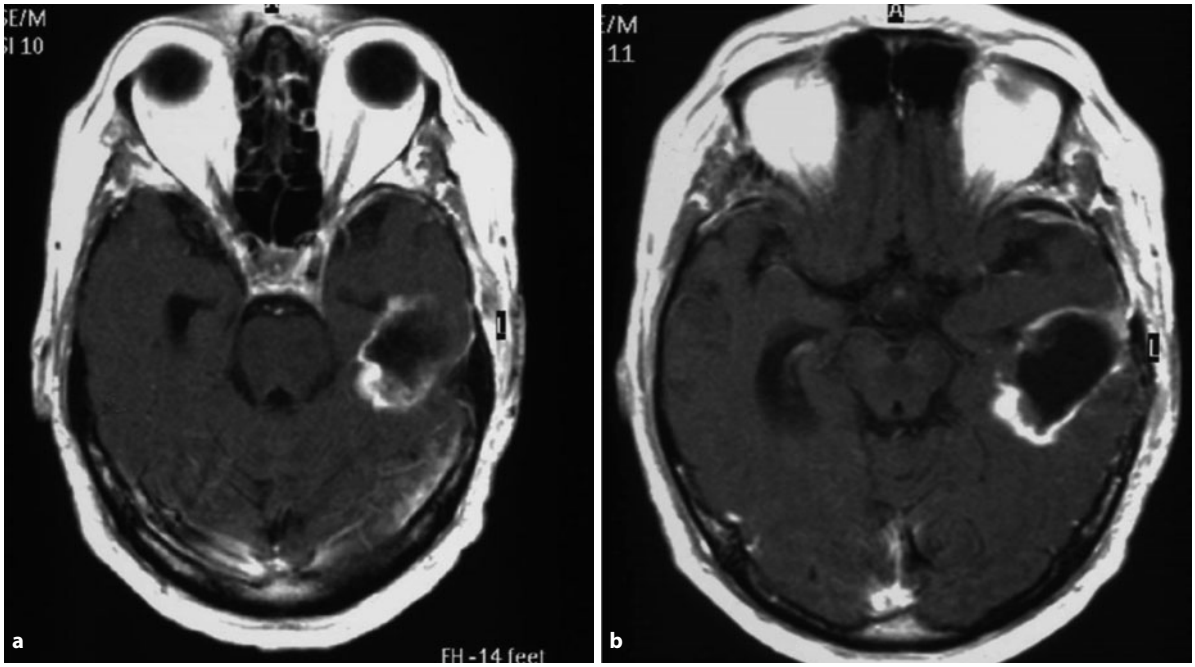

Fig. 41.2 a,b Contrast-enhanced MR SE T1-weighted sequences show the postsurgical appearance of a large cystic-like lesion with thick and irregular rim enhancement

Follow-up at 3 Months After Surgery and Adjuvant Tomotherapy-chemotherapy

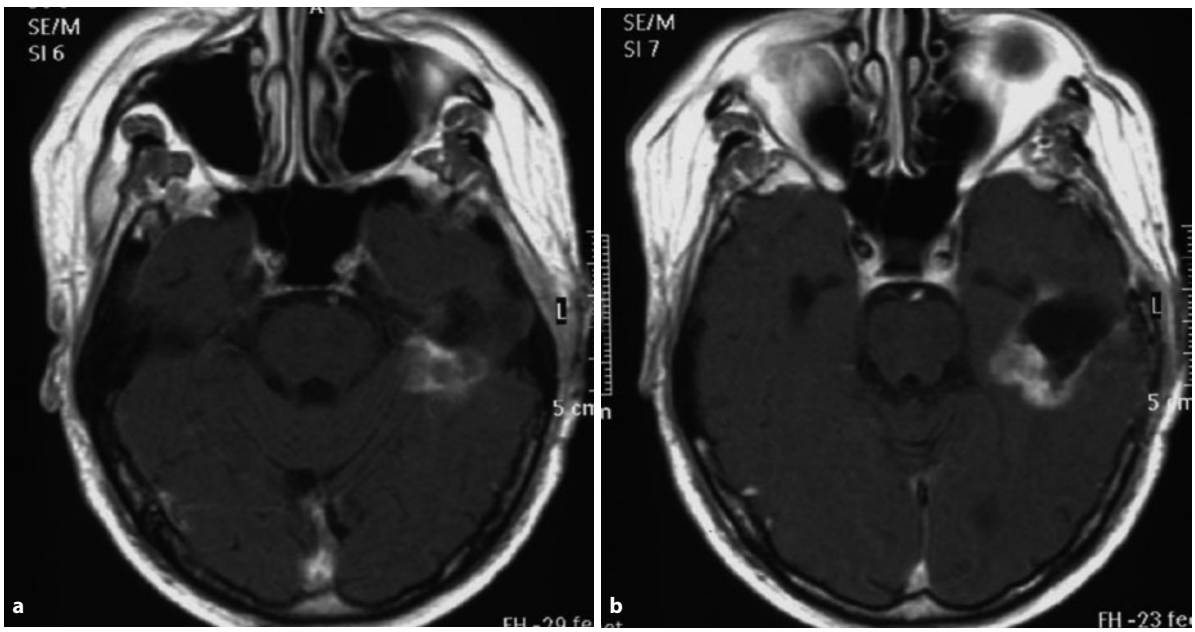

Fig. 41.3 a,b Contrast-enhanced MR SE T1-weighted sequences show an increase in the peripherally enhancing solid component

Follow-up at 9 Months

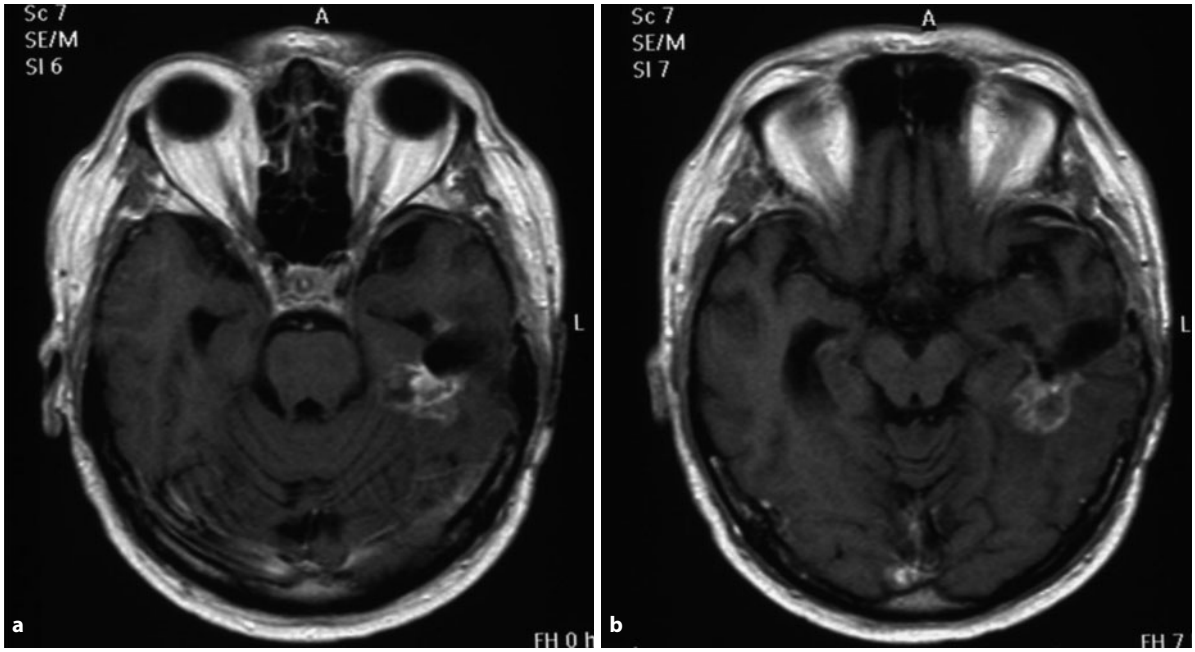

Fig. 41.4 a,b Contrast-enhanced MR SE T1-weighted sequence. A reduction in volume can be seen of both the cystic and solid portions with a substantial necrotic component

Follow-up at 12 Months

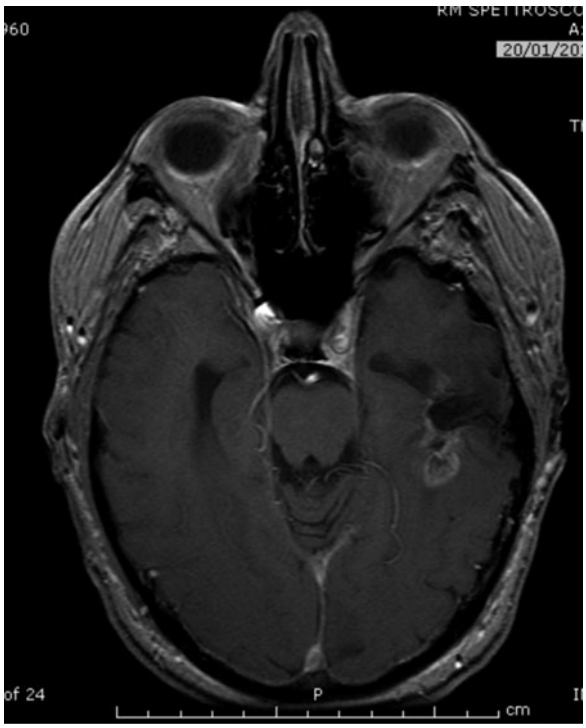

Fig. 41.5 Contrast-enhanced MR SE T1-sequence shows a further reduction in volume of the lesion

Case 42

Chemotherapy-induced Tumor Pseudoprogression with Disease Progression

3T Morphofunctional MR Follow-up in Anaplastic Astrocytoma

Massimo Caulo, Chiara Briganti, Valentina Panara, Simone Salice, Domenico Tortora and Armando Tartaro

- 59-year-old-patient with right frontal anaplastic astrocytoma treated with partial surgery and combined radiation therapy-chemotherapy
- 3T morphofunctional MR follow-up performed with morphologic imaging, diffusion-weighted imaging, perfusion study and spectroscopy at 7, 15 and 28 months after surgery and combined radiation-chemotherapy

Follow-up Performed at 7 Months After Surgery and Combined Radiation Therapy-chemotherapy

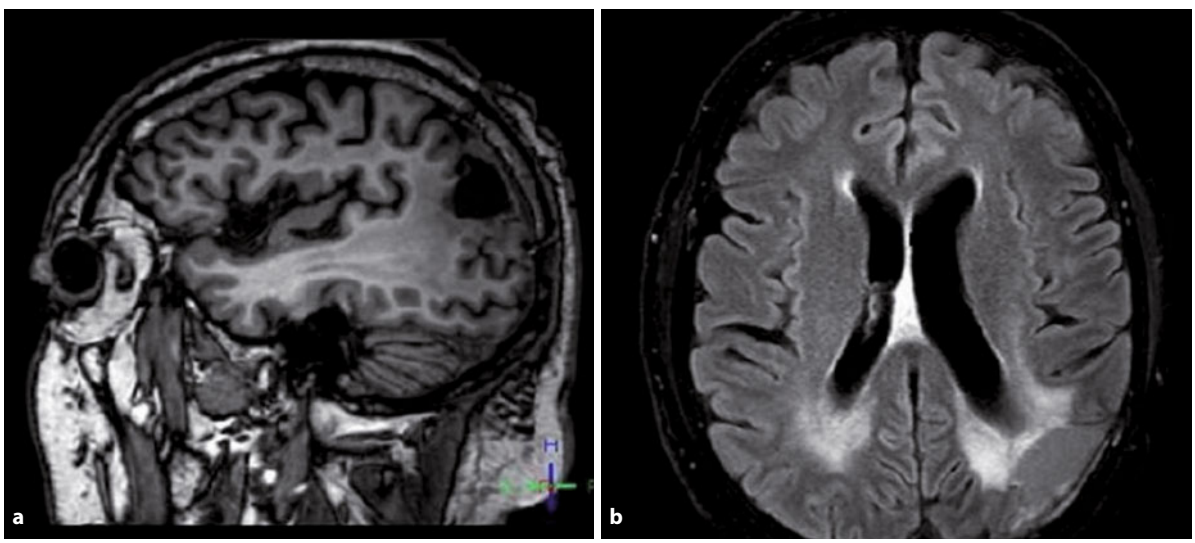

Fig. 42.1 Contrast-enhanced MR SE T1-weighted (**a**) and FLAIR (**b**) sequences show the postsurgical site in the left parietal lobe

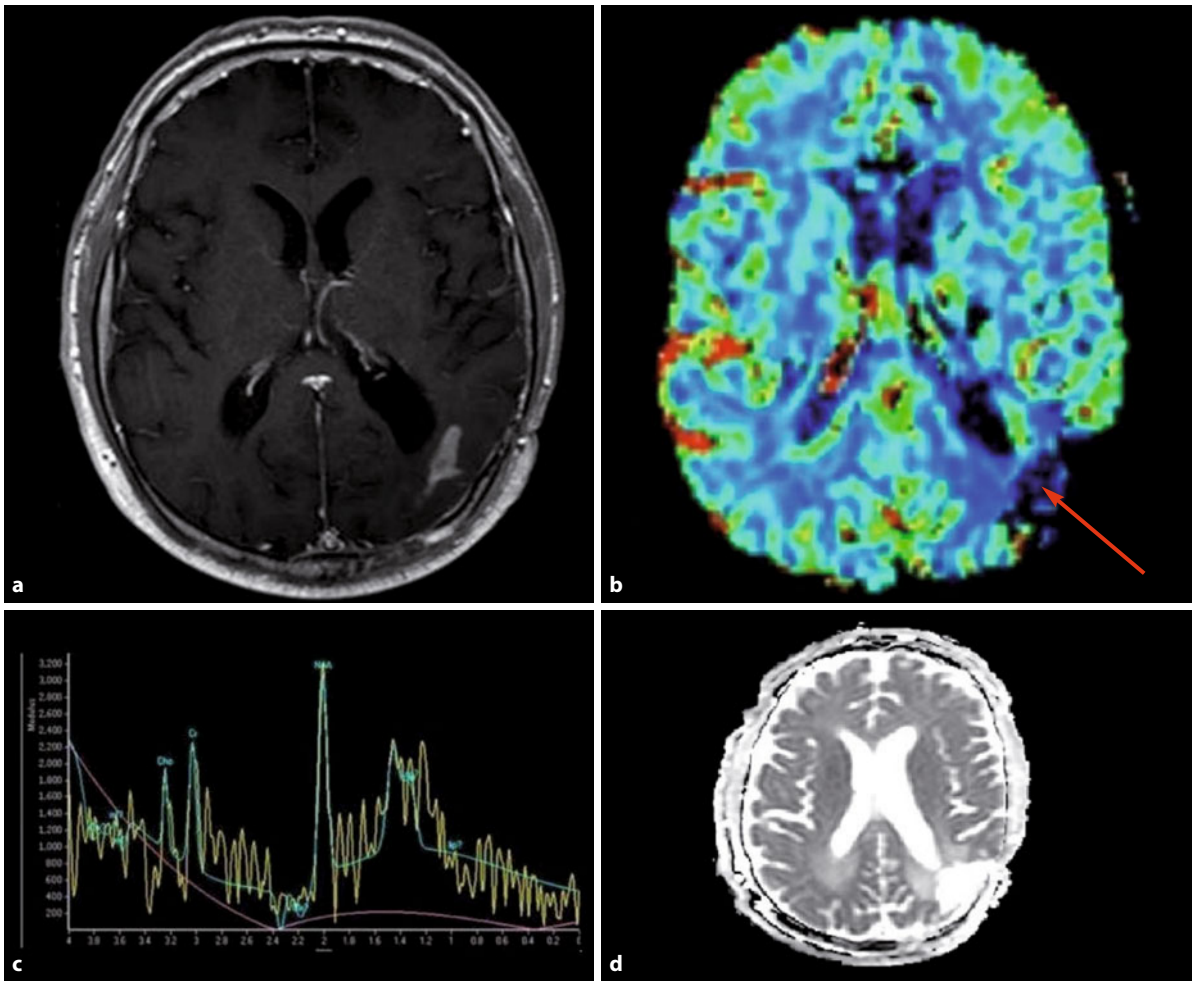

Fig. 42.2 **a** Contrast-enhanced MR SE T1-weighted sequence shows 3 mm nodular contrast enhancement at the anterior-medial portion of the surgical cavity. **b** MR perfusion study with CBV map. The value of rCBV [CBV lesion/contralateral white matter CBV = 2.2] has not increased at the nodular area of contrast enhancement (*red arrow*). **c** MR single/multivoxel spectroscopy. The Cho/Cr (1.2) and Cho/NAA (1.4) ratios are not indicative of high cell turn-over and the presence of the Lac peak confirms the presence of necrosis. **d** MR diffusion-weighted image with ADC map shows increased ADC values (1.323±0.336 mm^2/s) within the area of contrast enhancement

Follow-up Performed at 15 Months

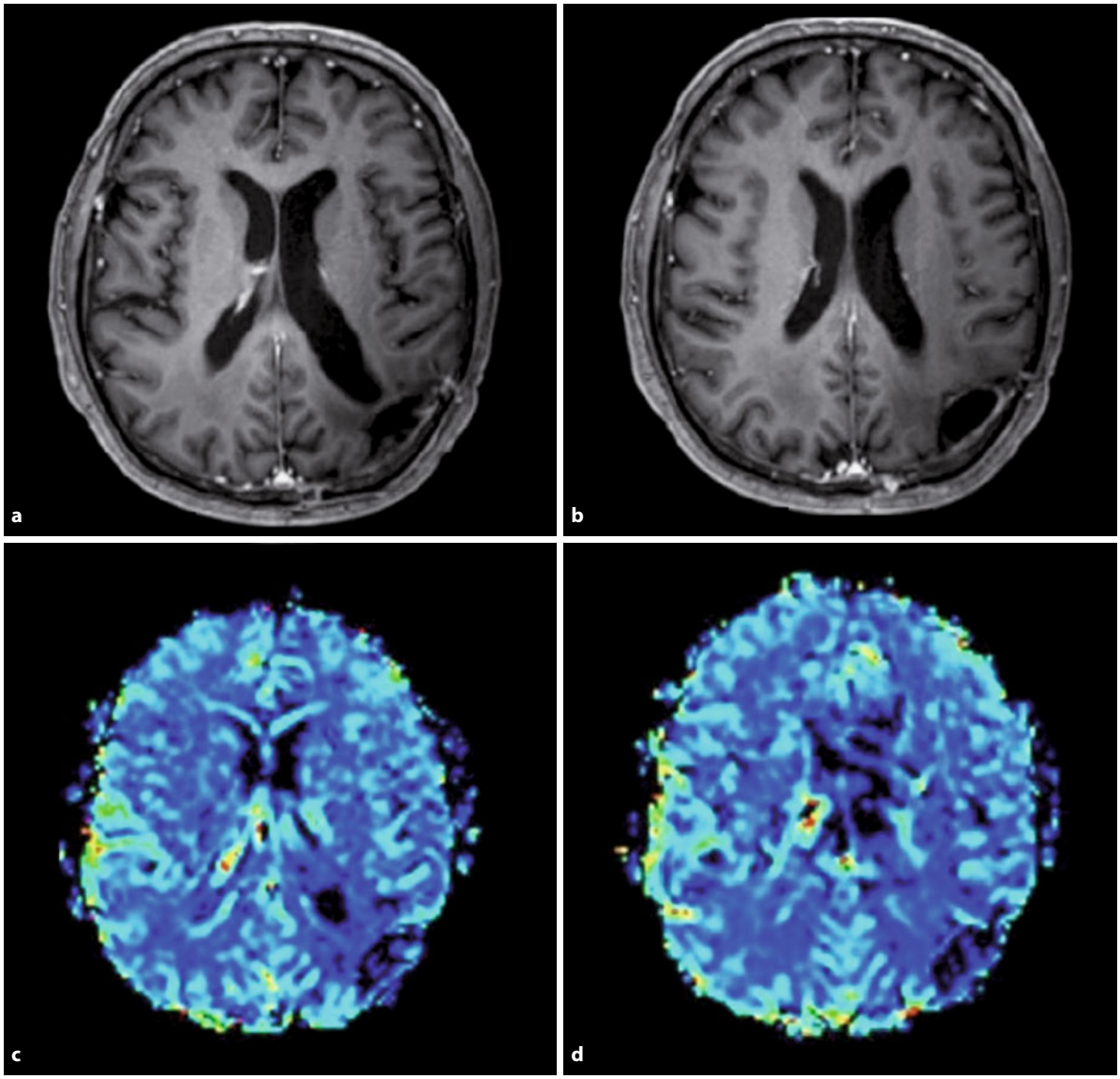

Fig. 42.3 Contrast-enhanced MR SE T1-weighted sequences and perfusion study show complete absence of contrast enhancement (**a,b**) associated with zero values of CBV (**c,d**), both indicative of the absence of disease progression

Follow-up Performed at 28 Months

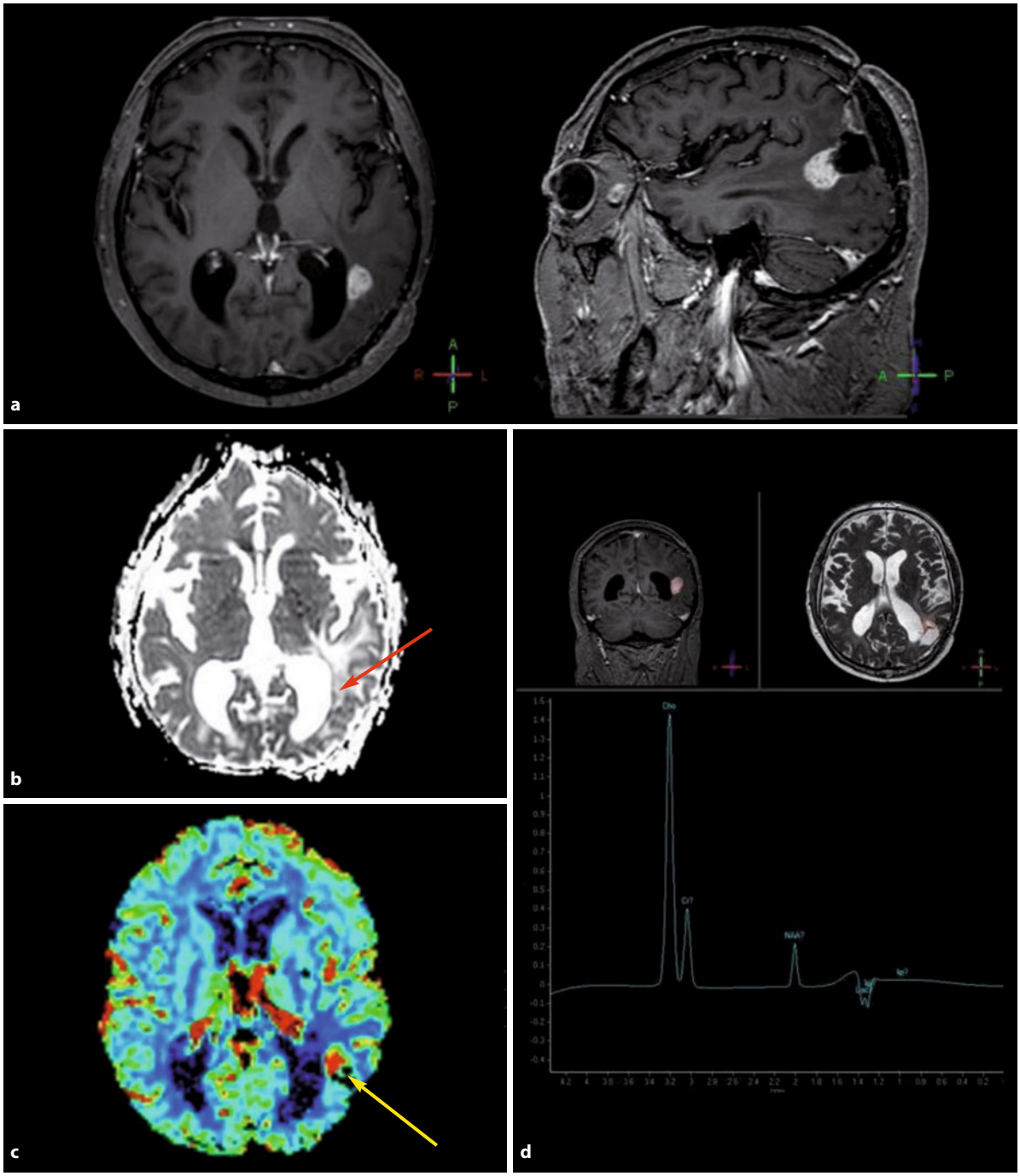

Fig. 42.4 **a** Contrast-enhanced MR SE T1-weighted sequence visualizes ependymal contrast enhancement on the surface of the lateral wall of the ventricular trigone and a nodule of contrast enhancement indicating tumor recurrence. **b** MR diffusion-weighted image with ADC map confirms the morphologic data with reduced ADC values (0.823±0.116 mm^2/s) at the nodule indicating increased cellularity (*red arrow*). **c** MR perfusion study with CBV map confirms the morphologic data of recurrence with significantly increased values of rCBV (5.2) [CBV lesion/contralateral white matter CBV] corresponding to the area of contrast enhancement close to the surgical cavity (*yellow arrow*). **d** MR single voxel spectroscopy shows a reversal of the Cho/Cr (3.8) and Cho/NAA (4.1) peaks at the area of disease progression. The presence of a lipids peak indicates necrosis

Case 43

Drug-induced Leukoencephalopathy

MR Follow-up After Corticosteroid Therapy

Teresa Popolizio, Maria Teresa Cascavilla, Nicola Sforza, Antonio Casillo and Alessandra Stranieri

- 42-year-old patient with Crohn's disease
- Early MR follow-up after steroid therapy

Early Follow-up After Steroid Therapy

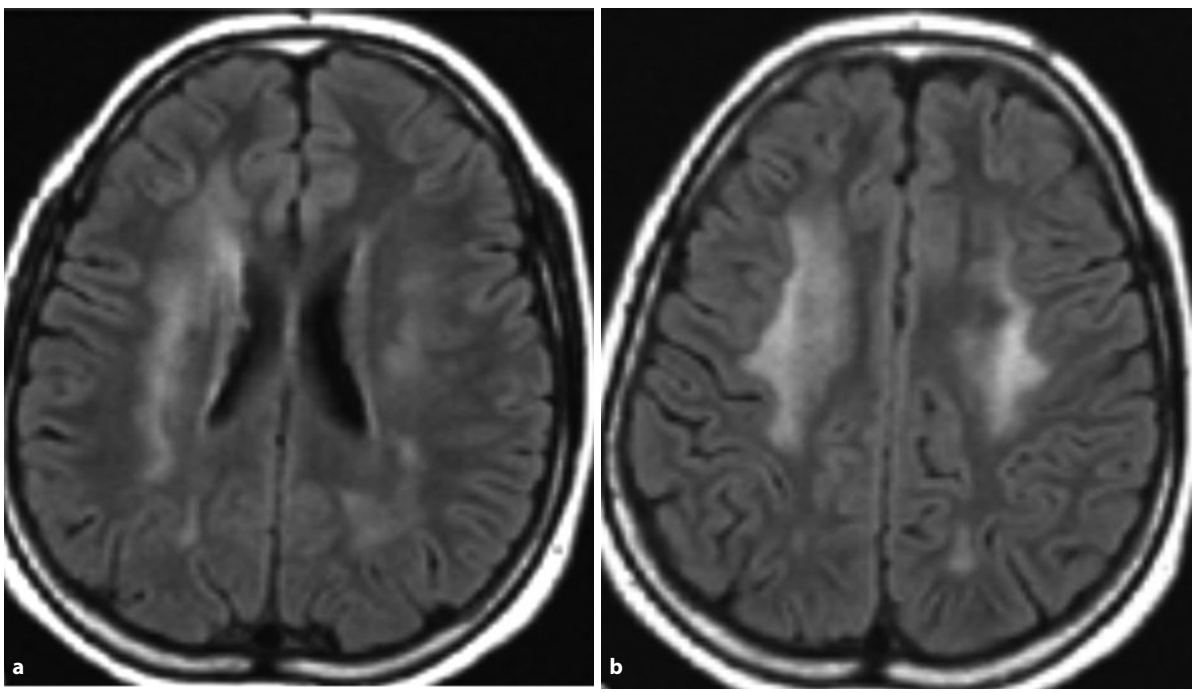

Fig. 43.1 a,b MR FLAIR sequences show diffuse bilateral hyperintensity of the periventricular white matter

Case 44

Drug-induced Leukoencephalopathy

MR Follow-up After Methotrexate Therapy

Teresa Popolizio, Maria Teresa Cascavilla, Nicola Sforza, Antonio Casillo and Alessandra Stranieri

- 52-year-old patient with Non-Hodgkin lymphoma
- MR follow-up in chronic phase after treatment with methotrexate

Late Follow-up After Chemotherapy

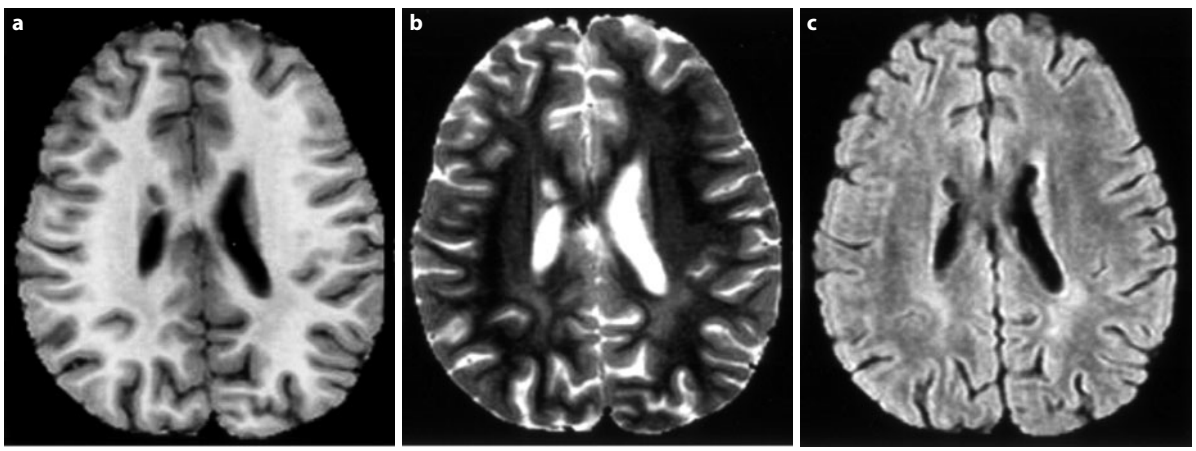

Fig. 44.1 MR SE T1-weighted (**a**), FSE T2-weighted (**b**) and FLAIR (**c**) sequences. Slight and circumscribed signal alteration (hypointensity in T1 and T2, hyperintensity in FLAIR) can be appreciated in the posterior periventricular white matter bilaterally

Case 45

Drug-induced Thrombosis

MR Follow-up After L-asparaginase Therapy

Teresa Popolizio, Maria Teresa Cascavilla, Nicola Sforza, Antonio Casillo and Alessandra Stranieri

- 8-year-old patient with acute lymphoblastic leukemia
- Early MR follow-up after L-asparaginase treatment

Early Imaging After Chemotherapy

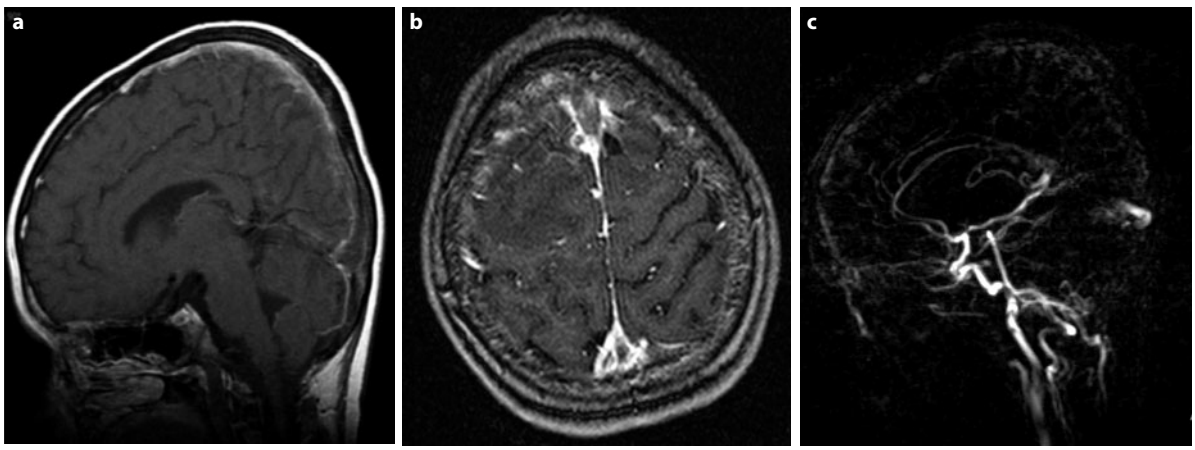

Fig. 45.1 MR SE T1-weighted sequence (**a**) and MR angiography (3D TOF in **b**, 2D PC MIP in **c**). Note the T1 hyperintensity from acute thrombosis with consequent "delta gap" sign in the single partition and no flow signal in the superior sagittal sinus in the MIP image

Case 46

PRES (Posterior Reversible Encephalopathy Syndrome)

MR Follow-up after Cyclosporine Therapy

Teresa Popolizio, Maria Teresa Cascavilla, Nicola Sforza, Antonio Casillo and Alessandra Stranieri

- 35-year-old patient with severe atopic dermatitis
- MR follow-up after treatment with cyclosporine

Imaging After Chemotherapy

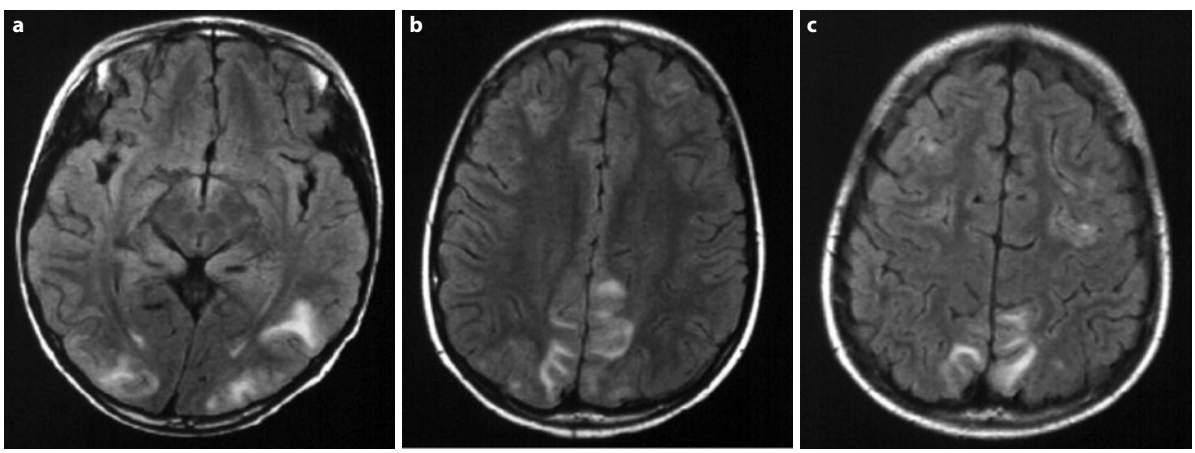

Fig. 46.1 a-c MR FLAIR sequences show symmetric and bilateral cortical-subcortical hyperintensity particularly in the parietal and occipital lobes but also in the frontal lobes attributable to vasogenic edema

Case 47

PRES (Posterior Reversible Encephalopathy Syndrome)

MR Follow-up after Cisplatin Therapy

Teresa Popolizio, Maria Teresa Cascavilla, Nicola Sforza, Antonio Casillo and Alessandra Stranieri

- 75-year-old patient with lung cancer
- MR follow-up after treatment with cisplatin

Imaging After Chemotherapy

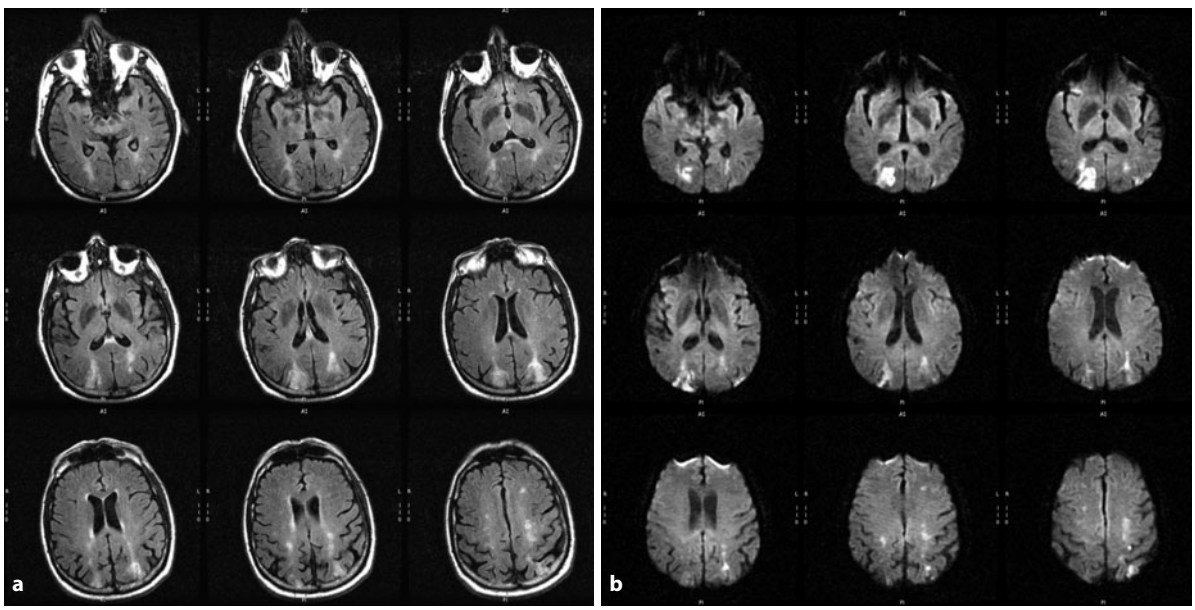

Fig. 47.1 MR FLAIR (**a**), diffusion-weighted (**b**), SE T1-weighted (**c**) and contrast-enhanced SE T1-weighted (**d**) sequences. The symmetrical and bilateral cortical-subcortical hyperintensity (**a,b**) involving the parietal and occipital lobes suggest vasogenic edema. The isointense lesions in T1 (**c**) display moderate enhancement (**d**) (*cont.* →)

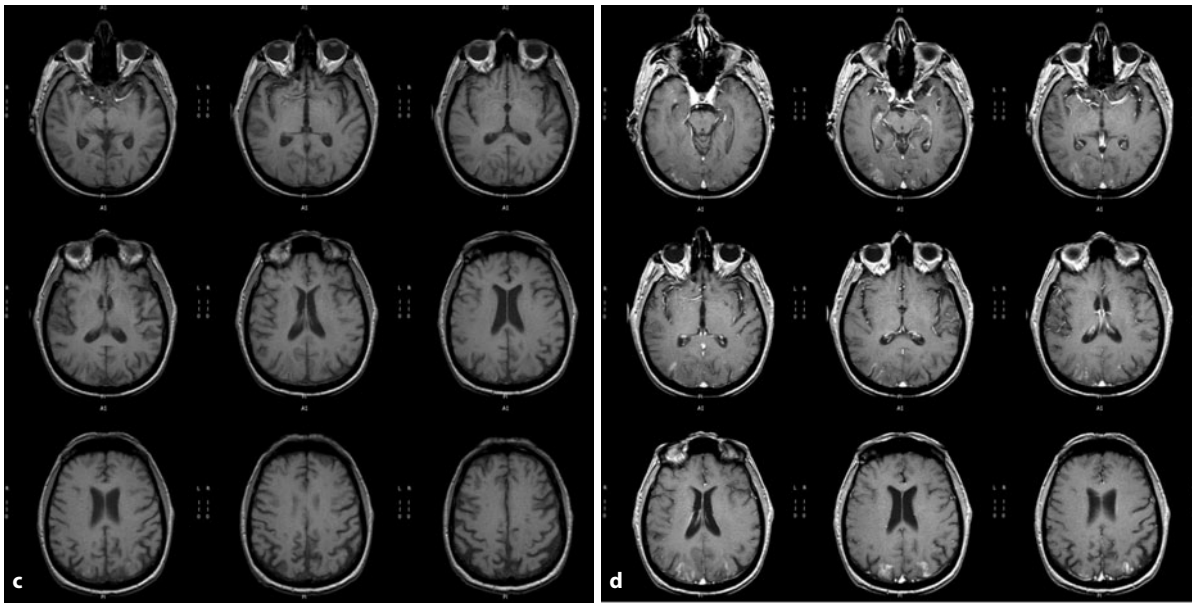

Fig. 47.1 (*continued*)

Case 48

Morphofunctional MR in the Diagnosis and Follow-up of Cerebral Gliomas

Tommaso Scarabino, Alberto Maggialetti, Saverio Pollice, Angela Lorusso, Gilda Morlino, Michela Capuano and Teresa Popolizio

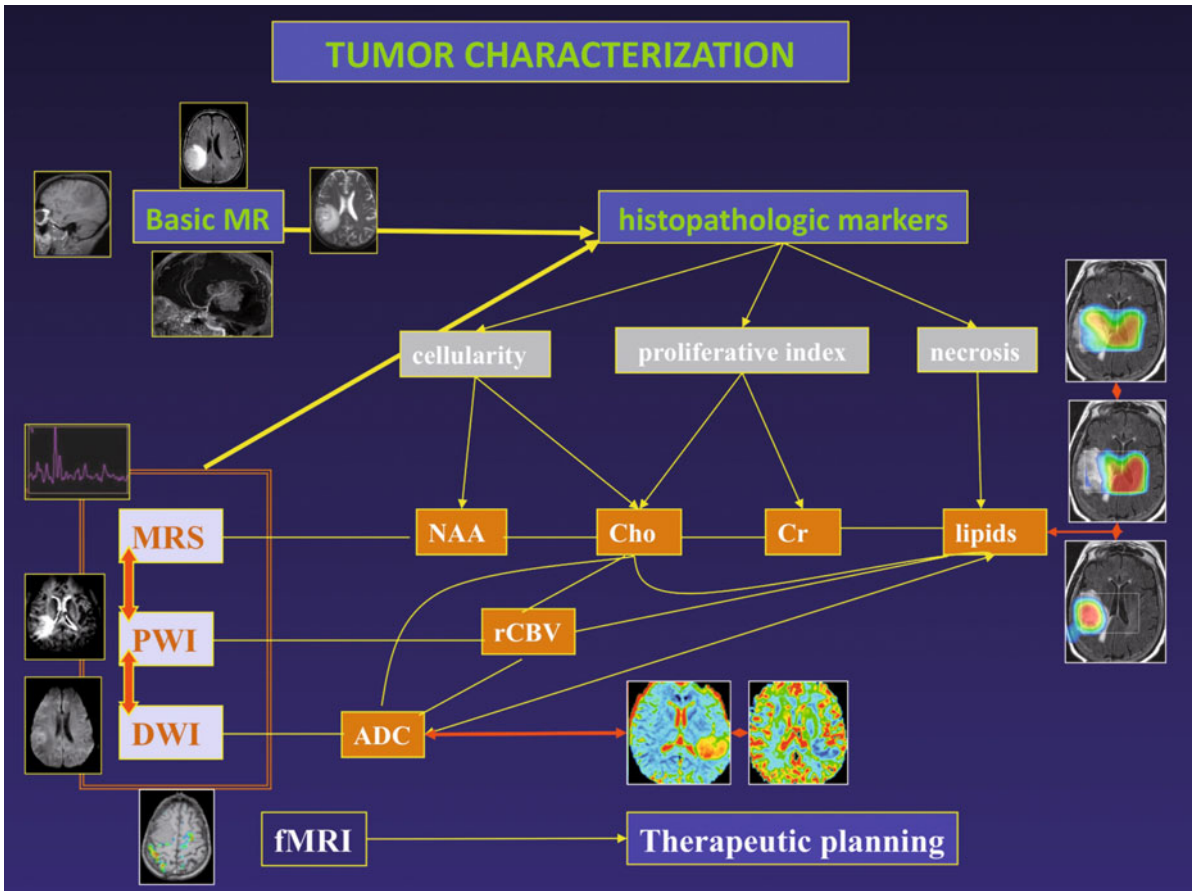

Fig. 48.1 Morphologic MR imaging without and with contrast medium is the examination of choice for the characterization of tumors in both diagnosis and follow-up. A thorough analysis of the radiologic signs, the comparison with the patient's clinical information and the therapy performed can lead to a correct diagnosis. However, some cases are difficult to diagnose because of the extreme tissue heterogeneity and the frequent coexistence of different pathologic patterns. The morphologic examination therefore may require the addition of advanced MR techniques, i.e. functional MR (spectroscopy, diffusion, perfusion, cortical activation), which enable a neuropathologic study in vivo. The functional and physiologic data on cell metabolism, as well as hemodynamic and diffusion parameters, provide a biologic interpretation of the heterogeneity and complexity typical of these tumors, thus improving the diagnostic accuracy, sensitivity and specificity of MR and enabling a more precise and comprehensive diagnosis for the surgeon